DEPOSITIONAL SYSTEMS, PALEOCLIMATE, AND PROVENANCE OF THE LATE MIOCENE TO PLIOCENE BELUGA AND STERLING FORMATIONS, COOK INLET FOREARC BASIN, ALASKA

Presented to the Faculty

of the University of Alaska Fairbanks

in Partial Fulfillment of the Requirements

for the Degree of

DOCTOR OF PHILOSOPHY

By

Jacob Mongrain, B.S., M.S.

Fairbanks, Alaska

December 2012

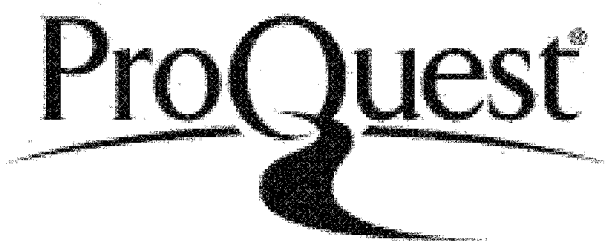

ProQuest LLC
789 East Eisenhower Parkway
P.O. Box 1346
Ann Arbor, MI 48106-1346

DEPOSITIONAL SYSTEMS, PALEOCLIMATE, AND PROVENANCE OF THE LATE MIOCENE TO PLIOCENE BELUGA AND STERLING FORMATIONS, COOK INLET FOREARC BASIN, ALASKA

By

Jacob Mongrain

RECOMMENDED:

Advisory Committee Chair

Chair, Department of Geology and Geophysics

APPROVED:

Dean, College of Natural Science and Mathematics

Dean of the Graduate School

August 31, 2012

Date

Abstract

The sedimentary record of forearc basins provides critical clues to the complex geologic history of subduction zones. This study focuses on Cook Inlet forearc basin, part of a larger forearc basin complex in southern Alaska. Specifically, I investigated the sedimentology, paleoclimate, and provenance of the Beluga and Sterling formations, comprising the late Miocene to Pliocene Cook Inlet basin record. These interpretations are used to reconstruct the Miocene-Pliocene basin history and better understand forearc development.

Before ~11 Ma anabranching/single channel depositional systems of the Beluga Fm. deposited sediment on the western and eastern margins of Cook Inlet. Sandstone compositional data suggest sediment from the eastern margin was sourced from the accretionary prism. Between ~11 Ma and ~8 Ma deposition of the Beluga Fm. waned and sandstone compositional data indicate increases in volcanic lithic fragments derived from the volcanic arc to the northwest. Deposition by the southward-directed, sandy braided fluvial systems of the Sterling Fm. started on the western margin of the basin and migrated eastward, reaching the eastern margin ~8 Ma. By ~6 Ma, sandstone compositional data suggest that the volcanic arc was the dominant sediment contributor to the basin.

Palynological results suggest that forests were predominately confined to coal swamps, and the surrounding floodplains were occupied by shrubs, herbs, and dispersed tree taxa. Thermophilic taxa persisted until at least ~6 Ma. Mean annual precipitation (MAP), estimated from $\delta^{13}C$ values, ranged from 420 to 3900 mm a^{-1} with the greatest variability ~8 Ma. This ~8 Ma event correlates with a decline in sea surface temperatures of the Alaska Gyre and a North Pacific climate optimum. Climate likely played a minor role in fluvial style change.

The dramatic change in depositional style between the Beluga and Sterling fms. is attributed to a change in sediment flux from the accretionary prism to the volcanic arc and western Alaska Range, most likely due to orogen-scale tectonic processes driven by far-afield flat-slab subduction of the Yakutat microplate. The change in fluvial style and sediment flux starting ~11 Ma suggests a previously unrecognized exhumation in the western Alaska Range at this time.

Table of Contents

Page

List of Figures

Page

List of Tables

Page

List of Appendices

Chapter 1

Introduction

1.1 Research Objectives

The main objective of this dissertation is to reconstruct Cook Inlet basin evolution during deposition of the Beluga and Sterling fms. The Beluga and Sterling fms. are fluvial sediments deposited in the Cook Inlet forearc basin during the Neogene. These formations are of particular interest as they record the tectonic evolution of southern Alaska during a pulse of exhumation in the Alaska Range and flat-slab subduction of the Yakutat microplate. In addition, both formations host significant oil, gas, and coal deposits (Stanley et al., 2011).

The first objective is to conduct field-based geologic studies of the fluvial sediments in order to reconstruct the depositional systems of these two formations. A significant change in depositional systems is found between the Beluga and Sterling fms. The second objective is to investigate possible causes for the significant change in depositional systems based on current understanding of the geological history of southern Alaska. This was accomplished by reconstructing paleoclimate, using palynology and stable isotope techniques, and tectonic changes, using petrographic data to infer provenance.

1.2 Document Format

This dissertation is presented in five chapters focused on the Beluga and Sterling fms. in Cook Inlet, southern Alaska. Chapter 1 introduces the document, provides a summary of the goals of this study, and highlights key results. Chapter 2 focuses on the sedimentology of these two formations and defines a significant difference in fluvial style between the humid/organoclastic anabranching/single channel streams of the Beluga Fm. and the sandy braided rivers of the Sterling Fm. Chapters 3 and 4 investigate

possible causes of the change in fluvial style due to climate and tectonics. Specifically, Chapter 3 reconstructs aspects of the Neogene climate in south-central Alaska using palynology and carbon stable isotopes. Chapter 4 discusses possible tectonic influences on fluvial style based on changes in provenance inferred from modal point count data of sandstone units.

1.3 Chapter Summaries

Chapter 2 is a synthesis of new sedimentological data including facies analysis, architectural analysis, paleocurrent data, and analog matching techniques. This synthesis allows us to reconstruct a major change in fluvial style, from anabranching/single channel fluvial systems of the Beluga Fm. to sandy braided fluvial systems of the Sterling Fm. We also identify modern analogs that are useful for understanding sand body geometry, facies models and reservoir architecture, all useful in the energy industry. The best modern analog for the fluvial depositional systems of the Beluga Fm. is the Cumberland Marshes reach of the Saskatchewan River. Only modest constraints can be placed on modern analogs for the Sterling Fm., as the scale of the streams is not well documented in the modern literature. The rivers that bracket the streams of the Sterling Fm. with respect to planform style, basin scale, and hydraulics are the smaller Platte River and the much larger Brahmaputra River. Based on climate and physiographic setting, the Susitna River is the closest match, but it is under-fit and may not be of predictive value with respect to reservoir architecture.

Chapter 3 reconstructs aspects of the Miocene and Pliocene paleoclimate using palynology and stable isotope analysis. These results suggest a slight decrease in temperature of a few degrees Celsius over the entire interval and variable mean annual precipitation (MAP) that ranged from 420 to 3900 mm a^{-1}. The interval with the most variable MAP occurs ~8 Ma and correlates with a decline in sea surface temperatures of the Alaska Gyre along with a North Pacific climate optimum.

Chapter 4 uses sandstone compositional data, new age constraints and interpretations of depositional systems to better understand Neogene Cook Inlet forearc basin evolution. This work hypothesizes that

the oldest Beluga Fm. sediment was derived from the accretionary prism and, as sediments become younger, the volcanic arc becomes more dominant, so that by the youngest Sterling Fm. sediments are derived almost entirely from the volcanic arc.

In all cases, I am responsible for the majority of the writing, data analysis, and sample collection. Supplementary data and all analytical work relevant to the main body of the text are found in appendices at the end of the dissertation.

1.4 References

STANLEY, R., CHARPENTIER, R.R., COOK, T.A., HOUSEKNECHT, D.W., KLETT, T.R., LEWIS, K.A., LILLIS, P.G., NELSON, P.H., PHILLIPS, J.D., POLLASTRO, R.M., POTTER, C.J., ROUSE, W.A., SALTUS, R.W., SCHENK, C.J., SHAH, A.K., and VALIN, Z.C., 2011, Assessment of Undiscovered Oil and Gas Resources of the Cook Inlet Region, South-Central Alaska: USGS National Assessment of Oil and Gas Fact Sheet, p. 2.

Chapter 2

Sedimentology of Neogene Terrestrial Deposits (Beluga and Sterling Formations), Cook Inlet Forearc Basin, Alaska[1]

2.1 Abstract

The geologic history of the convergent southern margin of Alaska is complex. Investigating the near-continuous Neogene depositional record of the Cook Inlet forearc basin will aid in better understanding this history. However, understanding basin development is hampered by conflicting interpretations of the depositional systems in the basin. Cook Inlet basin hosts up to ~ 600 million barrels of undiscovered, technically recoverable oil and ~19 trillion cubic feet of natural gas according to a recent assessment by the United States Geological Survey. A better understanding of depositional systems and sand body geometries will aid in exploration for additional hydrocarbon deposits. This paper focuses on depositional systems of the Neogene Beluga and Sterling formations, using detailed facies analysis, architectural analysis, and analog matching techniques, from exposures along the western and eastern margins of Cook Inlet, Alaska.

The Beluga Formation is dominated by anabranching, single thread fluvial systems. Channel dimensions of fluvial sand bodies indicate average flow depths of 2 m and channel widths of 11 m. On the eastern side of the basin, these fluvial systems flowed toward the west, away from the accretionary prism. Paleoflow on the western side of the basin is less well-constrained but flow was probably eastward. The Cumberland Marshes region of the Saskatchewan River, Canada, is a likely modern analog for fluvial systems of the Beluga Fm. in terms of scale and sedimentary

[1] Mongrain, J., McCarthy, P., LePain, D., In Prep, Sedimentology of Neogene Terrestrial Deposits (Beluga and Sterling Formations), Cook Inlet Forearc Basin, Alaska: Journal of Sedimentary Research.

facies. In contrast, the Sterling Formation records deposition in low sinuosity sandy braided fluvial systems. Calculated channel dimensions of these fluvial sand bodies indicate flow depths of 8-13 m and channel widths of 113-286 m. Rivers that deposited the Sterling Fm. flowed southward from the rising Alaska Range. No modern analog fits the scale of the fluvial systems of the Sterling Fm., however, the system was likely intermediate, between the modern Platte and the Brahmaputra rivers. The dramatic change in depositional style between the Beluga and Sterling formations is attributed to orogen-scale tectonic processes, likely driven by flat-slab subduction of the Yakutat microplate.

2.2 Introduction

The Cenozoic geologic history of Southern Alaska consists of a tectonically complex convergent margin composed of: 1) long-lived subduction since Jurassic time (Stock and Molnar, 1988; Nokleberg et al., 1994); 2) Paleocene to Eocene subduction of the Kula-Resurrection spreading ridge (Bradley et al., 2003; Haeussler et al., 2003); 3) Oligocene to Holocene flat-slab subduction of the Yakutat microplate (Haeussler et al., 2008; Finzel, 2010; Benowitz, 2011); and 4) Miocene to Holocene exhumation of the Alaska Range (Little and Naeser, 1989; Fitzgerald et al., 1995; Pavlis and Roeske, 2007; Haeussler et al., 2008; Finzel, 2010; Benowitz, 2011). Detailed studies of these events and their associated geologic records are needed to more fully understand hydrocarbon systems in Cook Inlet and the evolution of forearc basins during second-order subduction processes (i.e. spreading ridge subduction and flat-slab subduction; Ridgway et al., 2011).

Cook Inlet is a petroleum province from which more than 1.3 billion barrels of oil and 7.8 trillion cubic feet of gas have been produced since 1958 (Stanley et al., 2011). A recent assessment by the United States Geological Survey (USGS) indicates the probable existence of additional oil

and gas resources that are technically recoverable using current technology. The USGS estimates that the total undiscovered gas resource in Cook Inlet ranges between 4,976 and 39,737 billion cubic feet of gas (BCFG), with a mean estimate of 19,037 BCFG. The majority of this, about 72%, is predicted to reside in conventional hydrocarbon accumulations (Stanley et al., 2011).

The purpose of this paper is to interpret the sedimentary record of the terrestrial Late Miocene to Early Pliocene Cook Inlet forearc basin in order to better refine our understanding of forearc basin evolution during flat-slab subduction. We present new data on fluvial depositional systems and channel dimensions and use this information to estimate the size of Beluga and Sterling fms. streams and their corresponding catchment areas to aid in better prediction of reservoir geometries. We also use facies and architectural analysis to demonstrate a dramatic change in fluvial style from the Beluga Fm. to the Sterling Fm.

2.3 Geologic Setting

Cook Inlet basin is part of a northeast-trending, collisional forearc basin complex that extends from near Shelikof Strait in the southwest to the Wrangell Mountains in the northeast (Fig. 2.1). The Cook Inlet portion of this larger forearc complex is bounded on the west and north by granitic batholiths and volcanoes of the Aleutian-Alaska Range volcanic arc, and on the east and south by the Chugach and Kenai Mountains, which represent the emergent portion of the accretionary prism (Figs. 2.1, 2. 2; Nokleberg et al., 1994; Haeussler et al., 2000). High-angle faults, including the Bruin Bay and Castle Mountain faults, modify the western and northern sides of the forearc basin. The Border Ranges fault lies near the eastern edge of the forearc basin (Figs. 2.1, 2.2), and is locally overlain by Cenozoic forearc basin strata.

Ongoing collision and subduction of the Yakutat microplate is a major tectonic driver in southern Alaska. This event was initiated ~ 20-25 Ma (Plafker, 1987) and it may have begun as early as the late Eocene (Fig. 2.3; Finzel et al., 2011). The subducting portion of the Yakutat microplate likely consists of a 24-27 km-thick slab of mafic rocks which are more buoyant than typical oceanic crust; this slab is contiguous with typical oceanic crust that lies to the southwest (Plafker, 1987; Eberhart-Phillips et al., 2006; Haeussler and Saltus, 2011). Uplift of the western Alaska Range and inversion of the Matanuska Valley forearc basin are believed to result from this flat-slab subduction (Trop et al., 2003; Haeussler, 2008; Trop, 2008; Benowitz et al., 2011). Pulses of exhumation in the Tordrillo Mountains (Fig. 2.1) ~24 Ma and ~6 Ma, maybe due to rotation of the southern Alaska block (SAB) driven by the subducting Yakutat microplate (Haeussler, 2008; Benowitz, 2011). Folds in northern Cook Inlet are consistent in geometry and timing with rotation of the southern Alaska block. This rotation was coeval with the Neogene depocenter, as evidenced by a large low gravity anomaly in Cook Inlet Basin (Haeussler et al., 2000; Bruhn and Haeussler, 2006; Haeussler, 2008; Haeussler and Saltus, 2011). High rates of Neogene subsidence in Cook Inlet are attributed to the shallower-eastward geometry of the subducting Yakutat slab (Haeussler and Saltus, 2011) that resulted in a well-hydrated and serpentinized mantle wedge with lateral variation in heat flow. Differential heat flow is thought to result in enhanced corner flow in the mantle wedge between the subducting slab and the base of the continental crust under Cook Inlet (Haeussler and Saltus, 2011).

The volcanic arc near the Cook Inlet portion of the forearc basin was intermittently active until Late Oligocene to Early Miocene time (Nye et al., 2002). The arc was probably inactive from the early Miocene until the Quaternary, due to flat-slab subduction processes (Fig. 2.3; Nye et al., 2002; Finzel, 2010).

Cenozoic strata in Cook Inlet basin are underlain by a thick succession of dominantly marine Mesozoic rocks, exposed along the western and eastern basin margins (Fig. 2.2; Magoon et al., 1976; Wilson et al., 2009). The Cenozoic section (Fig. 2.3), which is up to 7,600 m-thick in the axial region of the basin, consists of a complex assemblage of alluvial fan, axial fluvial, and alluvial floodbasin deposits. The basic outline of this depositional model was first proposed by Hite (1976) and developed further by McGowen and Doherty (cited in Swenson, 2002) in the 1990s. With a combined thickness in excess of 4,600 m in the axial region of the basin (Calderwood and Fackler, 1972), the Beluga and Sterling fms. provide a detailed archive of depositional conditions in the basin and tectonic events that shaped its Neogene history. These tectonic changes are reflected in an up-section change in fluvial style recorded by the Beluga and Sterling fms., from muddy, low-energy fluvial systems in the former to sand-dominated, higher-energy systems in the latter (Flores et al., 2004; LePain et al., 2009).

2.3.1 Previous work on the Beluga and Sterling fms.

Previous interpretations of the depositional systems of the Beluga and Sterling fms. are varied. Hayes et al. (1976) interpreted the Beluga Fm. as the product of westward-prograding alluvial fans and westward-flowing braided fluvial streams emanating from the Kenai–Chugach Mountains. Boss et al. (1976) interpreted the Beluga Fm. as a "waste-basket" stratigraphic unit due to the range of fluvial-alluvial deposits included in the unit. Rawlinson (1984) interpreted the Beluga Fm. as the product of braided and meandering streams flanked by levee, floodplain, and flood-basin deposits sourced from the east in the Chugach-Kenai Mountains. Flores and Stricker (1992) interpreted the Beluga Fm. as the product of suspended-load, anastomosed streams. The maximum thickness of the Beluga Fm. is ~1800 m near the western margin of the basin, but it thins dramatically to the east (Calderwood and Fackler, 1972; Kirschner and Lyon, 1973). The provenance of the Beluga Fm. on the eastern side of the basin suggests that sediment was sourced from the Chugach-Kenai mountains (Calderwood and Fackler, 1972; Kirschner and

Lyon, 1973; Rawlinson, 1984; Chapter 4) and, perhaps, also from remnants of the Matanuska forearc basin (Trop et al., 2003; Trop, 2008; Chapter 4), while exposures on the western side were derived from the central and western Alaska Range (Calderwood and Fackler, 1972; Kirschner and Lyon, 1973; Chapter 4), the Kahiltna Assemblage (Helmold et al., In Review; Chapter 4), and areas possibly as far north as the Yukon composite terrane (Finzel, 2010).

Hayes et al. (1976) interpreted the Sterling Fm. as the product of meandering streams flowing southward from the Aleutian–Alaska ranges. Boss et al. (1976) interpreted the Sterling Fm. as having been deposited by braided rivers. Rawlinson (1984) interpreted deposits of the Sterling Fm. as the product of meandering streams flanked by overbank flood basin deposits, similar to those of the Beluga Fm., that were sourced from the east in the Chugach-Kenai Mountains. Flores and Stricker (1992) interpreted the lower to middle part of the Sterling Fm. as meandering stream deposits and the upper part of the Sterling Fm., near Clam Gulch, as the product of braided streams. Sediments were sourced from the Chugach-Kenai Mountains (Kirschner and Lyon, 1973; Rawlinson, 1984; Chapter 4), Talkeetna Mountains (Finzel, 2010), recycled Mesozoic forearc strata in the Matanuska Valley (Finzel, 2010; Helmold et al., In Review; Chapter 4), volcanic and plutonic sources in the Alaska Range (Nokleberg et al., 1994; Fitzgerald et al., 1995; Haeussler, 2008; Helmold et al., In Review; Chapter 4).

2.4 Methods

Sixty-three stratigraphic sections were measured from near-continuous exposures along the eastern shore of Cook Inlet and the western shore of Kachemak Bay, on the Kenai Lowland, and from isolated exposures on the western margin of Cook Inlet, along the Chuitna and Beluga Rivers (Fig. 2.1). Detailed descriptions include grain size, lithology, sedimentary structures, contact relationships, and vertical and lateral relationships. All exposures were photographed to

generate photomosaics and line-drawing interpretations of fluvial architecture. A hierarchical approach was used to interpret the scale of architectural elements from the smallest-scale cross-set boundaries to bar forms and large-scale scour surfaces separating fluvial stories. These data are integrated, where possible, with paleocurrent data and sand body dimensions. Drainage area estimates were calculated from geomorphological regional curves (Davidson and North, 2009) to aid in choosing the most appropriate modern analogs.

2.4.1 Channel Geometries

Exposures of Sterling Fm. sandstones are typically oriented along depositional dip, or oblique to dip. Channel margins are seldom observed, and complete channel geometries are rarely preserved. Interpreting sand body geometries, including channel widths and resulting width-to-depth ratios, is difficult given these outcrop orientations. Channel depth can be determined from measuring channel body thickness directly from outcrop or from equations relating sedimentary structures to flow depth (LeClaire and Bridge 2001). Most channel depths for the Sterling Fm. are calculated using the method of LeClaire and Bridge (2001), as internal erosional surfaces are abundant leading to underestimates of true depths using direct measurement methods. In contrast, small channels in the Beluga Fm. generally lack internal erosion surfaces and sedimentary structures are poorly preserved, so that direct measurement of channel depths from Beluga Fm. channel bodies is preferred over calculation. For both formations, channel depth was used to calculate channel width using relationships derived from Bridge and Mackey (1993).

2.4.2 *Channel Depths*

Estimates for depth of flow in the Beluga Fm. channels were approximated by measuring the thickness of the sand bodies from the base of the thalweg to the top of associated bar deposits. This method is limited to complete channel-filling successions where internal erosional surfaces are not present and is, therefore, not suitable for use in the Sterling Fm. Channel depths in the

Sterling Fm. are calculated instead. LeClaire and Bridge (2001) developed empirical relationships in which the average cross-bed set thickness is used as a proxy for flow depth. The method assumes that dune height is approximately equal to 2.97 (±0.7) (~ 3; McLaurin and Steel, 2007) of cross-bed thickness and that flow depth is six to ten times dune height.

Alternatively, dune height can be calculated using the following equation:

$$h_m = 5.3\beta + 0.001\,\beta^2 \qquad \text{Equation 2.1}$$

where h_m is equal to mean bedform height, β is $\approx s_m/1.8$, and s_m is the mean thickness of cross-sets (Bridge and Tye, 2000; Leclair and Bridge, 2001).

2.4.3 Channel Widths

Channel widths were calculated using the empirical regression equation of Bridge and Mackey (1993):

$$w_c = 8.88 d_m^{1.82} \qquad \text{Equation 2.2}$$

where w_c is equal to bankfull channel width and d_m is equal to mean bankfull depth. Bridge and Mackey (1993) indicate that mean bankfull depth is approximately equal to one-half the maximum bankfull depth.

2.4.4 Channel Sinuosity

Sinuosity was calculated following Bridge et al. (2000). Their equations assume that bends within channels can be represented as circular arcs or sine-generated curves:

$sn = \phi / \sin \phi$ (circular arc method) Equation 2.3

$sn = 4.84/(4.84 - \phi^2)$ (sine-generated curve method) Equation 2.4

where *sn* is equal to the sinuosity of the channel, and ϕ is equal to one-half of the maximum paleocurrent range in radians.

2.4.5 *Paleocurrent*

A total of 88 paleocurrent measurements were recorded at six locations from channel deposits of the Sterling Fm. (Fig. 2.4). The Beluga Fm. generally lacks well-preserved sedimentary structures that would yield reliable paleocurrent data. Measurements used to calculate mean paleocurrent direction were restricted to foresets in trough cross-stratified fine- to coarse-grained sand bodies. The Sterling Fm. consists of unconsolidated material, so excavation of trough cross-stratified sand bodies was undertaken to assure measurement down trough axes.

2.4.6 *Drainage Area and Discharge Estimates and Modern Analogs*

An analog is best chosen that matches as many characteristics (i.e. climate, physiographic setting, catchment scale, etc.) as the ancient example. Davidson and North (2009) suggest using geomorphological regional curves from modern climatic and physiographic settings that are similar to the ancient example to aid in characterizing the size of the drainage basin and selection of modern analogs.

The Koppen-Geiger climate classification system can be used to assign a modern climate regime that approximates, as closely as possible, the paleoclimate of the formations in order to generate

a geomorphological regional curve ("regional curve"). Paleoclimatic interpretations for the Beluga and Sterling fms. (Wolfe, 1994; Reinink-Smith and Leopold, 2005; Chapter 3) can be used to bracket the Beluga and Sterling fms. between maritime temperate (*Cfc*) and continental subarctic (*Dfc)* climates. For reference, Anchorage, Alaska, is categorized as a continental subarctic (*Dfc)* climate. Once an appropriate climate classification has been chosen, modern rivers with gauge station data in similar climates and physiognomic settings as the ancient formation of interest are used to create the regional curve. A range of river catchment basin sizes and discharge values are used to construct regional curves on log-log graphs and a best-fit trend-line is fit to the data using a power law function (drainage area vs. bankfull depth; drainage area vs. bankfull discharge; Fig. 2.5; Table 2.1).

The summary statistics from the sand body calculations, particularly mean depth, are used in conjunction with the equation defining the trend-line from the drainage area versus bankfull depth to estimate drainage area. The best fit power law equation takes the form:

$y = a(x)^b$ Equation #5

The coefficients and exponents, a and b, are unique to each regional curve. The equation can be substituted to yield the equation:

$d = a(DA)^b$ Equation #6

where d is bankfull depth and DA is drainage area. Using the estimated drainage area, DA, from equation #6 above and the exponents a and b from the drainage area vs. bankfull discharge best-fit power law equation, discharge can be determined.:

$Q = a(DA)^b$ Equation #7

where Q is the discharge. Drainage area, discharge, climate, planform, and physiographic setting are then used to find the best corresponding modern analog (Davidson and North, 2009).

2.5 Facies and Facies Associations

Nine facies are recognized in the Beluga and Sterling fms. (Fig 1.6; Table 2.2). These facies define four facies associations (Table 2.3).

2.5.1 Facies Association I: Sandy Braided Channels

2.5.1.1 Description

FA-I consists of facies F-1, F-2a/b, F-3a/b, F-4, F-5, and F-6 (Figs. 1.6, 1.7; Tables 2.2 and 2.3). FA-I is an erosionally based, multi-story sand body that fines upward to mudstone and may be capped by coal (Fig. 2.7). This facies association is only observed in the Sterling Fm. A mean paleocurrent direction of ~197°, with low dispersion about the mean was measured from these sandbodies (Fig. 2.4). Individual stories are composed of coarse- to very fine- grained sand typically of uniform grain size, but locally they include upward-fining grain-size trends in the uppermost decimeters to few meters before being truncated by a scour surface or grading into mudstone or coal. Trough cross-bedding (F-2 a/b; Fig. 2.6B) and convolute bedding (F-6; Fig 1.8) are common. Convolute bedding (F-6; Fig. 2. 8) occasionally occurs over several meters of stratigraphic section and extends laterally across entire outcrops. Large-scale (>1m), planar-tabular cross-bedding (F-3a) is prominent locally. Trough cross-beds are bounded by small-scale erosional surfaces, medium-grained, plane parallel beds, large-scale (>1m) high angle planar tabular cross-beds. Trough cross-beds overlie erosionally-based lags of pebbles to boulders and wood casts. In some areas, large-amplitude (>1m), high-angle, planar tabular cross-beds can be

correlated laterally in one direction with medium-grained, plane parallel beds and in the other direction with trough cross-beds immediately overlying a scour surface. The bases of most sand bodies, and individual stories within multi-story sand bodies, display concave-upward scours, locally overlain by mudstone rip-up clasts and, less commonly, by extra-basinal granitic, metasedimentary and metavolcanic clasts (Fig. 2.7). Extra-basinal clasts up to 45 cm (apparent long dimension) may be present along scour surfaces and as isolated clasts floating in a sandy matrix. Mudstone rip-up clasts, up to boulder size, are present and rare mudstone clasts, up to several meters in apparent long dimension, are observed above some scour surfaces.

2.5.1.2 Interpretation

FA-1 is interpreted as unit bar, compound bar, and channel thalweg deposits of large, low sinuosity, sandy, braided streams. The common occurrence of trough cross-bedded sand bodies bounded by relatively small-scale erosional surfaces, upper flow regime plane beds, and large-scale, high-angle planar tabular cross-beds in association with trough cross-stratified sand bodies overlying erosional basal lags is consistent with features documented from modern and ancient sandy braided rivers (Cant and Walker, 1978; Blodgett and Stanley, 1980; Crowley, 1983; Miall, 1988 and 1994; Bridge, 1993; Bridge et al., 1998, Best et al., 2003; Miall and Jones, 2003; Skelley et al., 2003; Sambrook Smith et al., 2005; Bridge and Lunt, 2006; Sambrook Smith et al., 2006).

Trough cross-stratified sand bodies bounded by relatively small-scale erosional surfaces, upper flow regime plane beds, and large-scale high-angle planar tabular cross-beds are interpreted to represent migrating bar forms (Bridge, 1993; Bridge et al., 1998, Best et al., 2003; Miall and Jones, 2003; Skelley et al., 2003; Sambrook Smith et al., 2005; Bridge and Lunt, 2006; Sambrook Smith et al., 2006). Smaller-scale erosional surfaces are interpreted to represent migration of bars along the channel bed and coalescence of bars into compound bars (Bridge, 1993; Bridge

and Lunt, 2006). Upper flow regime planar laminated sandstones are interpreted as bar-top deposits. High-angle planar tabular cross-beds are interpreted as downstream accretion or lateral accretion surfaces that formed at active margins of bars (Bridge, 1993; Bridge et al., 1998, Best et al., 2003; Miall and Jones, 2003; Skelley et al., 2003; Sambrook Smith et al., 2005; Bridge and Lunt, 2006; Sambrook Smith et al., 2006).

Conglomerate lags on scour surfaces are interpreted as channel thalweg deposits (Allen, 1964, 1965a; Nanson 1980; Plint 1983). Sets of trough cross-lamination record migration of 3-D dunes along the beds of channels (Allen, 1963, 1965b; Elliott 1976; Plint 1983; Ashley, 1990). Multistory channel-fill deposits, reflect scouring within the channel during flood events and bar-form migration (Elliott, 1976; Gibling, 2006; McLaurin and Steel, 2007). The absence of root traces in sand bodies suggests that these channels experienced continuous flow conditions inhibiting colonization by plants or, alternatively, that channels migrated rapidly from place-to-place across the braidplain.

Convolute bedding in sand bodies may indicate high sedimentation rates leading to shearing of sediments by current drag while the sediments were still liquefied (Banks, 1973). The presence of convolute bedding over several meters of stratigraphic section and extending laterally across entire outcrops suggests more than a localized mechanism for generating these features (Fig 1.6D). Given the tectonic setting of this basin, it is intriguing to speculate that laterally and vertically extensive convolute beds composed of meter-scale, or larger, slump structures, deformed laminations, and load casts may have a seismogenic origin (Fig. 2.8; Owen, 1987; Neuwerth et al., 2006; Moretti and Sabato, 2007).

2.5.2 Facies Association II: Humid, Organoclastic Style Anabranching/Single Thread Channels

2.5.2.1 Description

FA-II consists of facies F-6, F-5, F-4 and rarely of F-2b and F-1 (Figs. 1.6, 1.9; Tables 2.2 and 2.3). A succession through FA-II is typically comprised of a single-story, medium- to very fine-grained sand body (F-6) that fines upwards to very fine-grained sand to silt and is encased in mudstone. Sand bodies are rarely multi-storied. Fining-upward sandstones in FA-II are typically poorly sorted and mud-rich. Sand bodies generally have a convex-up basal contact with rare mudstone rip-up clasts overlying a basal scour; extrabasinal clasts are rare at the base. Ripple cross-laminated sands (F-4) or wavy-laminated sands (F-4) are present locally, but are less common. The most striking feature of FA-II is the concave-up basal contact and flat-topped nature of the upper bounding contact. The sandy channel-fill is typically 2-5 m thick and encased in fine-grained mudstone. Where FA-II is extensively exposed, multiple, sandy channel-fills are typically present at, or near, the same stratigraphic level (Fig. 2.9).

2.5.2.2 Interpretation

FA-II is interpreted as laterally stable, ribbon sand bodies similar in facies and geometry to humid/organoclastic-style anabranching channels (Smith, 1976; Smith and Putnam, 1980; Smith and Smith, 1980; Eberth and Miall, 1991; Nadon, 1994; Nanson and Knighton, 1996; Makaske, 2001; North et al., 2007). FA-II is only found in the Beluga Fm.

The sand bodies of FA-II are interpreted to record deposition in single thread channels or, possibly, in anabranching channels. Regardless of plan-form geometry, these channel-fills were likely the product of a humid climatic setting (Reinink-Smith and Leopold, 2005; Chapter 3). In high-accommodation, aggradational settings characterized by frequent channel avulsions, anabranching and single thread channel-fills may create a very similar depositional record (North

et al., 2007). Given the presence of multiple channels at the same stratigraphic level, the humid/organoclastic-style anabranching interpretation is our preferred one.

Humid/organoclastic-style anabranching channels remain largely stable in position on the floodplain due to low stream power, low gradients, and high bank stability resulting from abundant silt, mud, and vegetation (Kirschbaum and McCabe, 1992; Tornqvist, 1993; Tornqvist et al., 1993; Nadon, 1994; Abbado et al., 2005; Guow and Berendsen, 2007). Humid/organoclastic-style anabranching channels are common in low-gradient systems containing abundant fine-grained material and high concentrations of suspended sediment (Smith 1983; Smith et al. 1989).

2.5.3 Facies Association III: Crevasse Splays and Crevasse Splay Complexes

2.5.3.1 Description

FA-III consists of facies F-4, F-5, F-6, F-7, and F-8 (Fig. 2.6, 1.10; Tables 2.2 and 2.3). A typical succession through FA-III is comprised of interbedded, relatively thin (decimeter to centimeter) sand beds (F-4, F-5, F-6), silt (F-7), and mudstone (F-8) with less common, small-scale (<2 m) channel-fill sand bodies (F-4, F-5, F-6; Fig. 2.11). Massive sandstones and siltstones (F-6, F-7) are common, but ripple cross-laminated sandstones and siltstones (F-4, F-5) are locally prominent, and trough cross-bedded sandstones (F-2) are rare.

Sand bodies are typically less than a meter thick and are interbedded with, decimeter scale siltstones and mudstones. Sand bodies are typically massive to ripple cross-laminated with sheet-like to lobate geometries. Root traces are locally present and the entire package of sand is typically encased in mudstone. However, in places an overall coarsening upward into a channel-fill sand of FA-I or FA-II is observed. FA-III is typically an overall fining-upward succession often culminating in a coal. Channel-fills of FA-III resemble those of FA-II, but they are significantly

smaller ($\leq$ 1 m), and comprised of massive sandstone (F-6) or ripple cross-laminated sandstone (F-4), with rare, trough or planar tabular cross-bedding (F-2 and F-3, respectively). FA-III is composed of thin sheet sand bodies that are lobate or elongate in plan view and lenticular along strike.

2.5.3.2 Interpretation

The distinguishing characteristics of this facies association are the laterally-extensive, decimeter-scale interbedding of sandstone and mudstone deposited by flow expansion and resultant loss of carrying capacity after floodwaters overtopped or breached natural levees (Fisk, 1944; Allen, 1965b; Elliott, 1974; Collinson, 1978; Bridge, 1984; Smith et al., 1989; Mjøs et al., 1993; Jorgensen and Fielding, 1996; Morozova and Smith, 2000). Associated channel-fills resulted from abandonment and preservation of crevasse channels feeding crevasse splays (Smith et al., 1989). Some researchers separate crevasse splays into two categories: 1) simple crevasse splays, and 2) large-scale composite crevasse splays (Elliott, 1974; Fielding, 1987; Smith et al., 1989; Mjøs et al., 1993; Smith and Pérez-Arlucea, 1994). Smith et al. (1989) have identified three stages of crevasse splay development. Crevasse splays in the Beluga and Sterling fms. typically resemble Stage I splays (Smith et al., 1989) that record initial crevasse formation on the trunk channel and consist of relatively thin sheet sand bodies lying directly on older floodplain sediments. Some Beluga Fm. splays resemble Stage II splays that evolve from stage I splays and consist of networks of active and abandoned channels (Smith et al., 1989). Stage III splays that capture the flow from the main channel during an avulsion are not observed in the Beluga and Sterling fms.

2.5.4 Facies Association IV: Floodplain

2.5.4.1 Description

FA-IV consists of facies F-5, F-6, F-7, F-8, and F-9 (Fig. 2.6, 1.11; Tables 2.2 and 2.3). A succession through FA-IV is composed of thick siltstone and mudstone beds, coal, and less commonly, fine- to very fine- grained sandstone (Fig. 2.11). Bioturbation is generally low or absent and, where present, it is represented by carbonized roots and burrows a few millimeters in diameter or less. Larger root traces are present locally, with diameters as large as a few centimeters. These typically extend as much as a few meters downward from a thick coal. Sedimentary structures are rare and, where present, include wavy laminations (F-5) and ripple cross-lamination (F-4; Fig. 2.12). Both sharp and gradational contacts separate FA-IV from underlying and overlying facies associations. FA-IV is commonly punctuated by one or more of the sandy facies associations (FA-I, FA-II, and FA-III), but FA-IV commonly fines upward from one of these sandy associations and, locally, coarsens upward toward the base of a sandy facies association (FA-II, FA-III).

Siltstones and mudstones are typically blocky to platy aggregates with less common laminated, wavy-laminated, and massive beds. Color varies from light grey to black. Organic components vary from sub-millimeter, finely macerated fragments to relatively large leaf impressions and vertically-oriented (growth position?) tree stumps. Rhythmically-laminated siltstone and silty claystone successions up to several meters thick are present locally and consist of alternating light- and dark-colored laminae ranging from sub-millimeter-scale to approximately one centimeter thick. Laminae are typically arranged in lamina sets to thin bedsets up to a few decimeters thick. These beds usually extend laterally the entire width of an outcrop.

Coal beds range from lignite to sub-bituminous and these commonly include splits of siltstone, claystone, carbonaceous mudstone, and volcanic ash (tonsteins; Flores et al., 2004). Ash layers

are typically disrupted and consist of randomly dispersed sub-millimeter- to millimeter-scale clusters of white to yellow crystals (feldspar and glass) and pumice fragments (Triplehorn et al., 1977; Reinink-Smith, 1995; Dallegge and Layer, 2004). Coals in the Beluga Fm. are of higher rank and quality than those in the Sterling Fm. (Merritt et al., 1987; Flores et al., 2004). They are also thicker, averaging approximately 39 cm with a maximum thickness of approximately 3.5 m. Coals in the Sterling Fm. are of lower rank (lignite) and quality (higher ash contents) and are thinner, averaging 31 cm with a maximum thickness of approximately 1.5 m.

2.5.4.2 Interpretation

FA-IV is interpreted as the record of deposition on low energy, poorly drained floodplains (Fig. 2.11). Vertically aggrading floodplain successions were primarily the result of suspension settling of fine-grained alluvium following floods in low-lying areas against a backdrop of steady subsidence. Interpretations for the locally coarsening-upward successions found in FA-IV are levee development near the margin of channel deposits and migration/avulsion of channels so that the floodbasins are progressively closer to higher-energy flood waters with greater sediment carrying capacity (Kraus, 1996; Heritage et al., 2001). Another possibility is that they represent splay delta deposits prograding into small floodplain lakes. Poor drainage and/or high aggradation rates are suggested by the lack of pedogenic features (e.g. well-developed peds, evidence of illuviation or eluviation, etc.), bioturbation, and pervasive rooted horizons.

Lacustrine intervals composed of siltstone and claystone with millimeter-thick undisturbed laminae in association with minor rippled sand and silt are common features in the deposits of small floodplain lakes and ponds (Talbot and Allen, 1996). These typically develop in topographic lows.

Organic-rich beds and coal seams are thought to record deposition in swamps, marshes, and mires removed from clastic input (Fielding 1987; Smith et al., 1989; Smith and Perez-Arlucea 1994). The thicker coal beds of the Beluga Fm suggest that conditions favoring peat accumulation persisted for long periods of time, possibly in raised mires, whereas the thinner, high-ash coals of the Sterling Fm. suggest deposition in shorter-lived, topogenous mires (Flores and Stricker, 1992; Flores et al., 2004). The presence of volcanic ash indicates common eruptions in the nearby volcanic arc. Scattered crystal clusters represent fragments of ash that were disrupted and dispersed by bioturbation (Reinink-Smith, 1995; Dallegge and Layer, 2004).

2.6 Channel Characteristics and Drainage Area and Discharge Constraints

2.6.1 Sterling Formation

Calculated average flow depths range from 8-13 m with maximum flow depths of 39 m (Table 2.4). Channel widths range between 113-286 m, with maximum widths of 1.9 km (Table 2.4). Typical width to thickness ratios (W/T) range between 14-21, with a maximum ratio of 51. These sand bodies are classified as medium width and medium thickness, with narrow sheet geometries (Gibling, 2006).

Paleocurrent measurements indicate a generally south-southwest (~197°) paleocurrent for the Sterling Fm., with low dispersion about the mean (~68°) (Table 2.4; Fig. 2.4). The circular arc and sine methods both generate fairly consistent sinuosities of ~1.1 from different exposures, suggesting that the Sterling Fm. was deposited in low sinuosity fluvial systems. The estimated drainage area for the Sterling Fm. is 415,000 km^2 and calculated bankfull discharge is 5,910 m^3/s (Table 2.1, Fig. 2.5).

2.6.2 Beluga Formation

Flow depths for channels in the Beluga Fm. range from 1-5 m, with an average flow depth of approximately 2 m. Channel width varies between 4 and 39 m, with an average width of ~11 m (Table 2.4). Width to thickness ratios vary between 3 and 9 with average W/T ratios of 5. These sand bodies comprise narrow to broad ribbon geometries using the classification scheme of Gibling (2006).

Paleocurrent indicators are difficult to obtain from the Beluga Fm. because grain size contrasts make sedimentary structures difficult to discern. Consequently, flow direction is poorly constrained in this formation. However, based on the size of channel sand bodies, the locations of exposures, and overall basin geometry, it seems reasonable to suggest that fluvial systems in the Beluga Fm. flowed toward the basin center from the margins (Swenson, 2002). The estimated drainage area for individual channels within the Beluga Fm. is 15,000 km^2 and bankfull discharge is calculated at 700 m^3/s (Table 2.1, Fig. 2.5).

2.7 Alluvial Architecture

Laterally continuous exposures allow a two-dimensional architectural analysis of the upper part of the Beluga Fm. and of the Sterling Fm., facilitating more accurate interpretations of fluvial style. In our analysis we integrate measured stratigraphic sections with interpreted photomosaics to aid in understanding lateral facies variations and their vertical stacking patterns. Outcrop orientation and paleocurrent data (where available) are shown on each photomosaic. Four architectural element associations (AE) are identified: 1) narrow sheets, 2) narrow ribbons, 3) crevasse splays and splay complexes, and 4) overbank successions. These four element associations correspond to facies associations outlined in the previous section. In this section we present information that allows inferences regarding the three-dimensional geometries of these deposits.

2.7.1 Architectural Element Association I: Narrow Sheets

2.7.1.1 Description

Sandy braided channel-fills of FA-I combine to build narrow sand sheets of AE-I (Fig. 2.13; Table 2.5, and 2.6; Gibling, 2006). AE-I is the dominant architectural element association in the Sterling Fm. Exposures of this element association are oriented slightly oblique to the mean paleocurrent direction of 197° (Figs. 1.4). AE-I is comprised of several smaller architectural elements, including sandy bedforms (SB), accreting bedforms (AB), scour-fill (SF), downstream accretion units (DA; Fig. 2.14), and laterally accretion units (LA; Fig. 2.15).

Three surfaces of different order are observed in AE-1. First-order surfaces bound individual stories. Sand bodies include as many as three stories. Second-order surfaces bound bars within individual channel-fills. Some second-order surfaces dip downstream and others dip at an oblique angle to paleocurrent. Third-order surfaces are within individual bar forms and occur as low-relief scours. These third-order surfaces are commonly oriented at high angles to paleocurrent and exposures oriented close to depositional strike typically have a complex internal organization. Scours at the base of the sand bodies may result in sand-on-coal contacts (Fig. 2.7; LePain et al., 2009).

Trough (F-2) and planar tabular (F-3) cross-bedding with subordinate horizontal laminations (F-5) bounded by second-order surfaces comprise larger-scale bar forms. Two types of bar forms are present: unit bars (Sambrook Smith et al., 2006; 'cross channel' bars of Cant and Walker, 1978) and compound bars (Cant and Walker, 1978; Ashworth et al., 2000; Sambrook Smith et al., 2005). Unit bars are less common and are composed of a few low-relief, internal erosion surfaces and one set of large-amplitude, planar tabular cross-bedded sands (F-3a) bounded by a second order surface. Solitary sets of large-scale planar cross-bedding of elements DA and LA

bound the cores of unit bars on downstream and lateral margins (Miall, 1994).Compound bars are bounded by second-order surfaces and include multiple, low-relief, internal erosion surfaces (third-order surfaces) that bound sets of large-scale planar cross-beds (F-3a) (Fig. 2.13). As unit bars coalesce into compound bars, DA and LA surfaces may be preserved within the compound bar as well as at the margins.

Mean paleocurrent direction allows recognition of downstream accretion (DA; Fig 1.14) and lateral-accretion (LA; Fig. 2.15) elements, and the larger scale of these elements allows their distinction from sandy bedforms (SB) and accreting bedforms (AB), which form the cores of unit bars (*sensu* Enyon and Walker, 1974; Ashworth et. al., 2000; Moreton et al., 2002; and Best et al., 2003). In some areas, horizontally-bedded sand (AB) can be traced downstream into large-scale planar cross-bedded sand (DA). Figure 1.14 shows a distinct unit bar that is interpreted to form part of a compound bar. The core of this unit bar consists of trough cross-bedded sand (SB) that grades downstream to large-scale, planar cross-bedded sand (DA).

2.7.1.2 Interpretation

The majority of the architectural element associations found in braided channels are sandy bedforms (SB) formed by dunes, followed in abundance by lateral accretion surfaces (LA), downstream accretion surfaces (DA), minor vertical accretion deposits (VA), and minor scour fills (SF). Paleocurrent direction and sinuosity calculations indicate that the Sterling Fm. is composed of southward-flowing, low sinuosity fluvial deposits, consistent with a sandy braided fluvial interpretation.

Large scale (~ a few meters in amplitude) downstream (DA) and lateral accretion (LA) elements are attributed to cross-channel bar migration into anabranches or expanding flow over the barhead that results in deposition at bar-margin avalanche faces (Best et al., 2003; Sambrook

Smith et al., 2005; Bridge and Lunt, 2006; Sambrook Smith et al., 2009). These accretion surfaces are documented from modern studies of large, low-sinuosity sandy braided systems, such as the Jamuna and Parana rivers (Best et al., 2003; Sambrook Smith et al., 2005; Sambrook Smith et al., 2009) and moderate to smaller sandy braided systems, such as the South Saskatchewan, Wisconsin, and Niobrara rivers (Skelly et al., 2003; Sambrook Smith et al., 2006; Mumpy et al., 2007; Sambrook Smith et al., 2009).

Sandy bedforms (SB) that are not bounded by upper flow regime VA (vertically accreting), DA and LA surfaces and are stratigraphically above the highest-order bounding surface are interpreted as dunes that migrated in the channel thalweg. The majority of sandy bedforms (SB) comprise dunes that stack to form complex successions of depositional and/or erosional events termed unit bars (Miall, 1977; Smith, 1978; Bridge and Lunt, 2006), with individual unit bars forming compound bars (Miall, 1977; "sand flats" of Cant and Walker, 1978; Smith, 1978; "sand shoals" of Allen 1983; and large- and medium- scale dunes of Best et al., 2003; Bridge and Lunt, 2006). Some researchers have distinguished the deposits of "bar cores" and "bar margins" (Eynon and Walker, 1974; Ashworth et al., 2000; Moreton et al., 2002; Best et al., 2003), although Bridge and Lunt (2006) note that 'there may be gradations between the core and margins of both unit and compound bars.' The deposits of simple, non-coalesced, unit bars in the Sterling Fm. tend to have clear distinctions between the core, composed of sandy bedforms(SB), and the bar margin, composed of steeply dipping beds. Vertical accretion (VA), upper flow regime, horizontal beds can be traced into adjacent steeply dipping beds with a core of sandy bedforms (SB) forming a unit bar (Fig. 2.14). However, the majority of preserved bars in the Sterling Fm. are compound bars composed of multiple unit bars. In these cases, distinguishing unit bar cores and margins in the overall compound bar is difficult, as the scale of an outcrop is typically smaller than the scale of an entire compound bar.

A partial compound bar, composed of at least two unit bars with lateral accretion (LA) surfaces is shown in Figure 1.15. The outcrop is oriented oblique to paleocurrent and allows one of the better near-strike views of fluvial architecture in the Sterling Fm. Separating the unit bars is an erosional surface with low relief that is overlain by a minor scour fill. The cores of the individual unit bars are composed of sandy bedforms (SB) that are fairly easy to identify, as is the bar margin, which has steeply-dipping lateral accretion surfaces (LA). These features are consistent with observations from modern sandy braided rivers (Best et al., 2003; Skelly et al., 2003; Sambrook Smith et al., 2005; Mumpy et al., 2007; Sambrook Smith et al., 2009) and depositional models of sandy braided deposits (Best el al., 2003; Bridge and Lunt, 2006).

2.7.2 Architectural Element Association II: Narrow Ribbon

2.7.2.1 Description

Muddy sand channel-fills of FA-II comprise AE-II whose width-to-thickness ratios correspond to Gibling's (2006) broad to narrow ribbons (Fig. 2.15). Ribbon sands of AE-II are always encased in flood plain siltstones and mudstones, and typically have widths ranging from 20 - 200 m and thicknesses from 2 - 5 m. AE-II is typical of the Beluga Fm., but persists up-section into the transition zone with the Sterling Fm. AE-II is typically comprised of apparently massive sand, but where sedimentary structures are visible, it consists mostly of two sub-elements: – sandy bedforms (SB) and scour fills (SF). Figure 1.15 shows broad channel-fills of AE-II encased in siltstones and mudstones. Note that more than one channel-fill is present at or near the same stratigraphic level. This is an important characteristic of AE-II.

2.7.2.2 Interpretation

Ribbon sand bodies of AE-II are interpreted to record deposition in single thread channels that may have been similar in plan-form geometry to anabranching channels (Fig. 2.10; Nadon, 1994;

Nanson and Knighton, 1996; North et al., 2007). Single thread, non-anabranching rivers could create similar deposits if: 1) large accommodation space was available due to high rates of subsidence; 2) sediment supply was mud-rich; and 3) frequent avulsions occurred (North et al., 2007). The first two of these have been documented for the Beluga Fm. (Haeussler and Saltus, 2011; Helmold et al., In Review; Chapter 4). Avulsion frequency is unconstrained in Cook Inlet basin during Late Miocene time when the Beluga Fm. and transition zone of the Sterling Fm. were deposited.

Anabranching channel patterns are difficult to document in the ancient record, and we cannot unequivocally demonstrate their presence during deposition. However, the presence of multiple sand bodies at the same stratigraphic level separated by floodplain deposits suggests that stable floodplain "islands" were present between coeval channels (Nadon, 1994; Flaig et al., 2011). This suggests a system of anabranching channels. Multistory ribbon sand bodies are present locally, but they are less common. The multi-storied sand bodies probably developed due to the relatively strong coherence of the floodplain material, making erosion and reoccupation of previous channels more likely (North et al., 2007). The rarity of multi-story channels in the Beluga Fm. may be due to the mud-rich matrix of the sands creating a substrate nearly as coherent as the surrounding mudstones, thus making erosion of the floodplain and previously occupied channel deposits almost equally likely (Helmold et al., In Review; Chapter 4).

2.7.3 Architectural Element Association III: Crevasse Splays and Crevasse Complexes

2.7.3.1 Description

The vertical and lateral juxtaposition of minor sheets (MS), minor lenses (ML), and interlaminated mixed sheets (IM) characterizes this architectural element association. Distinguishing characteristics of this architectural element association include sand that is interdigitated with

fine-grained material. In rare cases, minor sheets and lenses can be traced laterally into a larger channel sand (AE-I, AE-II) but, more commonly, these thin sands can be traced laterally until they fine and interfinger with the overbank architectural element association (AE-IV). Figure 1.16 depicts crevasse splay and crevasse complex architectural element several tens of meters thick primarily composed of interlaminated mixed sand, silt and mud sheets, minor sand sheets, and floodplain fines with relatively thin coals.

2.7.3.2 Interpretation

Smith et al. (1989) and Perez-Arlucea and Smith (1999) show that crevasse splays are typically not single events but, rather, they form as a result of a complex process. Crevasse splays observed in the Beluga Fm. are similar to stage II crevasse "splay complexes" (Smith et al., 1989) that evolve from simple sand lobes adjacent to trunk channels. This interpretation is supported by the numerous sheet sands and lenses interfingering with the overbank architectural element association (AE-IV; Fig. 2.16). Crevasse splays in the Sterling Fm. are predominantly simpler stage I splays and are less common than those in the Beluga Fm.

2.7.4 Architectural Element Association IV: Overbank

2.7.4.1 Description

The overbank architectural element association consists mainly of silt-mud sheets (SMS) (Fig. 2.17; Tables 2.5 and 2.6). This architectural element association is also associated with the presence of coal in beds up to several meters thick. The silt-mud interlaminated sheets are tabular and are typically several meters thick.

2.7.4.2 Interpretation

The overbank architectural element association is composed of several different sub-environments including floodplains, lakes, and peat swamps (Tables 2.5 and 2.6; Fig. 2.17). The thick coal, lacustrine, and floodplain deposits suggest stability on parts of the floodplain that received little sediment for long periods of time.

2.8 Geomorphological Regional Curves and Analog Matching

A range of options must be considered when choosing modern analogs for ancient fluvial systems as no single modern river fits exactly. With respect to climate, drainage area, and discharge, the Fraser and Columbia rivers are close matches to the river systems in the Sterling Fm. In terms of climate and physiographic setting, the Susitna River is the closest match to the Sterling Fm., but it is too small and may not be of predictive value with respect to reservoir architecture. The closest analogs to the Sterling Fm., with respect to planform style, basin scale, and discharge, are the smaller Platte River and the much larger Brahmaputra River. Therefore, the best rivers to use for predictive value from a reservoir architecture perspective are the Platte and Brahmaputra Rivers.

A range of potential options also exists for the Beluga Fm. The closest analog with respect to climate, drainage area, discharge and physiographic setting is the Chulitna River that drains into the modern Cook Inlet basin. In terms of climate, drainage area, discharge, and planform geometry, the Cumberland Marshes region of the Saskatchewan River, Canada, is a good candidate. The best analog for understanding reservoir architecture is likely the organic, humid-style anabranching (anastomosing) channels and floodplains of the Cumberland Marshes.

2.9 Discussion

2.9.1 Fluvial Style

2.9.1.1 Sterling Fm.

The Sterling Fm. is primarily composed of sandy braided channels (FA-I) that are defined by narrow sand sheets with the following sub-elements: sandy bedforms, accreting bedforms, and scour fills (Figs. 1. 6, 1.7, 1.13, 1.14, 1.15; Table 2.2, 2.3, 2.4, 2.5, 2.6; Cant and Walker, 1978; Blodgett and Stanley, 1980; Crowley, 1983; Miall, 1988 and 1994; Bridge, 1993; Bridge et al., 1998, Best et al., 2003; Miall and Jones, 2003; Skelley et al., 2003; Sambrook Smith et al., 2005; Bridge and Lunt, 2006; Sambrook Smith et al., 2006). Crevasse splays, crevasse splay complexes (*sensu* Smith et al., 1989) and floodplains also occur, but they are less common than channels, and are only locally important. Paleochannel depths range between 8-13 m and average channel width varies from 113-286 m (Table 2.4). Paleocurrent measurements are generally southward with a mean of 197° and low to moderate dispersion about the mean. Calculated sinuosities are low (~ 1.1), both at individual exposures and within the formation as a whole (Fig. 2.4).

Realistic constraints can be placed on the size, discharge, and drainage area of ancient fluvial systems using geomorphological regional curves based on modern rivers that occur in similar physiographic and climatic settings (Davidson and North, 2009). Fluvial channel dimensions determined from sand body geometry and basin area and discharge characteristics calculated from geomorphological regional curves indicate that paleo-channels in the Sterling Fm. were probably larger than the South Saskatchewan and Platte rivers but smaller than the

Brahmaputra/Jamuna River. This puts the streams that comprise the Sterling Fm. in the somewhat subjective category of 'medium-sized' sandy braided rivers.

Sambrook Smith et al. (2005) postulate that a single universal facies model for sandy braided rivers will remain elusive. While sandy braided systems exhibit both scale-dependent (e.g. bar planform width : depth ratio and scour depth) and independent features (e.g. trough stratification associated with dune migration), significant differences exist in the occurrence and abundance of other facies, most notably high-angle planar cross-stratification or low-angle stratification (Sapozhnikov and Foufoula-Georgiou, 1996, 1997; Foufoula-Georgiou and Sapozhnikov, 1998, 2001; Sapozhnikov et al., 1998; Sambrook Smith et al., 2005; Kelly, 2006). This is likely controlled by a number of factors including discharge, flow regime, local bar and channel topography, anabranch width:depth ratio, and type and abundance of vegetation (Sambrook Smith et al., 2005).

Based on measured and calculated parameters in this study (e.g. channel depth, discharge, width:depth ratio) the Sterling Fm. is dominated by medium-scale sandy braided rivers. High-angle planar strata in the Sterling Fm. that extend, from bar top to the thalweg, are more than a few meters in height, and extending laterally from 10s to a few 100s of meters are relatively common, suggesting that these bars migrated extensively and were fairly long-lived (Sambrook Smith et al., 2005). These features have not been reported in studies of the Calamus River, a relatively small braided river, but they do constitute a significant component of the South Saskatchewan and Brahmaputra/Jamuna rivers (Sambrook Smith et al., 2005). This supports the assertion that no universal facies model is likely to apply to all braided rivers, given that different scales of fluvial systems exist. Practically speaking, two or more facies models may be necessary to adequately characterize any given deposit.

Bridge and Lunt (2006) have developed process form models that characterize braided rivers based on studies of modern rivers and experimental work. Their sandy braided model provides several views of fluvial architecture including: 1) an along-stream section across a compound bar; 2) a cross-stream section through a compound bar; 3) a cross-stream section through a confluence scour; and 4) typical vertical sedimentological logs through compound bars and channel-fills. In general there is good agreement between the process form model of Bridge and Lunt (2006) and the Sterling Fm. For example, using the Bridge and Lunt (2006) model *a priori,* we can identify a cross-stream view of a compound braid bar in a downstream cross-sectional view (Fig. 2.13). When paleocurrent data are included, the interpretation of a compound braid bar is even more definitive because downstream accretion (DA) can be demonstrated.

Upper flow regime planar strata are generally lacking in exposures of the Sterling Fm. and, where observed, are only present in the bar top region of compound bars and unit bars. These planar strata can sometimes be traced into lateral or downstream accretion surfaces at or near the angle of repose (Fig. 2.14). The paucity of upper-stage planar strata may be explained by subsequent erosion and migration of bars, decreasing their upstream preservation potential (Skelly et al., 2003; Sambrook Smith et al., 2006). Alternatively, vertical accretion under upper flow regime conditions may not have been common.

2.9.1.2 Beluga Fm.

The Beluga Fm. is composed of humid, organoclastic-style anabranching/single thread channels. The channel systems contain the following sub-elements: ribbon sand channel-fills with minor sandy bedforms, scour-fills and sheet sands. Crevasse splay, crevasse splay complexes, and floodplains encasing sand bodies are common throughout. Sand bodies are small, between 1 and 5 meters with an average of 2 meters, and channel widths range from 4 to 39 m. Ribbon-like single channel morphologies are exposed in outcrop.

No single exposure allows views of the geometric expression of convergent and divergent channel-fills, or other means of testing for interconnected channel-fill (i.e. high-resolution age control, ground penetrating radar, or pressure communication) forming the anabranching style. However, several channel-fills do occur at or near the same stratigraphic level (Fig. 2.10), and many authors have suggested that this may indicate contemporaneous flow in ancient fluvial units (Nadon, 1994; Plint et al., 2001; Flaig et al., 2011). Since it is very uncommon to actually demonstrate a multi-channel plan view in the ancient record, interpretations of anabranching fluvial systems may be under-represented (Nadon, 1994; Makaske, 2001).

Comparing the Beluga Fm. to recent work on facies models in dryland anabranching rivers is instructive. Based on modern observations of dryland anabranching rivers, North et al. (2007) suggest dividing anabranching rivers into dryland and humid classes. If the Beluga Fm. truly is an anabranching fluvial system, the sedimentary record differs from the typical humid and dryland styles. Vertical stacking of channel bodies is thought to be common in humid-style anabranching rivers because of the relatively high cohesion contrast between channel bodies and floodplain sediments (Mohrig et al., 2000; Makaske et al., 2002; North et al., 2007). Levee deposits are also thought to be prominent in humid anabranching deposits (Smith and Smith 1980; Smith 1983; Makaske, 2001; North et al., 2007), leading to frequent avulsions and crevasse splay deposits. However, this is not universal. Several studies have interpreted facies relationships similar to those seen in the Beluga Fm. as anastomosing fluvial deposits (Nadon 1994; Plint et al., 2001; Flaig et al., 2011).

Outcrop expression of sand bodies in the Beluga Fm. may be subdued due to the high mud content, which renders individual channels may be difficult to detect. The mud-dominated nature of Beluga Fm. deposits is probably due to sediment provenance, as sediment on the Kenai

Peninsula is shed from the accretionary prism composed of weakly to moderately metamorphosed deep marine deposits (Rawlinson, 1984; Swenson, 2002; Helmold et al., In Review). This may, in part, explain the departure from classic humid anabranching (anastomosing) facies models. North et al. (2007) found similar issues with channel recognition in their summary of dryland anabranching systems. However, paleoclimate data clearly place the Beluga Fm. in a humid depositional environment (Wolfe, 1994; Reinink-Smith and Leopold, 2005). Consequently, Beluga Fm. rivers have characteristics similar to both humid and dryland anabranching systems and we suggest that sediment type is at least as important as climate in determining alluvial architecture and facies relationships in anabranching systems.

2.9.2 Controls on Fluvial Style

Flores and Stricker (1993) suggest that the Sterling Fm. evolved from low sinuosity braided to high sinuosity meandering systems. Interestingly, we find no appreciable change in fluvial style in the middle to lower Sterling Fm. as previously reported by Flores and Stricker (1993). One reason for this discrepancy is that they may have been comparing stratigraphic units of different ages in the absence of a high-resolution chronostratigraphic and biostratigraphic framework (Dallegge and Layer, 2004; Reinink-Smith, 2010). Without a chronostratigraphic framework it is impossible to adequately evaluate the stratigraphic position of widely dispersed exposures that are typically separated by high angle faults in Cook Inlet basin. In addition, we document southerly paleoflow data and channel geometries that demonstrate low sinuosity (~1.1), and some high-angle cross beds in the formation indicate downstream accretion typical of braided fluvial deposits (Figs. 1.4, 1.14; Bridge and Lunt; 2006).

On the Kenai Peninsula, the Beluga and Sterling fms. are conformable and the contact is transitional, typified by sheet sands of crevasse splays and crevasse splay complexes. Evidence of sandy braided channel forms occurs a short distance, ~20 m, above this transition. The

difference in fluvial style between the humid organic-style anabranching/single thread Beluga Fm. and the sandy braided Sterling Fm. is striking. The sediment source for the Beluga Fm. on the east side of the basin (i.e. the accretionary prism; Helmold et al., In Review; Chapter 4) would have still been present during deposition of the Sterling Fm., yet the axial fluvial sandy braided system is the principal component of the sedimentary record during deposition of the Sterling Fm.

Fluvial style is primarily controlled by base level, climate, and tectonics, and their effect on sediment supply (Blum and Tornqvist, 2000). Base level is not well constrained in Cook Inlet basin. Global sea-level curves indicate that sea level may have been falling during the Neogene (Miller et al., 2005), but global sea -level curves are not likely to be of much use in a relatively dynamic plate margin setting such as southern Alaska. There are no regional studies of Neogene sea level fluctuations in the vicinity of the Cook Inlet basin.

In most fluvial settings, base level changes are transmitted less than ~200 km updip (Miall, 1997). Only in extreme cases, in low-gradient settings, are the effects of base-level fluctuations transmitted farther upstream (Blum and Tornqvist, 2000). The Beluga and Sterling fms. do not contain any documented evidence of marine or brackish conditions and are completely terrestrial in the southern-most exposures. Paleoshoreline position is unconstrained but, in any case, the effects of any base-level fluctuations were not likely to be transmitted hundreds of km up-dip (Miall, 2006).

A paleoclimatic control on fluvial style is unlikely. Mean annual temperatures were gradually declining, from ~12° C to ~8° C (Wolfe, 1994; Reinink-Smith and Leopold, 2005), and precipitation was fairly consistent, averaging ~400 to 1100 mm/year, except for ~8 Ma when precipitation was higher and more variable with an average of ~1500 mm/year (Chapter 3). The taxonomic composition of the vegetation, as determined from fossil pollen and leaf margin

analysis (Wolfe, 1994; Reinink-Smith and Leopold, 2005; Chapter 3), did not change considerably between the deposition of the Beluga and Sterling fms. (Reinink-Smith and Leopold, 2005; Chapter 3) and, in any case, the documented temperature and precipitation changes are unlikely to have been of sufficient magnitude to have affected sediment supply in any significant manner (Blum and Tornqvist, 2000; Huggett, 2007). The change in fluvial style at the Beluga-Sterling boundary, is therefore, unlikely to have resulted from climatic changes.

Tectonic controls are the most likely cause for the observed changes in depositional style. Ongoing, flat-slab subduction of the Yakutat microplate resulted in exhumation of the central and western Alaska Range, either progressively (Finzel, 2010) or in pulses at ~24 Ma and ~6 Ma (Haeussler et al., 2008; Benowitz, 2011). Recent experimental work by Connell et al. (2012a, b) models the interactions of axial fluvial and transverse fluvial systems in an aggrading basin. Their findings suggest that whether axial or transverse systems dominate the basin is controlled by the relative sediment flux ("flux steering") being contributed to the system. When relative sediment flux was highest in the axial fluvial system, these rivers dominated the experimental basin. In contrast, when relative sediment flux was highest in the transverse fluvial systems, these rivers dominated the experimental basin, and were less influenced by the location and rate of subsidence.

Connell et al. (2012a, b) further suggested that their experimental results should be applicable to the sedimentary rock record. We propose, therefore, that during deposition of the Beluga Fm., sediment supply was dominated by erosion from the accretionary prism on the eastern side of the basin. It also seems likely, based on fluvial dimensions, aggradation rates and basin geometry that transverse streams flowed from the Kahiltna Assemblage on the western side of the basin toward the basin center although we cannot rule out the possibility that some Beluga rivers crossed the entire basin from east to west. As a result, we propose that the margins of the basin

were dominated by the small, transverse fluvial systems documented from the Beluga Fm. rather than by any record of larger axial fluvial systems. While it seems likely that some sort of axial fluvial system must have existed in Beluga time, the sediment flux rate at the basin margins was high enough that only transverse fluvial systems are preserved in outcrop.

As the western and central Alaska Range was exhumed (Haeussler et al., 2008; Finzel, 2010; Benowitz, 2011), the resulting sediment was deposited in axial fluvial braided rivers of the Sterling Fm. Dallegge and Layer (2004) calculated sediment accumulation rates for the Beluga and Sterling fms. that are not statistically different from each other. Consequently, a tectonically driven change in the amount and source of sediment near the Beluga-Sterling boundary provides a plausible explanation for the observed changes in fluvial style. If smaller transverse fluvial systems flowed from the basin margins, their sedimentary record was overwhelmed by the axial fluvial system dominating the basin during a period of high sediment flux (Connell et al., 2012a, b). This increase in sediment flux may be attributed to orogen scale changes in the Aleutian-Alaska Range leading to stream capture and increase discharge and sediment supply during deposition of the Sterling Fm. (Leckie and Craw, 1995; Craw and Leckie, 1996).

2.10 Conclusions

Detailed facies analysis, architectural analysis, and analog matching provide a new interpretation of the depositional setting of the Beluga and Sterling fms. The Beluga Fm. was deposited in a humid/organoclastic-style anabranching (anastomosing)/single thread system with average flow depths of two meters and channel widths of 11 m. Deposition of the Beluga Fm. on the eastern side of the Cook Inlet basin was west-directed while, on the western side of the basin, deposition was probably east-directed. No axial fluvial system is preserved at the basin margins. From a reservoir architecture perspective, the Cumberland Marshes region of the Saskatchewan River is a likely analog to the Beluga Fm.

The Sterling Fm. was deposited in low-sinuosity sandy braided streams with flow depths 8-13 m and channel widths of 113-286 m. Paleocurrent measurements suggest that axial fluvial braided rivers flowed southward from the volcanic and magmatic arc. The best modern analogs for a medium-sized braided fluvial system such as the Sterling Fm. ranges between the Platte River and the Brahmaputra River.

The Beluga and Sterling fms. provide insights on the tectonic development of southern Alaska during the Late Miocene to Pliocene. The forearc basin underwent significant changes in fluvial style between deposition of the Beluga and Sterling fms. Climate is relatively well constrained with gradually declining temperatures (≥ 10°C) and average mean annual precipitation of ~1100 mm a^{-1} (minimum value of 420 mm a^{-1}, maximum of 3900 mm a^{-1}; Chapter 3) with modest fluctuations in precipitation. Palynomorph assemblages from floodplain and lake deposits record a vegetational community composed primarily of shrubs, *Alnus*, and herbaceous plants with relatively sparse trees and open canopy conditions (Chapter 3). Coal swamps had denser tree populations (Reinink-Smith and Leopold, 2005). Modest changes in temperature, precipitation and floral communities do not seem to be of sufficient magnitude to effect depositional systems (Blum and Tornqvuist, 2000).

Base level fluctuations are not constrained regionally. However, the gradient of modern braided rivers is typically high so that base level changes should not have propagated very far upstream. Also, given the time-stratigraphic nature of sediment deposition, changes appear to have occurred in the hinterland (western Alaska Range) and progressed downstream. Tectonic changes in the hinterland are the likely cause for fluvial style change. The documented change in fluvial style between the Beluga and Sterling fms. is attributed to ongoing deformation in the western Alaska Range due to flat-slab subduction of the Yakutat microplate.

2.11 Figures

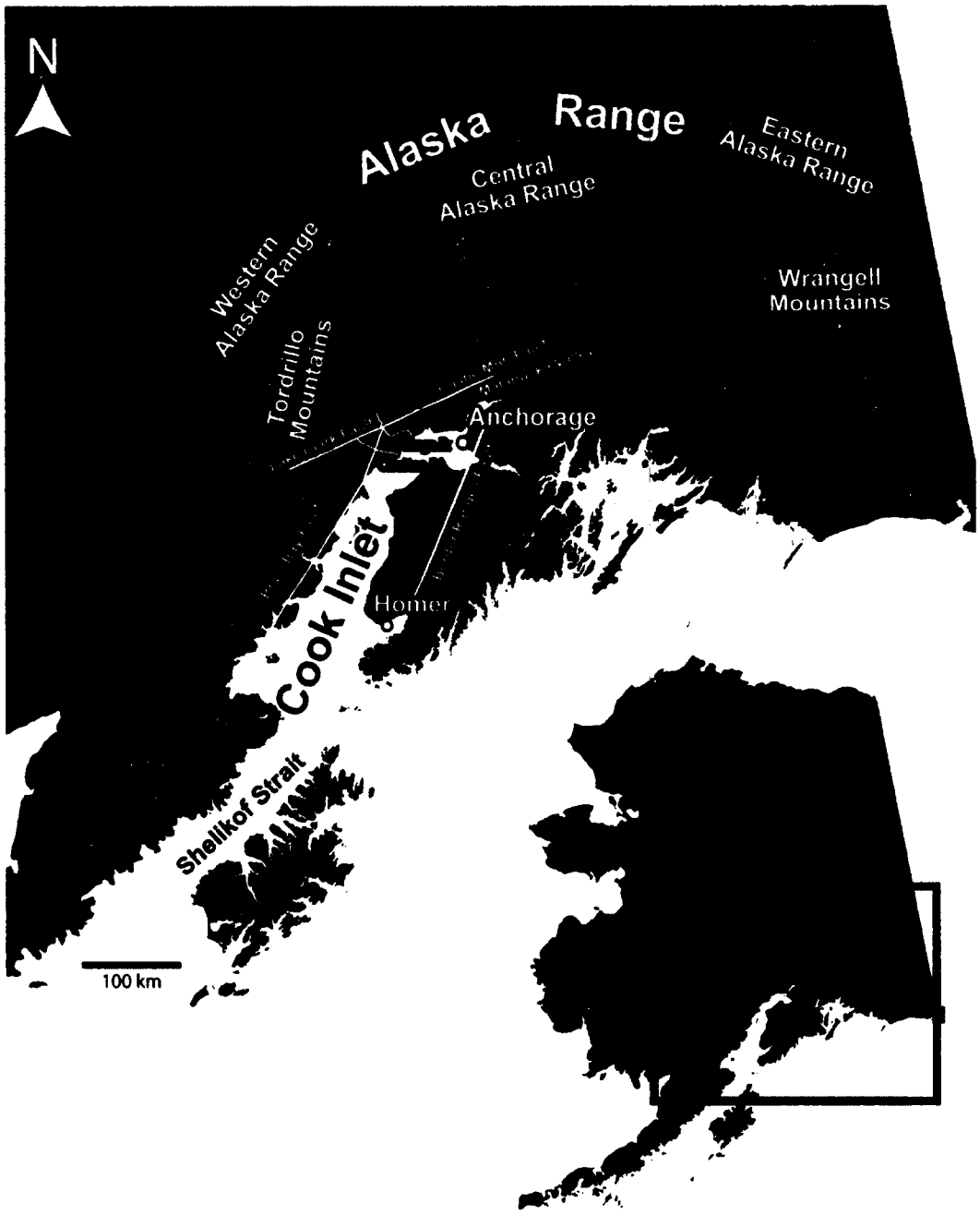

Figure 2.1: Digital elevation model (DEM) depicting the physiographic setting of south-central Alaska. Cook Inlet is on the western margin of a forearc basin that extends from Shelikof Strait to the Wrangell Mountains. Exposures of the Beluga and Sterling formations are found on the Kenai Peninsula near the town of Homer and on the western side of Cook Inlet west of Anchorage.

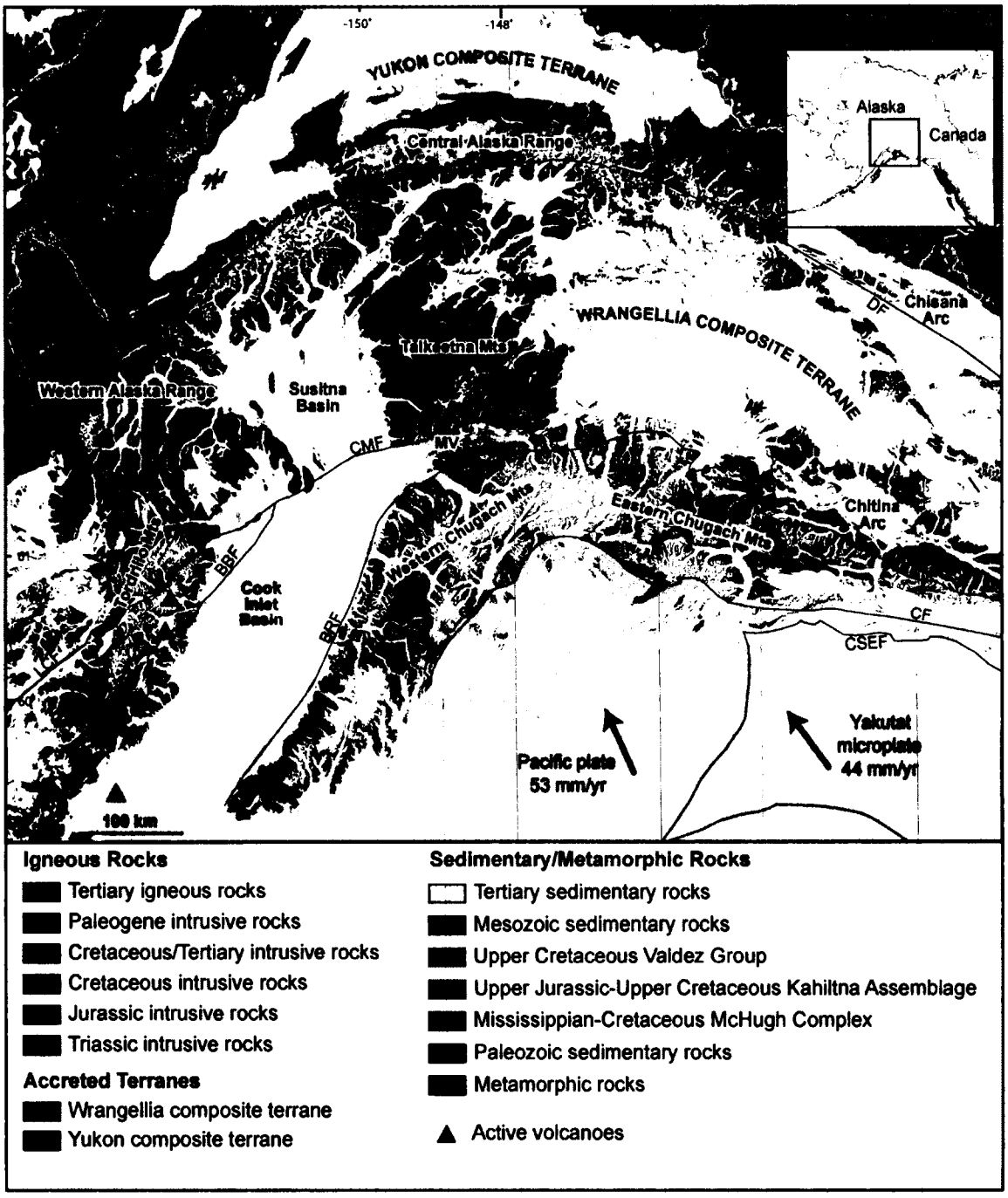

Figure 2.2: Simplified geologic map of southern Alaska showing arc region (western and central Alaska Range, Talkeetna Mountains), retroarc region (Yukon composite terrane), eastern region (Matanuska Valley (MV), western and eastern Chugach Mountains, Chisana and Chinitna arc) of the forearc basin. Arrows depict relative plate motions of the Pacific Plate and Yakutat Microplate. Major faults in the area are also shown: CSEF – Chugach-St. Elias Fault; CF – Contact Fault; BRF – Border Ranges Fault; BBF – Bruin Bay Fault; CMF – Castle Mountain Fault; LCF – Lake Clark Fault; DF – Denali Fault. Modified from Finzel (2010); Beikman (1980), Moll-Stalcup (1994), Greninger et al. (1999).

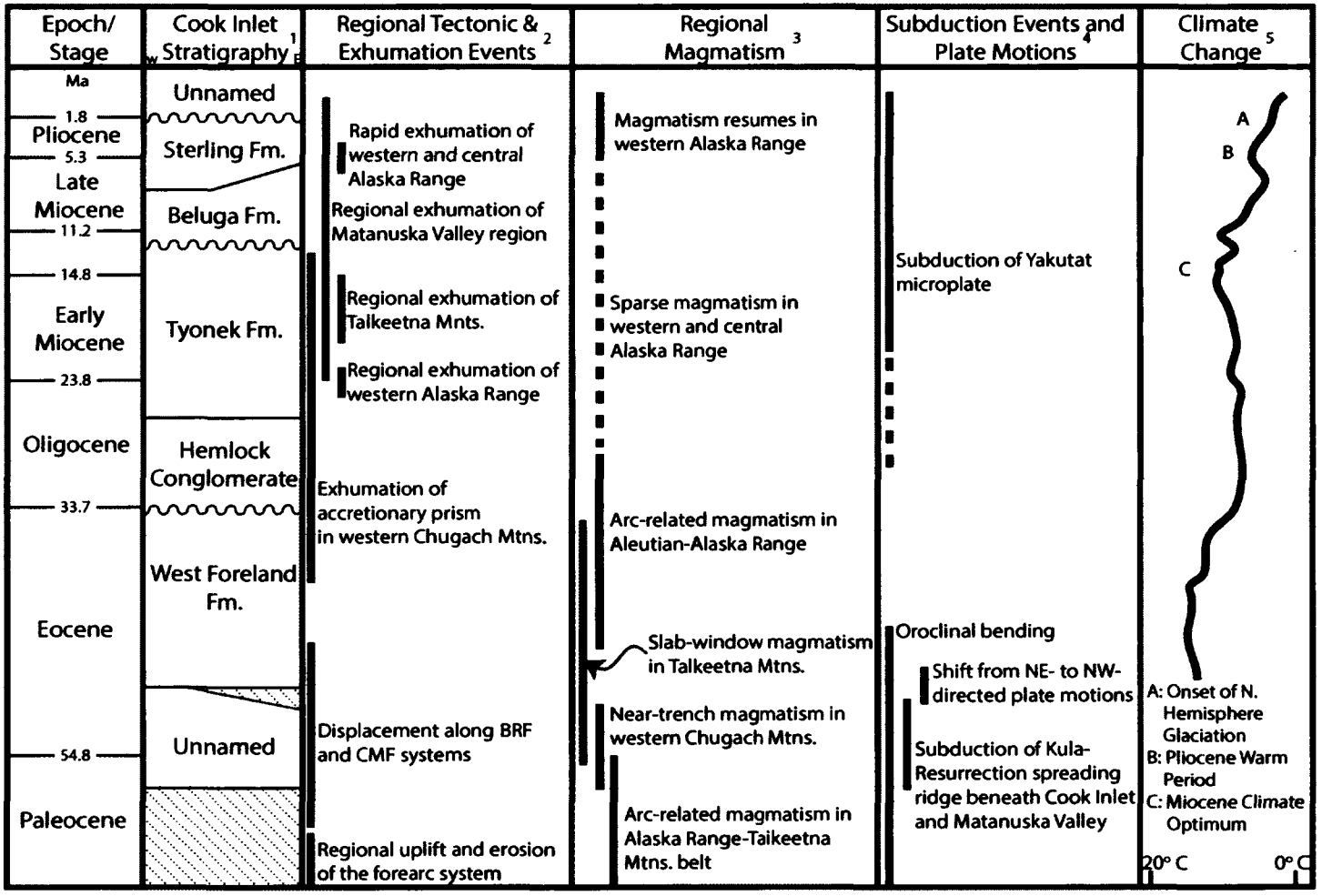

Figure 2.3: Age-event diagram for the Cenozoic Cook Inlet strata (Modified from Finzel, 2010). 1) Stratigraphy, from Flores et al., 2004; 2) Regional Tectonic and Exhumation Events, compiled from Fuchs, 1980; Little and Naeser, 1989; Fitzgerald et al., 1995; Pavlis and Roeske, 2007; and Haeussler et al., 2008; 3) Regional Magmatism, compiled from Moll-Stalcup, 1994; Plafker et al., 1994; Bradley et al., 2003; and Cole et al., 2006; 4) Subduction Events and Plate Motions, compiled from Stock and Molnar, 1988; Plafker et al., 1994; Haeussler et al., 2003; and Bradley et al., 2003); 5) Climate Change, from Zachos et al. 2001; and Wolfe et al., 1966.

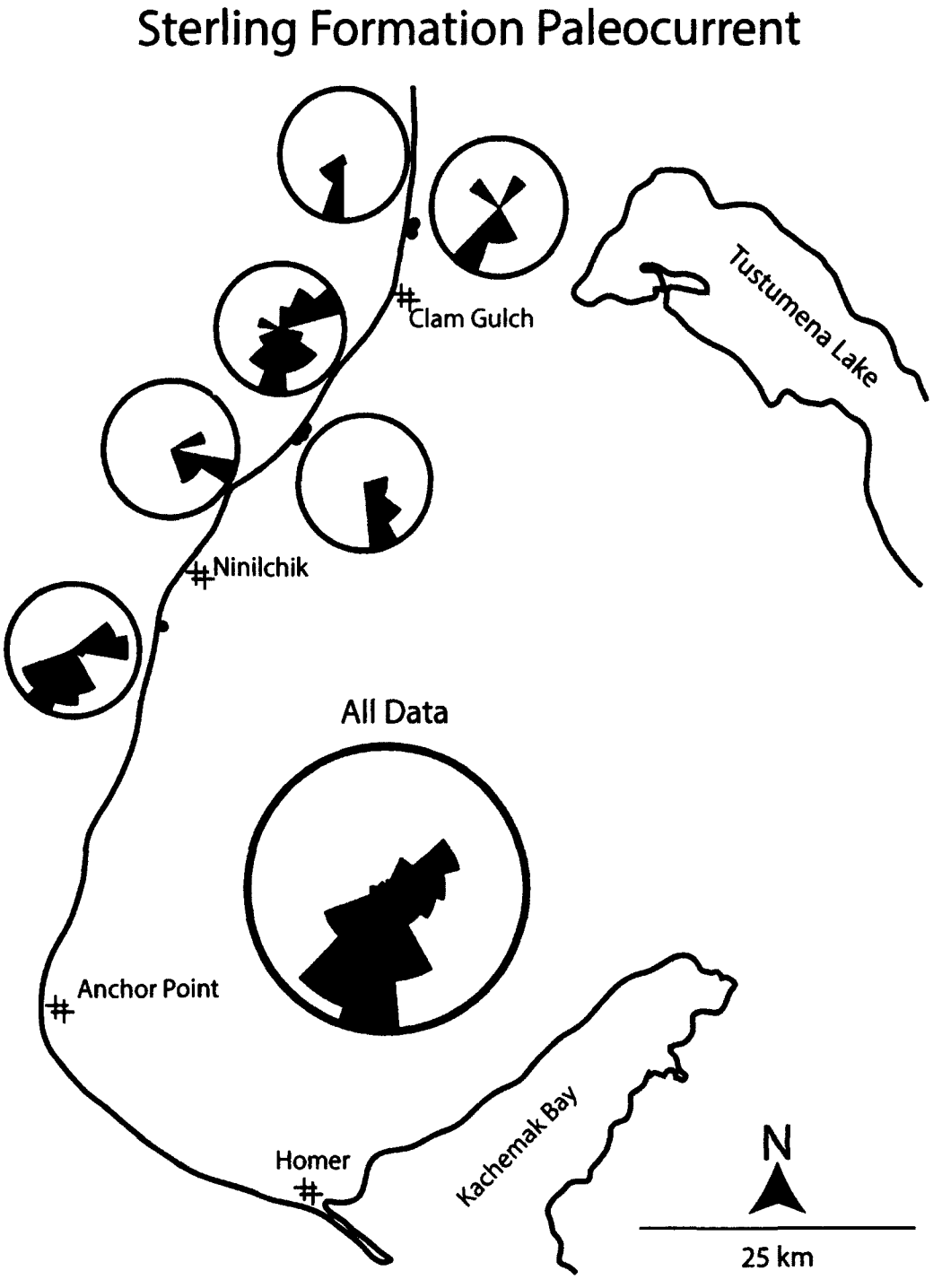

Figure 2.4: Paleocurrent data for the Sterling Fm. The paleocurrent vector mean is 197° with low dispersion about the mean leading to a low sinuosity of 1.1 (Table 4). Location noted in figure 2.1.

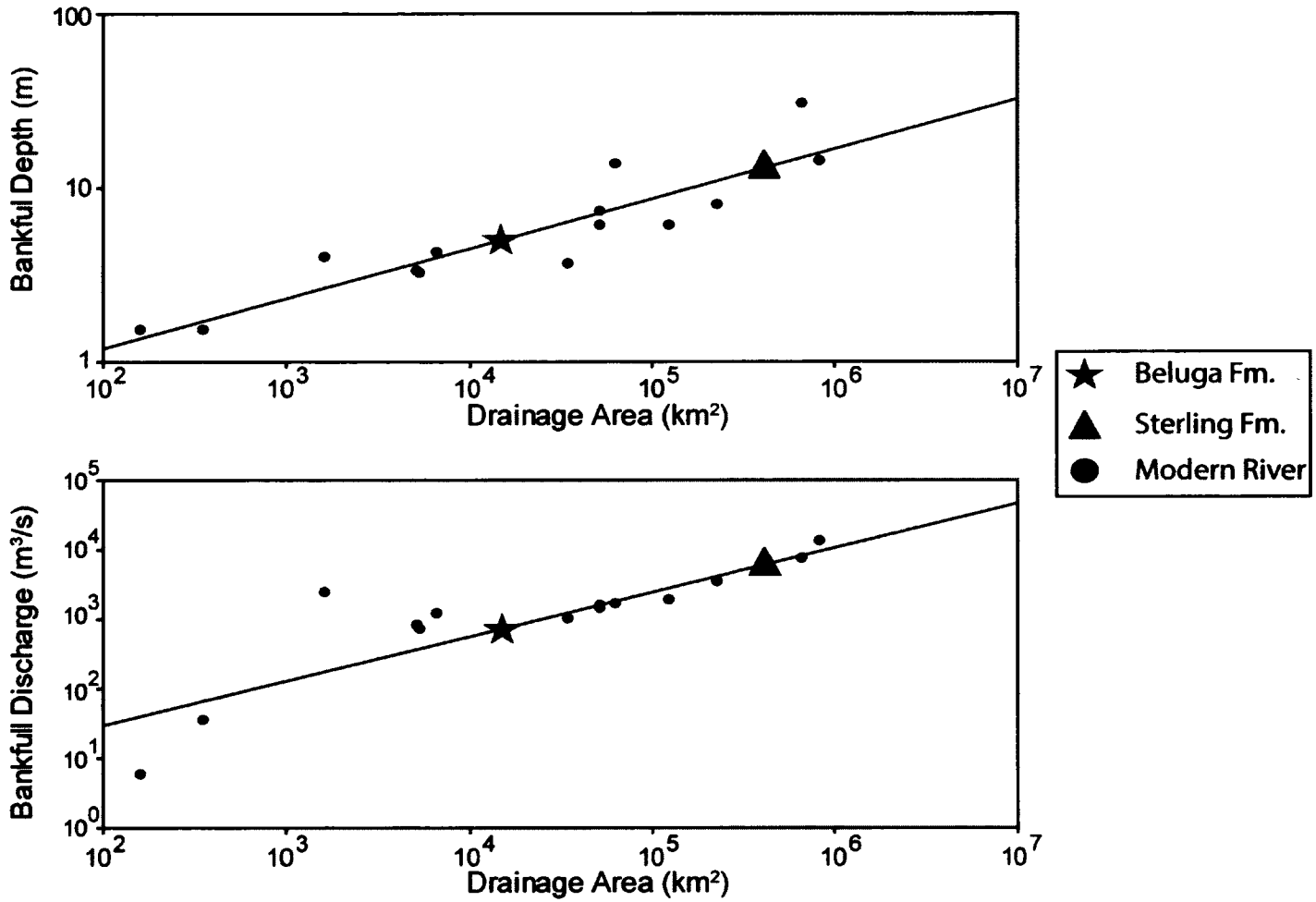

Figure 2.5: Modern regional hydraulic curves used to estimate drainage area (Davidson and North, 2009). The rivers used to generate these graphs are listed in Table 1. Estimated drainage area for the Sterling Fm. is ~415,000 km^2 and estimated bankfull discharge is ~5,910 m^3/s. Estimated drainage area for the Beluga Fm. is ~15,000 km^2 and estimated bankfull discharge is ~700 m^3/s.

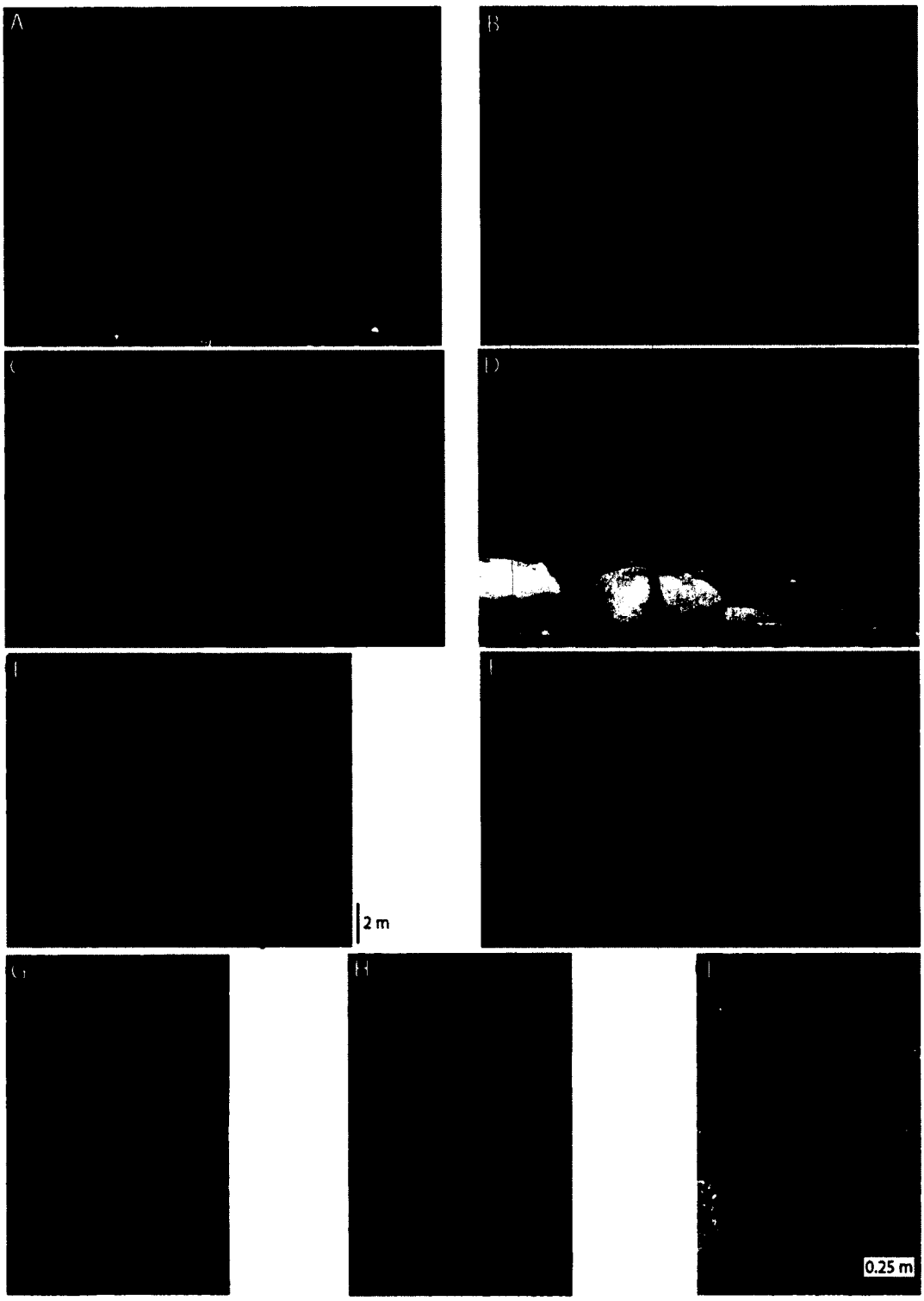

Figure 2.6: Typical facies of the Beluga and Sterling formations. A) Ripple cross-laminated sandstone; B) Trough cross-bedded sandstone; C) Plane parallel-laminated sand; D) Convolute bedded sandstone; E) Coal seams and fine-grained floodplain material; F) Matrix-supported conglomerate; G) Massive siltstone; H) Large amplitude planar tabular cross-beds; I) Carbonaceous siltstone.

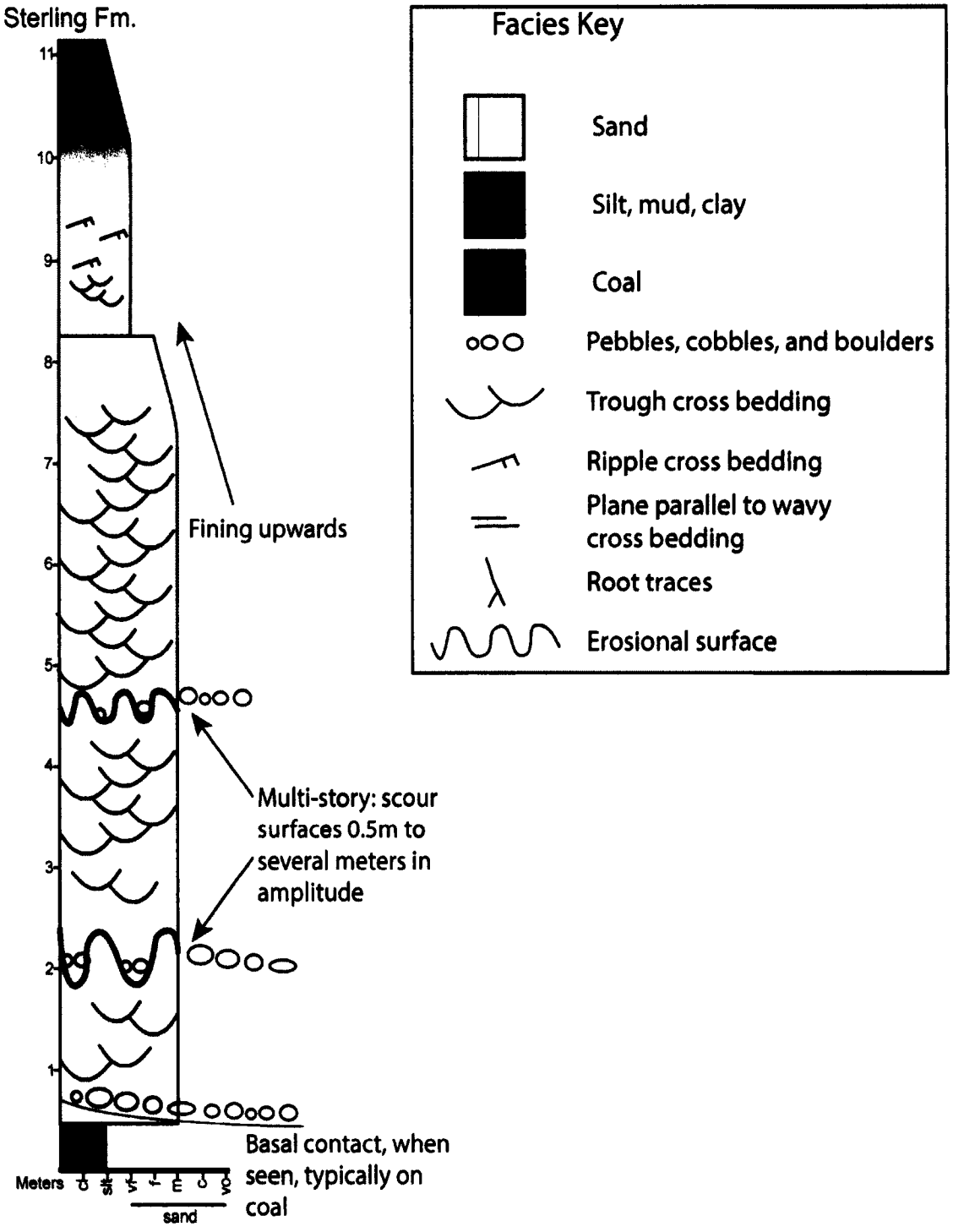

Figure 2.7: A typical measured section showing facies within the sandy braided channel facies association. Sandy bedforms are the most common feature along with pebble- to boulder- sized mud rip-up clasts on concave-upward scour surfaces separating multiple channel stories. Typically the sandy braided channel facies association fines upwards to floodplain facies sometimes culminating in a coal.

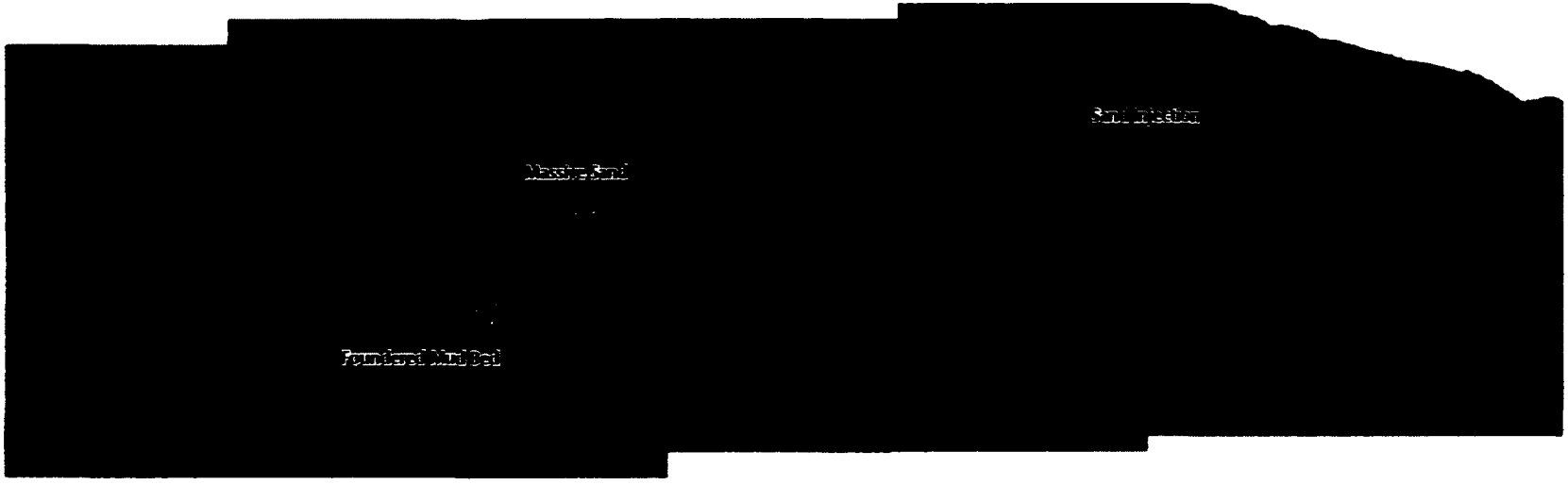

Figure 2.8: A) Composite photograph of large-scale bed disruptions that may be the result of seismogenic activity. B) Interpreted composite photograph showing a mud bed in a matrix of massive sand (arrow) that is detached from its corresponding bed on the right of the photograph (arrows). At right is a sand injection feature (arrow).

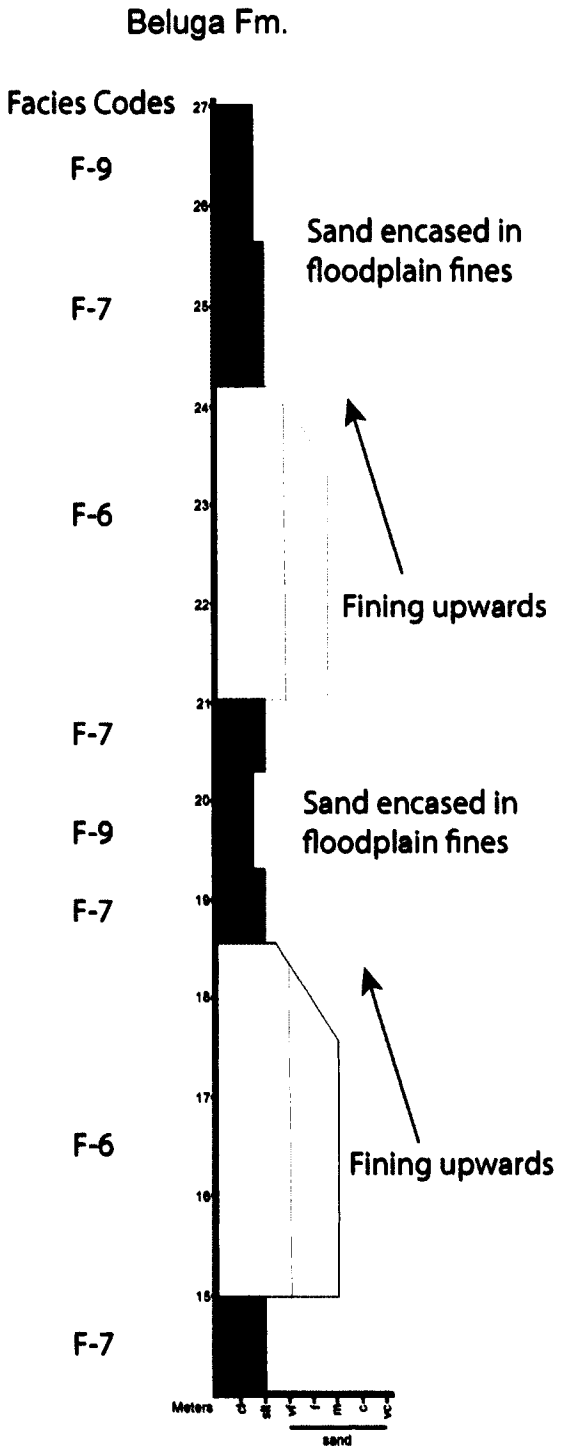

Figure 2.9: Typical measured section showing facies within the humid/organoclastic-style anabranching channel facies association. Single story sandbodies (F-6) that are encased in floodplain material (F-7) are the defining feature of this facies association. A typical succession starts with a concave-upward scour below a sandbody that fines upward to a flat-topped contact with floodplain material. Several sandbodies are usually seen in outcrop at or near the same stratigraphic level (Fig. 15) suggesting multiple channels were active at any one time.

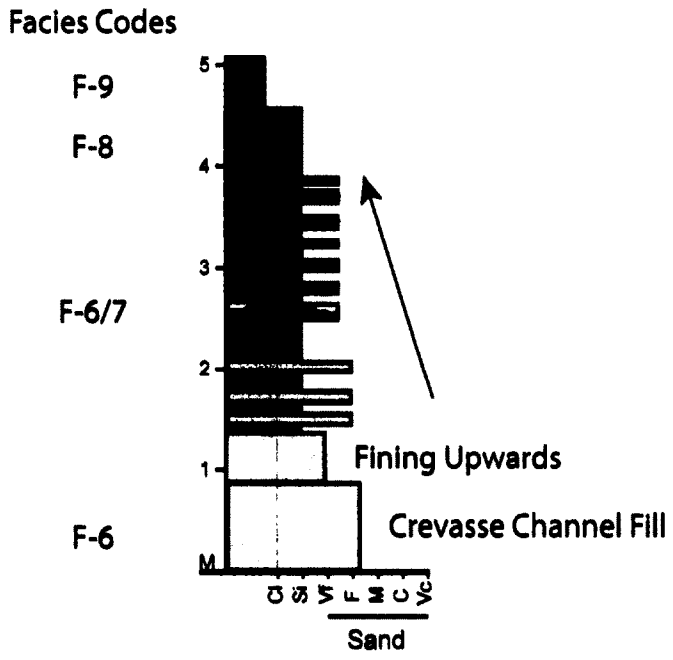

Figure 2.10: Typical measured section showing facies within the crevasse splay and crevasse complex facies association. Defining characteristics of this facies association include thin sandstones (F-6) interpreted as crevasse channels, and interdigitating sand (F-6) and fine-grained material (F-7) interpreted as splay deposits. Sand beds typically become thinner and finer-grained upward. This facies association is commonly capped by a coal (F-9) or, less commonly, by braided fluvial sandstone (FA-1) or humid organic anabranching/single channel sandstone (FA-2).

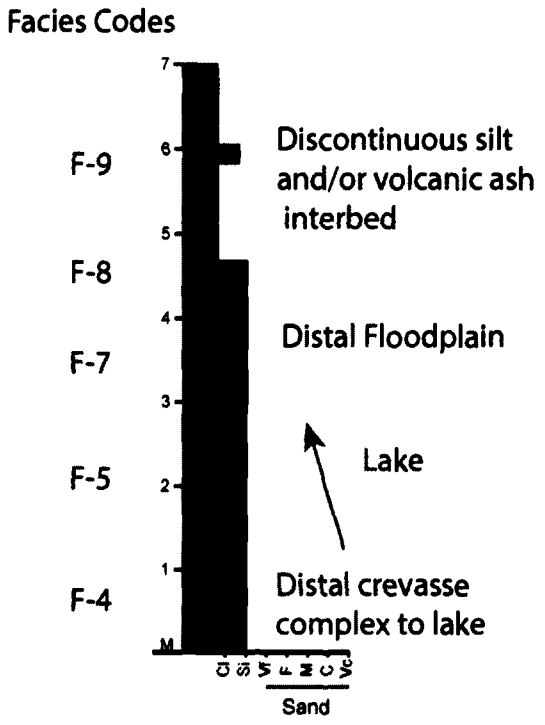

Figure 2.11: Typical measured section showing facies of the floodplain facies association. Defining characteristics of this facies association include relatively thick, laterally continuous beds of siltstone (F-7), mudstone (F-8), and coal (F-9).

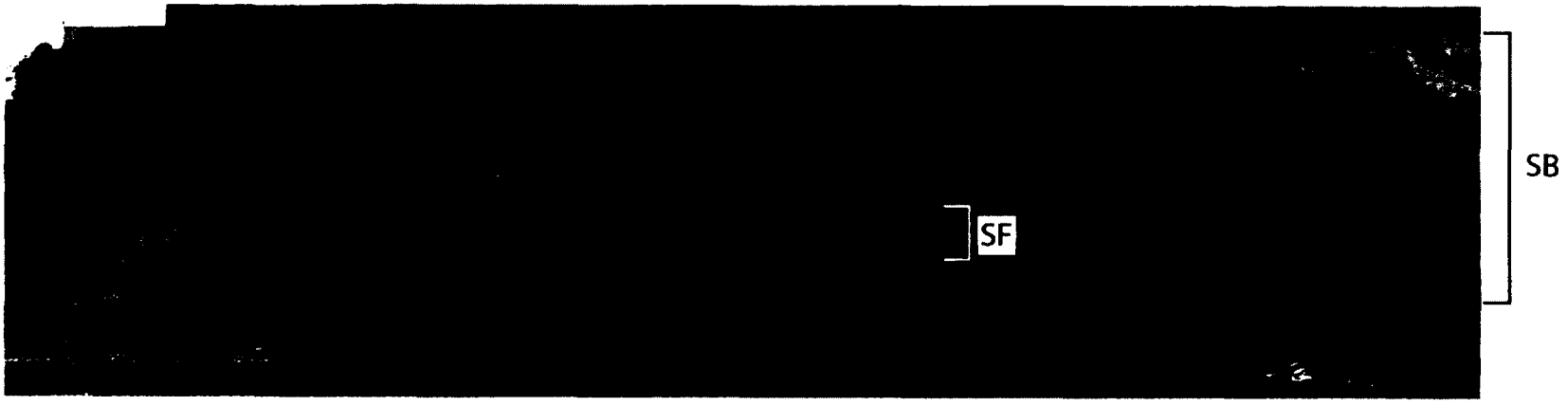

Figure 2.12: Typical outcrop of Sterling Fm. showing the sheet sands architectural element association. Sandy bedforms (SB) and scour fills (SF) are the most abundant features. Black line separates sand from overbank deposits, thick red lines represent major scours, and thin red lines represent sandy bedforms.

Figure 2.13: Downstream accreting beds (DA) in the Sterling Fm. Dashed thin red lines envelope DA beds. The outcrop is oriented nearly north-south and paleocurrent is south-directed at 196°. This outcrop is interpreted to be a simple unit bar with sandy bedforms (SB) in the core. DA beds can be traced to the north (left) where they become vertically accreting (VA) bar top beds. The locations of measured sections A and B (Fig. 2.13 cont.) are shown by vertical black lines.

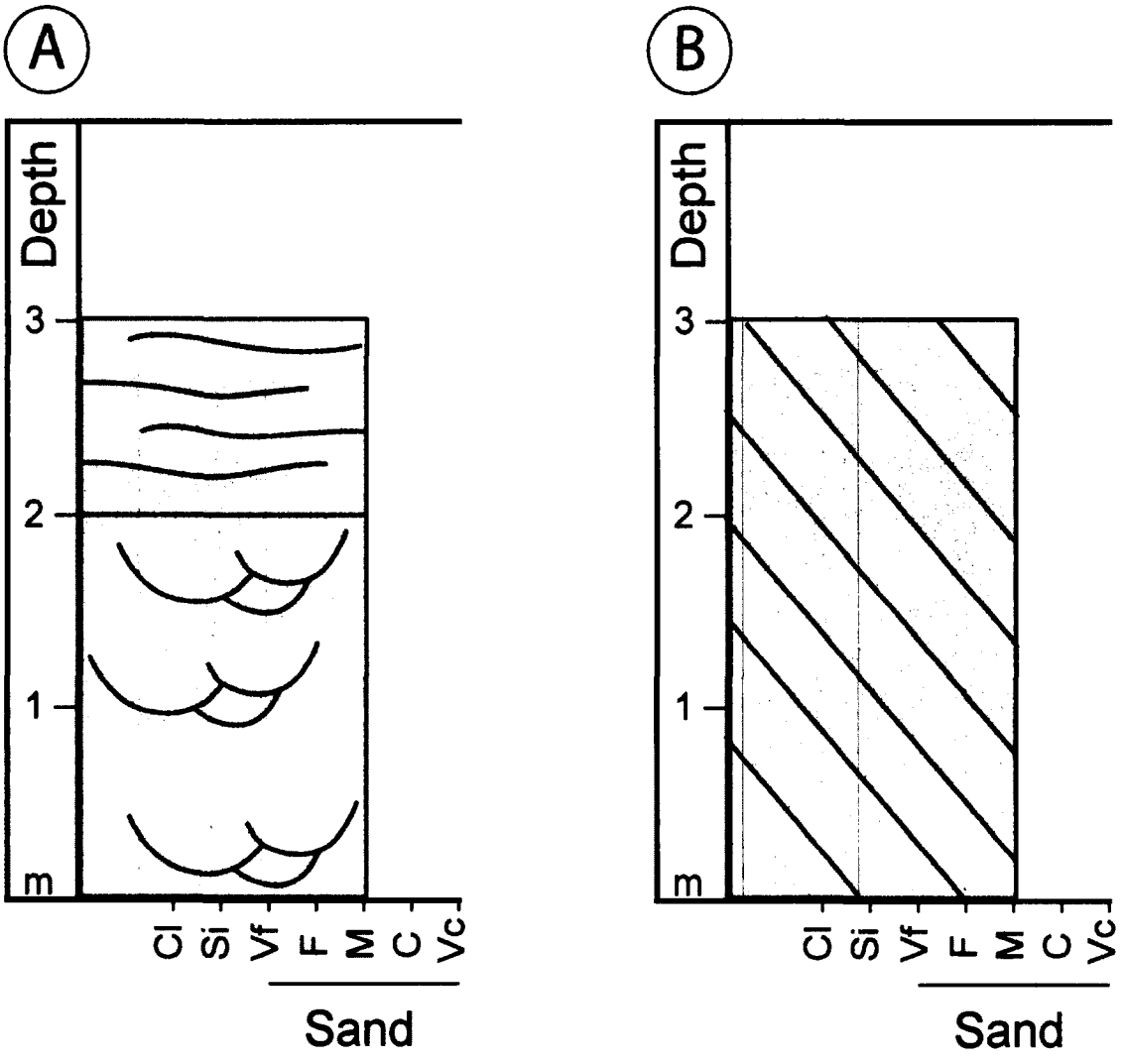

Figure 2.13: continued

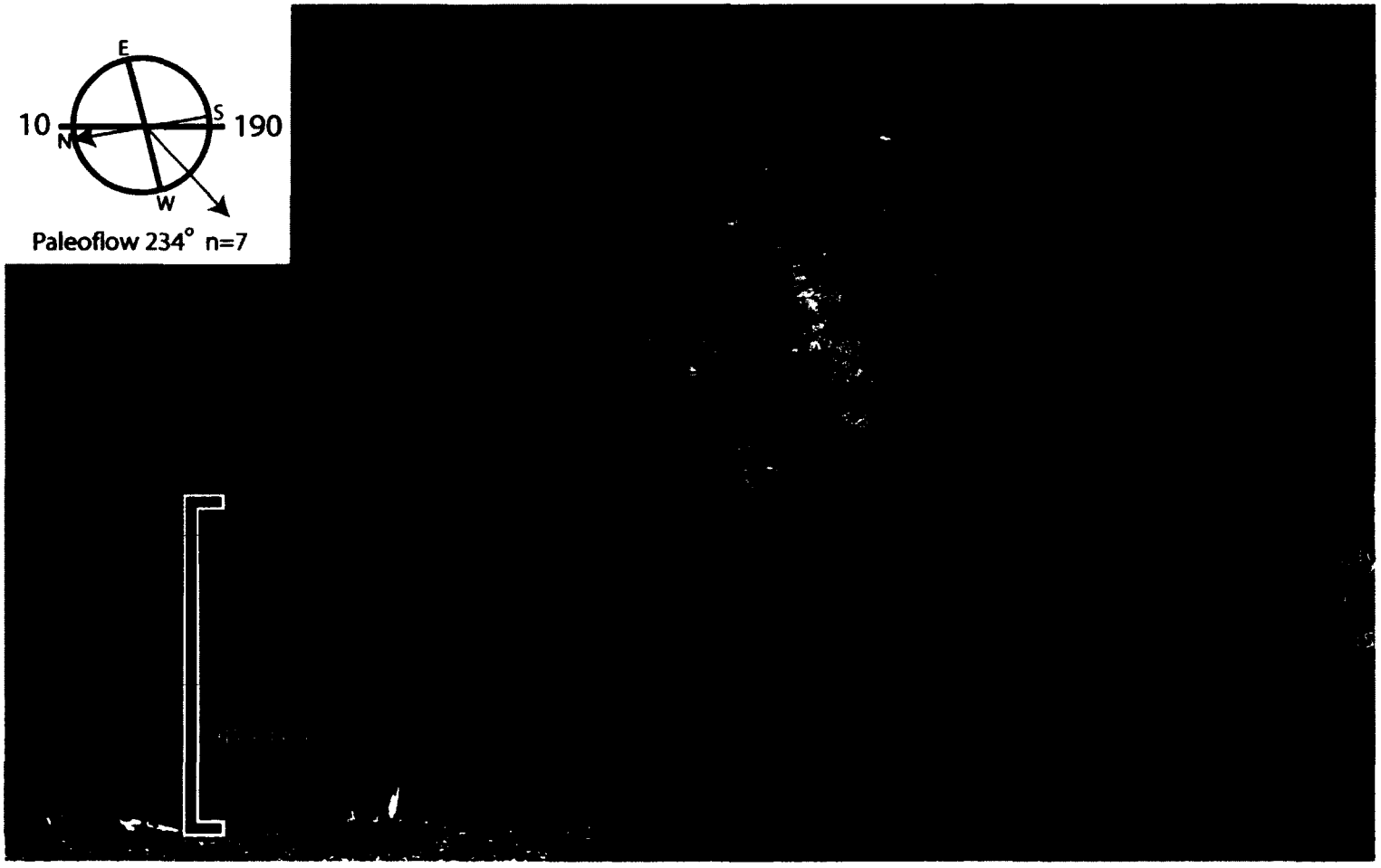

Figure 2.14: Laterally accreting beds (LA) of the Sterling Fm. Black line separates sand from overbank deposits, thick green lines represent major scours, and thin red lines represent bedforms. The outcrop is oriented nearly north-south and paleocurrent is west-southwest directed at 234°. This outcrop is interpreted to be a compound bar composed of at least two unit bars migrating across the paleocurrent direction that are separated by a major scour surface (green line). A composite measured section from this area is shown in Figure 2.14 cont.

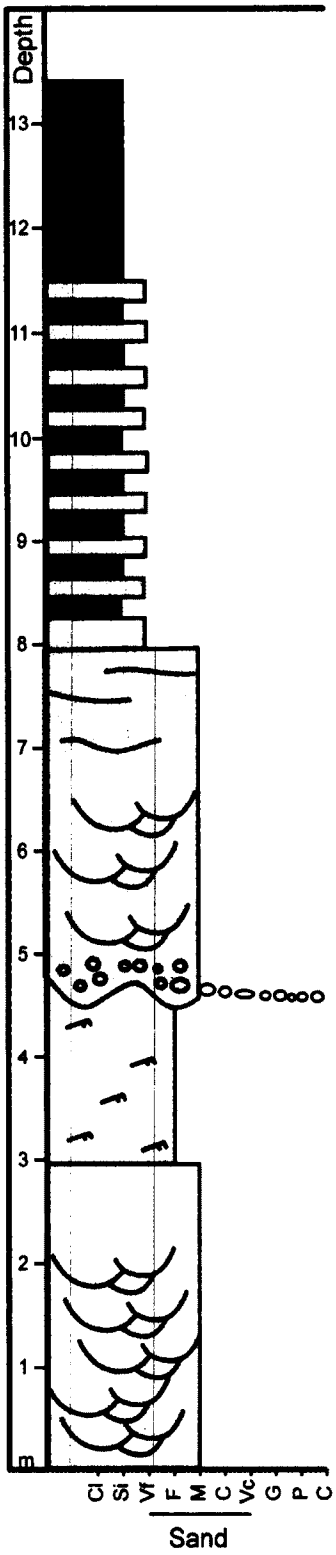

Figure 2.14: continued

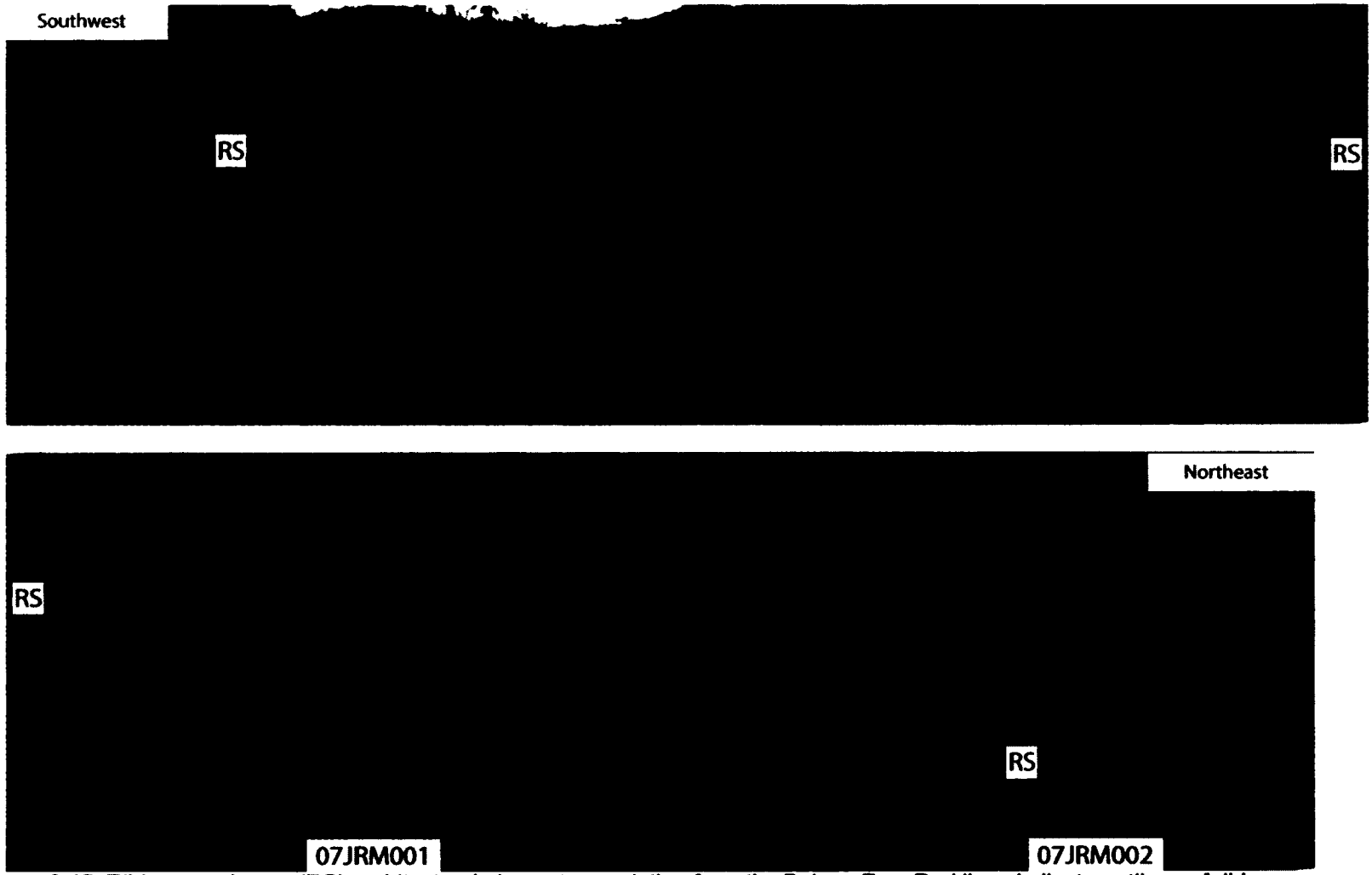

Figure 2.15: Ribbon sandstone (RS) architectural element association from the Beluga Fm. Red lines indicate outlines of ribbon sandbodies. Several sandbodies are at or near the same stratigraphic level suggesting multiple channels may have been active at any one time. Vertical black dashed line shows the position of overlap between the southwest and northeast panels. Solid black lines show locations of measured sections (Fig. 2.15 cont.).

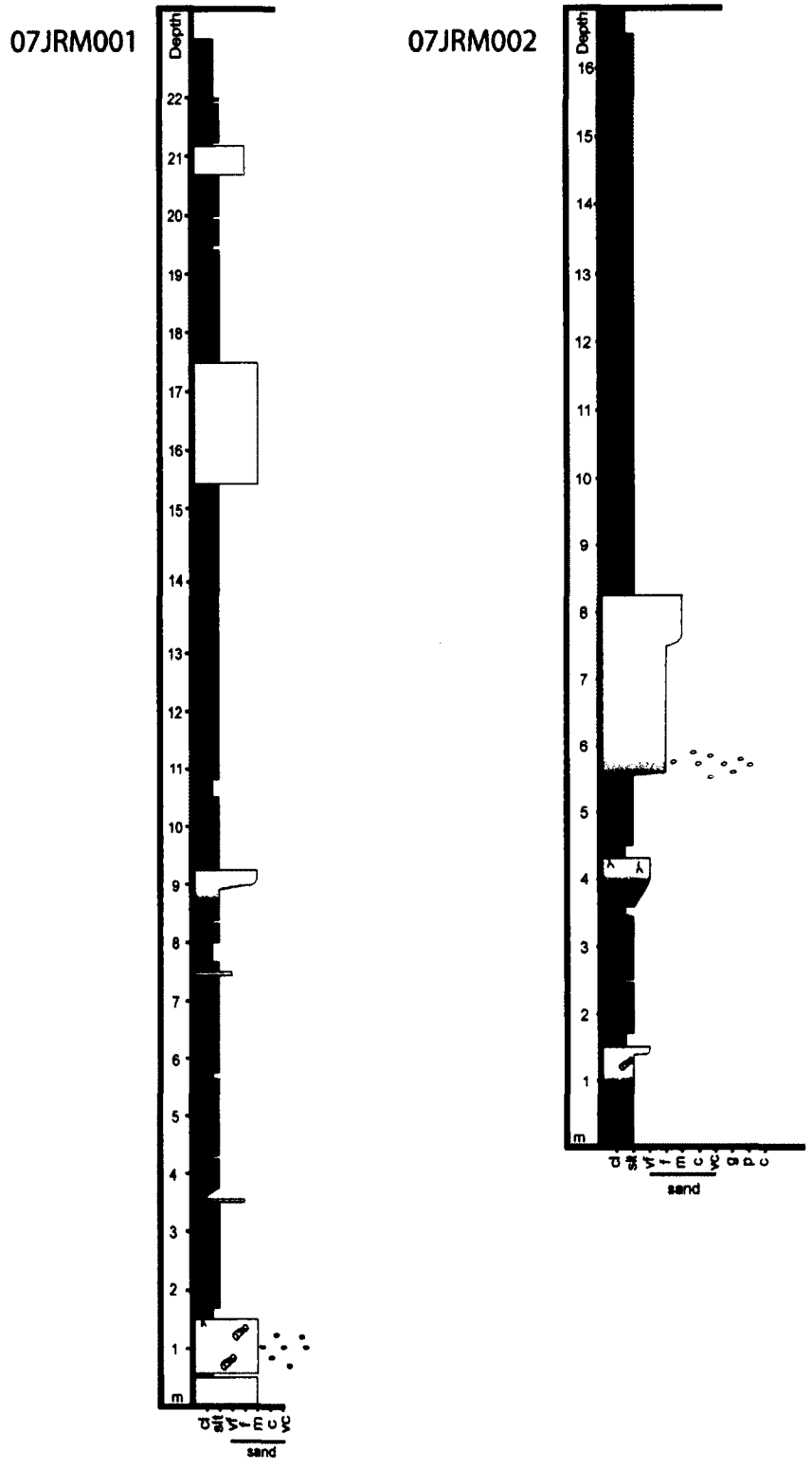

Figure 2.15: continued

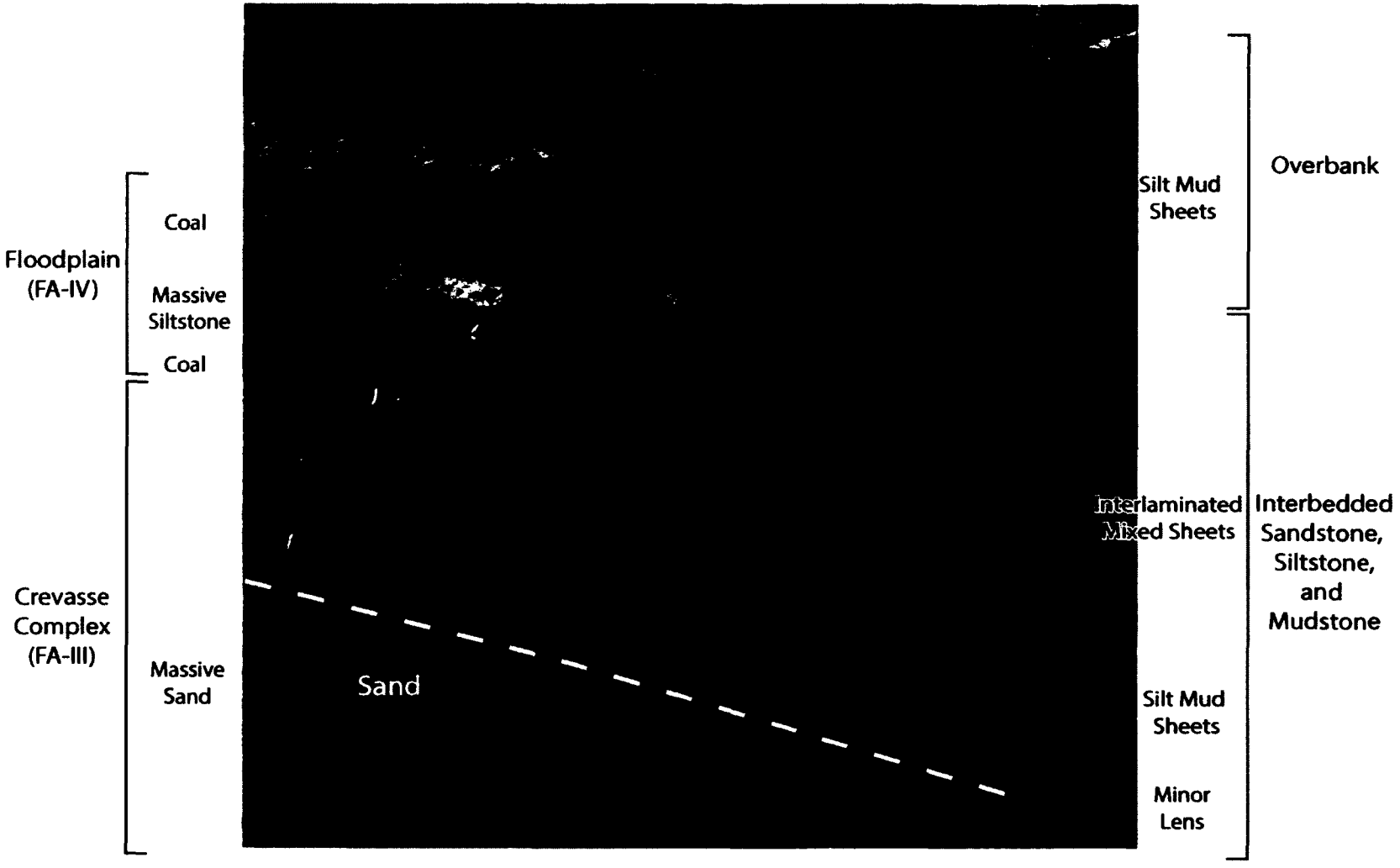

Figure 2.16: Crevasse Splay and Crevasse complex architectural element association from the Beluga Fm. Dashed white line separates minor lens (ML) from interlaminated mixed sheets (IMS), and silt-mud sheets (SMS). The interbedded sand decreases in thickness and silt becomes more abundant until the unit is capped by the overbank architectural element association.

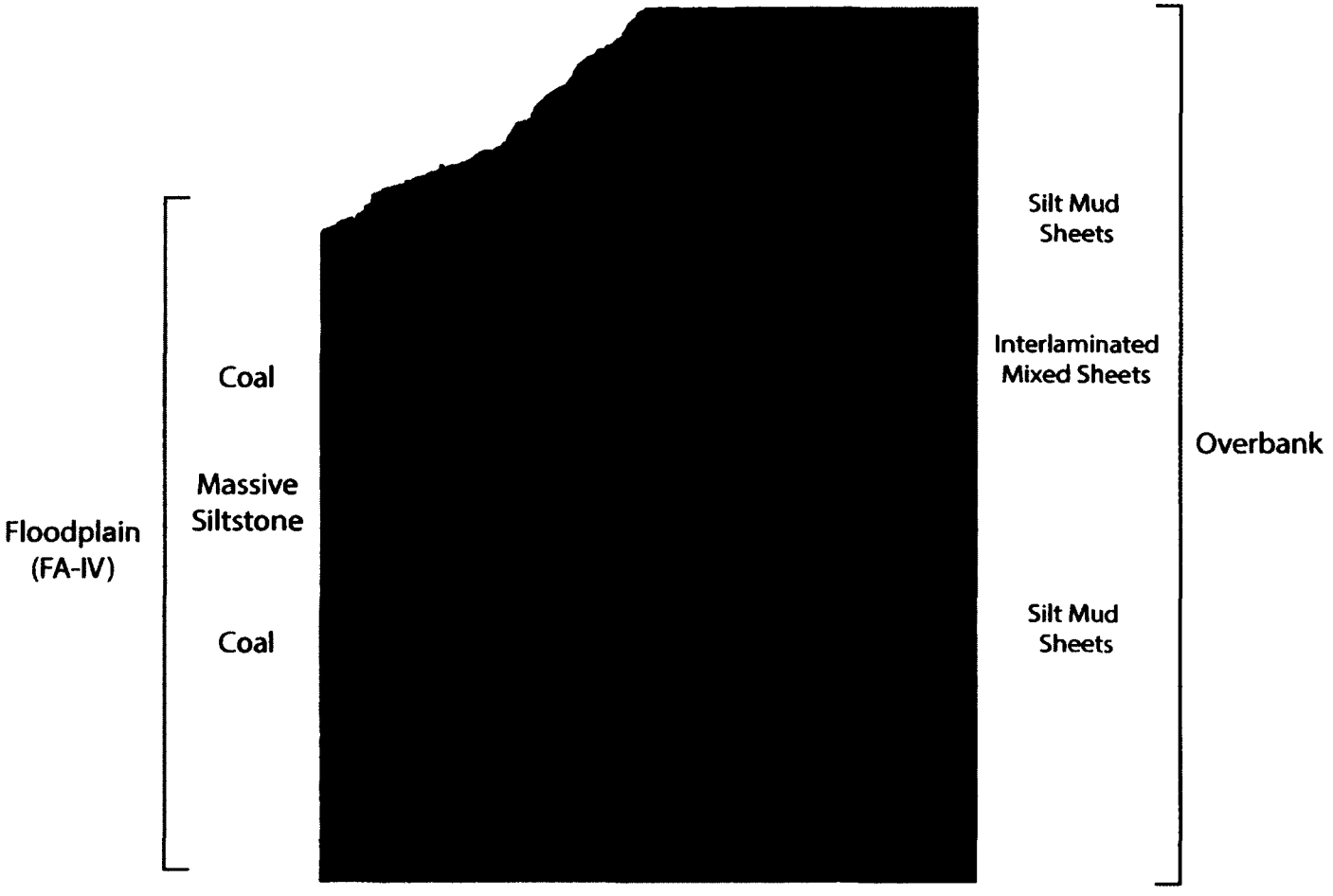

Figure 2.17: Overbank architectural element association from the Beluga Fm. This outcrop also shows a minor sheet (MS) of siltstone and silt-mud sheet (SMS) architectural elements. The most prominent feature is the thick coal seams.

2.12 Tables

Table 2.1: Data from modern rivers used to generate geomorphological regional curves

River	Modern River Length (km)	Bankfull Discharge (m^3/s)	Drainage Area (km^2)	Bankfull Depth (m)
Anchor	48	35	355	2
Beluga Fm.	—	710	14842	5
Chulitna	113	1211	6656	4
Columbia	2000	7504	668217	30
Copper River	460	1671	63196	14
Fraser	2213	3475	227999	8
Kenai	121	2450	1642	4
Kuskokwim	1165	1897	124319	6
Little Susitna	177	6	160	2
Matanuska	121	726	5361	3
Nushagak	459	1019	34706	4
Sterling Fm.	—	5911	414703	13
Stikine	610	1586	51800	7
Susitna River	504	1444	51800	6
Telkeetna	137	827	5170	3
Yukon	3701	13370	832681	14

Notes: Modern river data from USGS National Water Information System: http://waterdata.usgs.gov/usa/nwis/sw/

Table 2.2: Lithofacies in the Sterling and Beluga formations

Facies		Thickness	Description	Occurrence
F-1 Conglomerate		<0.5m Rare: ~6m	Matrix- to clast supported well-rounded pebble-to boulder-sized clasts of mudstone, coal, igneous, and silicified mudstone; matrix of medium-to coarse-grained sub-rounded to sub-angular sand.	Common: At base of braided and single channel sand bodies on scour surfaces
F-2 Trough cross bedded medium to fine grained sand	F-2a large amplitude (>~1m)	1-8 m	Composed of sub-rounded to sub-angular sand; only facies containing large-scale trough cross-laminations; when present usually in multi-stories.	Braided and single channel sand, crevasse channels and proximal crevasse splays
	F-2b small amplitude	0.3-1.5 m	Composed of fine-grained, sub-rounded to sub-angular sand; usually in single-stories	Same as F-2a
F-3 Planar tabular crossbeds in medium to fine sand	F-3a large amplitude (>~1m)	1.0-~3.5 m	Composed of sub-rounded to sub-angular sand. Only facies with planar tabular crossbeds	2-D dunes deposited in channels braided and single channel sand, crevasse channels and proximal crevasse splays; large features deposited from bar top to base of thalweg
	F-3b small amplitude	0.25-1 m	Same as F-3a	2-D dunes deposited in channels braided and single channel sand, crevasse channels and proximal crevasse splays
F-4 Ripple cross-laminated very fine to fine grained sand		0.25-1.5 m	When present ripple crossbeds are ubiquotous, usually with sub-mm macerated organic debris on ripples and less commonly with reddish-orange mottles	Low energy and/or small grain size in channalized to unchannelized sand found in crevassa channels and crevassa splays
F-5 Plane parallel- to wavy laminated silt, and very-fine to fine-grained sand		0.25-3 m	Composed of sub-rounded to sub-angular fine-grained to silt with plane-parallel and/or wavy stratification, Fe-oxide staining, and sub-mm macerated organic debris	Floodplain, distal crevasse splays, and lakes
F-6 Massive to convolute bedded medium to very fine grained sand		0.5-4 m	Found in a wide range of grain sizes; sand beds contain convolute beds including flame structures, ball and pillow structures, and distorted bed laminations. Massive beds show no sedimentary structures.	Range of depositional environments
F-7 Massive siltstone/mudstone		few cm's - 5 m	Lack of sedimentary structure and grain size; commonly with sub-mm macerated organic debris; rarely with plant compression fossils	Floodplain
F-8 Carbonaceous mudstone		few cm's - 2.5 m	Massive black mudstone	Swamp, floodplain, organic rich shallow lake deposits
F-9 Coal		few cm's - 4 m	Massive coal, carbonized wood and plant fragments, coalified logs; larger beds include interbeds of siltstone, mudstone, and tonsteins	Floodplain swamp

Table 2.3: Lithofacies associations in the Sterling and Beluga formations

Facies Associations	Component Facies	Diagnostic Features	Occurrence
FA-I: Braided Channel	F-1, F-2a, F-2b, F-3a, F-3b, F-4, F-5, F-6	5-15 m erosionally based, multi-story sand body	Only major channel form in the Sterling Fm.
FA-II: Humid/organoclastic-style anabranching channels	F-6, F-5, F-4; Rarely: F-2b, F-1	2-5 m muddy sand, typically massive, concave-up basal contact and flat top encased in fine-grained material	This channel style is common throughout the Beluga Fm. and is commonly encased in the floodplain depositional element
FA-III: Crevasse Complex	F-2b, F-3b, F-4, F-5, F-6, F-7, and F-8	Decimeter - <~2m sands, interbedded with silt and mud on the order of decimeters	This depositional element is found in association with all three channel elements. Most commonly found in the transition between the Beluga and Sterling Fms.
FA-IV: Floodplain	F-4, F-5, F-7, F-8, F-9	Variable thickness, contains the bulk of the fine-grained sediments and contains coal	Common throughout Beluga and Sterling Fms.

Table 2.4: Paleochannel characteristics for typical channel sandstones in the Sterling and Beluga formations

Sterling Fm.

Average flow depth	(m)
	8
	13
Average channel width	(m)
	113
	286
Average width/thickness	(m)
	14
	21

Bridge and Tye 2000 Method	
	(m)
Dune height	1.3
Range of flow depth	7.9
	13.2
Sinuosity (circular arc method)	1.1
Sinuosity (sine generated curve)	1.1

Beluga Fm.

Average flow depth	(m)
	2
Average channel width	(m)
	11
Average width/thickness	
	5

Table 2.5: Architectural elements in the Sterling and Beluga formations

Element	Symbol	Typical Facies	Geometry	Interpretation
Sandy Bedforms	SB	F-2a, F-2b, F-3b, F-4, F-6	Lens, sheet, wedge, with thicknesses of 10s of cm to several meters in thickness.	Occurs as channel fills, crevasse channels and proximal splays, and composes bar forms
Accreting Bedforms	AB	F-3a	Sheet, individual beds typically a few to 10s of cm thick and dip at approximately the angle of repose. Overall bedform is typically a few meters in thickness.	General form of accreting bedform when paleocurrent direction is unknown
	LA	F-3a		Accretion of sand near/at the angle of repose within ≥ 60°of perpendicular to the paleoflow direction
	DA	F-3a		Accretion of sand near/at the angle of repose within ≤ 60° of the paleoflow direction
	VA	F-5	Horizontal to wavy beds typically a few to 10s of cm thick	Vertical accretion of sand in upper flow regime conditions
Scour Fill	SF	F-1, F-2a, F-2b, F-3b	Irregular 'scoop' shaped usually with meter scale relief, much less commonly with a few 10's of cm	Erosional scour within a channel fill
Ribbon Sand	RS	F-6	Width to depth <15, usually one story, stories <5m	Anastomozing fluvial channel fill
Minor Lens	ML	F-2b, F-4, F-5, F-6	Width to depth <10, thickness less than ~2m	Crevasse channel, composes part of the crevasse complex depositional element
Minor Sheet	MS	F-4, F-5, F-7	Tabular, typically with flat base and top, thickness varies from a few cm to ~1 m	Sheet splay, composes part of the crevasse complex depositional element
Interlaminated Mixed Sheets	IM	F-4, F-5, F-6, F-7, F-8	Tabular, interbeds of sand and silt-mud. Individual sand and silt/mud beds a few to 10's of cm. Overall thickness is typically less than 2 m	Distal crevasse splay and/or proximal floodplain deposit; composes part of the crevasse complex depositional element
Silt-mud sheets	SMS	F-5, F-7, F-8, F-9	Tabular, beds a few to several meters thick usually with coal interbeds	Distal floodplain deposit

Table 2.6: Architectural element associations in the Sterling and Beluga formations

Architectural Element Associations	Architectural Element	Diagnostic Features	Occurrence
Narrow Sheets	SB, LA, DA,VA, AB, SF	Dominantly composed of sandy bedforms and bar forms. The migration of bar forms creates DA, LA, and AB	Only channel architectural element in the Sterling Fm.
Ribbon Sand	RS	Single story sandstone encased in overbank architectural element	Only channel architectural element in the Beluga Fm.
Crevasse Splays and Crevasse Complexes	ML, MS, IM, SMS Less Commonly: SB, SF	Interbedded silt and mud usually encased in the overbank architectural element; less commonly fining upwards from a sandstone	This depositional element is found in association with narrow sheets and ribbon sands; most commonly found in the transition between the Beluga and Sterling Fms.
Overbank	MS, IM, SMS	Relatively thick sheets dominated by fine-grained silt, mud, and clay	Common throughout Beluga and Sterling Fms.

2.13 References

ABBADO, D., SLINGERLAND, R., and SMITH, N.D., 2005, Origin of anastomosis in the upper Columbia River, British Columbia, *in* Blum, M.D., Mariott, S.B., and Leclair, S.F., eds., Fluvial Sedimentology VII, International Association of Sedimentologists, p. 3-15.

ALLEN, J.R.L., 1963, The classification of cross-stratified units with notes on their origin: Sedimentology, v. 2, p. 93–114.

ALLEN, J.R.L., 1964, Studies in fluvitile sedimentation: Six cyclothems from the lower Old Red Sandstone, Anglo-Welsh Basin: Sedimentology, v. 3, p. 163-198.

ALLEN, J.R.L., 1965a, Fining upward cycles in alluvial successions: Geological Journal, v. 4, p. 229-246.

ALLEN, J.R.L., 1965b, A review of the origin and characteristics of recent alluvial sediments: Sedimentology, v. 5, p. 89-191.

ALLEN, J.R.L., 1983, Studies in fluviatile sedimentation: Bars, bar-complexes and sandstone sheets (low-sinuosity braided streams) in the brownstones (L. devonian), welsh borders: Sedimentary Geology, v. 33, p. 237-293.

ASHLEY, G.M., 1990, Classification of large-scale subaqueous bedforms: a new look at an old problem: Journal of Sedimentary Petrology, v. 60, p. 160-172.

ASHWORTH, P.J., BEST, J.L., RODEN, J.E., BRISTOW, C.S., and KLAASSEN, G.J., 2000, Morphological evolution and dynamics of a large, sand braid-bar, Jamuna River, Bangladesh: Sedimentology, v. 47, p. 533-555.

BANKS, N.L., 1973, The origin and significance of some downcurrent-dipping cross-stratified sets: Journal of Sedimentary Petrology, v. 43, p. 423-427.

BEIKMAN, H.M., 1980, Geologic map of Alaska: U.S. Geological Survey Professional Paper PP0171, 1 plate, scale 1:250,000.

BENOWITZ, J.A., 2011, The Topographically Asymmetrical Alaska Range: Multiple Tectonic Drivers Through Space And Time: University of Alaska Fairbanks, Fairbanks, 291 p.

BENOWITZ, J.A., LAYER, P.W., ARMSTRONG, P., PERRY, S.E., HAEUSSLER, P.J., FITZGERALD, P.G., and VANLANINGHAM, S., 2011, Spatial variations in focused exhumation along a continental-scale strike-slip fault: The Denali fault of the eastern Alaska Range: Geosphere, v. 7, p. 455-467.

BEST, J.L., ASHWORTH, P.J., BRISTOW, C.S., and RODEN, J., 2003, Three-dimensional sedimentary architecture of a large, mid-channel sand braid bar, Jamuna River, Bangladesh: Journal of Sedimentary Research, v. 73, p. 516-530.

BLODGETT, R.H., and STANLEY, K., 1980, Stratification, bedforms, and discharge relations of the Platte braided river system, Nebraska: Journal of Sedimentary Research, v. 50, p. 139.

BLUM, M.D., and TORNQVIST, T.E., 2000, Fluvial responses to climate and sea-level change: a review and look forward: Sedimentology, v. 47, p. 2-48.

BOSS, R.F., LENNON, R.B., and WILSON, B.W., 1976, Middle Ground Shoal oil field, Alaska: AAPG Memoir, p. 1-22.

BRADLEY, D.C., KUSKY, T., HAEUSSLER, P., GOLDFARB, R., MILLER, M., DUMOULIN, J., NELSON, S.W., and KARL, S., 2003, Geologic signature of early Tertiary ridge subduction in Alaska, *in* Sisson, V.B., Roeske, S.M., and Pavlis, T.L., eds., Geology of a transpressional orogen developed during ridge-trench interaction along the north Pacific margin: Boulder, Geological Society of America, p. 19-49.

BRIDGE, J., 1984, Large scale facies sequences in alluvial overbank environments: Journal of Sedimentary Petrology, v. 54, p. 583-588.

BRIDGE, J., COLLIER, R., and ALEXANDER, J., 1998, Large scale structure of Calamus River deposits (Nebraska, USA) revealed using ground penetrating radar: Sedimentology, v. 45, p. 977-986.

BRIDGE, J.S., GUILLERMO, A.J., and GEORGIEFF, S.M., 2000, Geometry, lithofacies, and spatial distribution of Cretaceous fluvial sandstone bodies, San Jorge Basin, Argentina: Outcrop analog of the hydrocarbon-bearing Chubut Group: Journal of Sedimentary Research, v. 70, p. 341–359.

BRIDGE, J., and MACKEY, S., 1993, A theoretical study of fluvial sandstone body dimensions: The geological modelling of hydrocarbon reservoirs and outcrop analogues: International Association of Sedimentologists Special Publication, v. 15, p. 213–236.

BRIDGE, J., and TYE, R., 2000, Interpreting the dimensions of ancient fluvial channel bars, channels, and channel belts from wireline-logs and cores: AAPG Bulletin, v. 84, p. 1205.

BRIDGE, J.S., 1993, The interaction between channel geometry, water flow, sediment transport and deposition in braided rivers: Geological Society, London, Special Publications, v. 75, p. 13.

BRIDGE, J.S., and LUNT, I.A., 2006, Depositional models of braided rivers, *in* Sambrook Smith, G.H., Best, J.L., Bristow, C.S., and Petts, G.E., eds., Braided Rivers; Process, Deposits, Ecology and Management,, International Association of Sedimentologists, p. 11-50.

BRUHN, R.L., and HAEUSSLER, P.J., 2006, Deformation driven by subduction and microplate collision: Geodynamics of Cook Inlet basin, Alaska: Geological Society of America Bulletin, v. 118, p. 289-303.

CALDERWOOD, K.W., and FACKLER, W.C., 1972, Proposed Stratigraphic Nomenclature for Kenai Group, Cook Inlet Basin, Alaska: AAPG Bulletin, v. 56, p. 739-754.

CANT, D., and WALKER, R., 1978, Fluvial processes and facies sequences in the sandy braided South Saskatchewan River, Canada: Sedimentology, v. 25, p. 625-648.

COLE, R.B., NELSON, S.W., LAYER, P.W., and OSWALD, P.J., 2006, Eocene volcanism above a depleted mantle slab window in southern Alaska: Geological Society of America Bulletin, v. 118, p. 140-158.

COLLINSON, J.D., 1978, Vertical sequence and sand body shape in alluvial sequences, *in* Miall, A.D., ed., Fluvial Sedimentology, Canadian Society of Petroleum Geologists, Memoir 5, p. 577-587.

CONNELL, S.D., WONSUCK, K., PAOLA, C., and SMITH, G.A., 2012a, Fluvial Morphology and Sediment-Flux Steering of Axial Transverse Boundaries in an Experimental Basin: Journal of Sedimentary Research, v. 82.

CONNELL, S.D., WONSUCK, K., SMITH, G.A., and PAOLA, C., 2012b, Stratigraphic Architecture of an Experimental Basin with Interacting Drainages: Journal of Sedimentary Research, v. 82.

CRAW, D., and LECKIE, D.A., 1996, Tectonic controls on dispersal of gold into a foreland basin; an example from the Western Canada foreland basin: Journal of Sedimentary Research, v. 66, p. 559-566.

CROWLEY, K., 1983, Large-scale bed configurations (macroforms), Platte River Basin, Colorado and Nebraska: primary structures and formative processes: Bulletin of the Geological Society of America, v. 94, p. 117.

DALLEGGE, T.A., and LAYER, P.W., 2004, Revised chronostratigraphy of the Kenai Group from 40Ar/39Ar dating of low-potassium bearing minerals, Cook Inlet basin, Alaska: Canadian Journal of Earth Sciences, v. 41, p. 1159-1179.

DAVIDSON, S.K., and NORTH, C.P., 2009, Geomorphological Regional Curves for Prediction of Drainage Area and Screening Modern Analogues for Rivers in the Rock Record: Journal of Sedimentary Research, v. 79, p. 773-792.

EBERHART-PHILLIPS, D., CHRISTENSEN, D.H., BROCHER, T.M., HANSEN, R., RUPPERT, N.A., HAEUSSLER, P.J., and ABERS, G.A., 2006, Imaging the transition from Aleutian subduction to Yakutat collision in central Alaska, with local earthquakes and active source data: J. Geophys. Res., v. 111, p. B11303.

EBERTH, D.A., and MIALL, A.D., 1991, Stratigraphy, sedimentology, and evolution of a vertebrate-bearing braided to anastomosed fluvial system, Cutler Formation (Permian-Pennsylvanian), north-central New Mexico: Sedimentary Geology, v. 72, p. 225-252.

ELLIOTT, T., 1974, Interdistributary bay sequences and their genesis: Sedimentology, v. 21, p. 611-622.

ELLIOTT, T., 1976, The morphology, magnitude, and regime of a Carboniferous fluvial-distributary channel: Journal of Sedimentary Petrology, v. 46, p. 70-76.

EYNON, G., and WALKER, R.G., 1974, Facies relationships in Pleistocene outwash gravels, southern Ontario: a model for bar growth in braided rivers: Sedimentology, v. 21, p. 43-70.

FIELDING, C.R., 1987, Coal deposition models for deltaic and alluvial plain sequences: Geology, v. 15, p. 661-664.

FINZEL, E.S., 2010, Geodynamics of Flat-Slab Subduction, Sedimentary Basin Development, and Hydrocarbon Systems along the Southern Alaska Convergent Plate Margin: University of Purdue, West Lafayette, 401 p.

FINZEL, E.S., TROP, J.M., RIDGWAY, K.D., and ENKELMANN, E., 2011, Upper plate proxies for flat-slab subduction processes in southern Alaska: Earth and Planetary Science Letters.

FISK, H.N., 1944, Geological Investigation of the Alluvial Valley of the Lower Mississippi River: Digest of the Tulsa Geological Society, v. 15, p. 78.

FITZGERALD, P.G., SORKHABI, R.B., REDFIELD, T.F., and STUMP, E., 1995, Uplift and denudation of the central Alaska Range; a case study in the use of apatite fission track thermochronology to determine absolute uplift parameters: Journal of Geophysical Research, v. 100, p. 20,175-20,191.

FLAIG, P.P., MCCARTHY, P.J., and FIORILLO, A.R., 2011, A tidally-influenced, highlatitude coastal plain: the Late Cretaceous Prince Creek Formation, North Slope, Alaska, *in* North, C.P., Davidson, S., and Leleu, S., eds., From River to Rock Record: The Preservation of Fluvial Sediments and their Subsequent Interpretation, SEPM Special Publication 97, p. 233-264.

FLORES, R.M., and STRICKER, G.D., 1992, Some facies aspects of the upper part of the Kenai Group, southern Kenai Peninsula, Alaska, *in* Bradley, D.C., and Dusel-Bacon, C., eds., Geologic studies in Alaska by the U.S. Geological Survey, 1991: Reston, VA, U. S. Geological Survey, p. 160-170.

FLORES, R.M., and STRICKER, G.D., 1993, Reservoir framework architecture in the Clamgulchian type section (Pliocene) of the Sterling Formation, Kenai Peninsula, Alaska, *in* Dusel-Bacon, C., and Till, A.B., eds., Geologic studies in Alaska by the U.S. Geological Survey, 1992, U. S. Geological Survey Bulletin 2068, p. 118-129.

FLORES, R.M., STRICKER, G.D., and KINNEY, S.A., 2004, Alaska Coal Geology, Resources, and Coalbed Methane potential: U.S. Geological Survey DDS-77.

FOUFOULA-GEORGIOU, E., and SAPOZHNIKOV, V., 1998, Anisotropic scaling in braided rivers: An integrated theoretical framework and results from application to an experimental river: Water Resources Research, v. 34, p. 863-867.

FOUFOULA-GEORGIOU, E., and SAPOZHNIKOV, V., 2001, Scale invariances in the morphology and evolution of braided rivers: Mathematical Geology, v. 33.

FUCHS, W.A., 1980, Tertiary tectonic history of the Castle Mountain-Caribou fault system in the Talkeetna Mountains, Alaska: University of Utah, Salt Lake City, 152 p.

GIBLING, M.R., 2006, Width and Thickness of Fluvial Channel Bodies and Valley Fills in the Geological Record: A Literature Compilation and Classification: Journal of Sedimentary Research, v. 76, p. 731-770.

GRENINGER, M.L., KLEMPERER, S.L., and NOKLEBERG, W.J., 1999, Geographic Information Systems (GIS) compilation of geophysical, geologic, and tectonic data for the Circum-North Pacific: U.S. Geological survey Open File Report 99-422, p. 1.

GUOW, M.J.P., and BERENDSEN, H.J.A., 2007, Variability of channel-belt dimensions and the consequences for alluvial architecture: observations from the Holocene Rhine-Meuse Delta (the Netherlands) and Lower Mississippi Valley (U.S.A.): Journal of Sedimentary Research, v. 77, p. 124-138.

HAEUSSLER, P., BRUHN, R., and PRATT, T., 2000, Potential seismic hazards and tectonics of the upper Cook Inlet basin, Alaska, based on analysis of Pliocene and younger deformation: Geological Society of America Bulletin, v. 112, p. 1414.

HAEUSSLER, P., O'SULLIVAN, P., BERGER, A.L., and SPOTILA, J.A., 2008, Synchronous exhumation of the Tordrillo Mountains and Denali (Mt. McKinley), Alaska, around 6 Ma, *in* Freymueller, J.T., Haeussler, P.J., Wesson, R.L., and Ekstrom, G., eds., Active Tectonics and Seismic Potential of Alaska: Washington, D.C., American Geophysical Union, p. 269-286

HAEUSSLER, P.J., 2008, An overview of the neotectonics of interior Alaska: Far-field deformation from the Yakutat microplate collision, *in* Freymueller, J.T., Haeussler, P.J., Wesson, R., and Ekstrom, G., eds., Active Tectonics and Seismic Potential of Alaska: Washington, D.C., AGU Monograph, p. 83-108.

HAEUSSLER, P.J., BRADLEY, D.C., WELLS, R.E., and MILLER, M.L., 2003, Life and death of the Resurrection plate: Evidence for its existence and subduction in the northeastern Pacific in Paleocene–Eocene time: Geological Society of America Bulletin, v. 115, p. 867-880.

HAEUSSLER, P.J., and SALTUS, R.W., 2011, Location and Extent of Tertiary Structures in Cook Inlet Basin, Alaska, and Mantle Dynamics that Focus deformation and Subsidence, *in* Dumoulin, J.A., and Galloway, J.P., eds., Studies by the U.S. Geological Survey in Alaska 2008-2009: U.S. Geological Survey Professional Paper 1776-D, p. 26.

HAYES, J.B., HARMS, J.C., and WILSON, T., 1976, Contrasts between braided and meandering stream deposits, Beluga and Sterling formations (Tertiary), Cook Inlet, Alaska: Recent and ancient sedimentary environments in Alaska: Anchorage, Alaska, Alaska Geol. Soc.

HELMOLD, K.P., LEPAIN, D.L., WILSON, M.D., and PETERSON, S.C., *In Review*, Petrology and reservoir potential of Tertiary and Mesozoic sandstones, Cook Inlet, Alaska: A preliminary analysis of outcrop samples collected during 2007-2010 field seasons: Division of Geological & Geophysical Surveys Preliminary Interpretive Report.

HERITAGE, G.L., CHARLTON, M.E., and O'REGAN, S., 2001, Morphological Classification of Fluvial Environments: An Investigation of the Continuum of Channel Types: The Journal of Geology, v. 109, p. 21-33.

HITE, D.M., 1976, Some sedimentary aspects of the Kenai Group, Cook Inlet, Alaska, *in* Miller, T.P., ed., Recent and Ancient Sedimentary Environments in Alaska: Proceedings of the Alaska Geological Society Symposium, April 2-4, 1975: Anchorage, p. I1-I23.

HUGGETT, R.J., 2007, Fundamentals of Geomorphology: New York, Routledge.

JORGENSEN, P.J., and FIELDING, C.R., 1996, Facies architecture of alluvial floodbasin deposits: Three-dimensional data from the Upper Triassic Callide Coal Measures of east-central Queensland, Australia: Sedimentology, v. 43, p. 479-495.

KELLY, S., 2006, Scaling and Hierarchy in Braided Rivers and Their Deposits: Examples and Implications for Reservior Modeling, *in* Sambrook Smith, G.H., Best, J.L., Bristow, C.S., and Petts, G.E., eds., Braided Rivers; Process, Deposits, Ecology and Management,, International Association of Sedimentologists, p. 75-106.

KIRSCHBAUM, M.A., and MCCABE, P.J., 1992, Controls on the accumulation of coal and on the development of anastomosed fluvial systems in the Cretaceous Dakota Formation of southern Utah: Sedimentology, v. 39, p. 581-598.

KIRSCHNER, C., and LYON, C., 1973, Stratigraphic and tectonic development of Cook Inlet petroleum province: Arctic geology: American Association of Petroleum Geologists Memoir, v. 19, p. 396-407.

KRAUS, M.J., 1996, Avulsion deposits in lower Eocene alluvial rocks, Bighorn Basin, Wyoming: Journal of Sedimentary Research, v. 66, p. 354-363.

LECKIE, D.A., and CRAW, D., 1995, Westerly derived Early Cretaceous gold paleoplacers in the Western Canada foreland basin, southwestern Alberta: tectonic and economic implications: Canadian Journal of Earth Sciences, v. 32, p. 1079-1092.

LECLAIR, S., and BRIDGE, J., 2001, Quantitative interpretation of sedimentary structures formed by river dunes: Journal of Sedimentary Research, v. 71, p. 713.

LEPAIN, D.L., WARTES, M.A., MCCARTHY, P.J., STANLEY, R., SILLIPHANT, L.J., PETERSON, S., SHELLENBAUM, D.P., HELMOLD, K.P., DECKER, P.L., MONGRAIN, J.R., and GILLIS, R.J., 2009, Facies Associations, Sand Body Geometry, and Depositional Systems in Late Oligocene–Pliocene Strata, Southern Kenai Peninsula, Cook Inlet, Alaska: Report on Progress During the 2006–07 Field Seasons, *in* LePain, D.L., ed., Preliminary Results of Recent Geologic Investigations in the Homer-Kachemak Bay Area, Cook Inlet Basin: Progress During the 2006-2007 Field Season: Fairbanks, DGGS, p. 1-32.

LITTLE, T.A., and NAESER, C.W., 1989, Tertiary tectonics of the Border Ranges fault system, Chugach Mountains, Alaska; deformation and uplift in a forearc setting: Journal of Geophysical Research, v. 94, p. 4333-4359.

MAGOON, L.B., ADKINSON, W.L., and EGBERT, R.M., 1976, Map showing geology, wildcat wells, Tertiary plant fossil localities, K-Ar age dates, and petroleum operations, Cook Inlet area, Alaska: U.S. Geological Survey Miscellaneous Investigations Series Map I-1019, scale 1:250,000.

MAKASKE, B., 2001, Anastomosing rivers: A reviewof their classification, origin and sedimentary products: Earth-Science Reviews, v. 53, p. 149-196.

MAKASKE, B., SMITH, D.G., and BERENDSEN, H.J.A., 2002, Avulsions, channel evolution and floodplain sedimentation rates of the anastomosing upper Columbia River, British Columbia, Canada: Sedimentology, v. 49, p. 1049-1071.

McLAURIN, B.T., and STEEL, R.J., 2007, Architecture and origin of an amalgamated fluvial sheet sand, lower Castlegate Formation, Book Cliffs, Utah: Sedimentary Geology, v. 197, p. 291-311.

MERRITT, R.D., LUECK, L.L., RAWLINSON, S.E., BELOWICH, M.A., GOFF, K.M., CLOUGH, J.G., and REININK-SMITH, L.M., 1987, Southern Kenai Peninsula (Homer District) coal-resource assessment and mapping project: Alaska Division of Geological and Geophysical Surveys, p. Public Data File 87-15.

MIALL, A.D., 1977, A Review of the Braided River Depositional Environment: Earth Science Review, p. 1-62.

MIALL, A.D., 1988, Reservoir heterogeneities in fluvial sandstones: lessons from outcrop studies: AAPG Bulletin, v. 72, p. 682-697.

MIALL, A.D., 1994, Reconstructing fluvial macroform architecture from two-dimensional outcrops; examples from the Castlegate Sandstone, Book Cliffs, Utah: Journal of Sedimentary Research, v. 64, p. 146.

MIALL, A.D., 1997, The Geology of Stratigraphic Sequences: Berlin, Springer-Verlag, 427 p.

MIALL, A.D., 2006, The Geology of Fluvial Deposits : Sedimentary Facies, Basin Analysis, and Petroleum Geology: Berlin, Springer, 582 p.

MIALL, A.D., and JONES, B.G., 2003, Fluvial architecture of the Hawkesbury Sandstone (Triassic), near Sydney, Australia: Journal of Sedimentary Research, v. 73, p. 531.

MILLER, K.G., KOMINZ, M.A., BROWNING, J.V., WRIGHT, J.D., MOUNTAIN, G.S., KATZ, M.E., SUGARMAN, P.J., CRAMER, B.S., CHRISTIE-BLICK, N., and PEKAR, S.F., 2005, The Phanerozoic record of global sea-level change: Science (New York, N.Y.), v. 310, p. 1293-8.

MJØS, R., WALDERHAUG, O., and PRESTHOLM, E., 1993, Crevasse splay sandstone geometries in the Middle Jurassic Ravenscar Group of Yorkshire, UK, *in* Marzo, M., and Puigdefabregas, C., eds., Alluvial Sedimentation: International Association of Sedimentologists, Special Publication 17, p. 167-184.

MOHRIG, D., HELLER, P.L., PAOLA, C., and LYONS, W.J., 2000, Interpreting avulsion process from ancient alluvial sequences: Guadalope-Matarranya system (northern Spain) and Wasatch Formation (western Colorado): Geological Society of America Bulletin, v. 112, p. 1787-1803.

MOLL-STALCUP, E.J., 1994, Latest Cretaceous and Cenozoic magmatism in mainland Alaska, *in* Plafker, G., and Berg, H.C., eds., The Geology of Alaska: Boulder, Geological Society of America, p. 589-619.

MORETON, D.J., ASHWORTH, P.J., and BEST, J.L., 2002, The physical scale modelling of braided alluvial architecture and estimation of subsurface permeability: Basin Research, v. 14, p. 265-285.

MORETTI, M., and SABATO, L., 2007, Recognition of trigger mechanisms for soft-sediment deformation in the Pleistocene lacustrine deposits of the SantArcangelo Basin (Southern Italy): Seismic shock vs. overloading: Sedimentary Geology, v. 196, p. 31-45.

MOROZOVA, G.S., and SMITH, N.D., 2000, Holocene avulsion styles and sedimentation patterns of the Saskatchewan River, Cumberland Marshes, Canada: Sedimentary Geology, v. 130, p. 81-105.

MUMPY, A.J., JOL, H.M., KEAN, W.F., and ISBELL, J.L., 2007, Architecture and sedimentology of an active braid bar in the Wisconsin River based on 3-D ground penetrating radar, *in* Baker, G.S., and Jol, H.M., eds., Stratigraphic Analyses Using GPR, Geological Society of America, Special Paper 432, p. 111-131.

NADON, G.C., 1994, The genesis and recognition of anastomosed fluvial deposits: Data from the St. Mary River Formation, southwestern Alberta, Canada: Journal of Sedimentary Research, v. 64, p. 451-463.

NANSON, G.C., 1980, Point bar and floodplain formation of the meandering Beatton River, northeastern British Columbia: Sedimentology, v. 27, p. 3-29.

NANSON, G.C., and KNIGHTON, A.D., 1996, Anabranching rivers: their cause, character and classification: Earth surface processes and landforms, v. 21, p. 217-239.

NEUWERTH, R., SUTER, F., GUZMAN, C.A., and GORIN, G.E., 2006, Soft-sediment deformation in a tectonically active area: The Plio-Pleistocene Zarzal Formation in the Cauca Valley (Western Colombia): Sedimentary Geology, v. 186, p. 67-88.

NOKLEBERG, W.J., PLAFKER, G., and WILSON, F.H., 1994, Geology of south-central Alaska, *in* Plafker, G., and Berg, H.C., eds., The Geology of Alaska: Boulder, CO, Geological Society of America, p. 311-366.

NORTH, C.P., NANSON, G.C., and FAGAN, S.D., 2007, Recognition of the Sedimentary Architecture of Dryland Anabranching (Anastomosing) Rivers: Journal of Sedimentary Research, v. 77, p. 925-938.

NYE, C., WYSS, M., RATCHKOVSKI, N.A., and FLETCHER, H., 2002, Magmatism in the Denali Volcanic Gap, southern Alaska: Eos Transactions, American Geophysical Union, v. 83.

OWEN, G., 1987, Deformation processes in unconsolidated sands: Geological Society, London, Special Publications, v. 29, p. 11-24.

PAVLIS, T.L., and ROESKE, S.M., 2007, The Border Ranges Fault System, southern Alaska, *in* Ridgway, K.D., Trop, J.M., Glen, J.M.G., and O'Neill, J.M., eds., Tectonic growth of a collisional margin: crustal evolution of southern Alaska: Boulder, Geologic Society of America Special Paper, p. 95-128.

PLAFKER, G., 1987, Regional geology and petroleum potential of the northern Gulf of Alaska continental margin, *in* Scholl, D.W., Grantz, A., and Vedder, J.G., eds., Geology and resource potential of the continental margin of western North America and adjacent ocean basins-Beaufort Sea to Baja California Earth Science Series: Houston, Circum-Pacific Council for Energy and Mineral Resources, p. 229-268.

PLAFKER, G., MOORE, J.C., and WINKLER, G.R., 1994, Geology of the southern Alaska margin, *in* Plafker, G., and Berg, H.C., eds., The Geology of Alaska: Boulder, CO, Geological Society of America, p. 311-366.

PLINT, A.G., 1983, Sandy fluvial point-bar sediments from the Middle Eocene of Dorset, England, *in* Collinson, J.D., and Lewin, J., eds., Modern and Ancient Fluvial Systems, International Association of Sedimentologists, Special Publication.

PLINT, A.G., MCCARTHY J. PAUL, AND UBIRATAN, F. FACCINI, 2001, Nonmarine sequence stratigraphy: updip expression of sequence boundaries and systems tracts in a high resolution framework, Cenomanian Dunvegan Formation, Alberta foreland basin, Canada: AAPG Bulletin, v. 85, p. 1967-2001.

RAWLINSON, S.E., 1984, Environments of deposition, paleocurrents, and provenance of Tertiary deposits along Kachemak Bay, Kenai Peninsula, Alaska, *in* Nilsen, T.H., ed., Fluvial sedimentation and related tectonic framework, western North America: Amsterdam, Elsevier, p. 421-442.

REININK-SMITH, L., 2010, Variations in alder pollen pore numbers--a possible new correlation tool for the Neogene Kenai lowland, Alaska: Palynology, v. 34, p. 180-194.

REININK-SMITH, L., and LEOPOLD, E., 2005, Warm Climate in the Late Miocene of the South Coast of Alaska and the Occurrence of Podocarpaceae Pollen: Palynology, v. 29, p. 205-262.

REININK-SMITH, L.M., 1995, Tephra Layers as Correlation Tools of Neogene Coal-bearing Strata from the Kenai Lowland, Alaska: Geological Society of America Bulletin, v. 107, p. 340-353.

RIDGWAY, K.D., TROP, J.M., and FINZEL, E.S., 2011, Modification of continental forearc basins by flat-slab subduction processes: A case study from southern Alaska, *in* Busby, C., and Pérez, A.A., eds., Tectonics of Sedimentary Basins: Recent Advances: Hoboken, Wiley, p. 664.

SAMBROOK SMITH, G., ASHWORTH, P.J., BEST, J.L., WOODWARD, J., and SIMPSON, C.J., 2006, The sedimentology and alluvial architecture of the sandy braided South Saskatchewan River, Canada: Sedimentology, v. 53, p. 413-434.

SAMBROOK SMITH, G., GREGORY, H., ASHWORTH, P., BEST, J., WOODWARD, J., and SIMPSON, C., 2005, The morphology and facies of sandy braided rivers: some considerations of scale invariance.

SAMBROOK SMITH, G.H., ASHWORTH, P.J., BEST, J.L., WOODWARD, J., and SIMPSON, C.J., 2009, The Morphology and Facies of Sandy Braided Rivers: Some Considerations of Scale Invariance, *in* Blum, M.D., Marriott, S.B., and Leclair, S.F., eds., Fluvial Sedimentology VII: Oxford, Blackwell Publishing Ltd., p. 145-158.

SAPOZHNIKOV, V., and FOUFOULA-GEORGIOU, E., 1996, Self-affinity in braided rivers: Water Resources Research, v. 32, p. 1429-1439.

SAPOZHNIKOV, V., and FOUFOULA-GEORGIOU, E., 1997, Experimental evidence of dynamic scaling and self-organized criticality in braided rivers: Water Resources Research, v. 33, p. 1983-1991.

SAPOZHNIKOV, V., MURRAY, B., PAOLA, C., and FOUFOULA-GEORGIOU, E., 1998, Validation of braided-stream models: Spatial state-space plots, self-affine scaling and island shapes: Water Resources Research, v. 34, p. 2353-2364.

SKELLY, R.L., BRISTOW, C.S., and ETHRIDGE, F.G., 2003, Architecture of channel-belt deposits in an aggrading shallow sandbed braided river: the lower Niobrara River, northeast Nebraska: Sedimentary Geology, v. 158, p. 249-270.

SMITH, D.G., 1976, Effect of vegetation on lateral migration of anastomosed channels of a glacial meltwater river: Geological Society of America Bulletin, v. 87, p. 857-860.

SMITH, D.G., 1978, Some Comments on Terminology for Baus in Shallow Rivers, *in* Miall, A.D., ed., Fluvial Sedimentology, Canadian Society of Petroleum Geology Memoirs, p. 85-88.

SMITH, D.G., 1983, Anastomosed fluvial deposits: modern examples from Western Canada, *in* Collinson, J.D., and Lewin, J., eds., Modern and Ancient Fluvial Systems: , International Association of Sedimentologists, p. 155-168.

SMITH, D.G., and PUTNAM, P.E., 1980, Anastomosed river deposits: Modern and ancient examples in Alberta, Canada: Canadian Journal of Earth Sciences, v. 17, p. 1396-1406.

SMITH, D.G., and SMITH, N.D., 1980, Sedimentation in anastomosed river systems: examples from alluvial valleys near Banff, Alberta: Journal of Sedimentary Petrology, v. 50, p. 157-164.

SMITH, N.D., CROSS, T.A., DUFFICY, J.P., and CLOUGH, S.R., 1989, Anatomy of an avulsion: Sedimentology, v. 36, p. 1-23.

SMITH, N.D., and PEREZ-ARLUCEA, M., 1994, Fine-grained splay deposition in the avulsion belt of the Lower Saskachewan River, Canada: Journal of Sedimentary Research, v. 64, p. 159-168.

STANLEY, R., CHARPENTIER, R.R., COOK, T.A., HOUSEKNECHT, D.W., KLETT, T.R., LEWIS, K.A., LILLIS, P.G., NELSON, P.H., PHILLIPS, J.D., POLLASTRO, R.M., POTTER, C.J., ROUSE, W.A., SALTUS, R.W., SCHENK, C.J., SHAH, A.K., and VALIN, Z.C., 2011, Assessment of Undiscovered Oil and Gas Resources of the Cook Inlet Region, South-Central Alaska: USGS National Assessment of Oil and Gas Fact Sheet, p. 2.

STOCK, J., and MOLNAR, P., 1988, Uncertainties and implications of the Late Cretaceous and Tertiary position of North America relative to the Farallon, Kula, and Pacific Plates: Tectonics, v. 7, p. 1339-1384.

SWENSON, R., 2002, Introduction to Tertiary tectonics and sedimentation in the Cook Inlet basin, *in* Dallegge, T., ed., Geology and Hydrocarbon Systems of the Cook Inlet Basin, Alaska: American Association of Petroleum Geologists Pacific Section/Society of Petroleum Engineers Pacific Regional Conference, May 23-24, 2002, Anchorage, Alaska, p. 11-20.

TALBOT, M.R., and ALLEN, P.A., 1996, Lakes, *in* Reading, H.G., ed., Sedimentary Environments: Processes, Facies, and Stratigraphy: Oxford, Blackwell Scientific Publications, p. 83-124.

TORNQVIST, T.E., 1993, Holocene alternation of meandering and anastomosing fluvial systems in the Rhine-Meuse Delta (central Netherlands) controlled by sea level rise and subsoil erodibility: Journal of Sedimentary Petrology, v. 63, p. 683-693.

TORNQVIST, T.E., VAN REE, M.H.M., and FAESSEN, E.L.J.H., 1993, Longitudinal facies architectural changes of a Middle Holocene anastomosing distributary system (Rhine-Meuse Delta, central Netherlands), *in* Fielding, C.R., ed., Current Research in Fluvial Sedimentology, Sedimentary Geology, p. 203-219.

TRIPLEHORN, D.M., TURNER, D.L., and NAESER, C.W., 1977, K-Ar and Fission-track Dating of Ash Partings in Coal Beds from the Kenai Peninsula, Alaska: A Revised Age for the Homerian Stage-Clamgulchian Stage Boundary: Geological Society of America Bulletin, v. 88, p. 1156-1160.

TROP, J.M., 2008, Latest Cretaceous forearc basin development along an accretionary convergent margin: South-central Alaska: Geological Society of America Bulletin, v. 120, p. 207-224.

TROP, J.M., RIDGWAY, K.D., and SPELL, T.L., 2003, Sedimentary record of transpressional tectonics and ridge subduction in the Tertiary Matanuska Valley-Talkeetna Mountains forearc basin, southern Alaska: Geological Society of America Special Papers, v. 371, p. 89-118.

WILSON, F.H., HULTS, C.P., SCHMOLL, H.R., HAEUSSLER, P., SCHMIDT, J.M., YEHLE, L.A., and LABAY, K.A., 2009, Preliminary geologic map of the Cook Inlet Region, Alaska-including parts of the Talkeetna, Talkeetna Mountains, Tyonek, Lake Clark, Kenai, Seward, Iliamna, Seldovia, Mount Katmai, and Afognak 1:250,000 Quadrangles: U.S. Geological Survey Open-File Report 2009-1108, scale 1:250,000.

WOLFE, J., 1994, An analysis of Neogene climates in Beringia: Palaeogeography, Palaeoclimatology, Palaeoecology, v. 108, p. 207-216.

ZACHOS, J., PAGANI, M., SLOAN, L., THOMAS, E., and BILLUPS, K., 2001, Trends, Rhythms, and Aberrations in Global Climate 65 Ma to Present: Science, v. 292, p. 686-693.

Chapter 3

A Terrestrial Multi-Proxy Late Miocene to Pliocene Climate Reconstruction, Cook Inlet Forearc Basin, Alaska[1]

3.1 Abstract

The Late Miocene to Pliocene Beluga and Sterling formations are comprised of alluvial sedimentary deposits that form part of a forearc basin exposed along the southern Kenai Peninsula and, intermittently, along the northwestern margin of Cook Inlet, southern Alaska. A multi-proxy analysis of these deposits, combining palynology and carbon stable isotopic values of palynological separates, is used to reconstruct paleoenvironmental conditions from ~11 Ma to ~6 Ma. Pollen of thermophilic taxa was recovered from both formations, indicating the persistence of relatively warm conditions until ~6 Ma in southern Alaska. Our samples record the presence of shrubs, herbs, and dispersed trees on floodplains. Estimates of mean annual precipitation (MAP) derived from carbon stable isotopes reveal the highest average MAP with the greatest variability at ~8 Ma, coeval with a North Pacific climate optimum and increased sea surface temperatures in the Alaska Gyre. Globally, this time period coincides with intensification of the Indian, Asian, and Andean monsoons, and increasing aridity in the Western United States. Improvements in temporal and spatial reconstructions with respect to the rise of the central and western Alaska Range indicate that a pulse of uplift occurred after deposition of the Beluga Fm. and most of the Sterling Fm. exposed in outcrop. Consequently, associated orographic effects are not likely drivers of regional paleoclimate.

---

[1] Mongrain, J., Wooller M., Fowell, S., McCarthy, P., In Prep, A Terrestrial Multi-Proxy Late Miocene to Pliocene Climate Reconstruction, Cook Inlet Forearc Basin, Alaska: for submission to Palaios.

3.2 Introduction

Alluvial sediments of the Late Miocene to Pliocene Beluga and Sterling formations comprise part of the terrestrial forearc basin strata of Cook Inlet, southern Alaska (Calderwood and Fackler, 1972; Boss et al., 1976; Swenson, 2002; LePain et al., 2009). These high latitude formations (paleolatitude approximately the same as modern; Stamatakos et al., 1988) were deposited during the Neogene, a time of relative warmth without elevated levels of greenhouse gasses, especially CO_2 (Pearson and Palmer, 2000; Royer et al., 2001; Tipple et al., 2010). This warm interval in Earth's history has been attributed to an enhanced water cycle (Lyle et al., 2008).

The Beluga and Sterling formations provide a valuable record of high latitude paleoclimate. This study couples palynological techniques with stable isotopic analyses of carbon derived from pollen concentrates, bulk sediment, and coal. The use of palynological separates for $\delta^{13}C$ analyses allows for direct comparison of these palynological and stable isotopic records. With recent advances in the use of $\delta^{13}C$ values to calculate mean annual precipitation (MAP; Diefendorf et al., 2010; Kohn, 2010), estimates of precipitation can be compared to reconstructions of vegetation cover.

Integration of regional studies from high latitudes with those from temperate and tropical latitudes is essential in order to improve our understanding of the transfer of water and heat from low and mid-latitudes toward the poles during the Miocene. In this paper, we document local and regional paleoenvironmental and paleoclimatic conditions, illustrate the utility of integrating palynological and stable isotopic data, and place these high latitude (~60°N) records in the context of other global events (e.g. aridification, monsoon initiation/intensification).

3.3 Geologic Setting

The Cook Inlet forearc basin is part of the northeast-southwest-trending forearc basin that extends from Shelikof Strait in the southwest to the Wrangell Mountains in the northeast (Fig. 3.1). The geologic history of the southern Alaska margin is complicated due to ongoing convergence and subduction from the Jurassic to the present (Fig. 3.2; Plafker et al., 1994).

Regional tectonics in this area is driven, in part, by on-going subduction of the Yakutat Microplate beginning as early as the late Oligocene (Enkelmann et al., 2010). Rotation of the southern Alaska crustal block, driven by the Yakutat Microplate around 6 Ma (Fig. 3.2), has been suggested as a mechanism for the rise of the western Alaska Range (Benowitz, 2011; Haeussler et al., 2008). Alternatively, uplift in the western Alaska Range may be due to progressive deformation inboard of the Yakutat Microplate and not to rotation of the southern Alaska crustal block (Finzel et al., 2011).

Chronostratigraphic control is provided by radiometric dates (^{40}Ar-^{39}Ar and U-Pb) of ash-fall deposits in the Beluga and Sterling Formations, which are preserved primarily in coal seams (Dallegge and Layer, 2004; R. Gillis, unpublished data). These dates allow for correlation of widely spaced stratigraphic sections offset by high angle reverse faults, often with an unknown amount of displacement. This work, along with previous geochronological research (Turner et al., 1980; Triplehorn et al., 1977), chemostratigraphy of ash layers (Reinink-Smith, 1995) and subsurface correlations (Calderwood and Fackler, 1972) provides a robust chronostratigraphic framework for our paleoclimatic interpretations.

3.4 Previous Paleoclimate Research in the Beluga and Sterling fms.

3.4.1 Climate Leaf Analysis Multivariate Program (CLAMP)

A previous study of Cenozoic leaf fossils from Cook Inlet by Wolfe (1994) focused primarily on reconstructing paleotemperature using the Climate Leaf Analysis Multivariate Program (CLAMP). Subsequent re-analysis of the leaf metrics by Yang et al. (2011) generated the entire suite of environmental variables available through CLAMP (Table 3.1). Estimated mean annual temperature (MAT) does not vary appreciably during deposition of the Beluga and Sterling formations, barring a slight increase in cold month mean temperature (CMMT) in the lower Sterling Fm., relative to other sampled intervals. The middle Beluga Fm. was deposited during a period of increased precipitation compared to other intervals in the Beluga and Sterling fms (Yang et al., 2011; Table 3.1). The lower Sterling Fm. has growing season precipitation (GSP), mean monthly growing season precipitation (MMGSP), and three wettest growing season months (3-Wet) precipitation that are similar to the middle and lower Beluga Fm., but the estimated precipitation for the three consecutive driest months (3-Dry) is considerably less than 3-Dry estimates from underlying and overlying samples.

3.4.2 Palynology

Three previous studies have investigated the palynology of the Beluga and Sterling formations. Wolfe et al. (1966) focused primarily on the stratigraphy of the Cook Inlet region. Reinink-Smith (2010) attempted to use changes in the number of pores on *Alnus* pollen grains as a correlation tool. *Alnus* plants produce pollen grains with four to eight pores. A systematic shift to grains with more pores is used to distinguish the Beluga and lower Sterling formations (dominated by grains with 4 pores) from the middle to upper Sterling Fm. (dominated by grains with 5 pores). Reinink-Smith and Leopold (2005) analyzed Homerian (Beluga Fm.) coal facies and found warmth-loving

taxa (thermophiles) including the gymnosperms *Podocarpus* and *Dacrydium*. Their interpretation of the palynological record indicates warmer temperatures than those suggested by CLAMP data (≥ 10°C) in a summer wet/coastal climate (Fig. 3.3).

3.4.3 Regional Paleoclimate Records

The global benthic oxygen isotope record, based on opal, indicates a prolonged climate optimum in the late Early to early Middle Miocene (Zachos et al., 2001). Generally, global temperatures declined throughout the Miocene after this event. However, calcium carbonate records from Ocean Drilling Project (ODP) Site 846, south of the Galapagos Islands, indicate several isotopic excursions that are interpreted to reflect warmer conditions in the Late Miocene (Shackleton et al., 1995).

North Pacific Miocene marine sequences record several negative oxygen isotopic excursions based on *Cibicoides* foraminifera tests (Kennett, 1985). These excursions are interpreted to reflect warm sea-surface temperatures. Barron and Baldauf (1990) refer to these as Climate Optimum 1, ranging from 16 to 15 Ma, Climate Optimum 2, ranging from 11.5 to 10.5 Ma, and Climate Optimum 3, ranging from 7.5 to 6.5 Ma. At ODP Site 572 in the eastern equatorial Pacific, relative increases of *Thalassionema nitzschioides* diatoms, an indicator of reduced equatorial upwelling and polar warming, occur between 8.2 and 7.3 Ma. *T. nitzschioides remains common at this site between* 6.1 and 4.0 Ma, but significant fluctuations in abundance are interpreted to record generally cool, but variable, high-latitude paleotemperatures (Baldauf, 1985; Barron and Baldauf, 1990). Taken together, these records indicate possible warm conditions between 8.2 and 7.3 Ma and cooler, but fluctuating, temperatures between 6.1 and 4.0 Ma (Barron and Baldauf, 1990).

The onset of glaciation in southern Alaska is first recorded by ice-rafted sediment around 6.5 Ma (Krissek, 1995). However, it is difficult to distinguish the effects of orogenesis and subsequent formation of alpine glaciers from the effects of global cooling. Diatoms present only in sea ice (e.g. *Bacteriosira fragilis, Detonula confervacea,* and *Porosira glacialis*) become widespread in the North Pacific by 5.5 Ma (Akiba, 1986; Gladenkov et al., 2002; Barron, 2003; Lyle et al., 2008), and tidewater glaciers are first documented in this region at ~4.3 Ma (Rea and Snoeckx, 1995; Barron, 2003).

3.5 Depositional Environments

3.5.1 Beluga Formation

On the eastern side of the basin, fluvial systems that deposited the Beluga Fm. flowed westward from the accretionary prism. The western side of the basin is less well constrained, but these fluvial systems probably flowed towards the east (Rawlinson, 1984; Helmold et al., 2012; Chapter 4). The Beluga Fm. was deposited predominantly by anastomosing/single thread fluvial systems (Fig. 3.4; Flores and Stricker, 1993; LePain et al., 2009; Chapter 2). A typical Beluga Fm. succession is comprised of a single story sand body that fines upward and is encased by fine-grained mudstone. Sand bodies are rarely multi-storied. Fining-upward sandstones are typically poorly sorted and mud-rich. The sand bodies generally have a convex-up basal contact with rare mudstone rip-up clasts overlying the basal scour; extrabasinal clasts are rarely present at the base (Chapter 2). The most striking feature of Beluga Fm. sand bodies is the concave-up basal contact and flat-topped nature of the upper bounding contact. The sandy fill is typically 2-5 m thick and encased in fine-grained material. When channels are present in laterally extensive outcrops, multiple sandy channel-fills are typically present at, or near, the same stratigraphic level.

3.5.2 Sterling Formation

The Sterling Fm. was deposited in southward-flowing, low sinuosity (Chapter 2), sandy braided fluvial systems sourced, in part, from the magmatic arc of the western Alaska Range (Fig. 3.5; Flores and Stricker, 1992; LePain et al., 2009; Chapter 4). The common occurrence of trough cross-stratified sand bodies bounded by relatively small-scale erosional surfaces, upper flow regime plane beds, and large-scale, high-angle planar tabular cross-beds in association with trough cross-stratified sand bodies overlying erosional basal lags is consistent with studies of modern and ancient sandy braided rivers (Cant and Walker, 1978; Blodgett and Stanley, 1980; Crowley, 1983; Bridge, 1993; Bridge et al., 1998, Best et al., 2003; Miall and Jones, 2003; Miall, 1988 and 1994; Skelley et al., 2003; Bridge and Lunt, 2006; Sambrook Smith et al., 2006; Sambrook Smith et al., 2009; Chapter 2).

3.5.3 Beluga and Sterling fms. overbank deposition

Fine-grained facies from both formations are interpreted as lakes, low-lying floodplains, and distal crevasse splay deposits (LePain et al., 2009; Chapter 2), while organic-rich beds and coal seams are thought to record deposition in swamps, marshes, and mires removed from clastic input (Fielding, 1987; Smith, et al. 1989; Smith and Pérez-Arlucea, 1994). Samples processed for palynological and isotopic analyses were derived primarily from overbank facies described below.

Siltstones and mudstones are typically blocky to platy aggregates with less common laminated, wavy laminated, and massive beds. Color varies from light grey to black. Organic remains range from sub-millimeter, finely macerated fragments to relatively large leaf impressions and vertically oriented tree stumps. Rhythmically-laminated siltstone and silty claystone successions up to several meters thick are present locally and consist of alternating light- and dark-colored laminae ranging from less than one millimeter to approximately one centimeter thick. Laminae are typically arranged in lamina sets to thin bedsets up to a few decimeters thick. Coal beds range from lignite

to sub-bituminous and these commonly include splits of siltstone, claystone, carbonaceous mudstone, and volcanic ash (tonsteins; Flores et al., 2004; LePain et al., 2009; Chapter 2).

Palynological and stable isotope samples are also from crevasse splays and crevasse splay complexes. Crevasse splays and crevasse splay complexes are composed of relatively thin sheet-like beds of sand, silt, and finer-grained material with less common, small-scale (<2m) channel-fill sand bodies. Massive sandstone and siltstone beds are common, with ripple cross-laminated sandstone and siltstone locally prominent, and rare trough cross-bedded sandstones (LePain et al., 2009; Chapter 2). The sheet-like sand bodies are typically less than a meter thick and are interbedded with finer-grained material, typically on a decimeter scale. Sand bodies are typically massive to ripple cross-laminated with sheet-like to lobate geometries. Root traces are locally present and the entire package of sand is typically encased in mudstone (Chapter 2).

3.6 Methods

Samples were collected from siltstone beds in 20 measured sections located on the eastern and western margins of Cook Inlet and the northern shore of Kachemak Bay on the Kenai Peninsula (Fig. 3.6). Where possible, samples were collected every 0.5 m. However, significant stratigraphic separation can occur between siltstone beds. Coal units were not sampled, as the work of Reinink-Smith and Leopold (2005) thoroughly documents the palynology of this facies.

3.6.1 Palynological Methods

Approximately 20 g of each sample was crushed and prepared following a modified version of the techniques outlined by Traverse (2008). Samples were placed in a 10% hydrochloric acid bath for 24 hours, followed by 24 hours in a hydrofluoric acid bath. Samples were rinsed and washed through a 250 μm sieve to remove larger organic and mineral fragments. Nitex cloth with a 10 μm mesh was used to remove clay. The largest departure from Traverse (2008) was the use of

sodium polytungstate for heavy liquid separation, instead of zinc chloride. Slides were prepared using glycerin jelly and sealed with clear nail polish to prevent oxidation. Some samples were outsourced for processing by Global Geolabs, Ltd., Medicine Hat, Alberta, Canada, using the method above. Counting (at least 300 grains per sample) was performed by A. Krumhardt, University of Alaska Geophysical Institute and P. Zippi at Biostratigraphy.com, LLC. The number of pores present on *Alnus* grains was recorded for small number of samples (n=9) from the oldest Beluga Fm. and the youngest Sterling Fm. in order to evaluate the reliability of this pollen genus as a correlative tool (Reinink-Smith, 2010). Palynomorphs were assigned to extant plant families based on comparison with modern reference slides.

Indices of canopy density and paludification were calculated (White et al., 1997). Paludification indicates the degree of saturation, based on the ratio of terrestrial angiosperm pollen grains to *Sphagnum* spores. A paludification ratio of 15 indicates the boundary between more saturated (~pond) and less saturated organic material (floodplain; White et al., 1997). Samples without *Sphagnum* are removed from the data set. Canopy density is determined by the ratio of shrub and herb pollen to tree pollen. *Betula*-type pollen are not included in the calculation of this index as this pollen type includes shrub and tree growing habits. Ratios less than approximately 0.15 indicate closed canopy forest conditions (White et al., 1997).

Due to factors such as differential pollen productivity (White et al., 1997), the frequency of a taxon in the pollen spectrum is not indicative of its frequency in the vegetation. Hence, reconstructions of saturation, canopy density or ground cover based on palynological indices are approximations, and changes in these indices do not translate to linear changes in vegetation cover. Furthermore, due to evolutionary changes in physiognomy and climate tolerance, the reliability of these indices decreases with increasing age. Consequently, these indices are most reliable for

the Holocene and generally not considered appropriate for samples older than the Cenozoic (e.g. Wing and Greenwood, 1993; Mosbrugger and Utescher, 1997; Little et al., 2010).

3.6.2 Carbon Stable Isotope Methods

The palynomorph-rich organic residue remaining after palynological processing was used for stable carbon isotope analyses. Samples were analyzed using an ECS4010 Elemental Analyzer (EA) attached via a Conflow III to a Thermo Finnigan Deltaplus Isotope Ratio Mass Spectrometer (IRMS) at the Alaska Stable Isotope Facility, University of Alaska Fairbanks. Results are expressed in standard per mil (‰) units relative to the Vienna Peedee Belemnite (VPDB).

We applied the equations developed by Diefendorf et al. (2010) and Kohn (2010) relating the isotopic carbon ratio of leaves to MAP. We elected to use both equations to better understand MAP, as different mathematical approaches and data sets were used to develop these equations (Freeman et al., 2011; Kohn, 2011). Equations for estimating MAP used herein are based on $\delta^{13}C$ values of leaves. In order to estimate MAP from palynological separates, we assume that the $\delta^{13}C$ values of pollen and spores are similar to those of leaves from the same plants. The carbon stable isotope difference between modern pollen, stem, and leaf tissues in the same species is ±3.00‰ for >90% of plants and much less for some phylogenetic clades (e.g., Cornales and Ericales; Jahren, 2004). Jahren (2004) infers that $\delta^{13}C$ values of fossil pollen can be used to infer $\delta^{13}C$ values of ancient plant communities to within 1.5‰.

The Diefendorf et al. (2010) equation is:

$$\Delta_{leaf} = 5.54(\pm 0.22) * \log10\,(MAP) + 4.07(\pm 0.70) \qquad \text{Equation 3.1}$$

Where Δ_{leaf} is equal to:

$\Delta_{leaf} = (\delta^{13}C_{atm} - \delta^{13}C_{leaf})/(1+\delta^{13}C_{leaf}/10^3)$ Equation 3.2

A significant departure from the approach applied by Diefendorf et al. (2010) is that these authors used plant functional type to adjust their Δ_{leaf} values (e.g. deciduous angiosperms and evergreen plants have a Δ_{leaf} difference of 2.7). Although we could have employed a similar correction based on the frequency of different functional types in the palynological assemblages, this assumes that non-pollen organic detritus in the residues has the same ratio of plant functional types as the pollen assemblages. This seemed unlikely, so we did not apply the correction.

The Kohn (2010) equation for estimating MAP based on the $\delta^{13}C$ value of C_3 leaves is:

$\delta^{13}C$ (‰, VPDB) = -10.29 + 1.9 x 10^{-4} Altitude (m) - 5.61 $\log_{10}$ (MAP + 300, mm a^{-1}) - 0.0124 Abs (latitude, °) Equation 3.3

We used modern latitudes, as plate reconstructions indicate little change in the position of the Cook Inlet basin since the Miocene (Nokleberg et al., 1998). Since the basin had a high subsidence rate (Haeussler and Saltus, 2011), altitude is assumed to be near sea level.

Using the chronologic framework of Dallegge and Layer (2004), updated with U-Pb ages from R. Gillis (unpublished data), we were able to determine the approximate ages of our samples and estimate atmospheric $\delta^{13}C$. Tipple et al., (2010) reconstructed atmospheric $\delta^{13}C$ values from benthic foraminifera for the last ~ 65 Ma. Atmospheric $\delta^{13}C$ values appear to be fairly stable from ~12 Ma until the Early Pliocene encompassing all of the samples in this study. The average $\delta^{13}C_{CO2}$ value during this interval is -6.5‰ (Tipple et al., 2010).

3.7 Results

Twenty-seven plant families are represented in the palynological assemblages, including 32 genera of tree and shrub taxa, 14 herbs and forbs, 11 aquatic taxa, 9 pteridophytes, 8 bryophytes, and 13 fungi taxa. Eleven genera are gymnosperms, including *Podocarpus* and *Dacrydium*, and 28 genera are angiosperms (Table 3.2). Palynological data are plotted in stratigraphic and chronological order; clusters of data are from the same outcrop with age offsets between outcrops, so that the age scale is not linear (Fig. 3.7). *Alnus* grains are dominated by the 4-pored variety throughout our record. Contrary to the results of Reinink-Smith (2010) no systematic shift to higher percentages of *Alnus* grains with more pores is found in younger strata (Table 3.3, Fig. 3.8).

The pollen and spore indices record dominance by shrubs, herbs and forbs (Fig. 3.9). Canopy density index indicates open canopy conditions in 89% of the samples (Fig. 3.9). The paludification index suggests that 40% of samples are from well-drained facies (Fig. 3.9).

The $\delta^{13}C$ values of the palynological separates vary from -24.7‰ to -29.7‰; (Fig. 3.10). The variations in MAP are due to variations in the $\delta^{13}C$ value. Estimates of MAP vary considerably in space and time, but the two equations give systematically different results. Estimates based on the Kohn (2010) equation (KE) average 380 mm a^{-1} with a minimum value of -26 mm a^{-1} and a maximum value of 1902 mm a^{-1} (Fig. 3.11, Table 3.4). Estimates based on the Diefendorf et al. (2010) equation (DE) average 1100 mm a^{-1} with a minimum value of 420 mm a^{-1} and a maximum of 3900 mm a^{-1} (Fig. 3.11, Table 3.4). KE estimates of MAP during deposition of the oldest Beluga Fm. sediments exposed in outcrop average 160 mm a^{-1} (minimum: -4 mm a^{-1}, maximum: 776 mm a^{-1}), DE estimates average 750 mm a^{-1} (minimum: 463 mm a^{-1}, maximum: 1825 mm a^{-1}; Fig. 3.11). MAP estimates for samples from the youngest Beluga Fm. average 290 mm a^{-1} (minimum: -26 mm a^{-1}, maximum: 689 mm a^{-1}) according to the KE and 970 mm a^{-1} (minimum:

423 mm a^{-1}, maximum: 1654 mm a^{-1}; Fig. 3.11) according to the DE. Samples from the transitional interval between the Beluga and Sterling Fms. and/or the oldest Sterling Fm. have average MAPs of 630 mm a^{-1} (KE minimum: 161 mm a^{-1}, KE maximum: 1902 mm a^{-1}) and 1600 mm a^{-1} (DE minimum: 736 mm a^{-1}, DE maximum: 3887 mm a^{-1}) and record the most variable MAP of any interval according to both equations. The youngest Sterling Fm. samples, including samples near the type section of the Clamgulchian Stage in Clam Gulch (Fig. 3.6), have average MAPs of 250 mm a^{-1} (KE minimum: 52 mm a^{-1}, KE maximum: 692 mm a^{-1}) and 900 mm a^{-1} (DE minimum: 554 mm a^{-1}, DE maximum: 1664 mm a^{-1}; Fig. 3.11; Table 3.4).

3.8 Discussion

3.8.1 Implications of Floral Communities

Our palynological record is more diverse than the data previously presented by Wolfe et al. (1966). Our results, combined with previous data from coal facies (Reinink-Smith and Leopold, 2005), allow for a more complete understanding of the vegetational communities and their distribution among peat swamps, floodplain, and lake facies in the Beluga and Sterling formations. Overall, Reinink-Smith and Leopold (2005) report the highest diversity assemblages, including more abundant and diverse thermophile tree taxa. The coal facies likely record local conditions, while floodplain facies record both a local record and a more regional, integrated one due to stream transportation. However, the Beluga and Sterling formations are derived primarily from three main source areas: 1) the volcanic arc, 2) much older, weakly to pervasively metamorphosed marine sediments of the accretionary prism, and 3) igneous intrusions of the western Alaska Range (Finzel, 2010; Helmold et al., 2012; Chapter 4). These areas are not likely to be a source of reworked palynomorphs (Reinink-Smith and Leopold, 2005). Trop et al. (2003) suggested that eroded sediment from the Matanuska Forearc Basin was transported into the Cook Inlet Basin. However, the youngest sediments from the Matanuska basin are from the

Oligocene Tsadaka Fm.; neither we nor Reinink- Smith and Leopold (2005) recovered palynomorphs diagnostic of this age.

We extend the record of Mixed Northern Hardwood and Mixed Mesophytic forests (Wolfe et al., 1966; Reinink-Smith and Leopold, 2005) into the upper Sterling Fm., stratigraphically above the type section at Clam Gulch (Fig. 3.6). Thermophilic taxa are missing from the youngest sample (Fig. 3.7), and their absence may represent the cooling of southern Alaska past the threshold tolerance of these warmth-loving trees.

Two pollen indices help to better understand the paleoenvironment of the Beluga and Sterling formations (Fig. 3.9). The canopy density index indicates open canopy conditions existed on the floodplains and that shrubs, mostly *Alnus*, dominated these environments (Fig. 3.9). Variability within an outcrop (i.e., over a small time interval) is fairly low with respect to these two indices and open canopy conditions are recorded by the majority of samples. Closed canopy conditions are usually characterized as coming from well-drained facies, and they are found in both the Beluga and Sterling fms. and on both sides of the basin. The paludification index is the most variable, suggesting that our samples are from a variety of well-drained floodplain and saturated organic facies.

The correlation technique developed by Reinink-Smith (2010) indicated that Beluga and lower Sterling fms. were dominated by 4 -pored *Alnus* grains and that the upper Sterling Fm. was dominated (32-67%) by 5-pored *Alnus* grains with an accompanying increase in 6-, 7-, and 8-pored grains. No dominance of *Alnus* grains with 4+ pore numbers is observed in any of our samples (Fig. 3.8; Table 3.3). This suggests that this correlation technique is either unreliable or applicable only to coal facies.

Our data suggest that the floodplains were characterized by open canopy conditions with shrubs and, less commonly, herbs dominating the vegetation (Fig. 3.9). Reinink-Smith and Leopold (2005) did not estimate canopy density, but their figure 3.9 indicates closely-spaced fossilized tree stump horizons within a coal seam; this would probably have been a closed canopy forest. Additionally, Reinink-Smith and Leopold (2005) document the presence of vitrite, a microlithotype characteristic of forested swamps, indicating that trees were likely a larger component of the vegetation in the coal facies.

3.8.2 Precipitation Estimates

MAP estimates based on the DE are always larger than those based on the KE, with an average difference of 740 mm a^{-1}, a minimum difference of 450 mm a^{-1} and a maximum difference of almost 2000 mm a^{-1} (Table 3.4). The KE probably underestimates MAP, as the vegetation communities found in the palynological analysis are not consistent with these low precipitation amounts (Fig. 3.7; Table 3.2). Furthermore, such low values contradict estimates based on other proxies. For example, estimates of July precipitation based on hardwood tree pollen for the upper Beluga Fm. are 60-200 mm (Reinink-Smith and Leopold, 2005; Thompson et al., 2000).

The CLAMP method is capable of estimating growing season precipitation and should at least be similar to MAP estimates. KE estimates also differ considerably from MAP determined by CLAMP analyses on Beluga and Sterling samples (Yang et al., 2011). Comparison of DE estimates of MAP with CLAMP analysis (Tables 3.1, 3.4) suggests that the DE produces more reliable MAP estimates for the Beluga and Sterling fms. than the KE.

Based on CLAMP, average growing season precipitation (GSP; Table 3.1) throughout the entire Beluga and Sterling Fm. is ~760 mm a^{-1} while the DE estimates MAP at ~1100 mm a^{-1} (Table 3.4). The difference between DE MAP estimates based on $\delta^{13}C$ values and GSP calculated by

CLAMP allows for an estimate of non-growing season precipitation. Using this method, we determine that the majority of precipitation fell during the growing season; ~25% to as little as ~8% fell outside the growing season.

3.8.3 Possible Regional Tectonic Effects

Climate may have been altered by local and/or regional tectonic events during deposition of the Beluga and Sterling Fms., including orographic effects associated with uplift of the Alaska Range. However, the topography of the western Alaska Range was probably not broad and/or high enough prior to ~6 Ma to significantly alter climate patterns (Haeussler et al., 2008; Benowitz, 2011; Finzel, 2010). Climate records from the interior of Alaska and northwest Canada indicate that, vegetation did not change to a colder and drier community until after ~6 Ma (White et al., 1997). Furthermore uplift in the western portion of the Alaska Range occurred ~6 Ma (Haeussler et al., 2008; Benowitz, 2011).

The transgression and drowning of the Bering Strait probably also influenced climate patterns in Alaska, but the strait is not thought to have been inundated by marine waters until around 5.3 Ma (Gladenkov et al., 2002). This regional event post-dates our samples, suggesting that it did not influence the vegetation or climate of the Sterling and Beluga formations.

3.8.4 Correlation with the Pacific Ocean Climate Record

Three climatic optima are identified in the North Pacific during the Middle to Late Miocene based, in part, on oxygen stable isotope ratios of foraminifera tests (Kennett, 1985; Barron and Baldauf, 1990). The latter two optima occurred ~11 Ma and ~7 Ma, during deposition of the Beluga and Sterling formations. The upper Beluga Fm., near the conformable boundary with the Sterling Fm. (Chapter 2) has an U-Pb age of ~11.1 Ma (R. Gillis, unpublished data). Samples from this interval have an average DE MAP of 650 mm a^{-1}, similar to modern precipitation levels at Homer,

AK (Alaska Climate Research Center, 2012). The average DE MAP estimates for ~11 Ma is 715 mm a^{-1} and this is slightly lower than the average Beluga Fm. DE MAP of 840 mm a^{-1} (Fig. 3.11). Given these results, the second thermal climate optimum (~11 Ma) of Barron and Baldauf (1990) seems to have a diminished effect on terrestrial precipitation.

The youngest of the three climatic optima is chronologically less well constrained. Lyle et al., (2008) caution that the biostratigraphic ages in Kennett (1985) used to construct the Barron and Baldauf (1990) climatic optimum chronology need to be adjusted to modern age models. This may require adjustments in the Miocene climatic optimum chronology of ~1 Ma or more.

Higher average MAP estimates with greater than average variability occur at ~8.5 Ma in the upper Beluga to lower Sterling fms (Fig 3.11). Results from CLAMP (Wolfe 1994; updated by Yang et al., 2011) indicate a warm interval during the Middle Homerian (equivalent to the middle Beluga Fm.). The MAP variability and elevated temperature estimates (Wolfe 1994; updated by Yang et al., 2011) are slightly older than ~7 Ma (± 1; Lyle et al. 2008), but may nevertheless represent the third climatic optimum, given errors in dating.

Summer sea surface temperatures (SST) during the Late Miocene in the Alaska Gyre, part of the North Pacific Gyre, are estimated to have been 5° C higher than today until ~8 Ma. Decreases in SST continued into the early Pliocene (Romine, 1985). The warm sea surface temperatures of the Alaska Gyre may be a regional expression of the third climate optimum of Barron and Baldauf (1990) and are likely responsible for northward transport of higher amounts of moisture and accompanying latent heat that allowed thermophilic taxa to remain as long as they did in Cook Inlet. The decline in SST may be responsible for variable precipitation ~ 8.1 Ma (Fig. 3.11) in the Cook Inlet region.

3.8.5 Implications for Southern Alaska

A significant increase in the abundance of Poaceae pollen (i.e., "true grasses") is associated with high and variable MAP at ~ 8.1 Ma (Fig. 3.7, 3.11). Pollen identification does not allow interpretation of photosynthetic pathways in grasses (e.g. C_3 vs. C_4); but the presence of C_4 plants in the Beluga and Sterling formations is very unlikely given that they spread from low latitudes and did not become abundant in what is now Oregon, USA until ~7 Ma (Retallack, 2001). Likewise, a simple two end-member mixing model using typical $\delta^{13}C$ values for C_4 and C_3 plants (Kohn, 2011; O'Leary, 1988) gives results too low to allow for much, if any, material from a C_4 source in the Beluga and Sterling fms. Therefore, the $\delta^{13}C$ values in our study are considered to be derived primarily or entirely from C3 plants.

An increase in grass pollen coincident with greater variation in MAP estimates may indicate a change in precipitation seasonality. However, changes in precipitation amount and timing must have been below the tolerance threshold for trees and shrubs, as there is no apparent turnover in taxa (Fig. 3.7). On the other hand, there is a significant change in the relative abundance of tree and shrub taxa during the ~8.1 Ma interval. Specifically, *Alnus* reaches its highest abundances at this time along with undifferentiated Pinaceae. Many of the other tree taxa decline, particularly Taxodiaceae/Taxaceae/Cupressaceae, *Picea* and, to a lesser degree, *Pinus*, *Larix/Psuedotsuga*, *Abies*-type, and the thermophiles (Fig. 3.7).

Alnus is associated with higher amounts of moisture in riparian zones and likely adapted to the higher MAP observed ~8 Ma (Burns and Hankala, 1990). The apparent decrease of many other tree and shrub taxa may be due to changes in the amount and timing of precipitation that allowed *Alnus* and Poaceae pollen to become relatively abundant. This is supported by CLAMP results (Table 3.1) that indicate that the lower Clamgulchian Stage (equivalent to the lower Sterling Fm.,

~8 Ma), shows a dramatic decrease in the mean three driest growing season months (Wolfe, 1994; Yang et al., 2011).

3.8.6 Correlation with Global Events

For the past 25 Ma atmospheric CO_2 concentrations have been stable at ~6.5 ‰, despite paleoclimate studies indicating relatively warm temperatures in the Miocene (Zachos et al., 2001; Pearson and Palmer, 2000; Royer et al., 2001; Pagani, et al., 1999a, b). The Miocene thermal maximum is attributed to an enhanced water cycle (Lyle et al., 2008); subsequent fluctuations and a general decrease in the water cycle coincide with the loss of thermophilic taxa in Alaska (Fig. 3.7; White et al., 1997).

The late Miocene terrestrial record includes a number of well-documented changes in precipitation and the timing of these events correlates with changes in MAP estimates for the Cook Inlet region. The intensification of the Asian and Indian monsoons occurred ~8 Ma (Filippelli, 1997; Hoorn et al., 2000) likely due to changes in the global water cycle (Lyle et al., 2008). This intensification is hypothesized to have resulted in changes in vegetation communities in the Himalayan foothills and Gangetic floodplain from subtropical and temperate broadleaf forests to grasslands at about 8 Ma. By about 6.5 Ma, grasslands were well established. Subsequent cooling of this region is evidenced by the spread of steppe taxa from ~6.5 to 5 Ma. Seasonal precipitation and drought due to monsoonal activity is thought to favor grassland in this region (Hoorn et al., 2000).

Intensification of the South American monsoonal climate in the Andes, starting at 7.9 Ma, is attributed to increases in sedimentation rates (Uba et al., 2007). Additionally, the record from the western United States indicates that a significant decrease in growing season temperature occurred around 13 Ma, concomitant with a slow decline in deciduous forests (Wolfe, 1994; Yang

et al., 2011). By 7 Ma grasslands were becoming widespread in North America as well as worldwide (Cerling et al., 1997; Retallack, 2001, Retallack et al., 2002). The rise of C_4 grasses was originally attributed to decreases in CO_2 (Cerling et al., 1997), but the spread of these grasslands is much more complex than originally thought. Higher temperatures, shifts in precipitation seasonality, and reduced precipitation all seem to favor the spread of these plants (Pagani et al., 1999a, b; Edwards et al., 2010).

3.9 Conclusions

This work documents the floodplain vegetation of the Beluga and Sterling Fms. Palynological data record the persistence of thermophilic taxa well into younger strata of the upper Sterling Fm. (~6 Ma). Palynomorph assemblages from floodplain and lake deposits record a vegetational community composed primarily of shrubs, *Alnus*, and herbaceous plants with relatively sparse trees and open canopy conditions. Coal swamps had denser tree populations (Reinink-Smith and Leopold, 2005).

Stable isotopic analysis of palynological separates provides another tool for reconstruction of the regional paleoclimate. This technique is robust due to the mostly inert chemical nature of the refractory detritus left over after palynological digestion. The similarity of leaf material to other plant tissues (Jahren, 2004), allows for estimation of MAP from palynological residues. MAP estimates based on the Diefendorf et al. (2010) equation from samples of the oldest Beluga Fm. average 750 mm a^{-1}. Transitional sediment samples from the upper Beluga and lower Sterling Fm. have an average MAP of 970 mm a^{-1}. Overlying samples within this transition zone (~ 8 Ma) reveal a significantly larger average MAP (1600 mm a^{-1}) and greater variability than younger and older samples (Fig. 3.11). Samples from the overlying portion of the transition zone have an average MAP of 600 mm a^{-1}.

Coupling palynology and stable carbon isotope data improves overall paleoclimate interpretations by allowing direct comparisons of vegetational communities with isotopically-based precipitation estimates. We extend the record of Mixed Northern Hardwood and Mixed Mesophytic forests into the upper Sterling Fm. Our results indicate that Poaceae pollen increase in abundance from a background of ~0% to upwards of almost 15% during intervals with high MAP variability. Likewise, *Alnus* is at the highest abundance and many tree species are at the lowest abundances during high MAP. This may reflect year-to-year variability and/or seasonality of the precipitation.

The amount and seasonality of precipitation in the Cook Inlet region may be caused by orographic effects from the rising Alaska Range. Current research places a pulse of uplift in the central and western Alaska Range at ~6 Ma (Haeussler et al., 2008; Benowitz, 2011). Previous to this uplift event, climate records of the interior of Alaska indicate these mountains were not yet tall and/or broad enough to create orographic effects (White et al., 1997). A majority of the sediments in this study predate the ~ 6 Ma regional increases in topography. Therefore, orographic effects associated with topography are not likely a cause for the persistence of thermophilic taxa in Cook Inlet. Our preferred interpretation links warm temperatures and increased precipitation to increased sea surface temperatures of the Alaska Gyre (Romaine, 1985). This may be a response to the third climatic optimum of Barron and Baldauf (1990) in the North Pacific.

Our findings are consistent with global changes in the hydrologic cycle that were widespread during the Late Miocene (Lyle et al., 2008). Increased (1600 mm a^{-1}) and highly variable (Fig. 3.11; Table 3.4) MAP approximately 8 Ma correlates with other global changes in climate at this time, including the intensification of the Asian, Indian, and Andean monsoons and aridification of the American West (Filippelli 1997; Hoorn et al., 2000; Retallack, 2001; Uba et al., 2007). The

correlation of these phenomena suggests that changes to the hydrologic cycle explain the climate record in Cook Inlet and likely impacted the climate of the northern high latitudes.

3.10 Figures

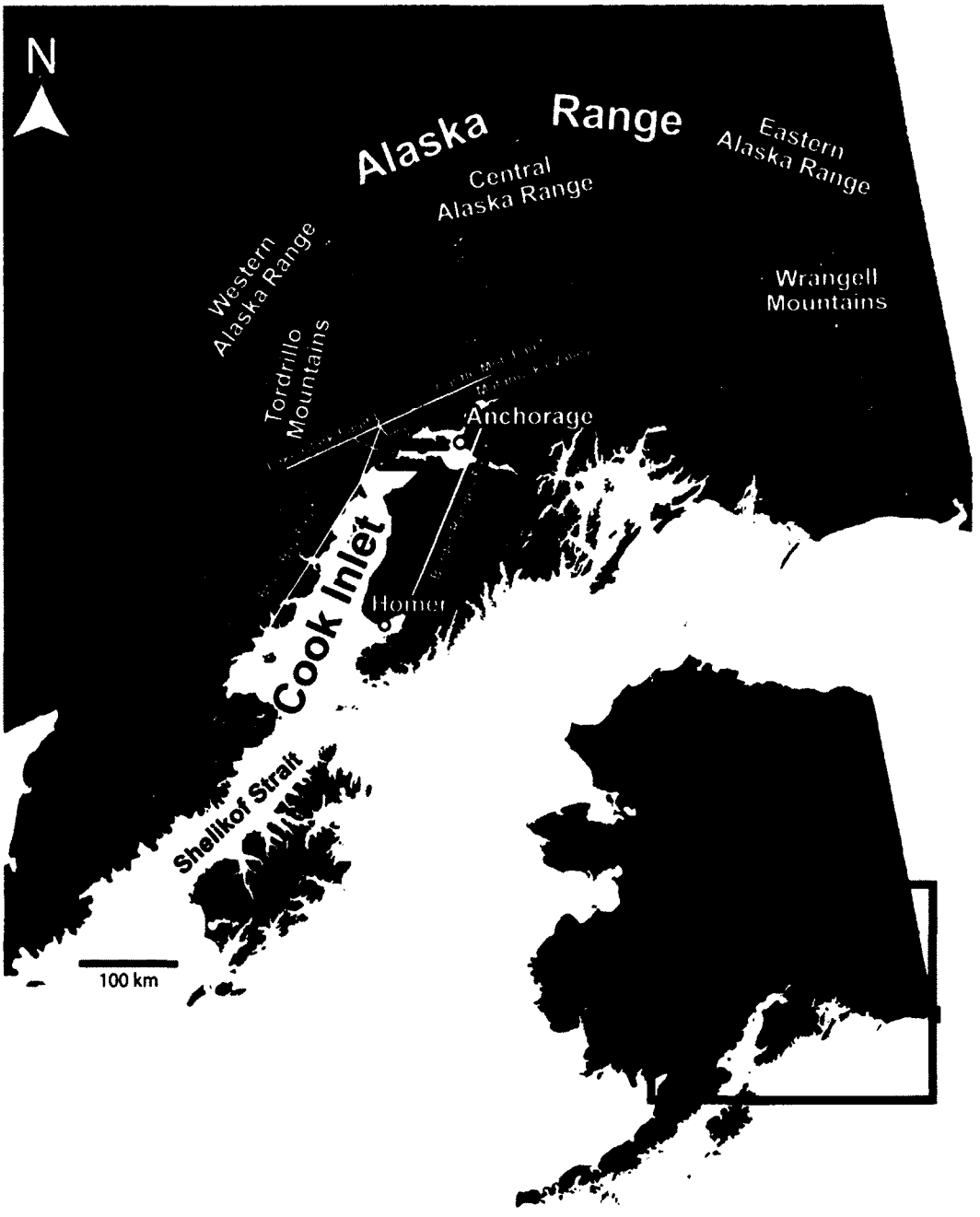

Figure 3.1: Digital elevation model (DEM) depicting the physiographic setting of Southern Alaska. Cook Inlet is situated in the forearc basin and extends from Shelikof Strait to the Wrangell Mountains. Exposures of the Beluga and Sterling formations are found on the Kenai Peninsula, near the town of Homer, and on the western side of Cook Inlet west of Anchorage near the Beluga and Chuitna Rivers.

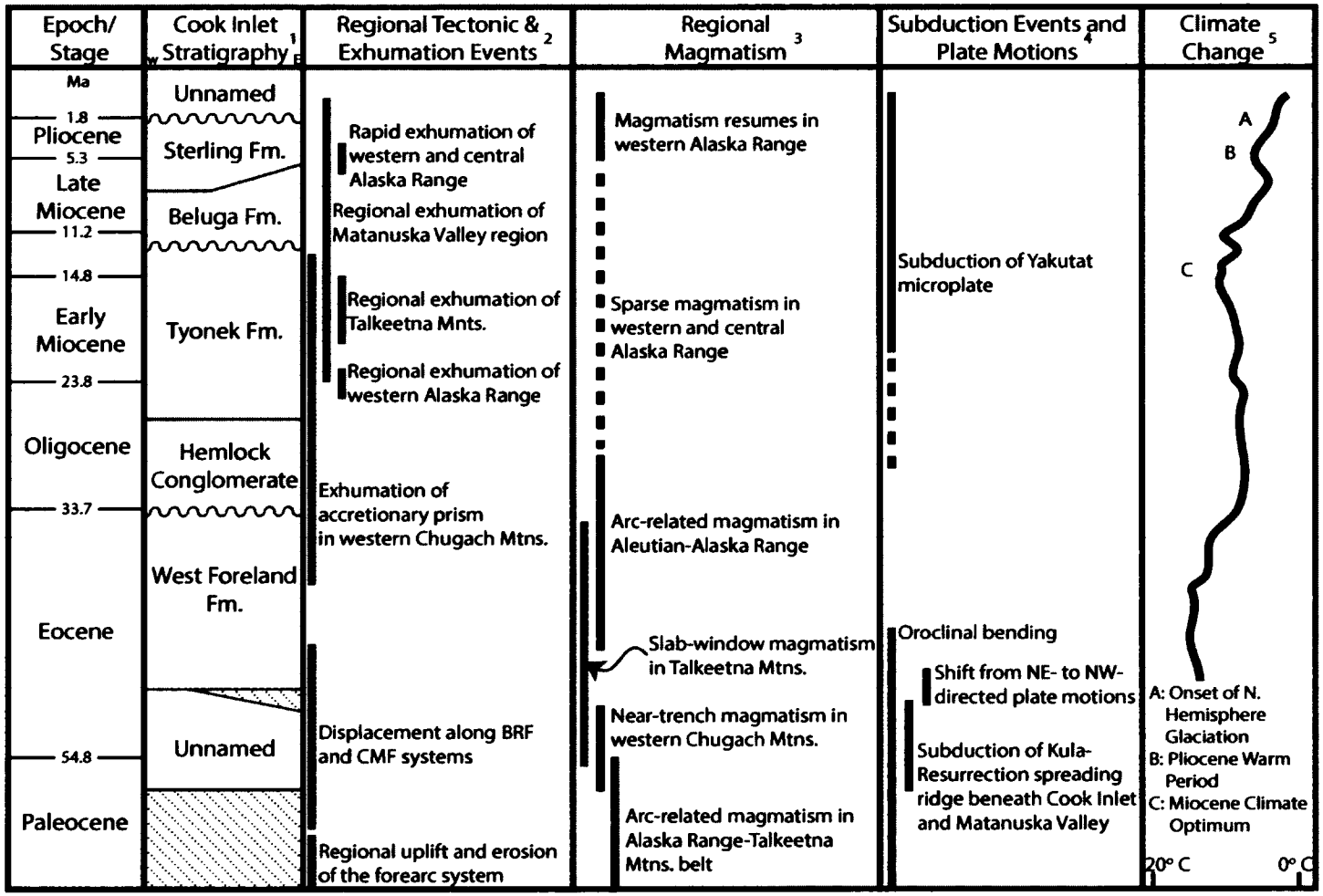

Figure 3.2: Age-event diagram for the Cenozoic Cook Inlet strata (Modified from Finzel, 2010). 1) Stratigraphy, from Flores et al., 2004; 2) Regional Tectonic and Exhumation Events, compiled from Fuchs, 1980; Little and Naeser, 1989; Fitzgerald et al., 1995; Pavlis and Roeske, 2007; and Haeussler et al., 2008; 3) Regional Magmatism, compiled from Moll-Stalcup, 1994; Plafker et al., 1994; Bradley et al., 2003; and Cole et al., 2006; 4) Subduction Events and Plate Motions, compiled from Stock and Molnar, 1988; Plafker et al., 1994; Haeussler et al., 2003; and Bradley et al., 2003); 5) Climate Change, from Zachos et al. 2001; and Wolfe et al., 1966.

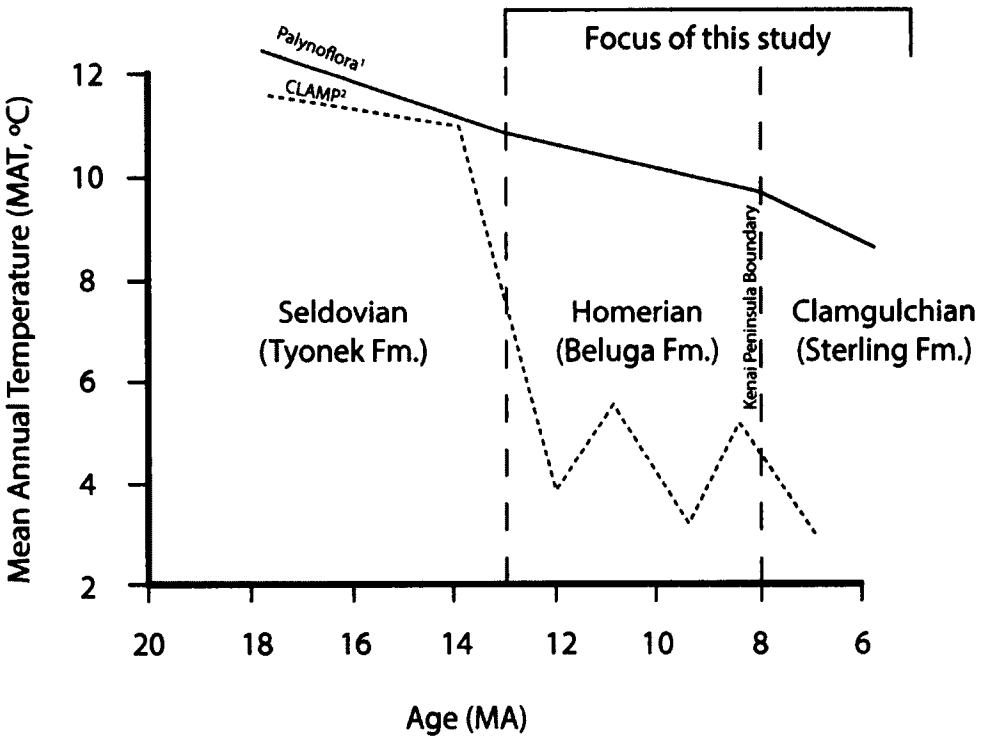

Figure 3.3: CLAMP (dotted line) and palynological (solid line) estimates of mean annual temperature (MAT) for the Seldovian (Tyonek Fm.), Homerian (Beluga Fm.), and Clamgulchian (Sterling Fm.) floral stages. Palynological estimates indicate a warmer climate than the CLAMP results. Palynology results indicate temperatures of ≥ 10°C in a summer wet/coastal climate, (modified from Reinink-Smith and Leopold, 2005). 1) Reinink-Smith and Leopold (2005); 2) Wolfe, 1994; Yang et al., 2011.

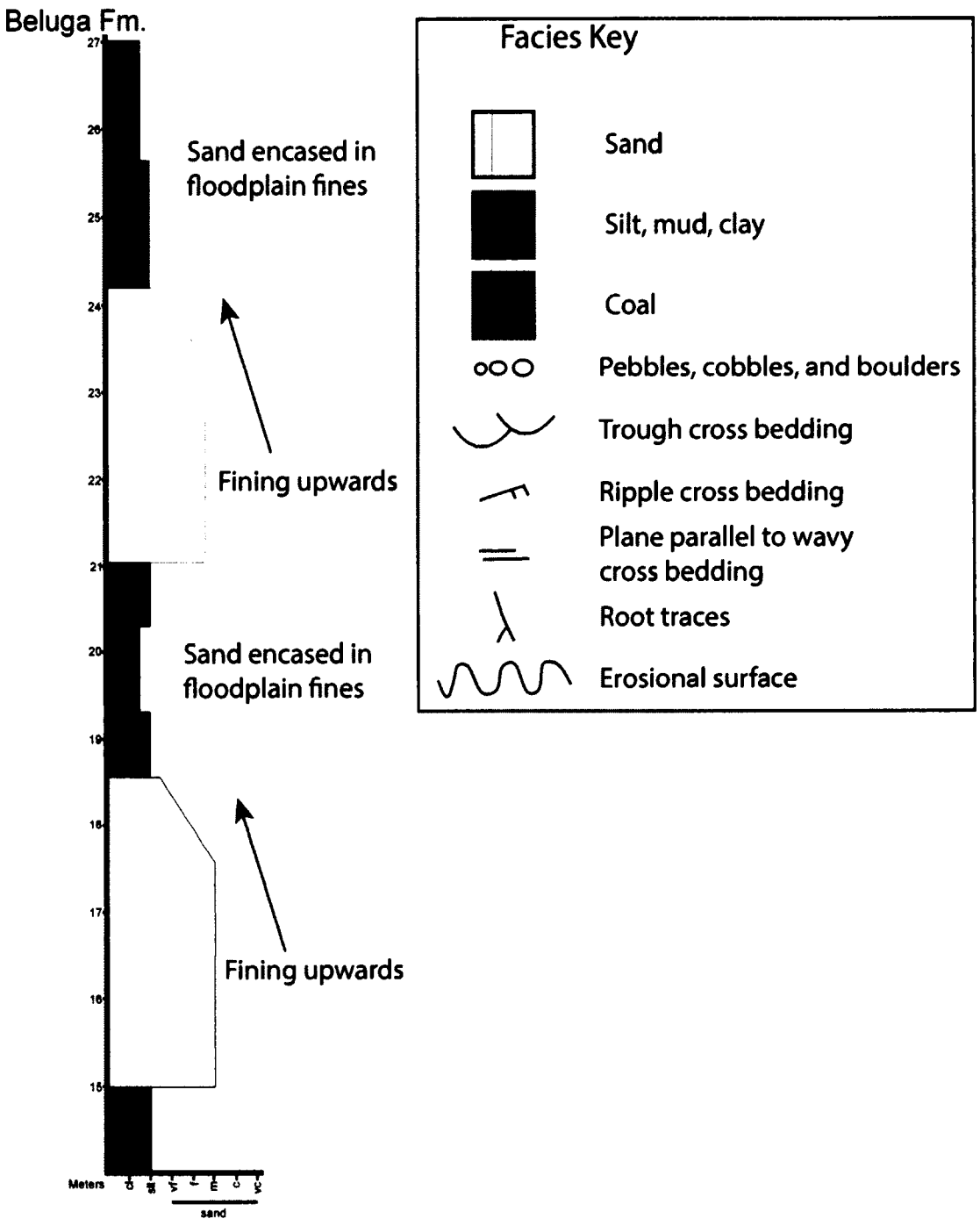

Figure 3.4: This is a typical measured section showing facies within the humid/organoclastic-style anabranching channels facies association of the Beluga Fm. The defining feature of this facies association is that the typically single story sand bodies are encased in floodplain material. A typical sequence starts with a concave upward scour with a sand body that fines upwards to a flat-topped contact with floodplain material. Several sand bodies are usually seen in an outcrop at or near the same stratigraphic level, suggesting multiple channels were active at any one time.

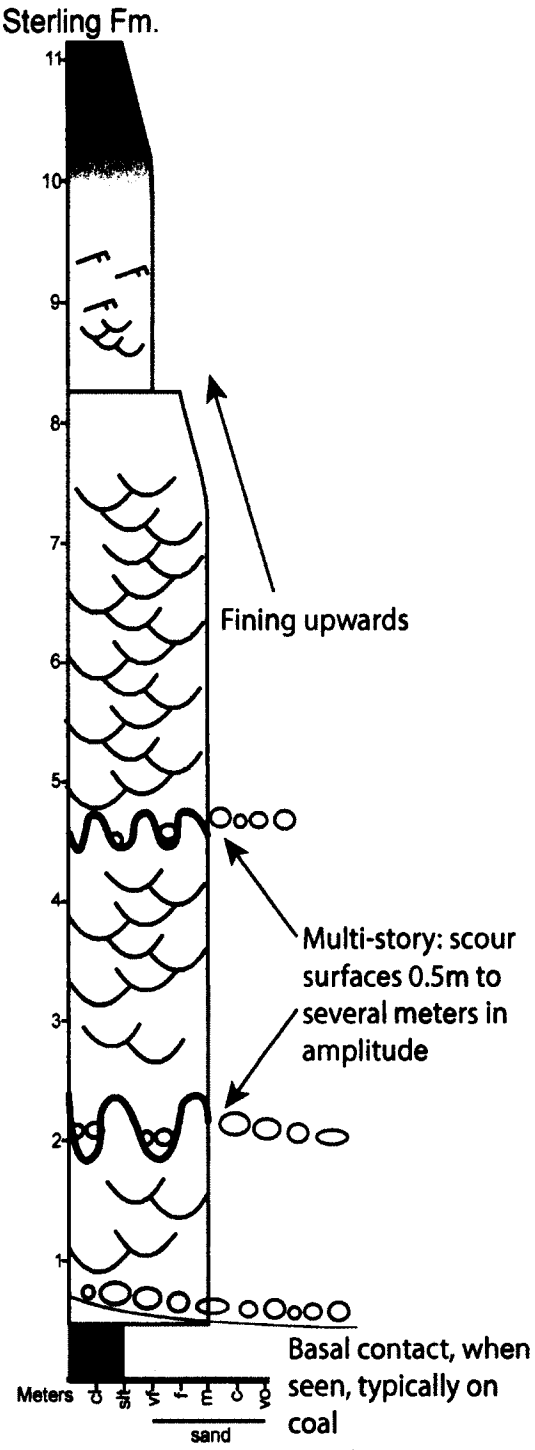

Figure 3.5: This is a typical measured section showing facies within the sandy braided channel facies of the Sterling Fm. Sandy bedforms are the most common feature along with pebbles to boulders of mud rip-up clasts on concave upward scour surfaces separating multiple channel stories. Most of the sandy braided channel facies association fines upwards to floodplain facies sometimes culminating in a coal.

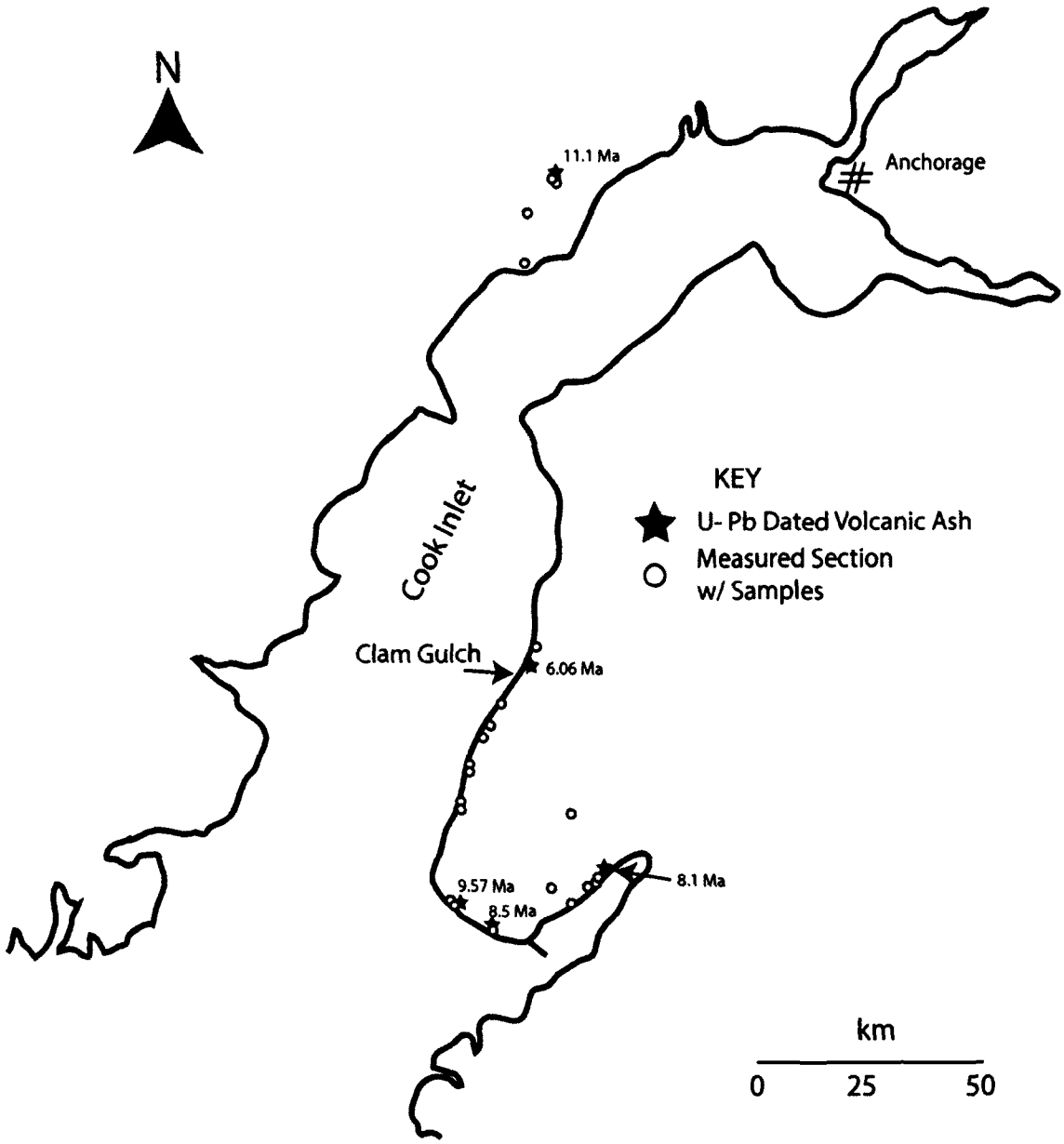

Figure 3.6: Sample locations and selected ages of Beluga and Sterling formations from around the Cook Inlet area. All samples are from measured sections discussed in Chapter 3, locations are noted in the appendix, ages are from R. Gillis (Personal Communication).

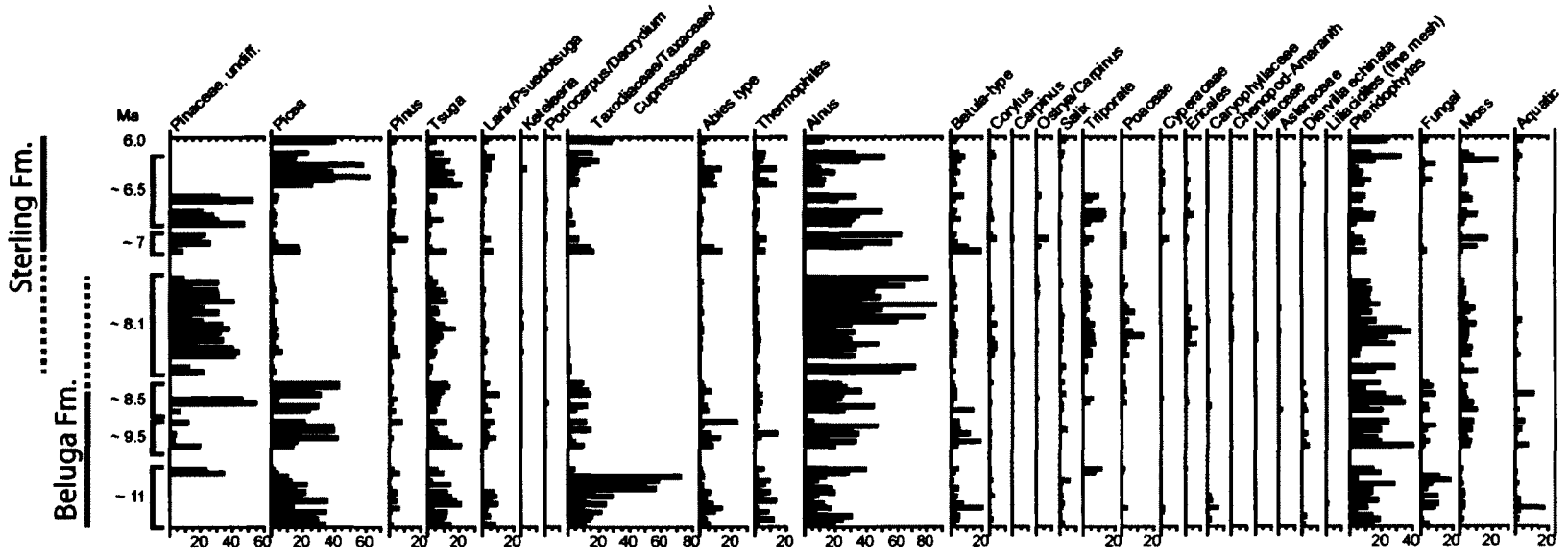

Figure 3.7: Pollen diagram showing percentages (fungal and mosses are actual numbers) for the Beluga and Sterling formations from floodplain and lake facies, excluding coal. Age offsets are between outcrops and absolute ages are based primarily on U-Pb dates from R. Gillis (unpublished data) and $^{40}Ar/^{39}Ar$ dates of Dallegge and Layer (2004).

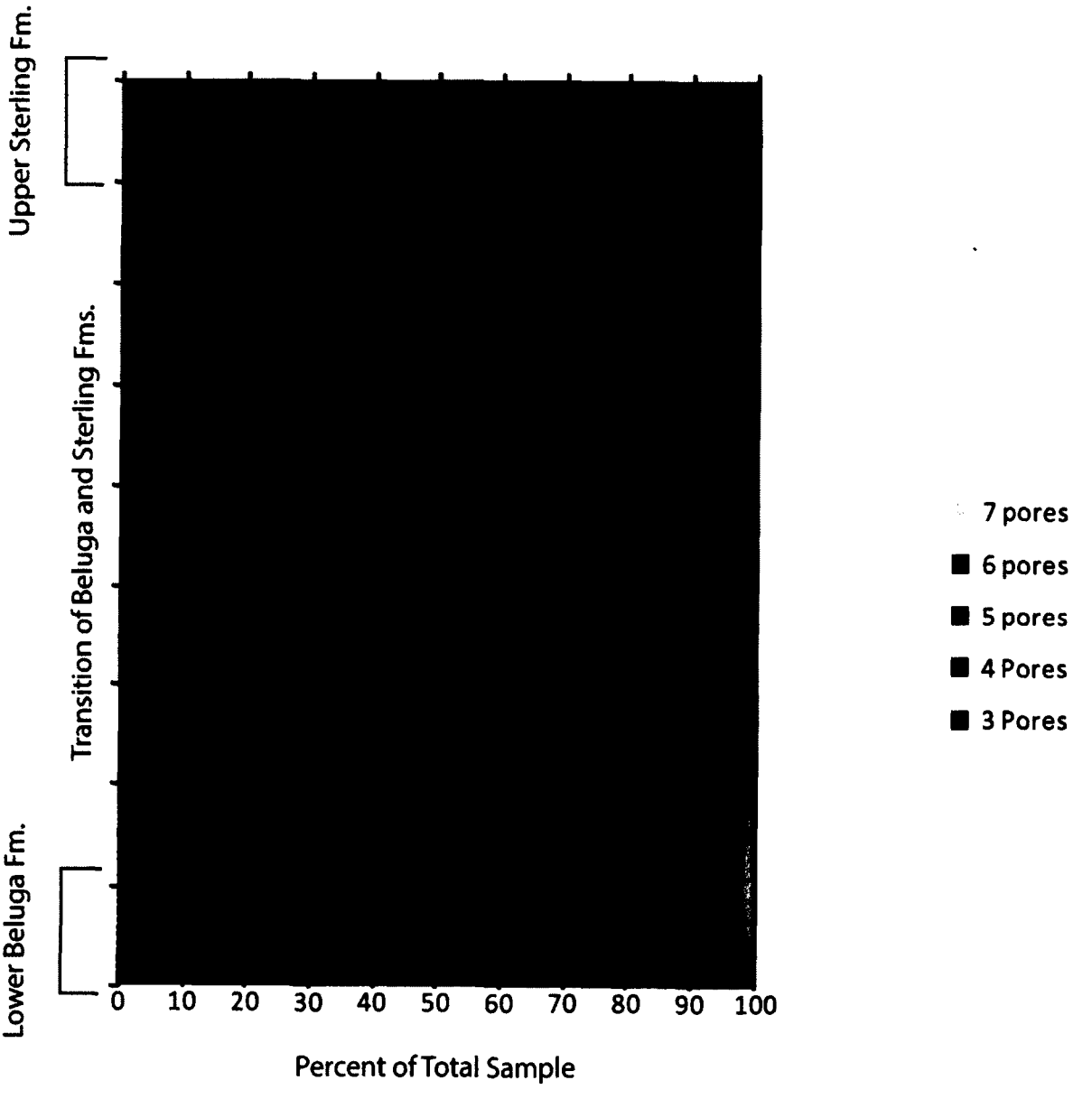

Figure 3.8: Graph of Beluga, transitional Beluga and Sterling, and Sterling fms. depicting percentages of Alnus pollen grains with different numbers of pores. The four-pored variety dominates the record; no shift is seen toward pollen grains with higher numbers of pores in these floodplain and lake facies.

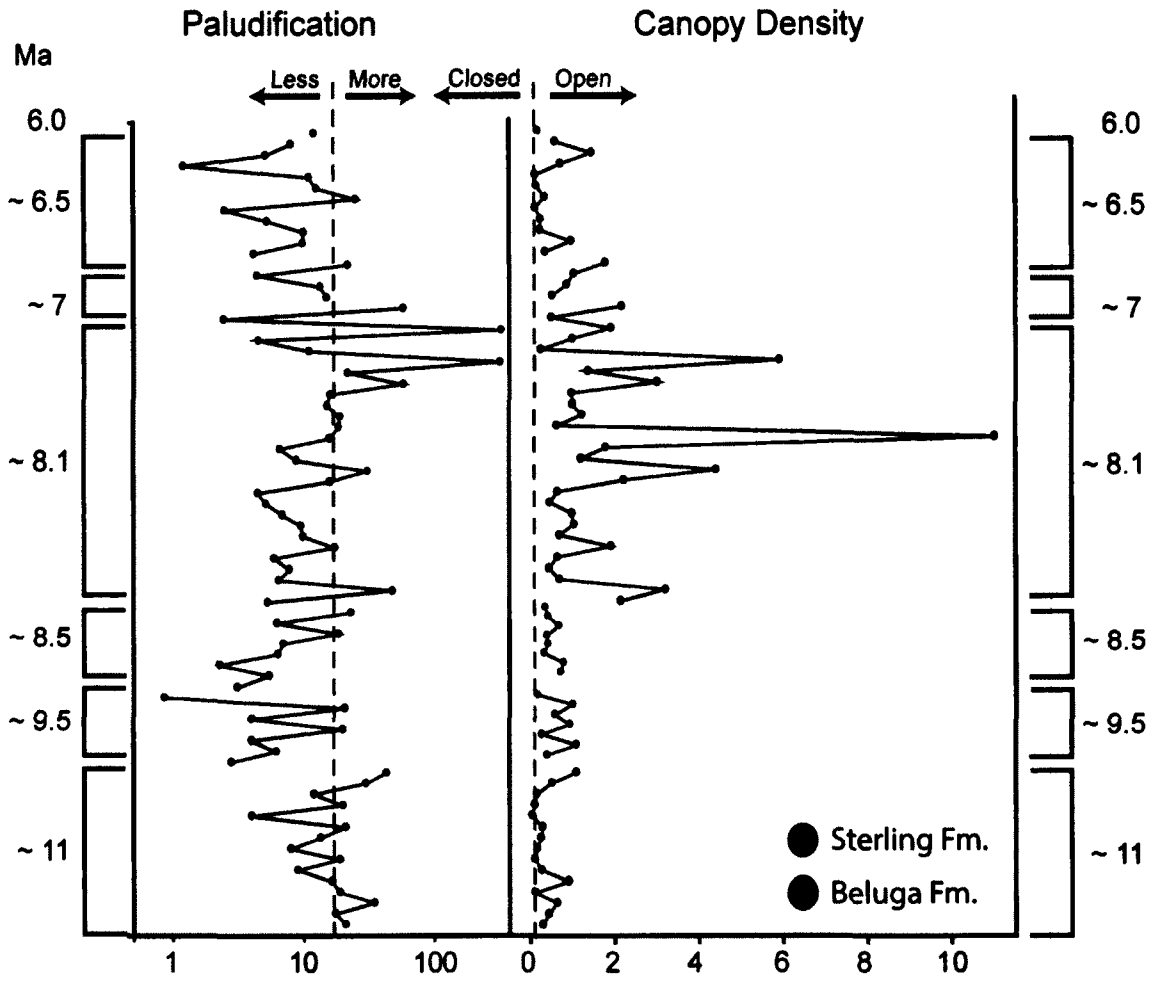

Figure 3.9: Palynological indices of paludification and canopy density. Red circles are Beluga Fm. while the blue circles are the Sterling Fm. The paludification index is a ratio of terrestrial angiosperms to Sphagnum. A value greater than 15 (dashed line) indicates saturated conditions. Samples without Sphagnum are excluded from the diagram. Canopy density is based on the r atio of tree pollen to shrubs and herb pollen. Open canopy conditions are typically taken as a ratio that is greater than ~0.15 (dashed line).

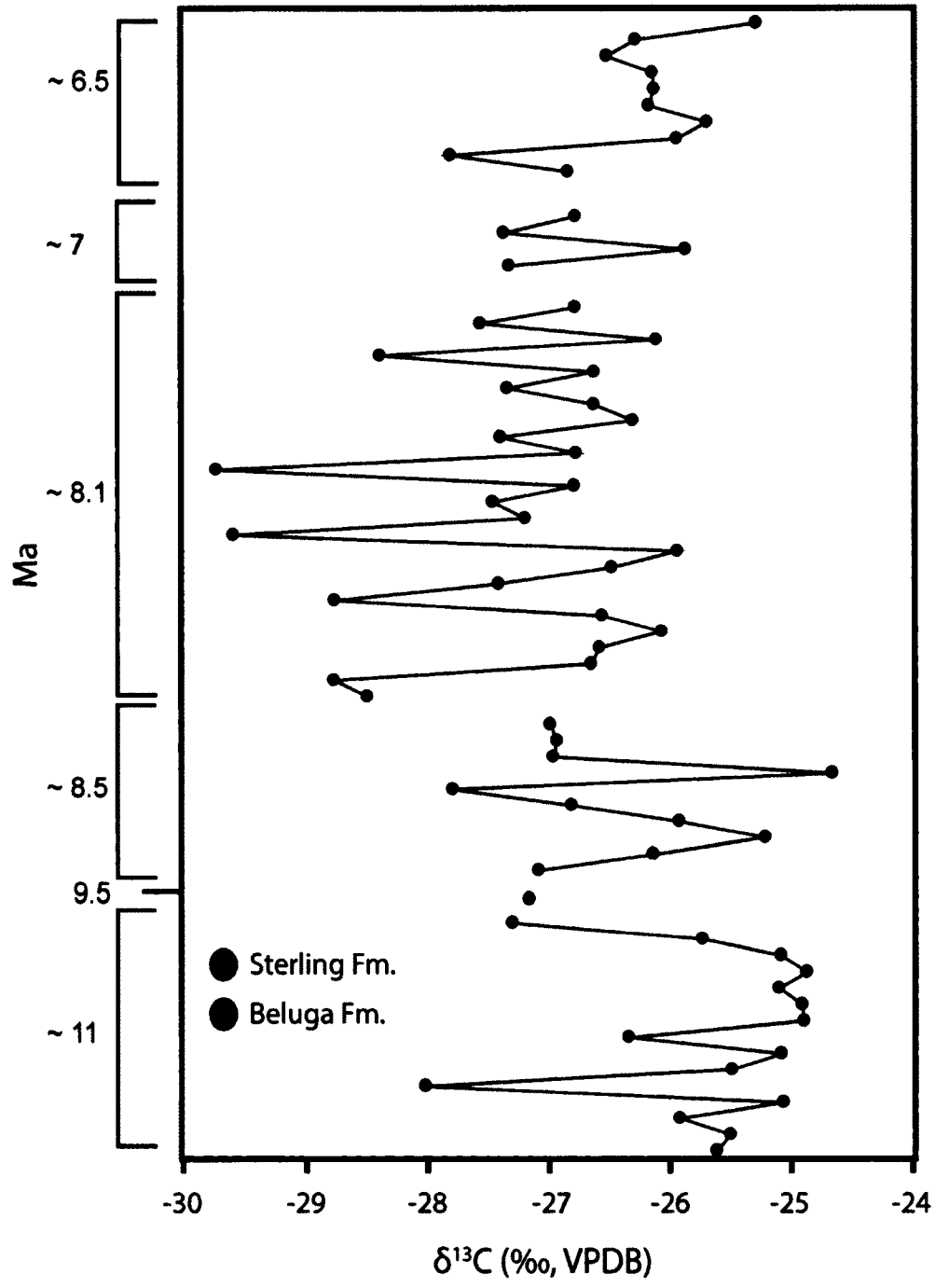

Figure 3.10: The $\delta^{13}C$ values of palynological separates are plotted. Results are expressed in standard per mil (‰) units relative to the Vienna Peedee Belemnite (VPDB) standard. Red circles are Beluga Fm. while the blue circles are the Sterling Fm.

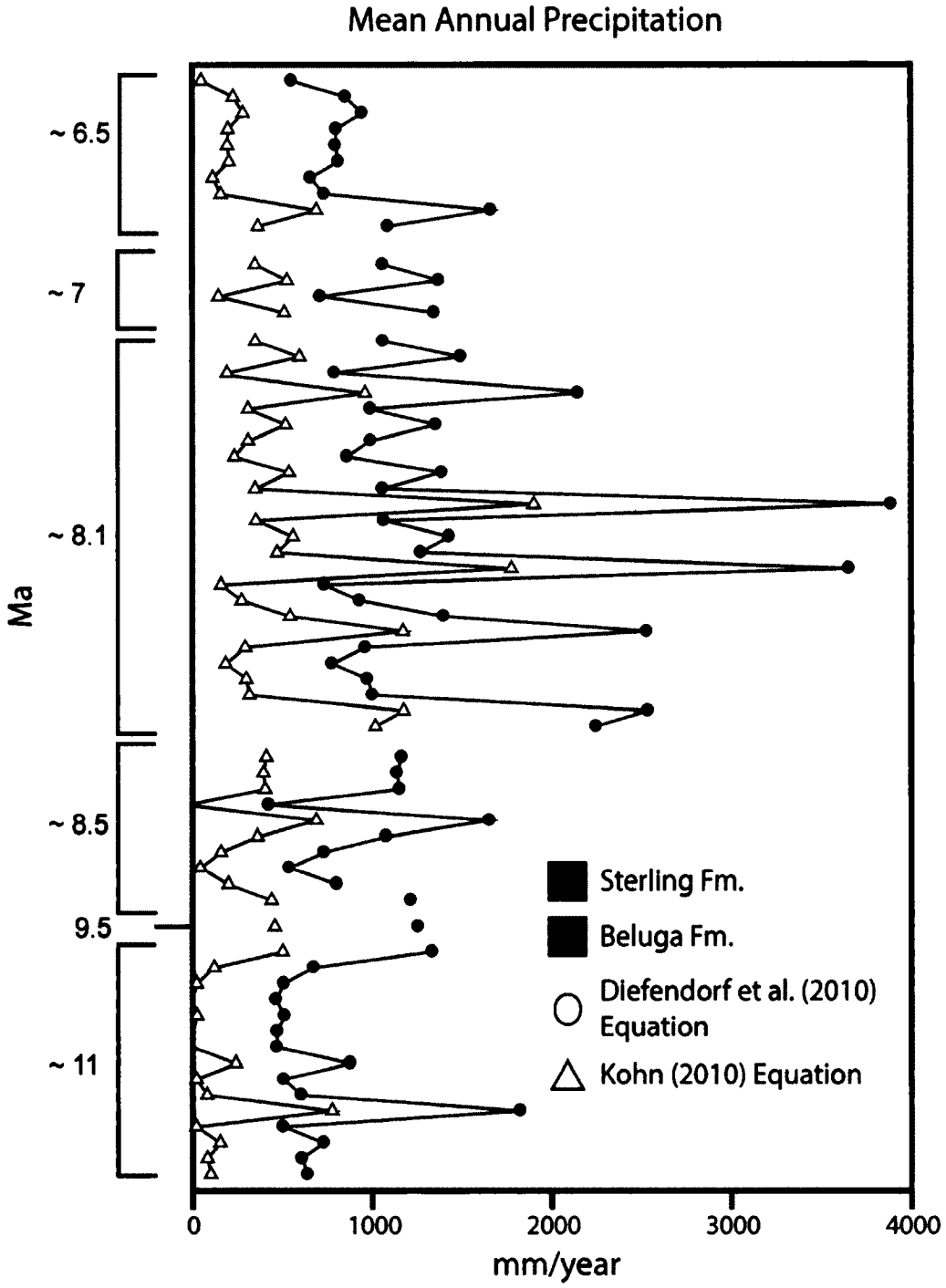

Figure 3.11: Mean annual precipitation (MAP) estimates from the $\delta^{13}C$ values of palynological separates. Calculation of MAP follows Kohn (2010) and Diefendorf et al., (2010). Red colors are Beluga Fm. samples while blue colored samples are the Sterling Fm.; circles are values from the Diefendorf et al. (2010) equation while triangles are from the Kohn (2010) equation.

3.11 Tables

Table 3.1: CLAMP calculations for the Homerian (Beluga Fm.) and Clamgulchian (Sterling Fm.) from Yang et al. (2011)

	GSP	GSP	GSP	MMGSP	MMGSP	MMGSP	3-WET	3-WET	3-WET	3-DRY	3-DRY	3-DRY
	Loc.	Grid.	Grid Adj.	Loc.	Grid.	Grid Adj.	Loc.	Grid.	Grid Adj.	Loc.	Grid.	Grid Adj.
Lower Clamgulchian AK	79.1	54	70.4	8.7	7.6	8.3	38.8	61.1	45.8	12.3	6.1	7.8
Upper Homerian AK	73.7	55.2	72.1	10.5	9.4	10.6	40.9	58.5	39.8	21	9.2	16.5
Middle Homerian AK	83	70.6	93.5	11.7	10.9	12.6	45.7	61.1	45.9	24.1	12.3	25.2
Lower Homerian AK	68.8	53	69	9.5	8.7	9.8	37.8	58.7	40.2	17.9	9.6	17.6

	MAT	MAT	MAT	WMMT	WMMT	WMMT	CMMT	CMMT	CMMT	LGS	LGS	LGS
	Loc.	Grid.	Grid Adj.	Loc.	Grid.	Grid Adj.	Loc.	Grid.	Grid Adj.	Loc.	Grid.	Grid Adj.
Lower Clamgulchian AK	8.7	8.1	8.4	17.6	17.5	17.5	-0.1	-1	-0.5	5.6	5.2	5.5
Upper Homerian AK	7.8	7.2	7.4	18.7	18.3	18.4	-2.7	-3.4	-3.2	5.3	4.8	5
Middle Homerian AK	9.1	8.5	8.9	19.6	19.1	19.3	-0.7	-1.5	-1.1	5.9	5.4	5.8
Lower Homerian AK	7.2	6.9	7	17.1	16.9	16.8	-2.8	-3.1	-2.9	5	4.7	4.9

	RH	RH	RH	SH	SH	SH	Enthalpy	Enthalpy	Enthalpy
	Loc.	Grid.	Grid Adj.	Loc.	Grid.	Grid Adj.	Loc.	Grid.	Grid Adj.
	(%)	(%)	(%)	(g/kg)	(g/kg)	(g/kg)	(kJ/kg)	(kJ/kg)	(kJ/kg)
Lower Clamgulchian AK	56.2	57.3	55.3	3.5	3.4	3.3	292	295.6	291.2
Upper Homerian AK	61.3	62.7	60.4	3.8	3.6	3.5	291.8	295.4	291.2
Middle Homerian AK	66.1	67.7	65	5.2	4.9	4.7	296.5	301.4	295.6
Lower Homerian AK	62.4	65	62.5	3.8	3.8	3.7	291.4	296.1	291.6

Mean Annual Temperature (MAT) (° C)
Warm Month Mean Temperature (WMMT) (° C)
Cold Month Mean temperature (CMMT) (° C)
Length of the Growing Season (LGS) (months)
Growing Season Precipitation (GSP) (mm x 10)
Mean Monthly Growing Season Precipitation (MMGSP) (mm x 10)
Precipitation during the 3 Consecutive Wettest Months (3WET) (mm x 10)
Precipitation during the 3 Consecutive Driest Months (3DRY) (mm x 10)
Relative Humidity (RH) (%)
Specific Humidity (SH) (g/kg)
Enthalpy (ENTHAL) (kJ/kg)

Table 3.2: List of palynomorphs identified in this study from the Beluga and Sterling fms. Those marked with an asterix are thermophilic taxa.

Taxa
Pteridophta
Botrychium type
Cibotiumspora
Cyathidites spp
Davallia type
Osmunda type
Polypodium (Laevigatosporites) spp
Polypodium undiff.
Verrumonoletes (coarse)
Verrumonoletes (fine low verrucae)
Fungal
Anatolinites sp
Arthrinium cf kamtschaticum
Brachysporites
Dicellaesporites cf largelongatus
Didymosporonites spp
Diporisporites
Fungal misc.
Hypoxylonites spp
Monoporisporites basidii
Monoporisporites magnus
Monoporisporites spp
Monoporisporites triangularis
Pluricellaesporites/Quilonia
Trichothyrites
Moss
Lycopodium cf. L. annotinum
Lycopodium lucidum (Foveotrilete)
Lycopodium selago
Lycopodium undiff
Polytrichum spp
Selaginella undiff
Sphagnum
Stereisporites
Gymnosperm
Abies type
Dacrydium
Keteleeria type*
Larix/Pseudotsuga
Picea
Pinaceae, undiff.
Pinus
Podocarpus*
Taxodiaceae/Taxaceae/Cupressaceae
Tsuga

Angiosperm (trees and shrubs)
Acer*
Alnus
Betula (pllcata type)
Carpinus type
Carya type*
Corylus type
Fagus type*
Ilex*
Juglandaceae undiff*
Magnolia*
Ostrya
Pterocarya/Cyclocarya*
Quercus spp*
Rutaceae*
Salix
Sciadopitys spp*
Sequoiapollenites spp*
Tilia*
Ulmus type*
Weigelia*
Diervilla echinata
Angiosperm (herbs)
Asteraceae
Caryophyllaceae
Chenopod-Amaranth
Cyperaceae
Equisetum
Ericales
Liliaceae
Liliacidites (fine mesh)
Poaceae
Aquatic
Algal cyst indet
Mougeotia
Nymphaea
Ovoidites (Spirogyra) spp
Ovoidites ligneolus
Potamogeton?
Sigmopollis hispidus
Sigmopollis psilatus
Sparganium
Typha

Table 3.3: Alnus pore number counts

	Alder Pore Number				
Measured Section	3	4	5	6	7
08JRM011-9.0	3	255	74	4	0
08JRM015-0	5	302	73	2	1
08JRM015-72.5	2	243	86	0	0
08JRM17-5.0	0	189	140	1	0
08JRM17-9.5	0	285	73	2	0
08JRM17-10.5	1	255	73	0	0
08JRM18-1.0	0	142	89	1	0
09JRM100-2	1	96	38	18	3
08JRM200-4.6	3	194	85	15	3

Table 3.4: $\delta^{13}C$ values and MAP estimates (see appendix A-E for sample locations)

			Kohn Equation	Diefendorf Equation
Sample Name	δ13C ‰	Latitude	MAP	MAP
09JRM003-0.0	-25.281	60.26	52	554
09JRM006-12.0	-26.276	60.13	229	854
09JRM006-10.0	-26.515	60.13	284	947
09JRM006-7.0	-26.138	60.13	200	804
09JRM006-6.5	-26.124	60.13	197	799
09JRM006-6.0	-26.168	60.13	206	815
09JRM006-5.5	-25.687	60.13	116	661
09JRM006-5.0	-25.937	60.13	161	737
08JRM001-7.0	-27.806	60.11	692	1664
08JRM004-4.5	-26.839	60.11	367	1091
08JRM011-9.0	-26.777	59.95	351	1062
08JRM012-3.0	-27.367	59.95	529	1374
08JRM006-1.5	-25.866	60.08	148	714
08JRM005-13.5	-27.323	60.07	514	1348
08JRM015-72.5	-26.781	59.71	353	1064
08JRM015-38.0	-27.561	59.71	599	1495
08JRM015-0.0	-26.106	59.71	195	793
08JRM017-10.5	-28.39	59.73	963	2148
08JRM017-10.0	-26.624	59.73	312	994
08JRM017-9.5	-27.339	59.73	521	1357
08JRM017-9.0	-26.625	59.73	312	994
08JRM017-8.5	-26.301	59.73	236	863
08JRM017-8.0	-27.395	59.73	540	1391
08JRM017-7.5	-26.773	59.73	350	1060
08JRM017-6.5	-29.744	59.73	1902	3887
08JRM017-6.0	-26.788	59.73	355	1067
08JRM017-5.5	-27.46	59.73	562	1431
08JRM017-5.0	-27.193	59.73	473	1273
08JRM017-4.5	-29.603	59.73	1778	3654
08JRM017-4.0	-25.934	59.73	161	736
08JRM017-3.25	-26.476	59.73	276	931
08JRM017-3.0	-27.411	59.73	545	1400
08JRM017-2.5	-28.765	59.73	1173	2531
08JRM017-2.0	-26.556	59.73	295	965
08JRM017-1.0	-26.063	59.73	186	778
08JRM017-0.5	-26.58	59.73	301	975
08JRM017-0.0	-26.648	59.73	318	1004
08JRM018-1.0	-28.771	59.73	1177	2538
08JRM020-5.75	-28.495	59.73	1019	2249
09JRM009-16.5	-26.988	59.65	411	1164
09JRM009-14.0	-26.933	59.65	395	1137
09JRM009-13.0	-26.965	59.65	404	1153
09JRM010-9.0	-24.662	59.71	-26	423
09JRM009-5.9	-27.792	59.65	689	1654
09JRM010-4.0	-26.811	59.71	361	1078
09JRM010-3.5	-25.92	59.71	158	731
09JRM010-2.1	-25.212	59.71	43	537
08JRM014-14.5	-26.135	59.68	201	803
08JRM016-14.25	-27.085	59.68	440	1215
08JRM200-4.6	-27.16	61.03	457	1255
08JRM206-40.0	-27.299	61.22	501	1334
08JRM201-4.0	-25.729	61.22	121	673
09JRM100-47.0	-25.082	61.12	23	508
09JRM100-46.0	-24.871	61.12	-4	463
09JRM100-43.0	-25.1	61.12	25	512
09JRM100-40.75	-24.909	61.12	1	471
09JRM100-10.0	-24.895	61.12	-1	468
09JRM100-7.0	-26.338	61.12	240	877
09JRM100-6.5	-25.079	61.12	22	507
09JRM100-6.0	-25.486	61.12	81	605
09JRM100-5.5	-28.017	61.12	776	1825
09JRM100-5.0	-25.063	61.12	20	504
08JRM100-2.0	-25.916	61.12	154	730
09JRM100-1.5	-25.498	61.12	83	609
09JRM100-1.0	-25.611	61.12	101	639

3.12 References

AKIBA, F., 1986, Middle Miocene to Quaternary Diatom Biostratigraphy in the Nankai Trough and Japan Trench, and Modified Lower Miocene through Quaternary Diatom Zones for the Middle-to-High Latitudes of the North Pacific, in Kagami, H., Karig, D.E., and Coulbourn, W.T. eds., Initial Reports DSDP: Deep Sea Drilling Project, p. 393-481.

ALASKA CLIMATE RESEARCH CENTER, 2012, Alaska Climatology: http://climate.gi.alaska.edu/.

BALDAUF, J., 1985, A High Resolution Late Miocene-Pliocene Diatom Biostratigraphy for the Eastern Equatorial Pacific, *in* Mayer, L., and Theyer, F., eds., Initial Reports, DSDP: Deep Sea Drilling Project, p. 457-475.

BARRON, J., 2003, Appearance and extinction of planktonic diatoms during the past 18 m.y. in the Pacific and Southern oceans: Diatom Research, v. 128, p. 203-224.

BARRON, J., and BALDAUF, J., 1990, Development of biosiliceous sedimentation in the North Pacific during the Miocene and early Pliocene, *in* Tsuchi, R., ed., Pacific Neogene Events: University of Tokyo Press, Tokyo, p. 43-63.

BENOWITZ, J.A., 2011, The Topographically Asymmetrical Alaska Range: Multiple Tectonic Drivers through Space and Time: Ph.D., University of Alaska Fairbanks, Fairbanks, 291 p.

BEST, J.L., ASHWORTH, P.J., BRISTOW, C.S., and RODEN, J., 2003, Three-dimensional sedimentary architecture of a large, mid-channel sand braid bar, Jamuna River, Bangladesh: Journal of Sedimentary Research, v. 73, p. 516-530.

BLODGETT, R.H., and STANLEY, K., 1980, Stratification, bedforms, and discharge relations of the Platte braided river system, Nebraska: Journal of Sedimentary Research, v. 50, p. 139.

BOSS, R.F., LENNON, R.B., and WILSON, B.W., 1976, Middle Ground Shoal oil field, Alaska: AAPG Memoir, p. 1-22.

BRADLEY, D.C., KUSKY, T., HAEUSSLER, P., GOLDFARB, R., MILLER, M., DUMOULIN, J., NELSON, S.W., and KARL, S., 2003, Geologic signature of early Tertiary ridge subduction in Alaska, *in* Sisson, V.B., Roeske, S.M., and Pavlis, T.L., eds., Geology of a transpressional orogen developed during ridge-trench interaction along the north Pacific margin: Geological Society of America, Boulder, p. 19-49.

BRIDGE, J., COLLIER, R., and ALEXANDER, J., 1998, Large scale structure of Calamus River deposits (Nebraska, USA) revealed using ground penetrating radar: Sedimentology, v. 45, p. 977-986.

BRIDGE, J.S., 1993, The interaction between channel geometry, water flow, sediment transport and deposition in braided rivers: Geological Society, London, Special Publications, v. 75, p. 13.

BRIDGE, J.S., and LUNT, I.A., 2006, Depositional models of braided rivers, *in* Sambrook Smith, G.H., Best, J.L., Bristow, C.S., and Petts, G.E., eds., Braided Rivers; Process, Deposits, Ecology and Management,: International Association of Sedimentologists, p. 11-50.

BURNS, R.M., and HONKALA, B.H., 1990, Silvics of North America: USDA Forest Service, Washington, DC, 675 p.

CALDERWOOD, K.W., and FACKLER, W.C., 1972, Proposed Stratigraphic Nomenclature for Kenai Group, Cook Inlet Basin, Alaska: AAPG Bulletin, v. 56, p. 739-754.

CANT, D., and WALKER, R., 1978, Fluvial processes and facies sequences in the sandy braided South Saskatchewan River, Canada: Sedimentology, v. 25, p. 625-648.

CERLING, T.E., HARRIS, J.M., MACFADDEN, B.J., LEAKEY, M.G., QUADE, J., EISENMANN, V., and EHLERINGER, J.R., 1997, Global vegetation change through the Miocene/Pliocene boundary: Nature, v. 389, p. 153-158.

COLE, R.B., NELSON, S.W., LAYER, P.W., and OSWALD, P.J., 2006, Eocene Volcanism Above a Depleted Mantle Slab Window in Southern Alaska: Geological Society of America Bulletin, v. 118, p. 140-158, doi: 10.1130/b25658.1.

CROWLEY, K., 1983, Large-scale bed configurations (macroforms), Platte River Basin, Colorado and Nebraska: primary structures and formative processes: Bulletin of the Geological Society of America, v. 94, p. 117.

DALLEGGE, T., and LAYER, P., 2004, Revised chronostratigraphy of the Kenai Group from 40Ar/39Ar dating of low-potassium bearing minerals, Cook Inlet Basin, Alaska: Canadian Journal of Earth Science, v. 41, p. 1159-1179.

DIEFENDORF, A.F., MUELLER, K.E., WING, S.L., KOCH, P.L., and FREEMAN, K.H., 2010, Global patterns in leaf ^{13}C discrimination and implications for studies of past and future climate: Proceedings of the National Academy of Sciences, v. 107, p. 5738-5743, doi: 10.1073/pnas.0910513107.

EDWARDS, E.J., OSBORNE, C.P., STRÖMBERG, C.A.E., SMITH, S.A., and CONSORTIUM, C.G., 2010, The Origins of C4 Grasslands: Integrating Evolutionary and Ecosystem Science: Science, v. 328, p. 587-591, doi: 10.1126/science.1177216.

ENKELMANN, E., ZEITLER, P., GARVER, J., PAVLIS, T.L., and HOOKS, B., 2010, The thermochronological record of tectonic and surface process interaction at the Yakutat-North American collision zone in southeast Alaska: American Journal of Sciences, v. 310, p. 231-260, doi: 10.2475/04.2010.01.

FIELDING, C.R., 1987, Coal deposition models for deltaic and alluvial plain sequences: Geology, v. 15, p. 661-664.

FILIPPELLI, G.M., 1997, Intensification of the Asian monsoon and a chemical weathering event in the late Miocene–early Pliocene: Implications for late Neogene climate change: Geology, v. 25, p. 27-30, doi: 10.1130/0091-7613(1997)025<0027:iotama>2.3.co;2.

FINZEL, E.S., 2010, Geodynamics of Flat-Slab Subduction, Sedimentary Basin Development, and Hydrocarbon Systems along the Southern Alaska Convergent Plate Margin: Ph.D., University of Purdue, West Lafayette, 401 p.

FINZEL, E.S., FLESCH, L.M., and RIDGWAY, K.D., 2011, Kinematics of a diffuse North America–Pacific–Bering plate boundary in Alaska and western Canada: Geology, v. 39, p. 835-838, doi: 10.1130/g32271.1.

FITZGERALD, P.G., SORKHABI, R.B., REDFIELD, T.F., and STUMP, E., 1995, Uplift and denudation of the central Alaska Range; a case study in the use of apatite fission track thermochronology to determine absolute uplift parameters: Journal of Geophysical Research, v. 100, p. 20,175-20,191.

FLORES, R.M., and STRICKER, G.D., 1992, Some facies aspects of the upper part of the Kenai Group, southern Kenai Peninsula, Alaska, in Bradley, D.C., and Dusel-Bacon, C. eds., Geologic studies in Alaska by the U.S. Geological Survey, 1991: U. S. Geological Survey, Reston, VA, p. 160-170.

FLORES, R.M., and STRICKER, G.D., 1993, Reservoir framework architecture in the Clamgulchian type section (Pliocene) of the Sterling Formation, Kenai Peninsula, Alaska, in Dusel-Bacon, C., and Till, A.B. eds., Geologic Studies in Alaska by the U.S. Geological Survey, 1992: U.S. Geological Survey Bulletin 2068, Reston, p. 118-129.

FLORES, R.M., STRICKER, G.D., and KINNEY, S.A., 2004, Alaska Coal Geology, Resources, and Coalbed Methane potential: U.S. Geological Survey DDS-77.

FREEMAN, K.H., MUELLER, K.E., DIEFENDORF, A.F., WING, S.L., and KOCH, P.L., 2011, Clarifying the influence of water availability and plant types on carbon isotope discrimination by C3 plants: Proceedings of the National Academy of Sciences, v. 108, p. E59-E60, doi: 10.1073/pnas.1102556108.

FUCHS, W.A., 1980, Tertiary tectonic history of the Castle Mountain-Caribou fault system in the Talkeetna Mountains, Alaska: Ph.D., University of Utah, Salt Lake City, 152 p.

GLADENKOV, A.Y., OLEINIK, A.E., MARINCOVICH JR, L., and BARINOV, K.B., 2002, A Refined Age for the Earliest Opening of Bering Strait: Palaeogeography, Palaeoclimatology, Palaeoecology, v. 183, p. 321-328, doi: 10.1016/s0031-0182(02)00249-3.

HAEUSSLER, P., O'SULLIVAN, P., BERGER, A., and SPOTILA, J., 2008, Synchronous exhumation of the Tordrillo Mountains and Denali (Mt. McKinley), Alaska, around 6 Ma, *in* Freymueller, J., Haeussler, P., Wesson, R., and Ekstrom, G., eds., Active Tectonics and Seismic Potential of Alaska: American Geophysical Union, Washington D.C., p. 269-286.

HAEUSSLER, P., and SALTUS, R.W., 2011, Location and Extent of Tertiary Structures in Cook Inlet Basin, Alaska, and Mantle Dynamics that Focus Deformation and Subsidence: U.S. Geological Survey, v. 1776-D, p. 34.

HAEUSSLER, P.J., BRADLEY, D.C., WELLS, R.E., and MILLER, M.L., 2003, Life and death of the Resurrection plate: Evidence for its existence and subduction in the northeastern Pacific in Paleocene–Eocene time: Geological Society of America Bulletin, v. 115, p. 867-880, doi: 10.1130/0016-7606(2003)115<0867:ladotr>2.0.co;2.

HELMOLD, K.P., LEPAIN, D.L., WILSON, W.D., and PETERSON, S.C., 2012, Petrology and Reservoir Potential of Tertiary and Mesozoic Sandstones, Cook Inlet, Alaska: A Preliminary Analysis of Outcrop Samples Collected During 2007-2010 Field Seasons: Preliminary Investigative Report Alaska Division of Geological and Geophysical Surveys.

HOORN, C., OHJA, T., and QUADE, J., 2000, Palynological evidence for vegetation development and climatic change in the Sub-Himalayan Zone (Neogene, Central Nepal): Palaeogeography, Palaeoclimatology, Palaeoecology, v. 163, p. 133-161, doi: 10.1016/s0031-0182(00)00149-8.

JAHREN, A.H., 2004, The carbon stable isotope composition of pollen: Review of Palaeobotany and Palynology, v. 132, p. 291-313, doi: 10.1016/j.revpalbo.2004.08.001.

KENNETT, J.P., 1985, Miocene to early Pliocene oxygen and carbon isotope stratigraphy in the southwest Pacific, Deep Sea Drilling Project Leg 90, *in* Kennett, J., and von der Borch, C., eds., Initial Reports of the Deep Sea Drilling Program, College Station, p. 1383-1411.

KOHN, M.J., 2010, Carbon isotope compositions of terrestrial C3 plants as indicators of (paleo)ecology and (paleo)climate: Proceedings of the National Academy of Sciences, v. 107, p. 19691-19695, doi: 10.1073/pnas.1004933107.

KOHN, M.J., 2011, Reply to Freeman et al.: Carbon isotope discrimination by C3 plants: Proceedings of the National Academy of Sciences, v. 108, p. E61, doi: 10.1073/pnas.1103222108.

KRISSEK, L., 1995, Late Cenozoic ice-rafting records from Leg 145 sites in the North Pacific; late Miocene onset, late Pliocene intensification, and Pliocene-Pleistocene events: Proceedings Ocean Drilling Program Scientific Results, v. 145, p. 179-194.

LEPAIN, D.L., WARTES, M.A., MCCARTHY, P.J., STANLEY, R., SILLIPHANT, L.J., PETERSON, S., SHELLENBAUM, D.P., HELMOLD, K.P., DECKER, P.L., MONGRAIN, J.R., and GILLIS, R.J., 2009, Facies Associations, Sand Body Geometry, and Depositional Systems in Late Oligocene–Pliocene Strata, Southern Kenai Peninsula, Cook Inlet, Alaska: Report on Progress During the 2006–07 Field Seasons, in LePain, D.L. ed., Preliminary Results of Recent Geologic Investigations in the Homer-Kachemak Bay Area, Cook Inlet Basin: Progress During the 2006-2007 Field Season: DGGS, Fairbanks, p. 1-32.

LITTLE, S.A., KEMBEL, S.W., and WILF, P., 2010, Paleotemperature Proxies from Leaf Fossils Reinterpreted in Light of Evolutionary History: PLoS ONE, v. 5, p. e15161, doi: 10.1371/journal.pone.0015161.

LITTLE, T.A., and NAESER, C.W., 1989, Tertiary tectonics of the Border Ranges fault system, Chugach Mountains, Alaska; deformation and uplift in a forearc setting: Journal of Geophysical Research, v. 94, p. 4333-4359.

LYLE, M., BARRON, J., BRALOWER, T., HUBER, M., OLIVAREZ LYLE, A., RAVELO, A., REA, D., and WILSON, P., 2008, Pacific Ocean and Cenozoic evolution of climate: Reviews of Geophysics, v. 46.

MIALL, A.D., 1988, Reservoir heterogeneities in fluvial sandstones: lessons from outcrop studies: AAPG Bulletin, v. 72, p. 682-697.

MIALL, A.D., 1994, Reconstructing fluvial macroform architecture from two-dimensional outcrops; examples from the Castlegate Sandstone, Book Cliffs, Utah: Journal of Sedimentary Research, v. 64, p. 146.

MIALL, A.D., and JONES, B.G., 2003, Fluvial architecture of the Hawkesbury Sandstone (Triassic), near Sydney, Australia: Journal of Sedimentary Research, v. 73, p. 531.

MOLL-STALCUP, E.J., 1994, Latest Cretaceous and Cenozoic magmatism in mainland Alaska, *in* Plafker, G., and Berg, H.C., eds., The Geology of Alaska: Geological Society of America, Boulder, p. 589-619.

MOSBRUGGER, V., and UTESCHER, T., 1997, The coexistence approach — a method for quantitative reconstructions of Tertiary terrestrial palaeoclimate data using plant fossils: Palaeogeography, Palaeoclimatology, Palaeoecology, v. 134, p. 61-86, doi: 10.1016/s0031-0182(96)00154-x.

NOKLEBERG, W.J., PARFENOV, L.M., MONGER, J.W.H., NORTON, I.O., KHANCHUK, A.I., STONE, D.B., SHOLL, D.W., and FUJITA, K., 1998, Phanerozoic tectonic evolution of the circum-north Pacific: U.S. Geological Survey.

O'LEARY, M.H., 1988, Carbon Isotopes in Photosynthesis: Bioscience, v. 38, p. 328-336.

PAGANI, M., ARTHUR, M.A., and FREEMAN, K.H., 1999a, Miocene Evolution of Atmospheric Carbon Dioxide: Paleoceanography, v. 14, p. 273-292, doi: 10.1029/1999pa900006.

PAGANI, M., FREEMAN, K.H., and ARTHUR, M.A., 1999b, Late Miocene Atmospheric CO2 Concentrations and the Expansion of C4 Grasses: Science, v. 285, p. 876-879, doi: 10.1126/science.285.5429.876.

PAVLIS, T.L., and ROESKE, S.M., 2007, The Border Ranges Fault System, southern Alaska, *in* Ridgway, K.D., Trop, J.M., Glen, J.M.G., and O'Neill, J.M., eds., Tectonic growth of a collisional margin: crustal evolution of southern Alaska: Geologic Society of America Special Paper, Boulder, p. 95-128.

PEARSON, P.N., and PALMER, M.R., 2000, Atmospheric carbon dioxide concentrations over the past 60 million years: Nature, v. 406, p. 695-695-9, doi: 10.1038/35021000.

PLAFKER, G., MOORE, J., and WINKLER, G., 1994, Geology of the southern Alaska margin, *in* Plafker, G., and Berg, H., eds., The geology of North America: Geological Society of America, Boulder, p. 389-449.

RAWLINSON, S.E., 1984, Environments of deposition, paleocurrents, and provenance of Tertiary deposits along Kachemak Bay, Kenai Peninsula, Alaska, in Nilsen, T.H. ed., Fluvial sedimentation and related tectonic framework, western North America: Elsevier, Amsterdam, p. 421-442.

REA, D., and SNOECKX, H., 1995, Sediment fluxes in the Gulf of Alaska: Paleoceanographic record from site 887 on the Patton-Murray seamount platform, *in* Rea, D., Basov, I., Scholl, D., and Allan, J., eds., Proceedings of the Ocean Drilling Program Scientific Results: Ocean Drilling Program, College Station, Texas, p. 247-256.

REININK-SMITH, L., 2010, Variations in alder pollen pore numbers--a possible new correlation tool for the Neogene Kenai lowland, Alaska: Palynology, v. 34, p. 180-194, doi: 10.1080/01916122.2010.495544.

REININK-SMITH, L., and LEOPOLD, E., 2005, Warm Climate in the Late Miocene of the South Coast of Alaska and the Occurrence of Podocarpaceae Pollen: Palynology, v. 29, p. 205-262, doi: 10.2113/29.1.205.

REININK-SMITH, L.M., 1995, Tephra Layers as Correlation Tools of Neogene Coal-bearing Strata from the Kenai Lowland, Alaska: Geological Society of America Bulletin, v. 107, p. 340-353, doi: 10.1130/0016-7606(1995)107<0340:tlacto>2.3.co;2.

RETALLACK, G.J., 2001, Cenozoic Expansion of Grasslands and Climatic Cooling: The Journal of Geology, v. 109, p. 407-426.

RETALLACK, G.J., TANAKA, S., and TATE, T., 2002, Late Miocene advent of tall grassland paleosols in Oregon: Palaeogeography, Palaeoclimatology, Palaeoecology, v. 183, p. 329-354, doi: 10.1016/s0031-0182(02)00250-x.

ROMINE, K., 1985, Radiolarian biogeography and paleoceanography of the North Pacific at 8 Ma, *in* Kennett, J., ed., The Miocene Ocean: Paleoceanography and Biogeography: Geological Society of America, Boulder, p. 237-273.

ROYER, D.L., WING, S.L., BEERLING, D.L., and JOLLEY, D.W., 2001, Paleobotanical evidence for near present-day levels of atmospheric CO(2) during part of the tertiary: Science, v. 292, p. 2310-2310-3.

SAMBROOK SMITH, G., ASHWORTH, P.J., BEST, J.L., WOODWARD, J., and SIMPSON, C.J., 2006, The sedimentology and alluvial architecture of the sandy braided South Saskatchewan River, Canada: Sedimentology, v. 53, p. 413-434.

SAMBROOK SMITH, G., ASHWORTH, P.J., BEST, J.L., WOODWARD, J., and SIMPSON, C.J., 2009, The Morphology and Facies of Sandy Braided Rivers: Some Considerations of Scale Invariance, *in* Blum, M.D., Marriott, S.B., and Leclair, S.F., eds., Fluvial Sedimentology VII: Blackwell Publishing Ltd., Oxford, p. 145-158.

SHACKLETON, N.J., HALL, M.A., and PATE, D., 1995, Pliocene stable isotope stratigraphy of Site 846, in Pisias, N.G., Janacek, L.A., Palmer-Julson, A., and Van Andel, T.H. eds., Proceedings of the Ocean Drilling Program, Scientific Results, Leg 138: Ocean Drilling Program, College Station, TX, p. 337-355.

SKELLY, R.L., BRISTOW, C.S., and ETHRIDGE, F.G., 2003, Architecture of channel-belt deposits in an aggrading shallow sandbed braided river: the lower Niobrara River, northeast Nebraska: Sedimentary Geology, v. 158, p. 249-270.

SMITH, N.D., CROSS, T.A., DUFFICY, J.P., and CLOUGH, S.R., 1989, Anatomy of an avulsion: Sedimentology, v. 36, p. 1-23.

SMITH, N.D., and PEREZ-ARLUCEA, M., 1994, Fine-grained splay deposition in the avulsion belt of the Lower Saskachewan River, Canada: Journal of Sedimentary Research, v. 64, p. 159-168.

STAMATAKOS, J.A., KODAMA, K.P., and PAVLIS, T.L., 1988, Paleomagnetism of Eocene plutonic rocks, Matanuska Valley, Alaska: Geology, v. 16, p. 618-622, doi: 10.1130/0091-7613(1988)016<0618:poeprm>2.3.co;2.

STOCK, J., and MOLNAR, P., 1988, Uncertainties and implications of the Late Cretaceous and Tertiary position of North America relative to the Farallon, Kula, and Pacific Plates: Tectonics, v. 7, p. 1339-1384, doi: 10.1029/TC007i006p01339.

SWENSON, R., 2002, Introduction to Tertiary tectonics and sedimentation in the Cook Inlet basin, *in* Dallegge, T., ed., Geology and Hydrocarbon Systems of the Cook Inlet Basin, Alaska: American Association of Petroleum Geologists Pacific Section/Society of Petroleum Engineers Pacific Regional Conference, May 23-24, 2002, Anchorage, Alaska, p. 11-20.

THOMPSON, R.S., ANDERSON, K.H., and BARTLEIN, P.J., 2000, Atlas of relations between climatic parameters and distributions of important trees and shrubs in North America-hardwoods: U.S. Geological Survey Professional Paper, v. 1650-B, p. 423.

TIPPLE, B., MEYERS, S., and PAGANI, M., 2010, Carbon isotope ratio of Cenozoic CO_2: A comparative evaluation of available geochemical proxies: Paleoceanography, v. 25, doi: 10.1029/2009pa001851.

TRAVERSE, A., 2008, Paleopalynology: Springer, Dordrecht, The Netherlands.

TRIPLEHORN, D.M., TURNER, D.L., and NAESER, C.W., 1977, K-Ar and Fission-track Dating of Ash Partings in Coal Beds from the Kenai Peninsula, Alaska: A Revised Age for the Homerian Stage-Clamgulchian Stage Boundary: Geological Society of America Bulletin, v. 88, p. 1156-1160, doi: 10.1130/0016-7606(1977)88<1156:kafdoa>2.0.co;2.

TROP, J.M., RIDGWAY, K.D., and SPELL, T.L., 2003, Sedimentary record of transpressional tectonics and ridge subduction in the Tertiary Matanuska Valley-Talkeetna Mountains forearc basin, Southern Alaska: Special Paper - Geological Society of America, v. 371, p. 89-118.

TURNER, D.L., TRIPLEHORN, D.M., NAESER, C.W., and WOLFE, J.A., 1980, Radiometric Dating of Ash Partings in Alaskan Coal Beds and Upper Tertiary Paleobotanical Stages: Geology, v. 8, p. 92-96, doi: 10.1130/0091-7613(1980)8<92:rdoapi>2.0.co;2.

UBA, C.E., STRECKER, M.R., and SCHMITT, A.K., 2007, Increased Sediment Accumulation Rates and Climatic Forcing in the Central Andes During the Late Miocene: Geology, v. 35, p. 979-982, doi: 10.1130/g224025a.1.

WHITE, J.M., AGER, T.A., ADAM, D.P., LEOPOLD, E.B., LIU, G., JETTÉ, H., and SCHWEGER, C.E., 1997, An 18 million year record of vegetation and climate change in northwestern Canada and Alaska: tectonic and global climatic correlates: Palaeogeography, Palaeoclimatology, Palaeoecology, v. 130, p. 293-306, doi: 10.1016/s0031-0182(96)00146-0.

WING, S.L., and GREENWOOD, D.R., 1993, Fossils and Fossil Climate: The Case for Equable Continental Interiors in the Eocene: Philosophical Transactions of the Royal Society of London. Series B: Biological Sciences, v. 341, p. 243-252, doi: 10.1098/rstb.1993.0109.

WOLFE, J., 1994, An analysis of Neogene climates in Beringia: Palaeogeography, Palaeoclimatology, Palaeoecology, v. 108, p. 207-216, doi: 10.1016/0031-0182(94)90234-8.

WOLFE, J.A., HOPKINS, D.M., and LEOPOLD, E.B., 1966, Tertiary Stratigraphy and Paleobotany of the Cook Inlet Region, Alaska: U.S. Government Printing Office, Washington D.C., 37 p.

YANG, J., SPICER, R., SPICER, T., and LI, C.-S., 2011, 'CLAMP Online': a new web-based palaeoclimate tool and its application to the terrestrial Paleogene and Neogene of North America: Palaeobiodiversity and Palaeoenvironments, v. 91, p. 163-183, doi: 10.1007/s12549-011-0056-2.

ZACHOS, J., PAGANI, M., SLOAN, L., THOMAS, E., and BILLUPS, K., 2001, Trends, Rhythms, and Aberrations in Global Climate 65 Ma to Present: Science, v. 292, p. 686-693, doi: 10.1126/science.1059412.

Chapter 4

Petrology, Provenance, and Cenozoic Evolution of the Terrestrial Cook Inlet Basin, Alaska[1]

4.1 Abstract

Most provenance studies of forearc basins have determined the sediments filling the basins are primarily derived from the accretionary prism and volcanic arc. Most compositional data from the Beluga Formation suggests sediment sources within the accretionary prism, although the stratigraphically youngest samples from the Beluga Formation show an increase in volcanic lithic fragments. This trend continues into the oldest samples from the Sterling Formation and, by the time the youngest Sterling strata are deposited, the volcanic arc is the dominant sediment source. These results aid in understanding the late Miocene-Pliocene evolution of the Cook Inlet forearc basin. Prior to ~11 Ma, anastomosing channel depositional systems of the Beluga Formation carried sediment derived from the accretionary prism on the east side of Cook Inlet westward. Between ~11 Ma and ~8 Ma deposition of the Beluga Formation waned as Sterling Formation depositional systems began to dominate the basin. The Sterling Formation was deposited by a southward-flowing, sandy braided system. The oldest units in this formation crop out along the western margin of Cook Inlet. These sandy braided fluvial systems migrated eastward by ~8 Ma as deposition of the Beluga Formation in the eastern part of Cook Inlet waned. By ~6 Ma the volcanic arc was the dominant sediment contributor to the basin. These findings suggest that exhumation of the volcanic arc and the western Alaska Range started as early as ~11 Ma, earlier than previously acknowledged affecting depositional systems and provenance.

[1]Mongrain, J., McCarthy, P., LePain, D., Helmold, K., In Prep, Petrology, Provenance, and Cenozoic Evolution of the Terrestrial Cook Inlet Basin, Alaska: Journal of Sedimentary Research

4.2 Introduction

The sedimentary record of forearc basins provides a detailed history that can be used to decipher the tectonic development of convergent margins. The complex history of southern Alaska includes accretion of terranes, subduction of a spreading center, and flat-slab subduction of relatively buoyant oceanic crust (Stock and Molnar, 1988; Plafker et al., 1994; Bradley et al., 2003; Haeussler et al., 2003; Haeussler et al., 2008; Benowitz, 2011; Finzel, 2010). Many studies detail the influence of the forearc trinity (Ridgway et al., 2011) on basin fill (i.e. the volcanic arc, forearc basin, and accretionary prism; Dickinson, 1995; Busby et al., 1998; Clift et al., 2000; McNeill et al., 2000; Kimbrough et al., 2001; DeGraff-Surpless et al., 2002; Trop, 2008; Fildani et al., 2008).

Our current understanding of forearc basins primarily comes from studies of protracted intervals of subduction between oceanic crust of normal thickness and density and continental crust (i.e. Ingersoll, 1978a, 1978b, 1979, 1983; Dickinson and Seely, 1979; Busby-Spera, 1986; Moxon and Graham, 1987; Morris and Busby-Spera, 1988; Linn et al., 1991, 1992; Dickinson, 1995; Busby et al., 1998; DeGraff-Surpless et al., 2002; Surpless et al., 2006). The sediment sources for forearc basins associated with these continent-ocean subduction zones are the accretionary prism and the volcanic arc. In contrast, the geologic history of southern Alaska indicates a protracted interval of flat-slab subduction due to spreading ridge subduction, followed by subduction of thick, buoyant oceanic crust (Plafker et al., 1989; Nokleberg et al., 1994; Plafker and Berg, 1994; Trop and Ridgway, 2007). Recent work suggests that sediment contributions from the retroarc area are possible during flat-slab subduction (Finzel, 2010; Ridgway et al., 2011). The data also suggest that by the mid-Miocene forearc basin sediments in south-central Alaska may have been derived from more typical accretionary prism and volcanic arc sources. This study of the late Miocene Beluga and Sterling fms. provides petrologic data integrated with the timing and location of depositional system interpretations to understand the history of the Cook Inlet forearc basin.

This paper focuses on the late Miocene Beluga and Sterling fms. of the southern Alaska terrestrial forearc basin situated in the modern Cook Inlet area (Fig. 4.1). Using quantitative compositional data from sandstones we present a detailed reconstruction of sediment provenance. These compositional data, along with additional age constraints and depositional system interpretations, allow us to reconstruct the evolution of the Cook Inlet forearc basin during this time. We propose that exhumation in the Western Alaska Range occurred in the Miocene, at ~11 Ma, earlier than previously recognized from thermochronological data. This explains provenance changes and a shift from anastomosing to sandy braided fluvial systems along the basin margins.

4.3 Geologic Setting and Previous Work

Southern Alaska consists of a complex assemblage of accreted terranes, subduction- related volcanic belts, sedimentary basins, and accretionary prism strata (Fig. 4.2; Plafker et al., 1989; Plafker and Berg, 1994; Nokleberg et al., 1994; Trop and Ridgway, 2007). The Cook Inlet Basin (Fig. 4.1) is the southwestern portion of a forearc basin complex that extends from Shelikof Strait in the southwest to the Wrangell Mountains in the northeast. Major physiographic features bounding this basin include granitic batholiths and volcanoes of the Alaska Range to the north and the Aleutian volcanic arc to the southwest. The eastern and southern margins of the basin are bounded by the Chugach and Kenai Mountains that form part of the exhumed accretionary prism (Nokleberg et al., 1994; Haeussler et al., 2000). Major bounding faults to the north and west include the Bruin Bay and Castle Mountain faults (Fig 4.1). These faults juxtapose Mesozoic and Cenozoic sedimentary strata against each other and against arc intrusive bodies (Wilson et al., 2009). The east side of the basin is bounded by the Border Ranges fault that juxtaposes the Peninsular Terrane against the accretionary prism deposits of the Chugach terrane (Magoon et al., 1976; Bradley et al., 1999).

The Peninsular Terrane is thought to be a microcontinent accreted to inboard terranes during the Cretaceous; it is composed of late Paleozoic through Mesozoic strata (Kirschner and Lyon, 1973;

Magoon and Egbert, 1986; Plafker et al., 1989, 1994; Nokleberg et al., 1994). Mesozoic strata of the Peninsular Terrane form the foundation upon which the Cenozoic terrestrial forearc sediments are deposited. The Peninsular Terrane is exposed along the western and eastern margins of the forearc basin, where it has a regional composite thickness of ~12,000 m (Fisher and Magoon, 1978; Magoon and Egbert, 1986; Swenson, 2002). The Cenozoic forearc basin is ~7,500 m thick in the axial region of the basin and unconformably overlies the Peninsular terrane. The Neogene Beluga and Sterling fms. represent upwards of 4,500 m of the Cenozoic forearc fill (Flores et al., 2004).

4.3.1 Subduction History

The Cenozoic history of subduction in southern Alaska is punctuated by two distinct events: 1) Paleocene to Eocene subduction of a spreading ridge, and 2) Oligocene to Recent subduction of thick oceanic crust (Fig. 4.3). The Paleocene to Eocene subduction of a spreading ridge and its effects on southern Alaska are best recorded in the strata of the exposed Matanuska forearc basin (Ridgway et al., 2011). The Matanuska forearc basin is composed of >2,800 m of terrestrial alluvial sedimentary rocks in an overall coarsening upwards mega-sequence interpreted to be a response to syndepositional displacement of the Castle Mountain and Border Ranges fault systems and formation of the Caribou Creek volcanic field (Trop and Ridgeway, 2000; Trop et al., 2003; Ridgway et al., 2011). Sediments in the Matanuska basin are derived from erosion of remnant Mesozoic volcanic arcs, active Paleogene volcanic centers and the accretionary prism (Little and Naeser, 1989; Trop and Ridgeway, 2000; Ridgway et al., 2011).

The Oligocene to Recent history of subduction in southern Alaska is characterized, from west to east, as 'normal' subduction, flat-slab subduction, and transform tectonics. The largest far-field driver of Neogene deformation in southern Alaska is the flat-slab subduction of the Yakutat microplate (Eberhart-Phillips et al., 2006; Haeussler, 2008; Finzel, 2010; Benowitz, 2011). The oldest constraint on subduction of this microplate is ~26 Ma, as evidenced by the onset of volcanism in the Wrangell volcanic field (Fig. 4.1; Richter et al., 1990). The estimated thickness of the subducted portion of the Yakutat microplate is 11-22 km. The unsubducted portion is estimated to be 25-30 km thick and consists of buoyant crust similar to

an oceanic plateau (Ferris et al., 2003; Eberhart-Phillips et al., 2006). Another result of subduction of the Yakutat microplate is rotation of the southern Alaska Block. This event may be responsible for deformation in the Western Alaska Range, specifically the Tordrillo Mountains that experienced rapid uplift at ~ 6 Ma (Haeussler et al., 2008; Benowitz, 2011).

4.3.2 Potential Sediment Sources

Displacement of potential source terranes in the Cook Inlet region along the regional Bruin Bay, Lake Clark, and Boarder Ranges faults has occurred, but the majority of movement took place prior to deposition of the Beluga and Sterling fms. (Fig. 4.3; Detterman and Hartsock, 1966; Detterman and Reed, 1980; Haeussler and Saltus, 2004). A documented example of strike-slip movement includes ~19-65 km of left-lateral offset along the Bruin Bay fault on the northwestern margin of the basin prior to the Oligocene (Fig. 4.1, 4.3; Detterman and Hartsock, 1966; Detterman and Reed, 1980). Farther northwest, the Lake Clark fault has experienced ~26 km of right-lateral offset since the late Eocene (Haeussler and Saltus, 2004). Less significant faults northwest of the Lake Clark fault have accumulated ~10-11 km of strike-slip offset since the Oligocene (Haeussler et al., 2004), but major faults have experienced limited lateral movement since Oligocene time. The current juxtaposition of sediment sources with the basin has been fairly consistent for most of the Cenozoic.

Possible sediment sources to the north and northeast of Cook Inlet include plutons of the Alaska Range-Talkeetna Mountains, the exhumed Matanuska forearc, the accretionary prism, and the Kahiltna assemblage (Fig. 4.3). Plutons of the Alaska Range-Talkeetna Mountains are composed of granitic and calc-alkaline igneous rocks (Wilson et al., 2009). Flat-slab subduction caused inversion of the Matanuska forearc basin (Ridgway et al., 2011). The Matanuska forearc is composed of Jurassic to Oligocene strata deposited as marine suspension fallout, turbidites, alluvial fans, braided to anastomosing streams, and pyroclastic flows. These forearc sediments consist of marine mudstones, carbonaceous mudstones, coals, fine- to medium-grained sandstones and volcaniclastic sandstones (Trop and Ridgway, 2000; Trop et al., 2003; Trop, 2008).

The Chugach Terrane, part of the accretionary prism, is a possible source area to the east of the basin (Fig. 4.3) and is predominantly composed of weakly metamorphosed cherts, siltstones, greywackes, arkoses, and conglomeratic sandstones. Basalts and metabasalts of the McHugh Complex (Bradley et al., 1999) and metasedimentary to greenschist facies, siltstones, slates, sandstones, greywackes, and conglomerates of the Valdez Group (Wilson et al., 2009; Bradley et al., 1999) are also present in the Chugach Terrane, along with less common granitic plutons of Paleocene age.

Potential source rocks to the west of the basin include the Kahiltna assemblage, plutons of the western Alaska-Aleutian Ranges, the Tuxedni Group, the Naknek Fm., and recycled older Cenozoic forearc strata eroded from the basin margin (Fig. 4.3). The Kahiltna assemblage is an informal unit applied to Mesozoic flysch-like strata of south-central and south-western Alaska (Beikman, 1980; Nokleberg et al., 1994; Plafker and Berg, 1994; Kalbas et al., 2007; Wilson et al., 2009). Significant variability exists along strike within the Kahiltna assemblage, which includes argillites, cherts, mudstones, siltstones, lithic and feldspathic greywackes, conglomerates and, locally, contact metamorphic rocks at the margins of intrusions (Wilson et al., 2009). Plutons of the Alaska-Aleutian Ranges consist of granitic and calc-alkaline igneous rocks. The Tuxedni Group consists of marine shales, siltstones, feldspathic to lithic greywackes, and conglomerates, typically with volcanic clasts (Wilson et al., 2009). The Naknek Fm. consists of siltstones, sandstones and conglomerates, all of which have a plutonic provenance (Wilson et al., 1998). An additional possible source is from recycling of older Cenozoic non-marine forearc formations, including the Tyonek Fm., Hemlock Conglomerate, and West Foreland Fm. that are exposed along the western margin of Cook Inlet in narrow, fault-bounded outcrop belts. These units are composed primarily of siltstones, coals, sandstones and conglomerates.

Potential sediment sources to the northwest include plutons of the western Alaska Range, primarily the Tordrillo Mountains, and the Kahiltna assemblage (Fig. 4.3). The Tordrillo Mountains are composed of Late Cretaceous to Paleocene granitic rocks (Reed and Lanphere, 1973; Magoon et al., 1976).

4.3.3 Geochronology and Correlation

There have been several attempts, using a variety of techniques, to correlate strata in the Cook Inlet basin. While K-Ar geochronology has its limitations (see McDougall and Harrison, 2000; Dickin, 2005 and references within), initial attempts at dating plagioclase and hornblende crystal phases in tephra partings in coals yielded ages consistent with the Homerian and Clamgulchian floral stages of Wolfe et al. (1966). The boundary between the Sterling and Beluga fms. on the Kenai Peninsula roughly correlates with the boundary between the Homerian and Clamgulchian stage boundaries (Adkison et al., 1975; Dallegge and Layer, 2004; Reinink-Smith and Leopold, 2005). Apatite and zircon fission track dating of tonsteins also put this boundary on the Kenai Peninsula at ~8 Ma (Turner et al., 1980; Triplehorn et al., 1977).

Dallegge and Layer (2004) applied the $^{40}Ar/^{39}Ar$ technique to tephra partings on the Kenai Peninsula and generated the largest publicly available chronological framework to date. Their data support the Beluga to Sterling transition at ~8 Ma, with an overall range for this transition across the Kenai Peninsula between 9.4 to 4.6 Ma. The $^{40}Ar/^{39}Ar$ framework presents data substantiating the time-transgressive nature of Cenozoic strata in Cook Inlet, an idea first presented in an energy industry fieldtrip guidebook (Swenson, 2001).

R. Gillis (unpublished data) further refines the chronostratigraphic framework of Dallegge and Layer (2004) using U-Pb geochronology. These data estimate the age of the Beluga/Sterling boundary to be ~8 Ma on the Kenai Peninsula and ~11 Ma on the western side of Cook Inlet. Interestingly, the area near Diamond Gulch (Fig. 4), yields an U-Pb age of ~ 9.5 Ma. Dallegge and Layer (2004) invoke a disconformity in the Diamond Gulch area to explain anomalously younger ages ranging from 4.57 ± 0.72 to 6.47 ± 1.68 and use the young ages as confirmation of the time-transgressive nature of the Beluga and Sterling fms. However, Dallegge and Layer (2004) do not provide field evidence for the disconformity. We, LePain et al. (2009), and Reinink-Smith and Leopold (2005) measured several sections through this area and could not find evidence for a disconformity (Chapter 2; Appendix A). The U-Pb ages suggest

that time-transgressive relationships do not exist on the Kenai Peninsula but do exist between sediments on the western and eastern sides of Cook Inlet.

Other attempts at correlation include Reinink-Smith's (1995) attempt to correlate tephra beds based on morphology and geochemistry, with limited success, and Reinink-Smith's (2010) use of the number of pores present on grains of alder pollen recovered from coal beds. Correlation based on alder pollen morphology has subsequently been found to be successful only in coal deposits (Chapter 3).

4.3.4 Sedimentology of the Beluga and Sterling Formations

The sediments of the Beluga and Sterling fms. record a terrestrial succession of fluvial and associated floodplain deposits. Facies analysis, architectural analysis, and paleocurrent data from outcrops and exposures around Cook Inlet have been employed to reconstruct the depositional environments of the Beluga and Sterling fms. (Chapter 2).

4.3.4.1 Beluga Formation

On the eastern side of the basin, fluvial systems that deposited the Beluga Fm. flowed westward from the accretionary prism (Rawlinson, 1984; Helmold et al., In Review). The western side of the basin is less well constrained. However, based on the small dimensions of the channels and overall basin geometry, it seems at least as likely that these fluvial systems flowed towards the east (Chapter 2). The Beluga Fm. was deposited predominantly by anabranching (anastomosing)/single thread fluvial systems (Flores and Stricker, 1993; LePain et al., 2009; Chapter 2). A typical Beluga Fm. succession is comprised of a single story sand body that fines upward and is encased by fine-grained mudstone. Sand bodies are rarely multi-storied. Fining-upward sandstones are typically poorly sorted and mud-rich. The sand bodies generally have a convex-up basal contact with rare mudstone rip-up clasts overlying the basal scour; extrabasinal clasts are rarely present at the base (Chapter 2). The most striking feature of Beluga Fm. sand bodies is the concave-up basal contact and flat-topped nature of the upper bounding contact. The

sandy fill is typically 2-5 m thick and encased in fine-grained material. When channels are present in laterally extensive outcrops, multiple sandy channel-fills are typically present at, or near, the same stratigraphic level.

4.3.4.2 Sterling Formation

The Sterling Fm. was deposited in southward-flowing, low sinuosity (Chapter 2), sandy braided fluvial systems sourced, in part, from the magmatic arc of the western Alaska Range (Flores and Stricker, 1992; LePain et al., 2009). The common occurrence of trough cross-stratified sand bodies bounded by relatively small-scale erosional surfaces, upper flow regime plane beds, and large-scale, high-angle planar tabular cross-beds in association with trough cross-stratified sand bodies overlying erosional basal lags is consistent with studies of modern and ancient sandy braided rivers (Cant and Walker, 1978; Blodgett and Stanley, 1980; Crowley, 1983; Bridge, 1993; Bridge et al., 1998, Best et al., 2003; Miall and Jones, 2003; Miall, 1988 and 1994; Skelley et al., 2003; Sambrook Smith et al., 2005; Bridge and Lunt, 2006; Sambrook Smith et al., 2006; Chapter 2).

4.3.4.3 Overbank deposition in the Beluga and Sterling fms.

Fine-grained facies from both formations are interpreted as lakes, low-lying floodplains, and crevasse splay deposits (LePain et al., 2009; Chapter 2), organic-rich beds, and coal seams, thought to record deposition in swamps, marshes, and mires removed from clastic input (Fielding, 1987; Smith et al., 1989; Smith and Pérez-Arlucea, 1994). Siltstones and mudstones are typically blocky to platy aggregates with less common laminated, wavy laminated, and massive beds. Color varies from light grey to black. Organic remains range from sub-millimeter, finely macerated fragments to relatively large leaf impressions and vertically oriented tree stumps. Rhythmically-laminated siltstone and silty claystone successions up to several meters thick are present locally and consist of alternating light- and dark-colored laminae ranging from less than one

millimeter to approximately one centimeter thick. Laminae are typically arranged in lamina sets to thin bedsets up to a few decimeters thick. Coal beds range from lignite to sub-bituminous and these commonly include splits of siltstone, claystone, carbonaceous mudstone, and volcanic ash (tonsteins; Flores et al., 2004; LePain et al., 2009; Chapter 2).

4.4 Methods

Point counts of 89 primarily medium-grained sandstones from 26 measured stratigraphic sections were compiled to understand sandstone composition (Fig. 4.4). A few of the samples were taken from fine-grained or coarse- grained sandstones where medium-grained specimens were unavailable. Samples were taken from a wide range of geographic and stratigraphic locations in order to characterize available outcrops of Beluga Fm. and Sterling Fm. sandstones. Where possible, samples were collected close to dated horizons to aid in correlating discontinuous outcrops. Figure 4 depicts the distribution of ages and samples relevant to this study. See chapter 2 for additional information on measured stratigraphic sections.

Samples were prepared by Petrographic Services, Montrose, Colorado. Sandstones were impregnated with epoxy and cut into petrographic thin sections, etched, and stained for carbonate minerals (dual carbonate stain) and potassium feldspar. A minimum of 300 framework grains were counted per thin section. Additionally, the entire thin section was qualitatively scanned in order to produce a petrographic description. Classification and tabulation of grain types followed both the Gazzi-Dickinson (Gazzi, 1966; Dickinson, 1985) and 'traditional' methods (Ingersoll et al., 1984).

4.5 Petrology

There are no appreciable differences between the data obtained using the Gazzi-Dickinson and 'traditional' methods. The percentage of lithic fragments containing grains > 0.0625 mm in size averages 2%. The highest occurrence of lithic fragments containing grains > 0.0625 mm is ~14%.

4.5.1 Petrology of the Beluga Fm.

4.5.1.1 Sedimentary Lithic Fragments

Sedimentary lithic fragments compose an average of ~ 44% of the grains in each sample (Fig. 4.5; Table 4.2, 4.3, 4.4). These fragments are dominated by shale lithologies (average ~22%) comprising, in some cases, more than half of the total framework grains (Fig. 4.5; Table 4.1, 4.2, 4.3). Shale grains are typically clay-rich and traces of bedding are visible within the fragments. Lesser amounts of chert (average ~ 12%) and rare sandstone fragments (average ~ 5%) are also present. Chert fragments are commonly massive and black-to-grey in color. Sandstone fragments are dominantly composed of monocrystalline quartz and, less commonly, feldspar.

4.5.1.2 Metamorphic Lithic Fragments

Metamorphic lithic fragments comprise an average of ~17% of the grains in each sample (Table 4.2, 4.3, 4.4). These fragments are dominated by quartz-mica phyllite and schist (averages ~14%; Tables 4.2, 4.3, 4.4). Internally, grains of quartz-mica phyllite and schist are weakly to moderately foliated and composed of brown to reddish-brown clay. Grains of quartzite are also present (average ~3%).

4.5.1.3 Quartz

Quartz comprises an average of ~13% of the grains in each sample (Tables 4.2, 4.3, 4.4). Most of the quartz grains are monocrystalline with slight undulatory extinction (average ~8%; Table 4.2, 4.3, 4.4). Roughly equant grains of unfoliated to weakly foliated polycrystalline quartz are less common.

Sandstones from the Beluga Fm. have an average grain size of 0.26 mm (lower medium), poor sorting, moderate compaction, long to concave-convex grain contacts and little or no cement (Table 4.1; Fig. 4.5). Beluga Fm. samples are classified as litharenites or, less commonly, feldspathic litharenites (Folk, 1980; Fig. 4.6, Table 4.2, 4.3, 4.4). Ternary plots of Q+ F L- and Qm P K indicate lithic-rich sandstones with high plagioclase to total feldspar (P/F) ratios (Fig. 4. 6 and 4.7; See Table 4.2 for a list of abbreviations). The lithic fraction contains a high proportion of sedimentary rock fragments (SRF) as shown by Qp+ Lv Ls and Ls+ Lv Lm ternary diagrams (Fig. 4.8 and 4.9). Stratigraphically older samples tend to have a higher proportion of sedimentary rock fragments, while the stratigraphically younger samples tend to have a higher component of volcanic rock fragments (Figs. 4.8 and 4.9). A ternary plot of Qm F Lt indicates that the older Beluga Fm. samples plot in the lithic recycled portion of the diagram (Dickinson, 1985; Fig. 4.10; Table 4.4). The younger Beluga Fm. samples plot on the boundary between the undissected and transitional arc portions of the diagram (Dickinson, 1985; Fig. 4.10; Table 4.4).

4.5.1.4 Volcanic Lithic Fragments

The total volcanic lithic fragments comprise an average of ~ 8% of the counts (Table 4.2, 4.3, 4.4). This group is predominantly composed of grains with laths of plagioclase in a light to dark colored matrix (Fig. 4.5). This group also includes rare amounts of light to dark colored altered volcanic glass and vesicular glass.

4.5.2 Petrology of the Sterling Fm.

4.5.2.1 Quartz

Quartz comprises an average of ~ 33% of the grains in each sample (Fig. 4.5; Tables 4.2, 4.3, 4. 4). Most quartz framework grains are monocrystalline with slight undulatory extinction (average ~27%; Table 4.2, 4.3, 4.4). In a few instances grains have moderately developed euhedral boundaries with straight extinction, which is characteristic of volcanic quartz (Scholle, 1979). Unfoliated grains of roughly equant polycrystalline quartz are less common (average ~6%).

4.5.2.2 Volcanic Lithic Fragments

Volcanic lithic fragments comprise an average of ~ 27% of the grains in each sample (Fig. 4.5; Table 4.2, 4.3, 4.4). These fragments are dominated by grains with laths of plagioclase in a light- to dark-colored matrix (Fig. 4.5). Light- to dark-colored grains of altered volcanic glass and vesicular glass are also present.

4.5.2.3 Sedimentary Lithic Fragments

Sedimentary lithic fragments comprise an average of ~ 12% of the grains in each sample (Table 4.2, 4.3, 4.4). These fragments are dominated by chert (average ~7%), which is commonly massive and black-to-grey in color. Shale fragments (average ~4%) and sandstone grains (average ~1%) are also present.

4.5.2.4 Metamorphic Lithic Fragments

Metamorphic lithic fragments comprise an average of ~ 6% of the grains in each sample (Table 4.2, 4.3, 4.4). These fragments consist mainly of phyllite (average ~ 4%) with lesser amounts of quartz-mica schist (average ~2%). Phyllite grains are weakly to moderately foliated and composed of brown to reddish brown clay. Quartz-mica schist fragments are well foliated and composed primarily of mica and quartz.

Sandstones from the Sterling Fm. have an average grain size of 0.31 mm (lower medium), moderate sorting, minor compaction, tangential to long grain contacts and little or no cement (Table 4.1; Fig. 4.5). Sterling Fm. samples are characterized primarily as litharenites or, less commonly, feldspathic litharenites (Folk, 1980; Fig. 11; Table 4.2, 4.3, 4.4). Ternary plots of Q F L, Q+ F L- and Qm P K show that the Sterling Fm. is comprised of lithic-rich sandstones with high plagioclase to total feldspar (P/F) ratios (Figs. 4.11, 4.12; Table 4.3, 4.4). Lithic compositions plotted on Qp+ Lv Ls and Ls+ Lv Lm ternary diagrams show a high proportion of volcanic rock fragments (VRF) (Figs. 4.13, 4.14; Tables 4.3, 4.4). The stratigraphically oldest Sterling Fm. samples typically have higher proportions of sedimentary rock

fragments, while stratigraphically younger samples have a higher portion of volcanic rock fragments (Figs. 4.13, 4.14; Tables 4.3, 4.4). A ternary plot of Qm F Lt indicates that the majority of older samples plot in the undissected arc while the younger samples plot in the transitional arc portion of the diagram (Dickinson, 1985; Fig. 4.15; Table 4.3, 4.4).

4.6 Discussion

4.6.1 Provenance of the Beluga and Sterling Formations

The composition of sandstone in the Beluga and Sterling fms. suggests that the accretionary prism and volcanic arc were the primary source terrains. Beluga Fm. sandstones from the Kenai Peninsula have high proportions of argillaceous lithic fragments (see Qp+ Lv Ls and Ls+ Lv Lm ternary plots in Figs. 4.8, 4.9), indicating derivation from the accretionary prism. Younger sandstones from the Beluga Fm. contain a higher proportion of volcanic rock fragments, and the ternary plots reveal that the composition of sandstones from the basal Sterling Fm. is similar to that of youngest Beluga Fm. sandstones. The shift to dominance by volcanic lithic fragments does not occur until ~6 Ma and is found only in the stratigraphically youngest samples from the type section of the Sterling Fm. at Clam Gulch (Figs. 4.16 and 4.17).

The petrologic compositions of the Beluga and Sterling fms. reflect a change in source area due to progressive basin evolution. Starting with the oldest exposures of the Beluga Fm., lithic framework grains are dominated by shale and slate-phyllite fragments and plot in the recycled lithic grains section of the Qm F Lt ternary diagram (Dickinson, 1985; Fig. 4.10). Rawlinson (1984) indicates a paleocurrent direction of ~300°on a composite measured section of the Beluga Fm. along the northern shore of Kachemak Bay, suggesting that the accretionary prism is the most likely source area. Additionally, the catchment area for the Beluga Fm. was fairly small, similar in scale to that of the modern Chulitna River that currently drains into Cook Inlet basin (Chapter 2). These lines of reasoning suggest that the likely source areas for the Beluga Fm. on the Kenai Peninsula side of the basin are the McHugh Complex and Valdez Group of the Chugach and Kenai accretionary prism complex. No evidence currently exists in

outcrop on the basin margins to suggest an axial fluvial system for the Beluga Fm., so the strata on this side of the basin are likely basin-margin fluvial systems draining to the west that probably fed an axial fluvial system in the basin center.

Beluga Fm. strata on the western side of the modern Cook Inlet basin also contain a shale and slate-phyllite, lithic-rich component, and the depositional systems are similar in size, scale and morphological expression to those of the eastern side of the basin (Chapter 2). One possible explanation is that the fluvial systems on the Kenai Peninsula reached this far west, although their relatively small size makes this unlikely. Another possibility, and our favored interpretation, is that these outcrops were sourced from the west and drained to the east. In that case, the preserved lithic fragments are probably derived from the Kahiltna Assemblage, which has a composition similar to that of the McHugh Complex and Valdez Group (Figs. 4.3 and 4.4).

4.6.2 Miocene evolution of the Cook Inlet forearc basin

Prior to ~11 Ma, anastomosed fluvial systems deposited sediments of the Beluga Fm. on the western and eastern margins of the basin. The eastern side of the basin was sourced from the accretionary prism. The western side of the basin was most likely sourced from the Kahiltna Assemblage, but the Kahiltna Assemblage and the accretionary prism produce similar lithic fragments, so contributions from an accretionary prism source cannot be ruled out.

At ~11 Ma, depositional systems and provenance started to change along the western margin of the basin (Figs. 4.18 and 4.19), where deposition of the Beluga Fm. ceased as southward-flowing braided stream depositional systems of the Sterling become dominant. These braided depositional systems migrated eastward until they filled the entire basin; they are first recorded on the Kenai Peninsula at ~8 Ma (R. Gillis unpublished data; Dallegge and Layer, 2004; Turner et al., 1980; Triplehorn et al., 1977).

Haeussler et al. (2008) provide evidence of rapid exhumation and uplift in the western and central Alaska Range as early as ~24 Ma, creating topography, and generating sediment, in the Tordrillo Mountains and the Western Alaska Range. Additional or continued uplift in this region may explain why Sterling Fm. sandstones first appear on the western side of the basin, adajacent to the Tordrillo Mountains.

On the Kenai Peninsula, the Beluga-Sterling transition is characterized by changes in sand body geometry and depositional systems from anastomosing channels of the Beluga Fm. to sandy braided channels of the Sterling Fm. (chapter 2; LePain et al. 2009). Kirschner and Lyon (1973) document an increase in heavy mineral suites in progressively younger sediments on the Kenai Peninsula. They interpret this increase to signify that a greater proportion of sediment was being derived from the Alaska Range. The significant increase in the proportion of volcanic lithic fragments in Sterling Fm. sandstone found in this work supports a change in provenance at this time. As the source changed from the accretionary prism to the volcanic arc and western Alaska Range, the depositional systems changed from anastomosed rivers to axial sandy braided streams (Fig. 4.19).

The type section of the Sterling Fm. at Clam Gulch was deposited at ~ 6 Ma (Dallege and Layer, 2004; Fig. 4.20). By this time the sandy braided depositional systems of the Sterling Fm. were firmly established on the Kenai Peninsula and volcanic lithic fragments dominate sandstone (Figs. 4.8, 4.9, 4.13, 4.14, 4.16, 4.17) sourced from the volcanic arc. There is also a significant fraction of sand that was likely sourced from the western Alaska Range (Kirschner and Lyon, 1973). Younger strata are not exposed, but this basin configuration likely remained until further deterioration of climate and major reorganization of drainage systems by glaciation (Haug et al., 1995).

4.6.3 Late Miocene Exhumation Events

Kirschner and Lyon (1973) examined heavy mineral suites of the Sterling Fm. and concluded that the sediment was likely derived from the Alaska Range. Fitzgerald et al. (1995) and Haeussler et al. (2008)

indicate that the central Alaska Range and the Tordrillo Mountains are responsible for the voluminous Pliocene sediments in Cook Inlet. Haeussler et al. (2008) further note that rapid cooling of the Tordrillo Mountains occurred ~23 Ma and ~6 Ma, based on apatite fission track and apatite helium data. The timing of both exhumations indicates that these were uplift events, and they have been linked to counter-clockwise rotation of southern Alaska due to far-field effects of the collision of the Yakutat microplate (Benowitz, 2011; Haeussler et al., 2008). Outcrops of the older Sterling Fm. on the west side of Cook Inlet suggest denudation in the central and western Alaska Range at ~11 Ma, earlier than previously acknowledged (Haeussler et al., 2008; Benowitz, 2011; Figs. 4.2, 4.4). At ~11 Ma on the western side of the basin depositional systems changed from basin margin anastomosing to southward-directed axial braided fluvial (chapter 2). The southward-flowing axial fluvial system was likely sourced from the western Alaska Range and the volcanic arc to the northwest and west (chapter 2). There is no volcanic edifice to the north, suggesting that the change in sediment supply was the result of an exhumation event and/or stream capture in the western Alaska Range. This new work suggests that additional thermochronological sampling in the Western Alaska Range is warranted.

4.7 Conclusions

The lower to middle Beluga Fm. is primarily derived from the accretionary prism, while the upper Beluga Fm. has a higher proportion of volcanic lithic fragments. Sandstones of the upper Beluga and lower Sterling fms. have similar proportions of volcanic lithic fragments, and younger Sterling Fm. sandstones have even higher proportions. This trend suggests a progressive change in provenance from the accretionary prism to volcanic arc throughout deposition of the Beluga and Sterling fms.

A reconstruction of the late Miocene basin history is now possible thanks to improved stratigraphic control (Dallegge and Layer, 2004; R. Gillis, Personal Communication), a better understanding of the depositional systems (Chapter 2; LePain et al., 2009), and provenance data (Helmold et al., 2012). Prior to ~11 Ma, deposition along the eastern basin margin was dominated by anastomosing rivers sourced

primarily from the accretionary prism. Younger strata of the Beluga Fm. reveal an increasing contribution from the volcanic arc. Between ~11 Ma and ~8 Ma depositional systems changed to southward-directed, sandy braided fluvial channels with mixed accretionary prism and volcanic arc sources. After ~8 Ma the sandy braided systems were established across the entire basin and the volcanic arc became the dominant sediment source. This Miocene basin history suggests that a previously undocumented exhumation event occurred ~ 11 Ma.

4.8 Figures

Figure 4.1: Digital elevation model (DEM) depicting the physiographic setting of Southern Alaska. Cook Inlet is situated in the forearc basin position and extends from Shelikof Strait to the Wrangell Mountains. Exposures of the Beluga and Sterling fms. are found on the Kenai Peninsula near the town of Homer and on the western side of Cook Inlet west of Anchorage.

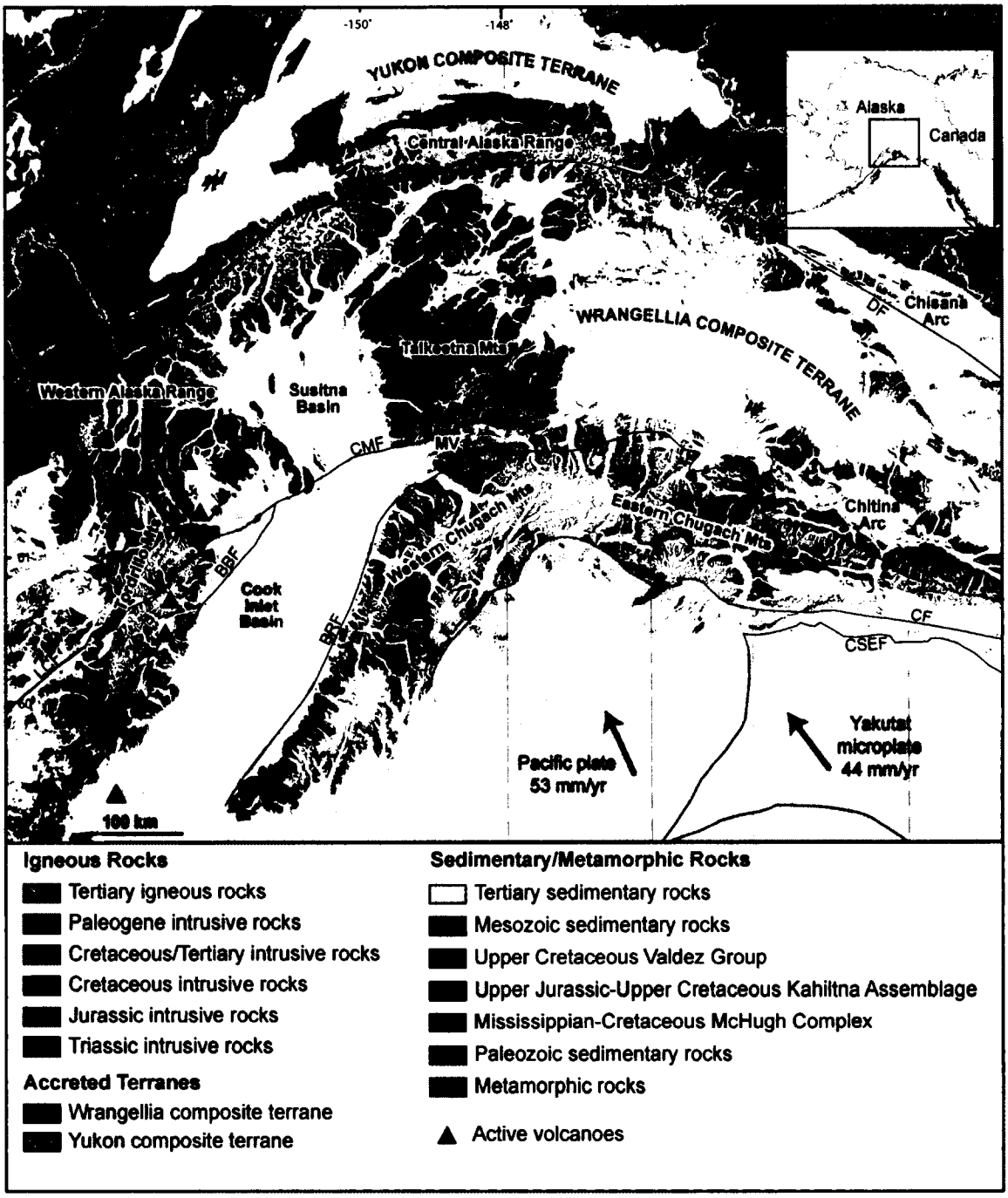

Figure 4.2: Simplified geologic map of southern Alaska showing arc region (western and central Alaska Range, Talkeetna Mountains), retroarc region (Yukon composite terrane), eastern region (Matanuska Valley (MV), western and eastern Chugach Mountains, Chisana and Chinitna arc) of the forearc basin. Arrows depict relative plate motions of the Pacific Plate and Yakutat Microplate. Major faults in the area are also shown: CSEF – Chugach-St. Elias Fault; CF – Contact Fault; BRF – Border Ranges Fault; BBF – Bruin Bay Fault; CMF – Castle Mountain Fault; LCF – Lake Clark Fault; DF – Denali Fault. Modified from Finzel (2010); Beikman (1980), Moll-Stalcup et al. (1994), Greninger et al. (1999).

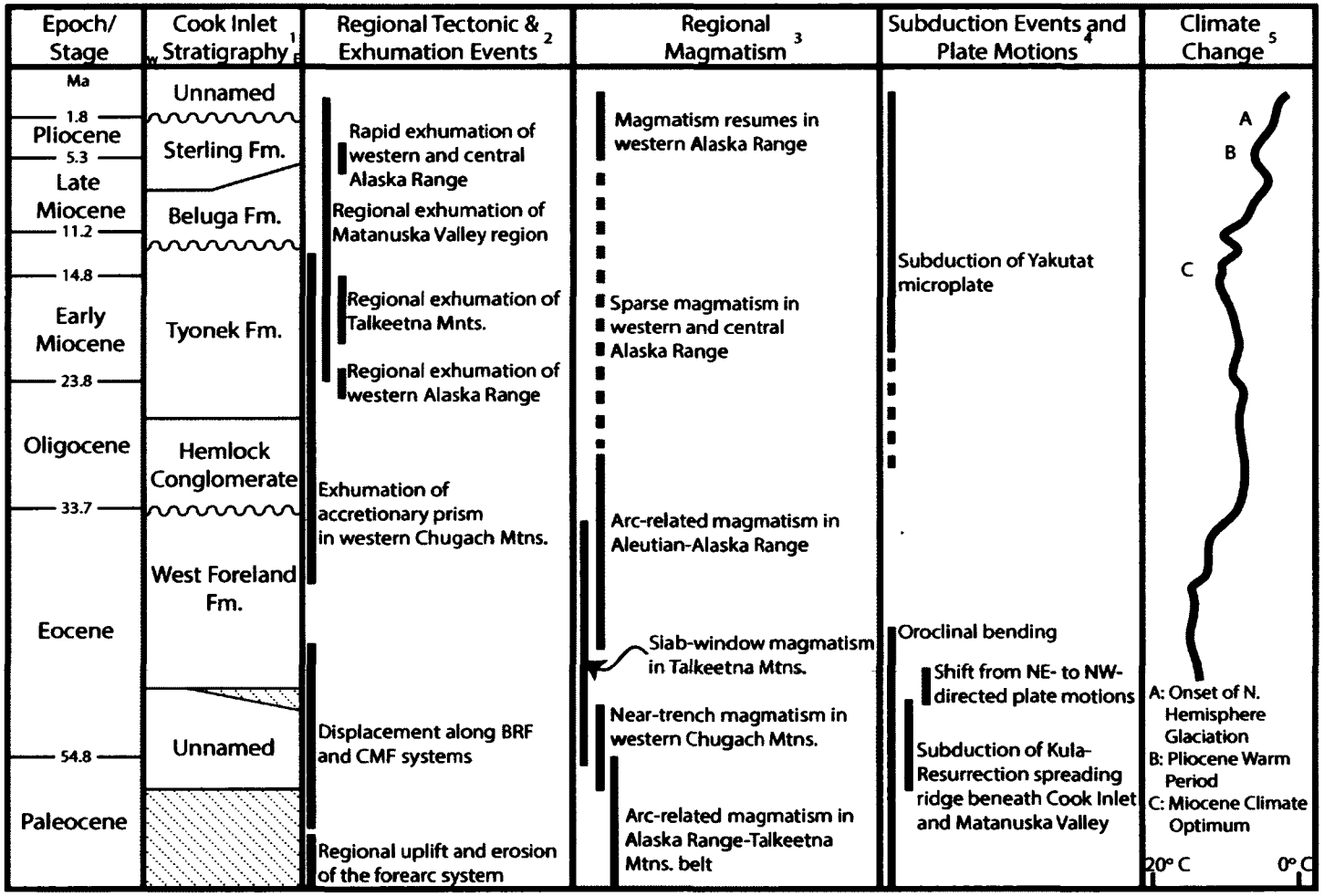

Figure 4.3: Age-event diagram for the Cenozoic Cook Inlet strata (Modified from Finzel, 2010). 1) Stratigraphy, from Flores et al., 2004; 2) Regional Tectonic and Exhumation Events, compiled from Fuchs, 1980; Little and Naeser, 1989; Fitzgerald et al., 1995; Pavlis and Roeske, 2007; and Haeussler et al., 2008; 3) Regional Magmatism, compiled from Moll-Stalcup et al., 1994; Plafker et al., 1994; Bradley et al., 2003; and Cole et al., 2006; 4) Subduction Events and Plate Motions, compiled from Stock and Molnar, 1988; Plafker et al., 1994; Haeussler et al., 2003; and Bradley et al., 2003); 5) Climate Change, from Zachos et al., 2001; and Wolfe et al., 1966.

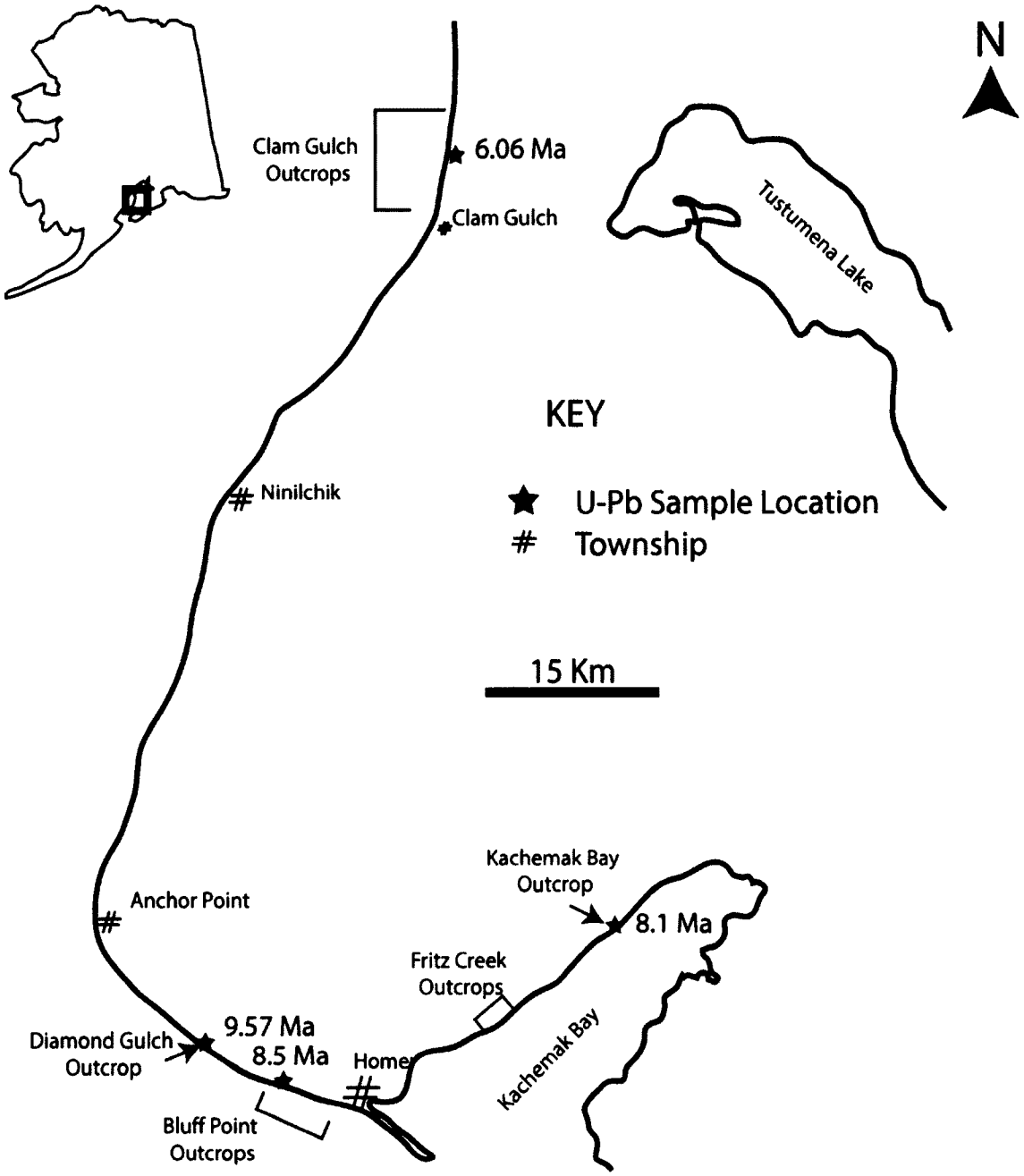

Figure 4.4: Location of outcrops and published age dates used in this study in the Cook Inlet area.

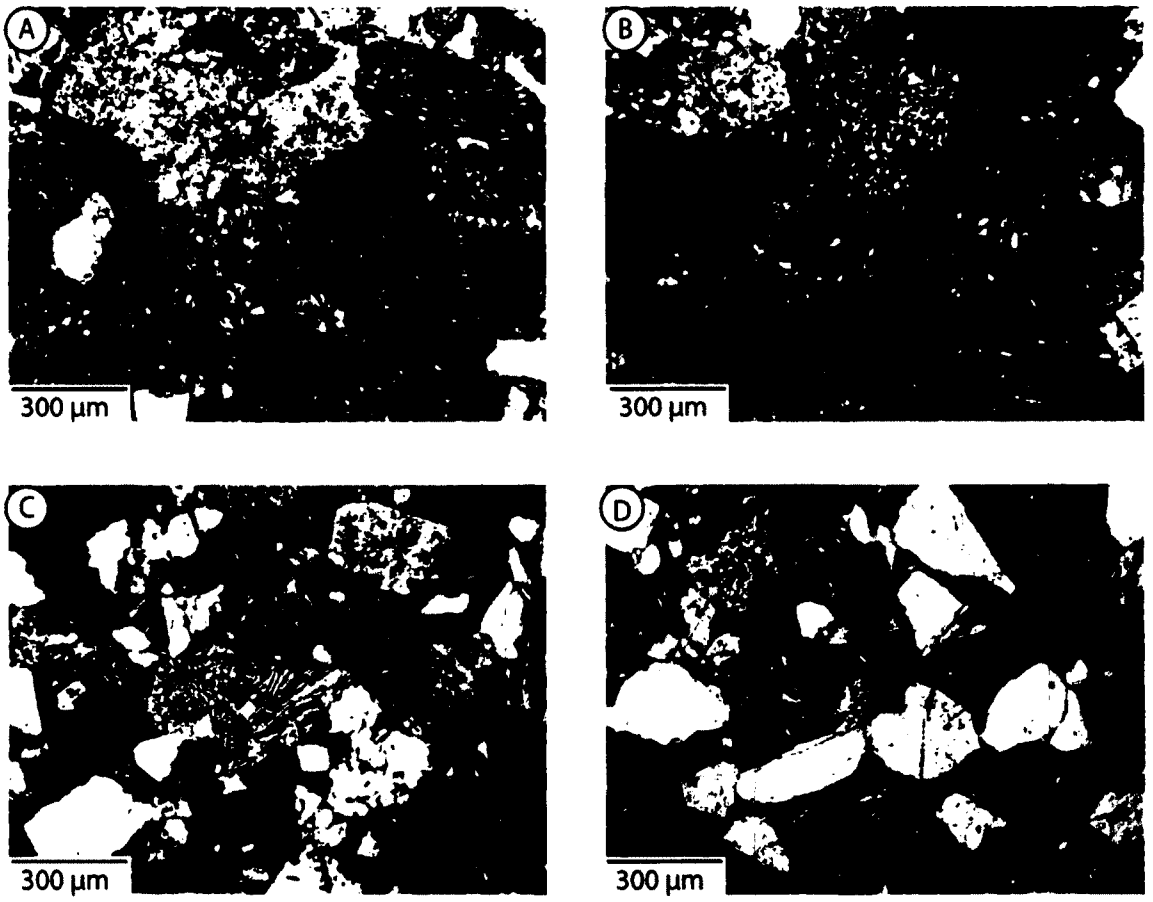

Figure 4.5: Photomicrographs of the Beluga and Sterling fms. Photomicrographs A and B are from the Beluga Fm. Note the moderate grain deformation and shale lithologies common in these sandstones. Photomicrographs C and D are from the Sterling Fm. These sandstones have less evidence of grain deformation and abundance of volcanic lithic fragments.

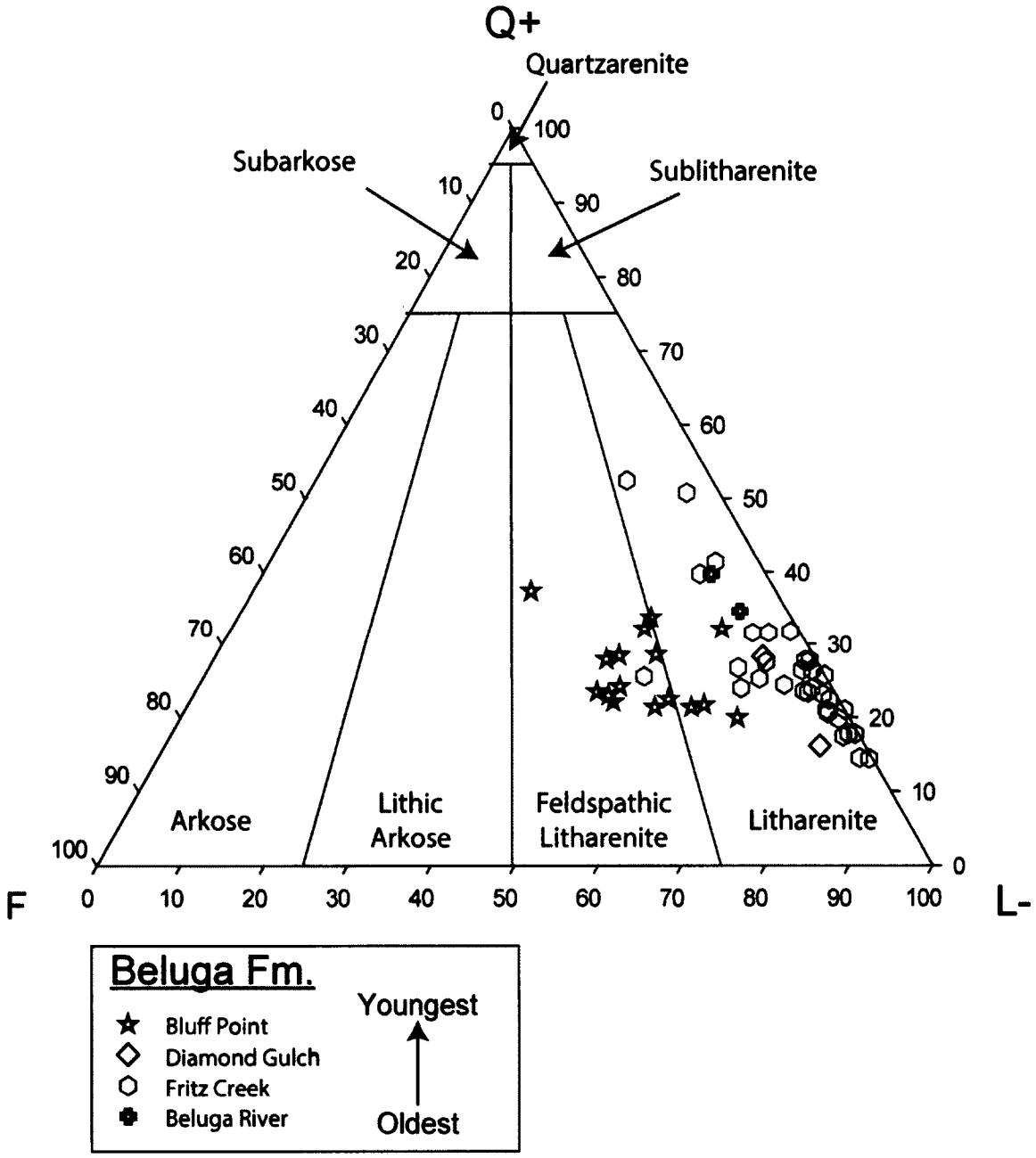

Figure 4.6: Beluga Fm. Q+ F L- ternary diagram. Q+: total quartz and chert, F: total feldspar (i.e. plagioclase, alkali feldspar, undifferentiated feldspar), L-: total lithics not including detrital minerals. Beluga River samples are from the oldest outcrops and Bluff Point samples are from the youngest Beluga Fm. outcrops. Most samples are litharenites, the remaining samples are feldspathic litharenites.

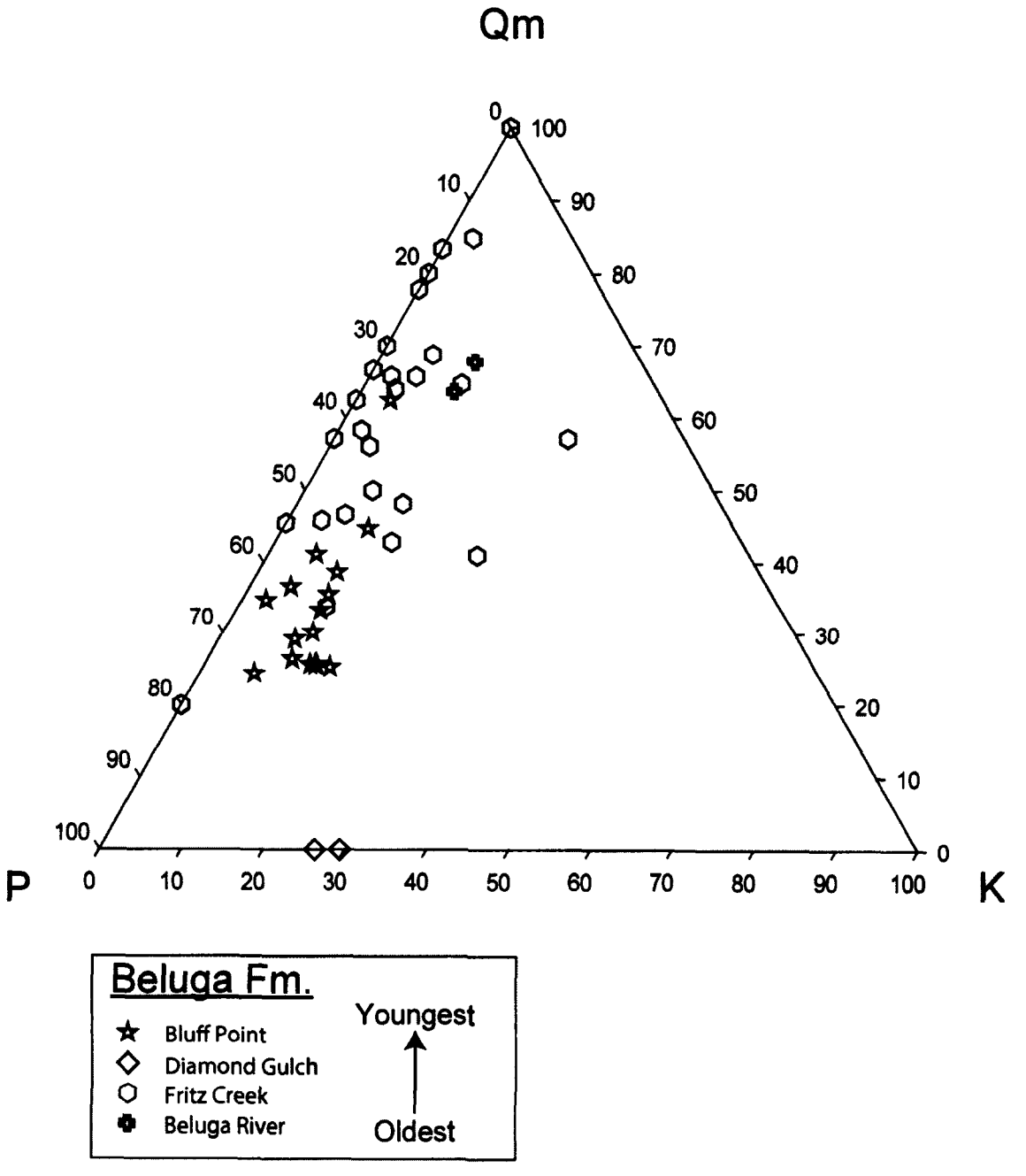

Figure 4.7: Beluga Fm. Qm P K ternary diagram. Qm: monocrystalline quartz, P: total plagioclase, K: total alkali feldspar. Beluga River samples are from the oldest outcrops and Bluff Point samples are from the youngest Beluga Fm. outcrops. Most samples plot along the Qm P side of the diagram indicating a high plagioclase to total feldspar ratio.

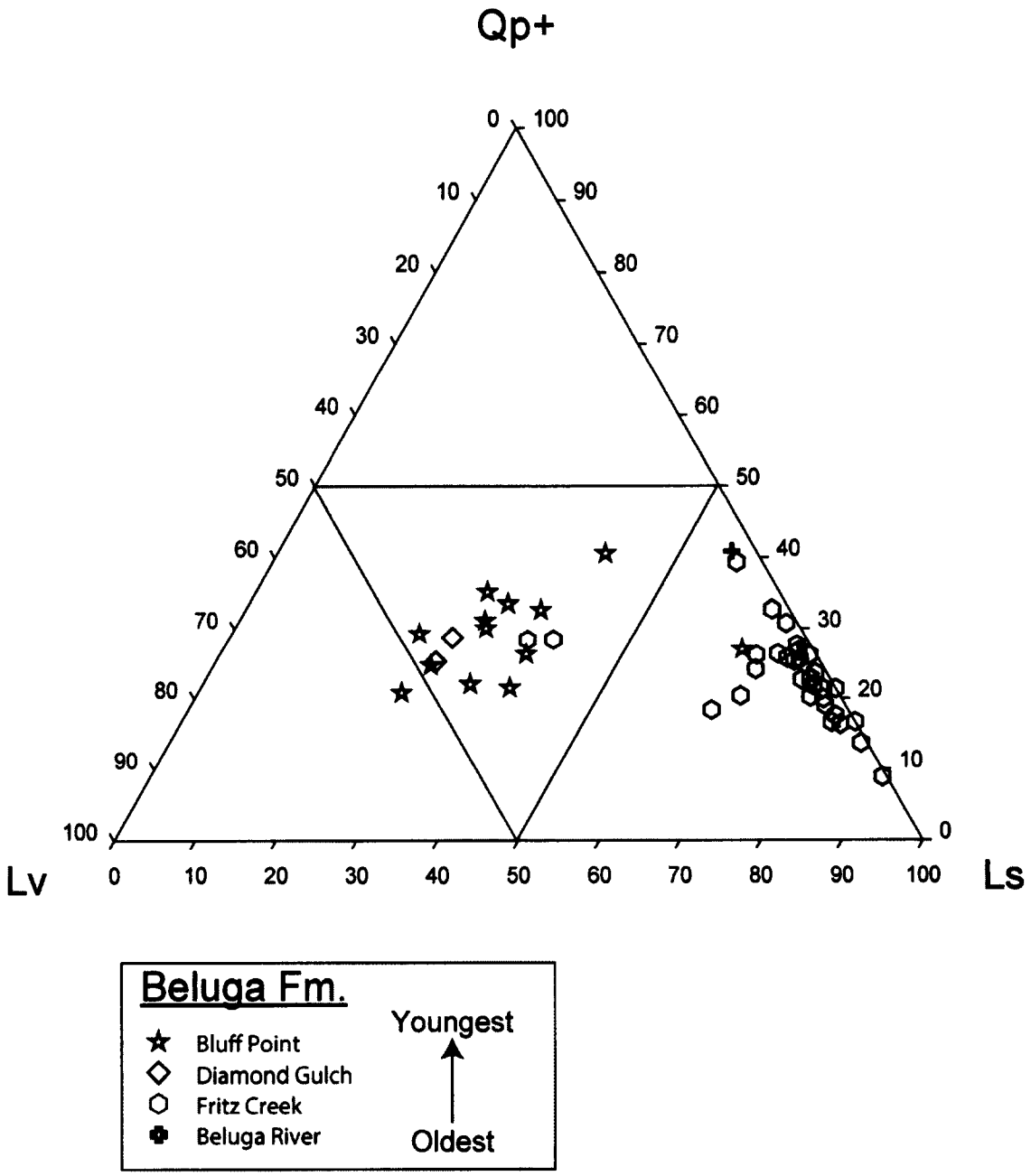

Figure 4.8: Beluga Fm. Qp+ Lv Ls ternary diagram. Qp+ polycrystalline quartz plus chert, Lv: total volcanic lithic fragments, Ls: total sedimentary lithic fragments. Beluga River samples are from the oldest outcrops and Bluff Point samples are from the youngest Beluga Fm. outcrops. The younger samples tend to have a higher proportion of volcanic lithic fragments interpreted as evidence for a change in provenance from the accretionary prism to the volcanic arc.

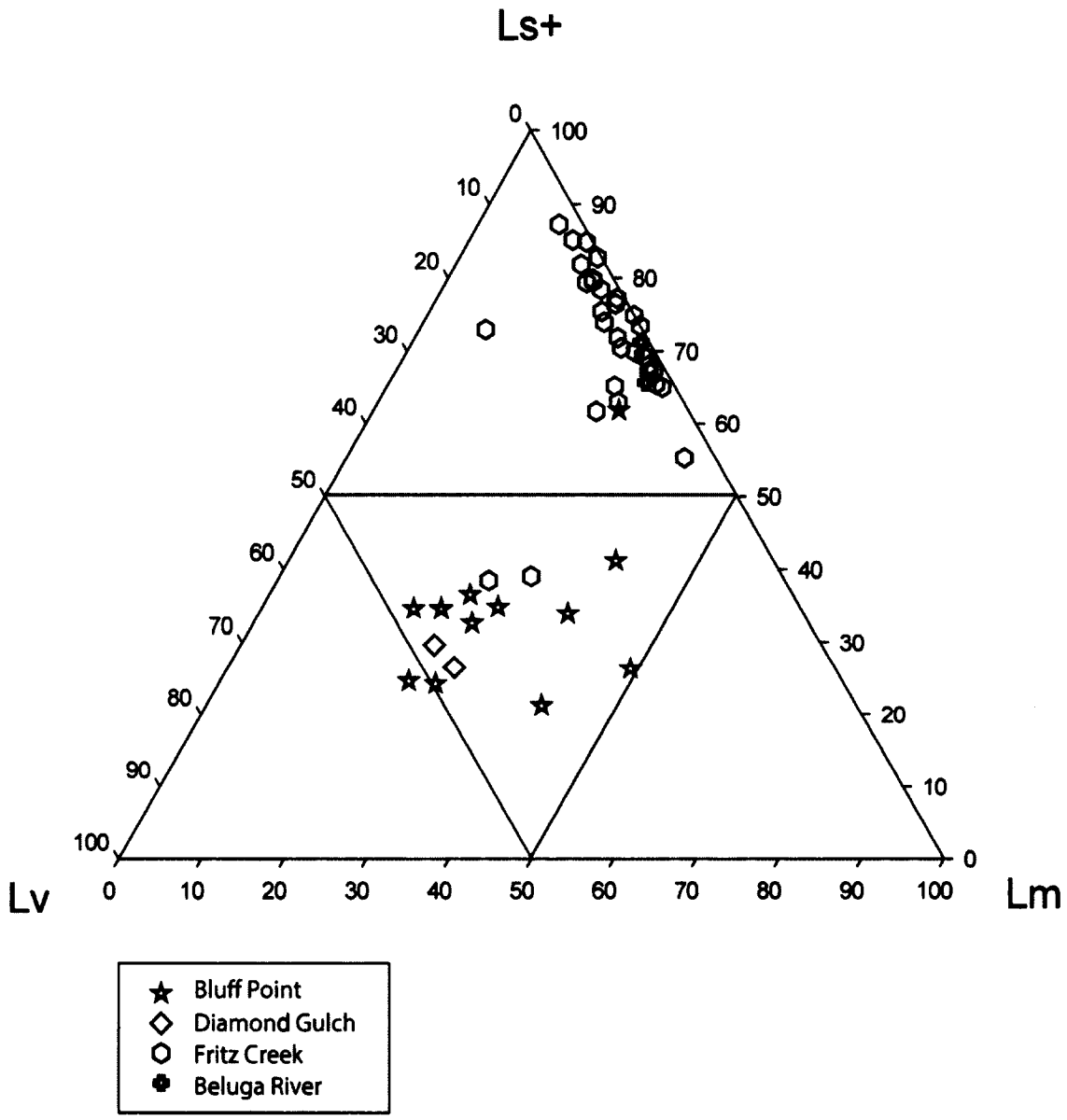

Figure 4.9: Beluga Fm. Ls+ Lv Lm ternary diagram. Ls+: differentiated sedimentary lithic fragment plus chert plus intrabasinal sedimentary lithic fragment, Lv: total volcanic lithic fragments, Lm: total metamorphic lithic fragments. Beluga River samples are from the oldest outcrops and Bluff Point samples are from the youngest Beluga Fm. outcrops. This is a similar plot to the Qp+ Lv Ls ternary diagram showing a trend towards a higher proportions of volcanic lithic fragments in stratigraphically younger samples, interpreted as evidence for change of provenance from the accretionary prism to the volcanic arc.

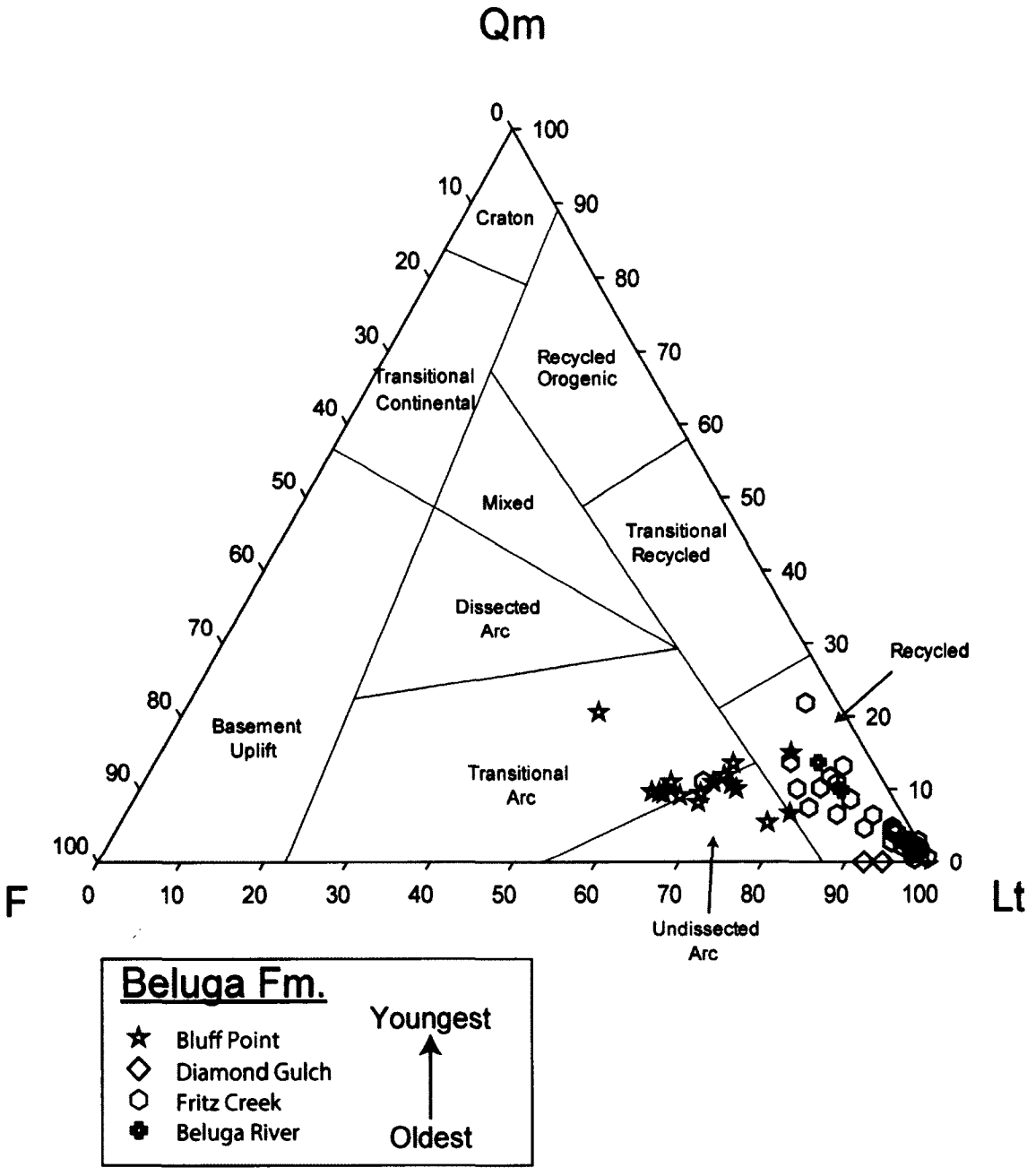

Figure 4.10 Beluga Fm. Qm F Lt ternary diagram. Qm: monocrystalline quartz, F: total feldspar (i.e. plagioclase, alkali feldspar, undifferentiated feldspar), Lt: total lithic fragments. Beluga River samples are from the oldest outcrops and Bluff Point samples are from the youngest Beluga Fm. outcrops. The younger samples tend to plot in the undissected to transitional arc of Dickinson (1985). This is interpreted as evidence for a shift in provenance from the accretionary prism to the volcanic arc.

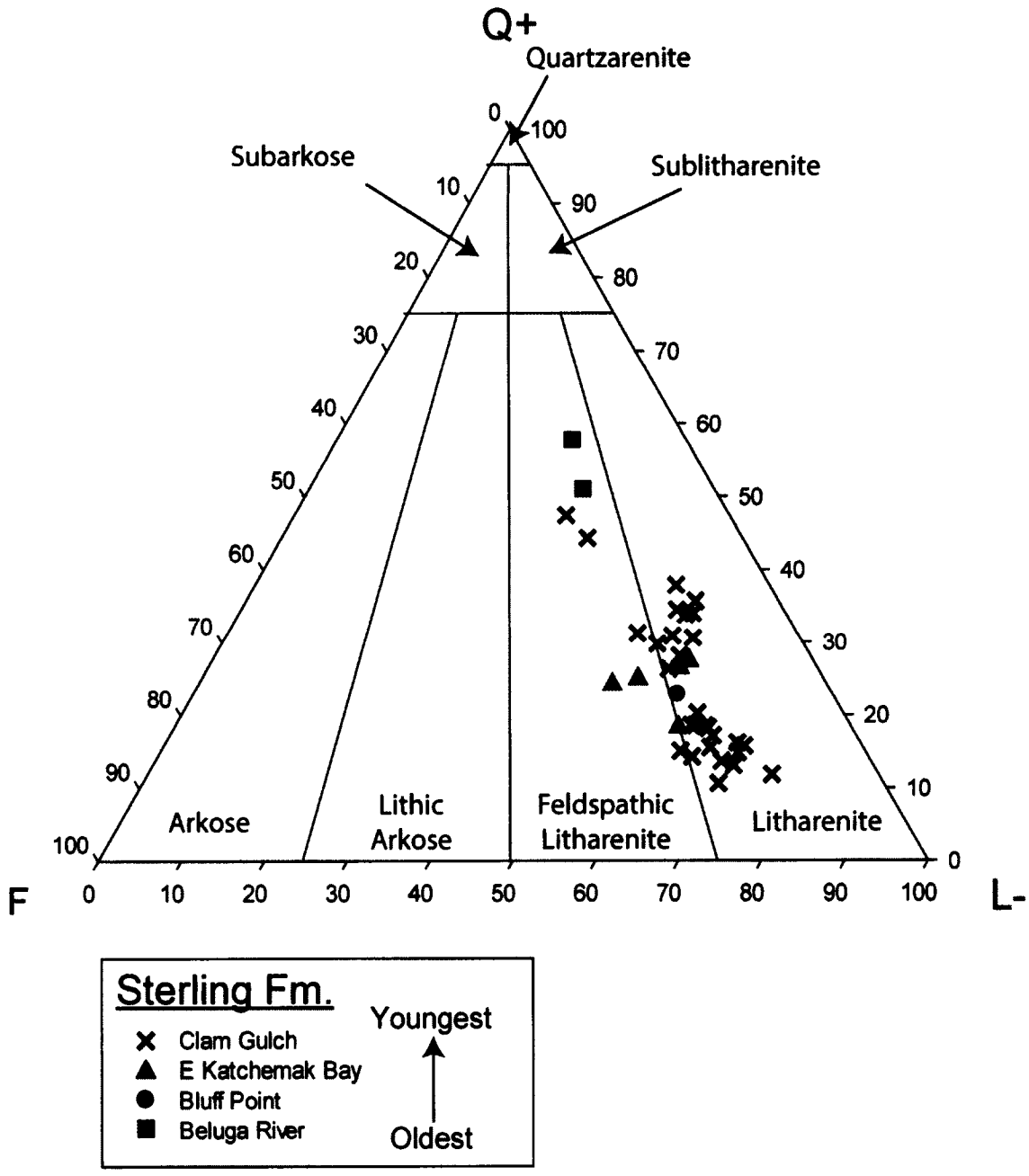

Figure 4.11: Sterling Fm. Q+ F L- ternary diagram. Q+: total quartz and chert, F: total feldspar (i.e. plagioclase, alkali feldspar, undifferentiated feldspar), L-: total lithics not including detrital minerals. The Beluga River samples are from the oldest outcrops and Clam Gulch samples are from the youngest Sterling Fm. outcrops. Most samples are litharenites while the remaining samples are feldspathic litharenites.

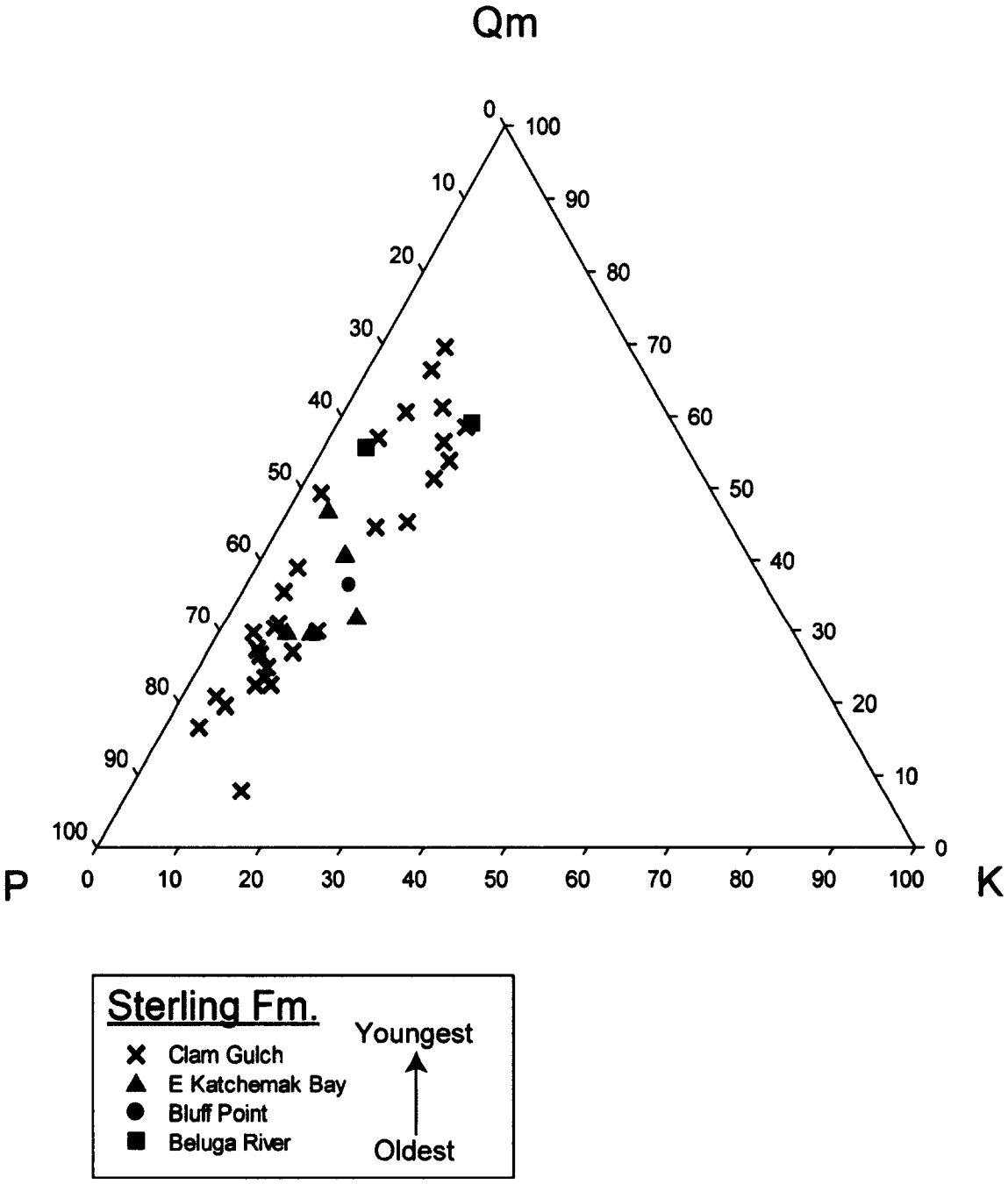

Figure 4.12: Sterling Fm. Qm P K ternary diagram. Qm: monocrystalline quartz, P: total plagioclase, K: total alkali feldspar. Beluga River samples are from the oldest outcrops and Clam Gulch samples are from the youngest Sterling Fm. outcrops. Most samples plot along the Qm P side of the diagram indicating a high plagioclase to total feldspar ratio interpreted as evidence for an intermediate igneous provenance.

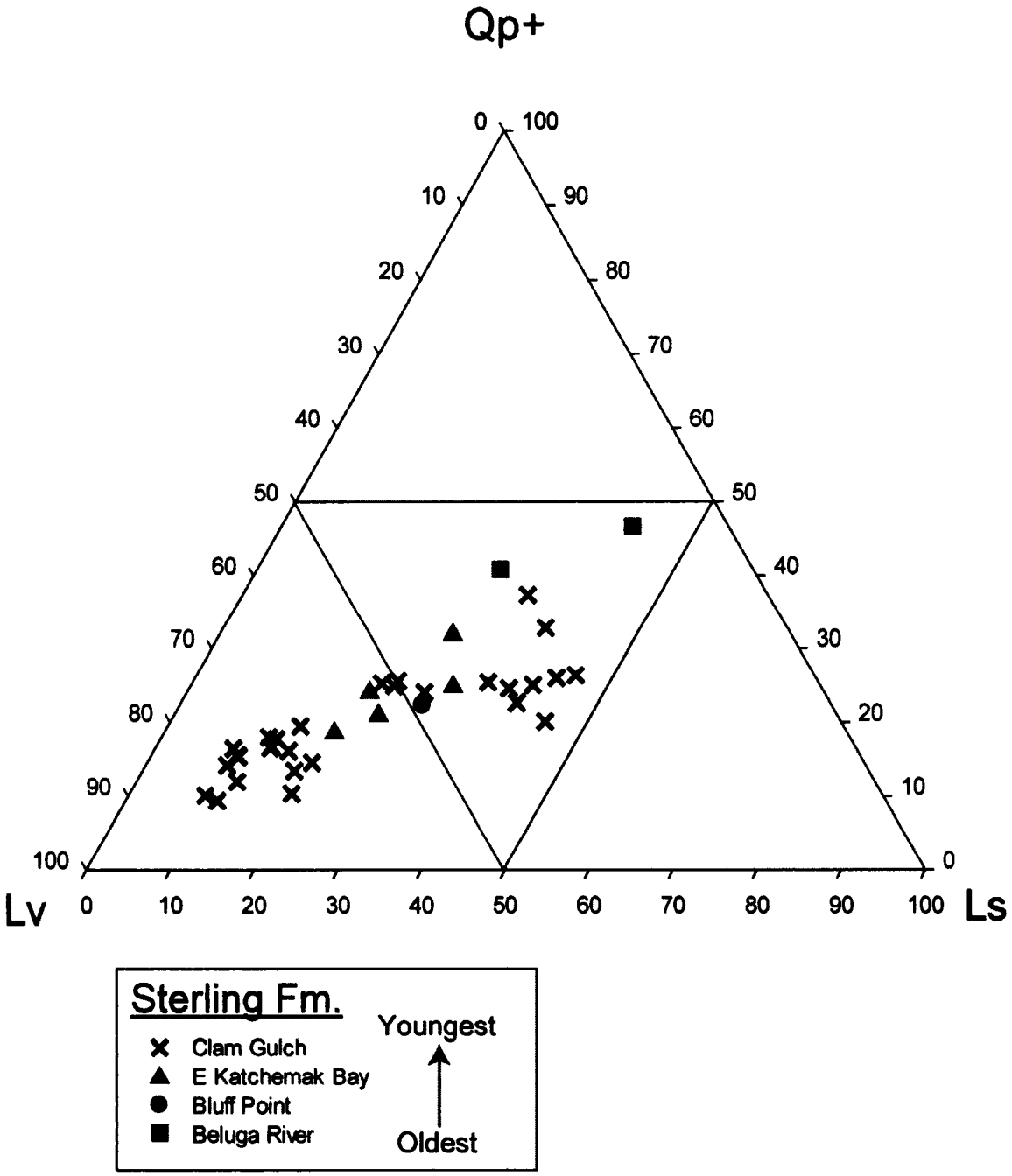

Figure 4.13: Sterling Fm. Qp+ Lv Ls ternary diagram. Qp+ polycrystalline quartz plus chert, Lv: total volcanic lithic fragments, Ls: total sedimentary lithic fragments. Beluga River samples are from the oldest outcrops and Clam Gulch samples are from the youngest Sterling Fm. outcrops. The younger samples tend to have a higher proportion of volcanic lithic fragments. This is interpreted as evidence for a change in provenance from a mixed accretionary prism and volcanic arc source to a dominantly volcanic arc source.

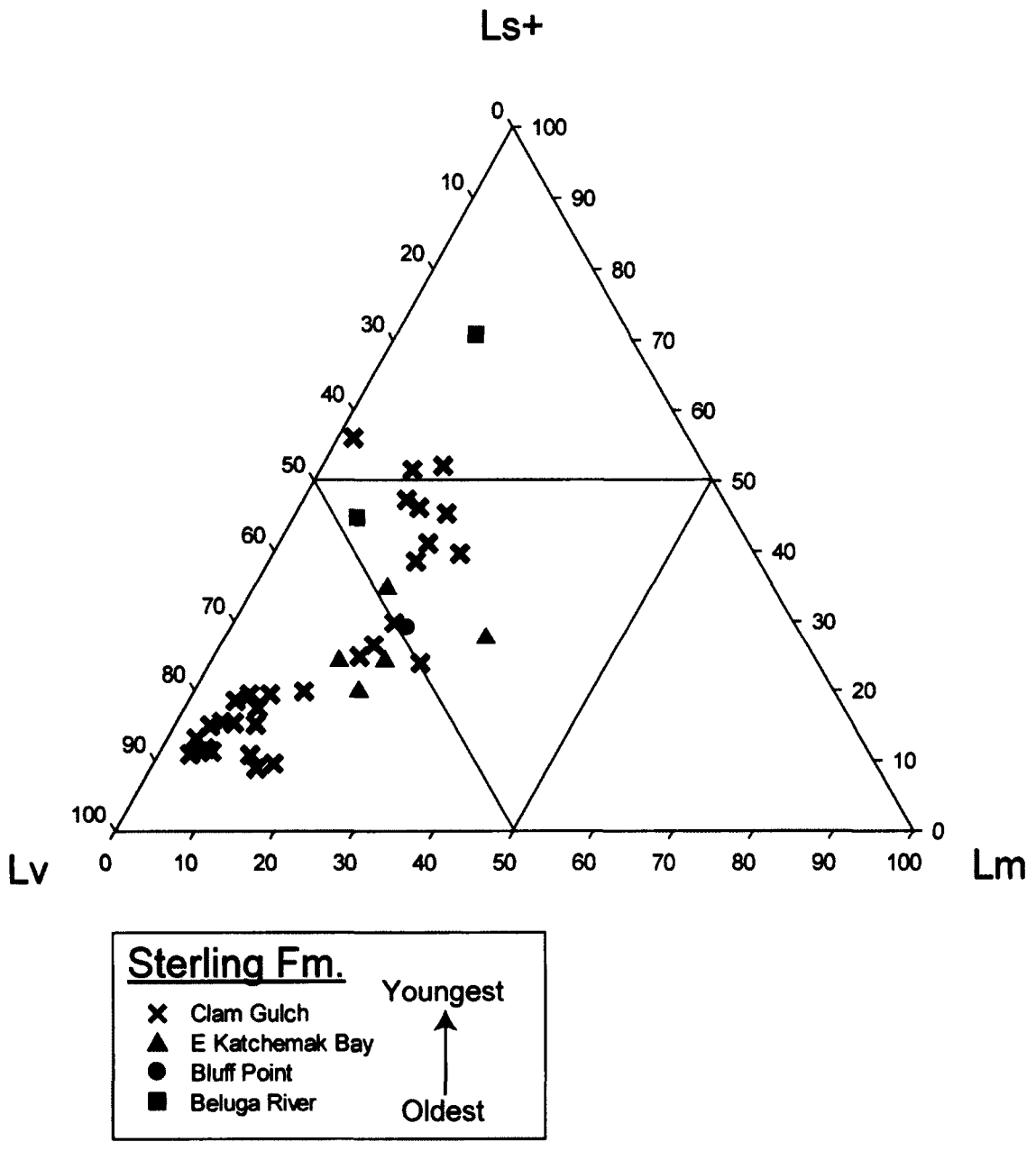

Figure 4.14: Sterling Fm. Ls+ Lv Lm ternary diagram. Ls+: differentiated sedimentary lithic fragment plus chert plus intrabasinal sedimentary lithic fragment, Lv: total volcanic lithic fragments, Lm: total metamorphic lithic fragments. Beluga River samples are from the oldest outcrops and Clam Gulch samples are from the youngest Sterling Fm. outcrops. This is a similar plot to the Qp+ Lv Ls ternary diagram showing a trend towards a higher proportion of volcanic lithic fragments in stratigraphically younger samples. This is interpreted as evidence for a change in provenance from a mixed accretionary prism and volcanic arc source to a dominantly volcanic arc source.

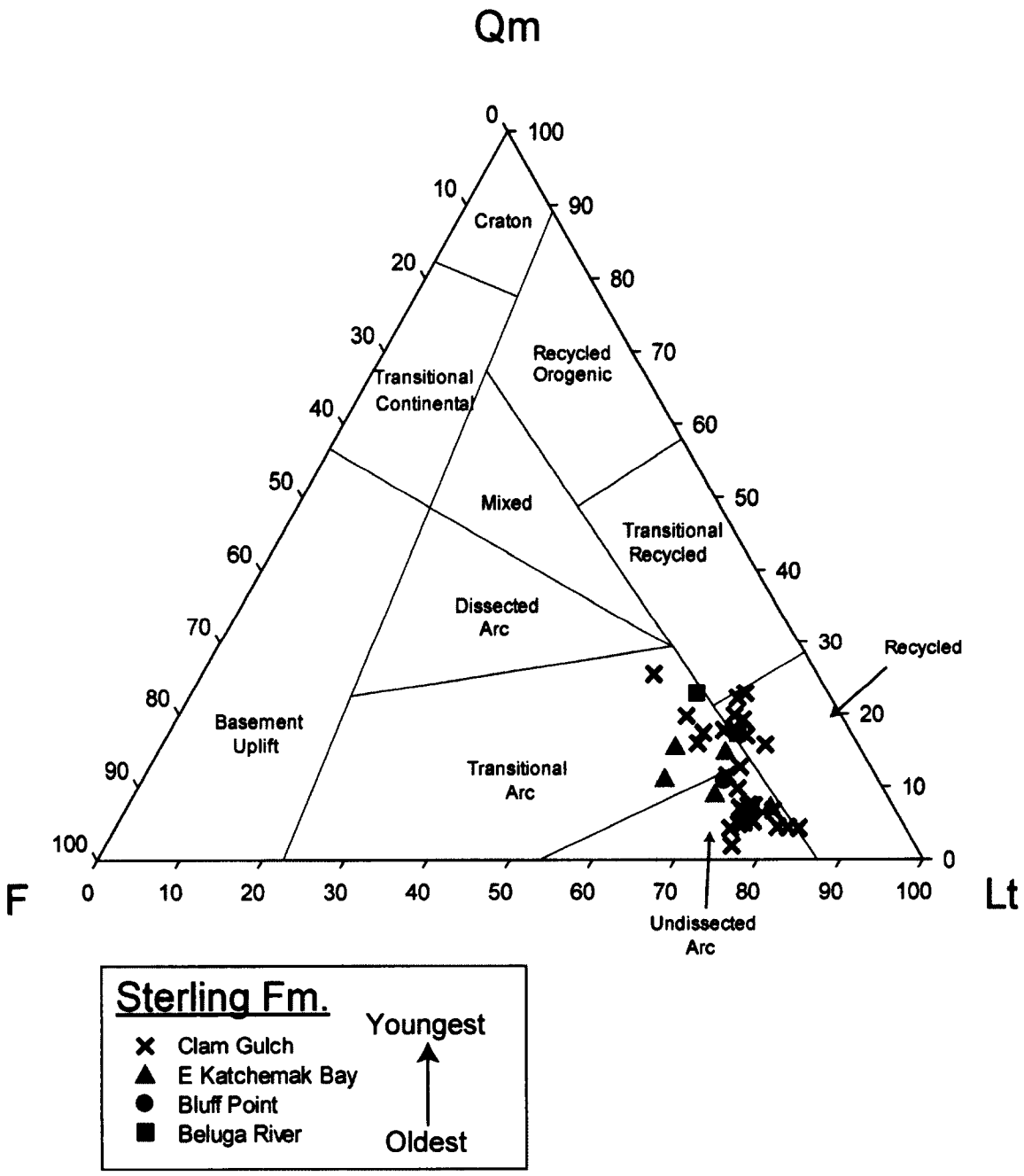

Figure 4.15: Sterling Fm. Qm F Lt ternary diagram. Qm: monocrystalline quartz, F: total feldspar (i.e. plagioclase, alkali feldspar, undifferentiated feldspar), Lt: total lithic fragments. Beluga River samples are from the oldest outcrops and Clam Gulch samples are from the youngest Sterling Fm. outcrops. The younger samples tend to plot in the undissected to transitional arc of Dickinson (1985). This is interpreted as evidence for a shift in provenance from a mixed accretionary prism volcanic arc source to a dominantly volcanic arc source.

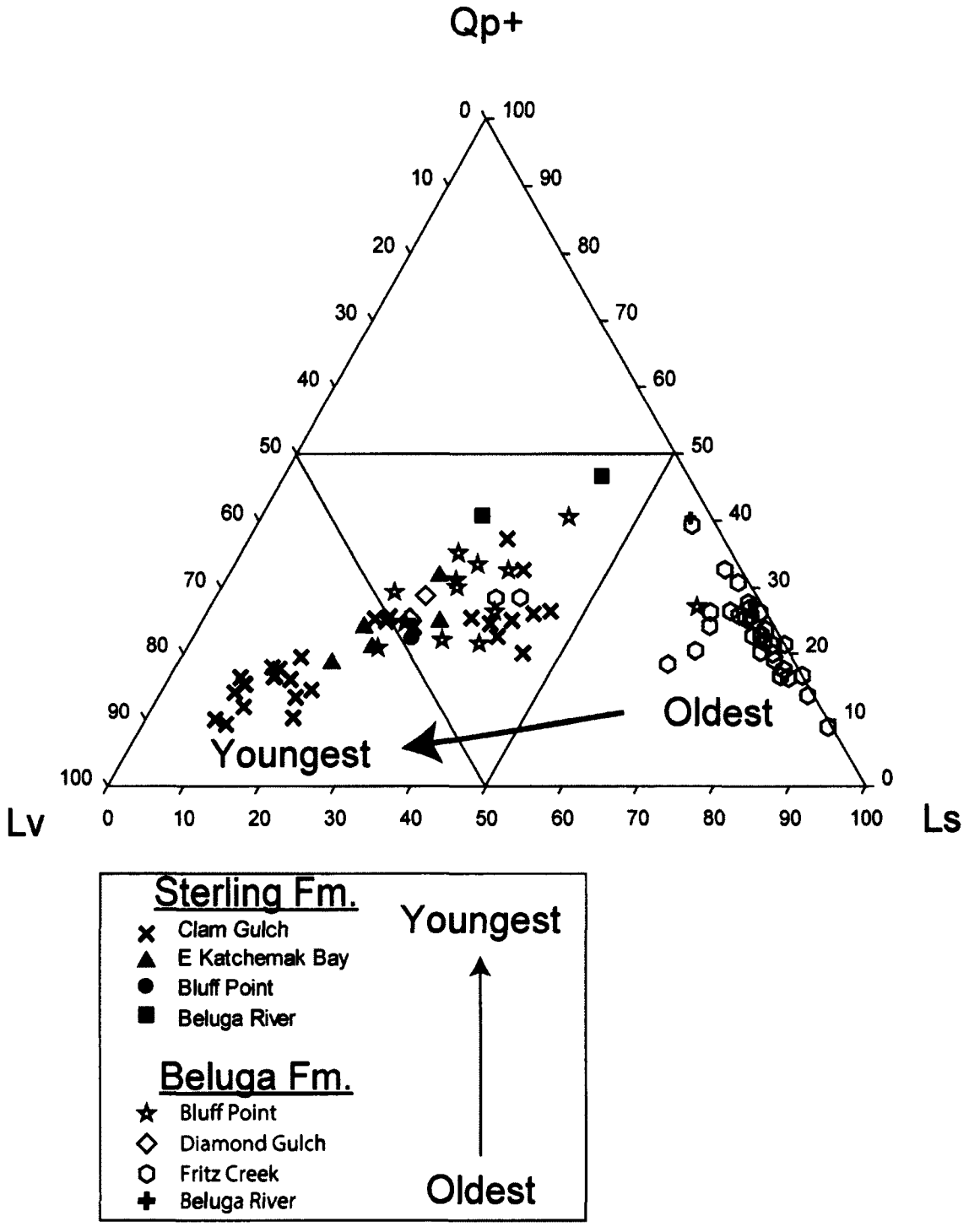

Figure 4.16: Beluga and Sterling fms. Qp+ Lv Ls ternary diagram. Qp+ polycrystalline quartz plus chert, Lv: total volcanic lithic fragments, Ls: total sedimentary lithic fragments. The samples are in stratigraphic order from the oldest Beluga Fm Beluga River samples to the Sterling Clam Gulch samples. When plotted together the change in provenance from the accretionary prism to volcanic arc becomes clear.

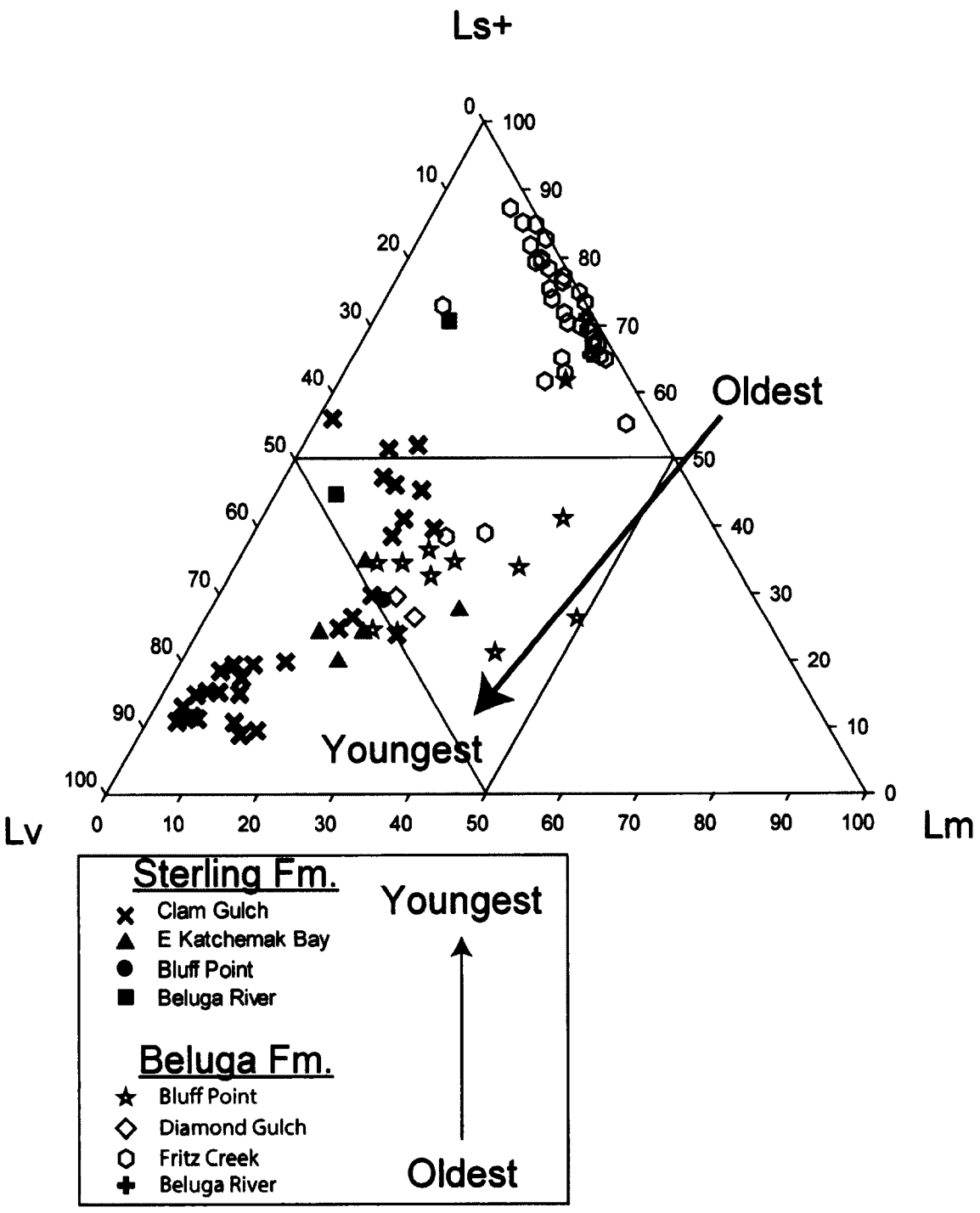

Figure 4.17: Beluga and Sterling fms. Ls+ Lv Lm ternary diagram. Ls+: differentiated sedimentary lithic fragment plus chert plus intrabasinal sedimentary lithic fragment, Lv: total volcanic lithic fragments, Lm: total metamorphic lithic fragments. The samples are in stratigraphic order from the oldest Beluga Fm. Beluga River samples to the Sterling Clam Gulch samples. When plotted together the change in provenance from the accretionary prism to volcanic arc becomes clear.

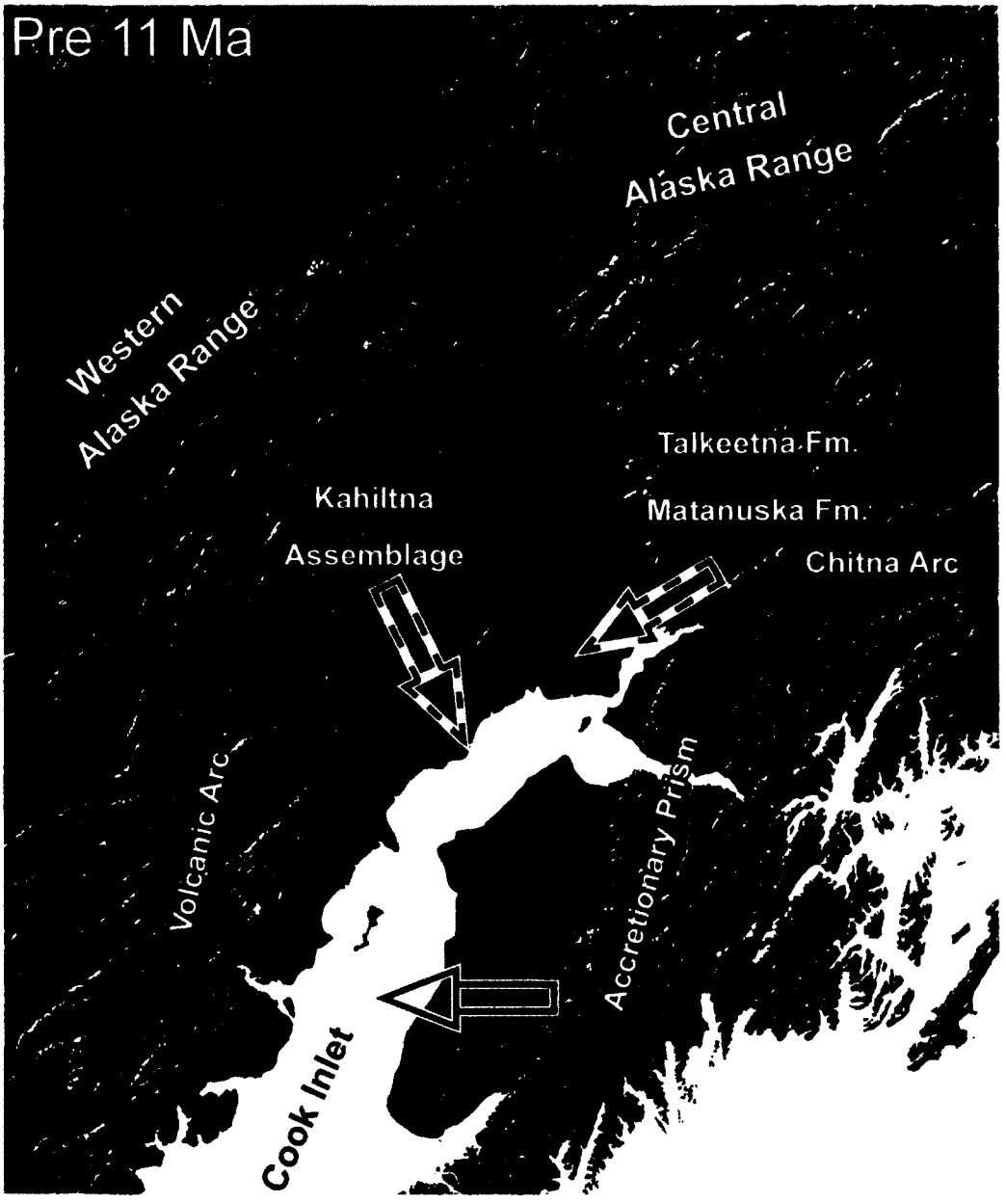

Figure 4.18: Pre 11 Ma sediment provenance of Cook Inlet forearc basin. The estward flowing single channel to anastomosing depositional systems are fairly well constrained on the east side of the basin. The paleocurrent direction of the depositional systems on the western margin is interpreted as is evidence for an axial fluvial system. The Matanuska Valley forearc basin to the northeast is contributing sediment (Finzel, 2010; Trop et al., 2003).

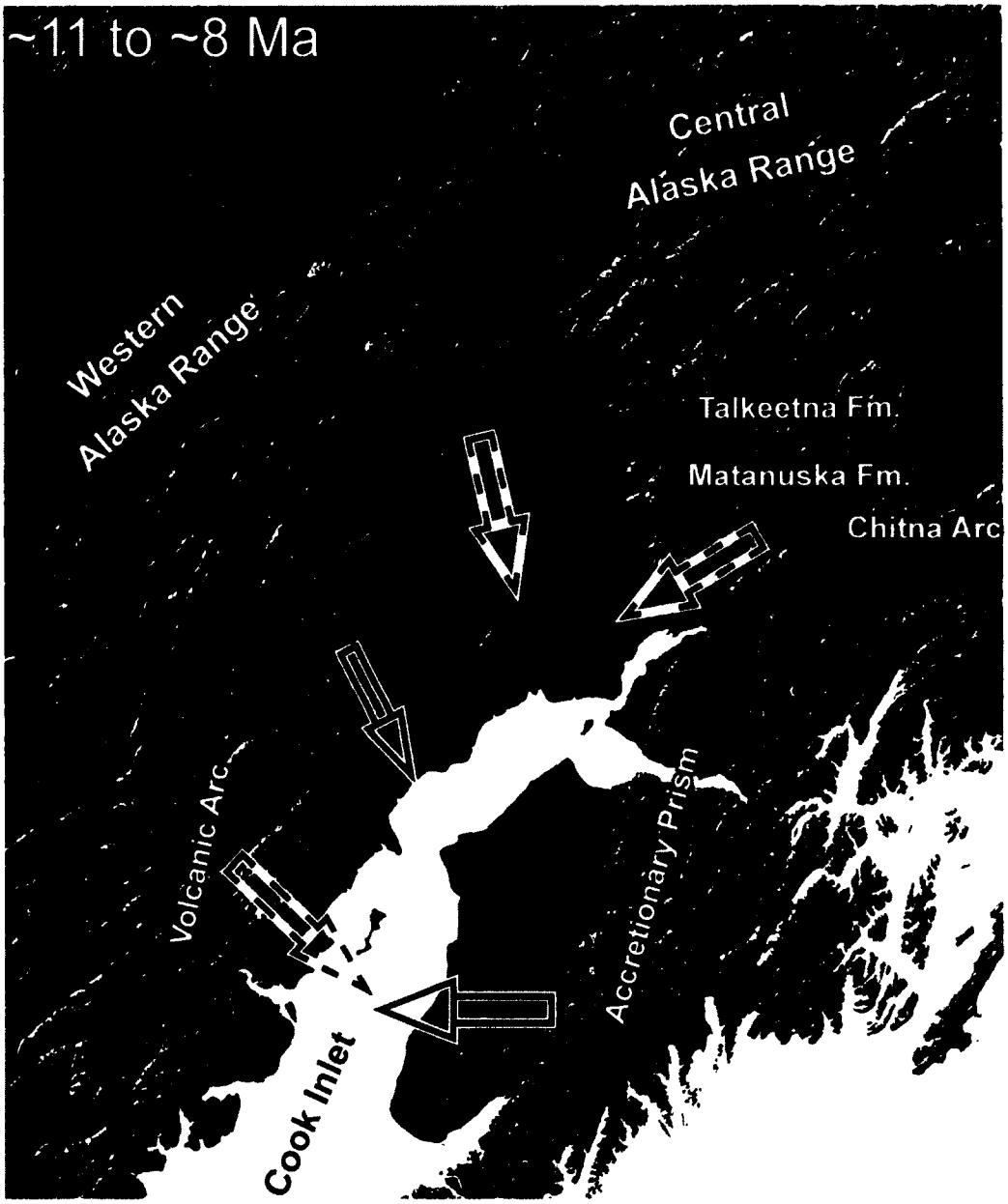

Figure 4.19: The ~11 to ~8 Ma sediment provenance of Cook Inlet forearc basin. Sandy braided depositional systems of the Sterling Fm. formed first on the west side of the basin and reached the east by ~8 Ma when deposition of the Beluga Fm. ceased.

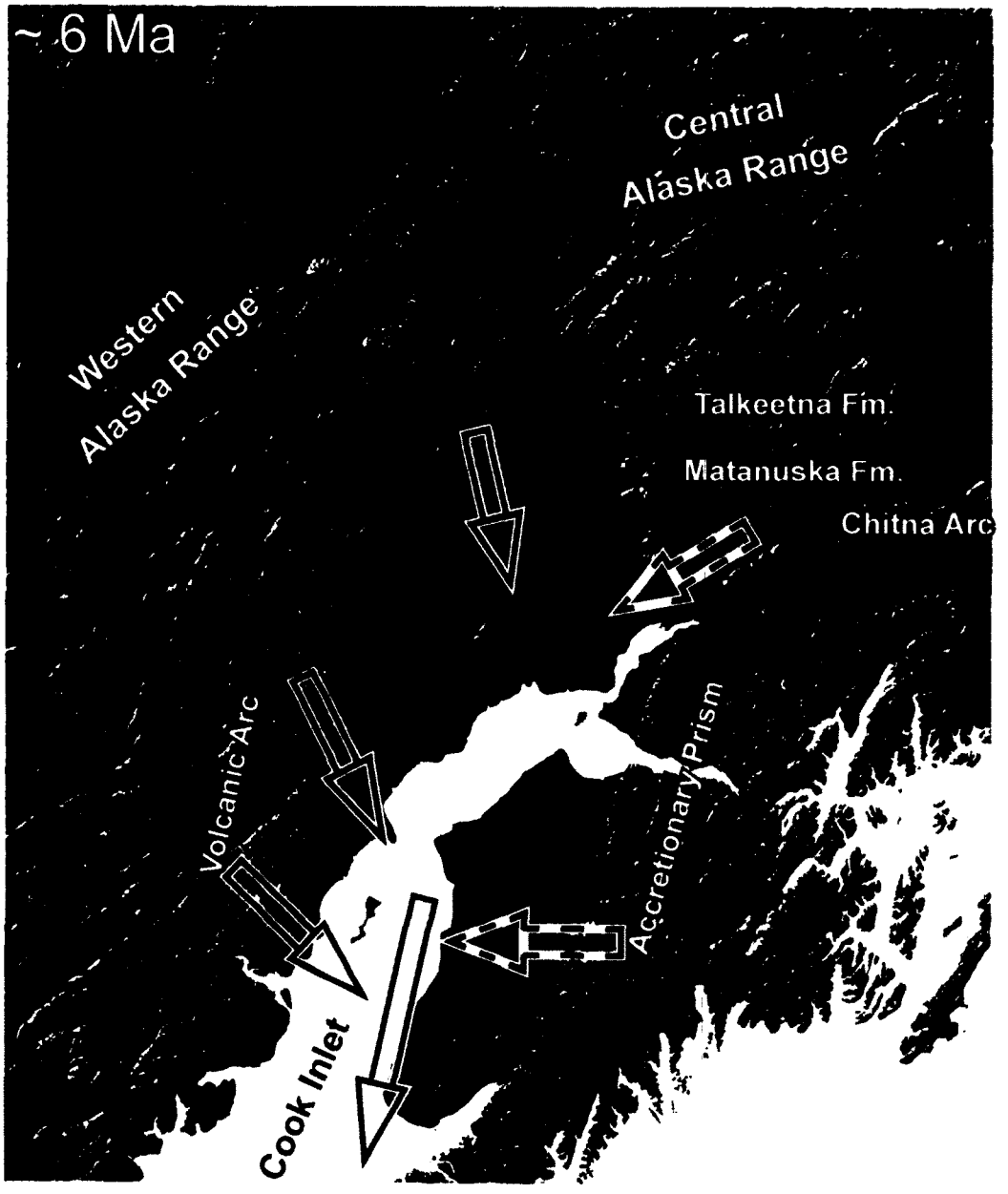

Figure 4.20: The less than ~8 Ma sediment provenance of Cook Inlet forearc basin. Sandy braided depositional systems of the Sterling Fm. are well established after ~ 8 Ma. Contributions from the accretionary prism are waning such that by ~6 Ma the sediments are derived almost entirely from the volcanic arc.

Table 4.1: Summary petrographic descriptions of the Beluga and Sterling fms.

Sterling Fm.	Characteristics
Grain Size	0.31 mm
Sorting	0.55 (moderate)
Classification	litharenites
Mineralogy	Quartz, Volcanic Lithic Fragments, Metamorphic Lithic Fragments, Sedimentary Lithic Fragments

Beluga Fm.	Characteristics
Grain Size	0.26 mm
Sorting	1.27 (poor)
Classification	litharenites
Mineralogy	Sedimentary Rock Fragments, Metamorphic Lithic Fragments, Quartz

Table 4.2: List of abbreviations

Abbreviations	Included Crystal Phases
C	Chert
F	Total Feldspar = Plagioclase + Alkali Feldspar + Undifferentiated Feldspar
K	Total Alkali Feldspar
L	Total Lithic Fragments + Detrital Minerals
Lm	Total Metamorphic Rock Fragment
Ls	Total Sedimentary Rock Fragment
Ls+	Differentiated Sedimentary Rock Fragment + Chert + Intrabasinal Sedimentary Rock Fragment
Lv	Total Volcanic Rock Fragment
P	Total Plagioclase
Q	Total Quartz = Monocrystalline Quartz + Polycrystallir Quartz + Undifferentiated Quartz
Q+	Total Quartz + Chert
Qm	Monocrystalline Quartz
Qp+	Polycrystalline Quartz + Chert

Table 4.3: Recalculated Beluga and Sterling fms. point count data

Sterling Formation	Qm	Qp	C	Q	Q+	K	P	F	Ls+	Ls	Lv	Lm	L
09JRM003-0	21.9	5.1	10.3	27.0	37.3	2.6	8.5	11.1	25.2	25.2	21.1	8.2	60.4
09JRM003-1	12.5	5.0	10.3	17.5	27.9	3.3	12.3	15.6	18.1	18.1	30.4	12.3	66.0
09JRM003-2	15.4	5.6	12.4	21.1	33.4	4.2	6.7	11.0	30.9	30.9	19.4	9.0	66.3
09JRM003-3	19.3	9.5	14.8	28.9	43.6	5.9	12.5	18.4	28.5	28.5	21.3	1.0	51.1
09JRM003-4	22.4	6.6	6.0	29.0	35.0	2.5	7.3	9.8	22.4	22.4	20.8	13.2	59.3
09JRM003-5	16.7	5.9	11.4	22.6	34.0	1.8	10.9	12.6	28.7	28.7	20.5	6.5	63.3
09JRM003-6	17.4	8.3	4.7	25.7	30.4	5.2	9.7	14.9	12.7	12.7	26.5	14.1	57.7
09JRM003-7	18.9	7.5	6.9	26.4	33.3	3.6	8.3	11.9	22.5	22.5	21.9	10.3	60.3
09JRM003-8	19.4	5.6	5.1	25.0	30.1	2.4	10.2	12.6	23.8	23.8	18.7	10.0	60.7
09JRM003-9	15.5	6.1	8.8	21.6	30.4	5.3	13.5	18.7	20.8	20.8	23.1	9.9	57.0
11JRM000-20	25.0	9.8	11.7	34.8	46.5	6.3	13.0	19.3	19.6	19.6	16.5	5.4	44.0
08DL008-001.0A	11.0	4.8	9.5	15.7	25.2	1.4	15.7	17.1	12.9	12.9	29.5	9.5	62.9
08DL008-003.0A	4.3	5.3	4.8	9.6	14.4	1.9	12.9	14.8	6.7	6.7	48.3	7.2	72.2
08DL008-007.0A	4.2	1.9	5.1	6.5	11.6	1.4	11.2	12.6	13.0	13.0	47.4	6.5	79.1
08DL008-008.6A	4.1	5.2	5.7	9.3	14.9	1.5	11.9	13.4	6.2	6.2	49.0	9.8	72.2
08DL008-011.3A	7.0	2.5	6.0	10.4	16.4	1.0	15.4	16.4	11.4	11.4	38.3	8.0	68.7
08DL008-015.8A	6.8	3.4	2.0	10.2	12.2	1.5	14.1	15.6	4.9	4.9	42.9	7.3	67.3
08DL008-025.9B	16.2	4.6	6.0	22.2	28.2	0.9	15.7	16.7	10.2	10.2	20.8	7.4	56.0
08DL007-000.8A	6.6	3.8	5.6	10.3	16.0	1.4	13.1	14.6	12.7	12.7	47.9	4.7	73.7
08DL007-001.0A	9.5	5.9	4.5	15.5	20.0	1.4	15.9	17.3	8.6	8.6	44.1	3.2	65.9
08DL007-004.0A	7.3	4.9	5.8	12.1	18.0	2.9	14.1	17.0	7.3	7.3	51.5	3.4	69.4
08DL007-008.5A	6.8	3.4	7.8	10.2	18.0	1.5	16.6	18.0	9.3	9.3	46.8	4.4	68.8
08DL007-010.5A	6.4	4.3	4.3	10.6	14.9	1.6	16.0	17.6	5.9	5.9	45.7	2.1	67.6
08DL007-011.8A	4.7	1.9	3.8	6.6	10.3	1.4	17.8	19.2	6.6	6.6	47.9	3.8	71.4
08DL006-000.3A	1.9	4.6	8.3	6.5	14.8	3.2	18.5	21.8	9.3	9.3	50.0	2.8	69.9
08DL006-000.4A	4.9	4.9	8.3	9.8	18.0	1.0	17.6	18.5	10.7	10.7	43.9	3.4	68.8
08DL006-003.9A	4.0	4.5	5.0	8.5	13.6	1.0	19.1	20.1	9.5	9.5	40.2	5.0	66.3
08DL006-006.2A	6.3	3.8	7.2	10.6	17.8	2.4	14.4	16.8	8.7	8.7	42.8	5.8	68.8
08DL006-010.8A	5.0	2.7	5.5	7.7	13.2	1.8	15.5	17.3	8.2	8.2	51.8	2.3	71.4
08JRM006-0	32.4	5.1	1.1	37.5	38.6	9.0	24.5	33.5	1.9	1.9	2.4	0.0	28.2
08JRM006-1	42.6	6.8	3.1	49.4	52.6	7.7	22.2	29.8	4.0	4.0	3.4	0.0	19.3
08JRM006-2	28.7	5.4	1.7	34.1	35.8	12.1	30.4	42.5	2.0	2.0	1.1	0.3	22.3
08JRM006-3	35.1	4.8	1.8	39.9	41.7	9.8	23.0	32.8	2.5	2.5	4.8	0.8	25.8
11JRM001-0	34.0	4.7	1.8	38.7	40.6	7.9	25.4	33.2	3.7	3.7	1.6	1.8	27.0
11JRM001-1	34.2	6.3	1.6	40.5	42.1	7.2	20.5	27.7	3.0	3.0	2.6	0.9	30.2
11JRM001-2	29.7	7.1	0.2	36.9	37.1	5.7	26.5	32.2	0.2	0.2	1.2	1.0	29.5
11JRM001-3	33.6	10.1	3.1	43.7	46.8	7.8	24.4	32.2	4.2	4.2	2.0	0.8	22.4
07JRM011-002.4A	10.2	3.4	9.3	13.7	22.9	2.9	21.5	24.4	16.1	16.1	22.4	7.8	56.6
07JRM011-007.4A	13.7	6.3	4.9	20.0	24.9	1.5	14.1	15.6	10.2	10.2	25.4	6.8	58.5
07JRM011-017.3A	8.5	2.8	6.6	11.3	17.9	3.3	17.0	20.3	10.4	10.4	31.1	10.8	66.0
07JRM011-020.7A	14.3	5.6	3.6	19.9	23.5	3.6	17.3	20.9	10.7	10.7	24.0	9.7	53.1
07JRM011-026.5	6.7	8.1	11.4	14.8	26.2	3.3	11.0	14.3	17.1	17.1	24.8	20.5	66.7
07DL002-003.7A	10.5	5.0	6.8	15.5	22.3	3.6	14.5	18.2	15.5	15.5	25.9	11.8	64.1
09JRM101	21.8	11.7	15.1	33.6	48.7	6.0	9.1	15.1	18.8	19.1	19.8	3.4	47.0
09JRM102	16.6	14.2	24.9	30.8	55.7	1.5	11.7	13.2	35.1	35.1	9.5	4.9	52.3

Table 4.3: Cont.

Beluga Formation	Qm	Qp	C	Q	Q+	K	P	F	Ls+	Ls	Lv	Lm	L
08DL001-005.5B1	5.3	5.3	9.1	12.5	21.6	1.4	14.9	16.3	21.6	21.6	29.3	11.5	70.7
08DL001-008.8A	7.8	7.3	10.6	17.0	27.5	4.1	18.3	22.5	17.4	17.4	22.0	11.0	57.3
08DL001-013.0B1	8.7	6.8	7.2	15.9	23.2	3.4	20.8	24.2	11.1	11.1	22.7	12.1	55.6
08DL002-002.4A1	9.7	5.1	5.6	15.3	20.8	2.8	14.8	17.6	11.6	11.6	20.8	22.2	64.4
08DL002-004.8	11.3	6.1	9.9	17.4	27.2	2.8	15.0	17.8	17.8	17.8	15.0	19.7	60.1
08DL002-006.1A	10.4	4.3	6.1	15.7	21.7	0.9	18.7	19.6	12.6	12.6	27.0	11.7	61.3
08DL003-001.9A	6.2	5.7	6.2	12.4	18.7	1.9	10.5	12.4	17.2	17.2	16.3	32.1	68.4
08DL003-004.0A1	8.8	2.8	7.4	12.9	20.3	2.8	18.4	21.2	18.0	18.0	18.9	14.7	60.4
08DL003-018.5	10.6	5.8	9.1	18.3	27.4	3.8	20.7	24.5	15.4	15.4	19.2	12.5	55.3
08DL003-020.3A1	13.2	6.6	12.8	20.3	33.0	3.1	13.2	16.3	18.5	18.5	19.8	12.3	61.2
08DL003-021.8A	18.5	5.3	9.5	24.3	33.9	2.6	23.8	26.5	14.8	14.8	6.9	14.3	39.7
08DL003-026.1A	14.3	6.7	9.5	21.0	30.5	1.0	7.6	8.6	38.6	38.6	5.2	18.6	65.2
08DL004-000.6A	10.2	10.7	9.3	21.9	31.2	1.4	16.3	17.7	16.3	16.3	20.5	10.2	57.2
08DL004-002.0A	8.8	3.2	8.3	12.4	20.7	4.6	20.7	25.3	12.4	12.4	21.7	12.9	55.8
08DL004-003.0A	9.0	8.0	4.5	17.4	21.9	5.5	20.9	26.4	11.9	11.9	18.9	9.5	49.3
08DL004-003.1A1	9.0	7.0	4.5	17.6	22.1	4.5	21.6	26.1	15.1	15.1	14.1	10.1	52.3
08JRM016-6	0.0	2.5	2.8	25.0	27.8	1.6	4.4	6.0	54.7	54.7	0.3	11.1	67.4
08JRM016-16	0.0	5.7	5.7	10.4	16.1	1.6	3.8	5.4	71.0	71.0	0.6	12.0	83.6
07JRM009-005.5A	1.5	3.1	9.6	4.6	14.2	0.0	0.4	0.4	63.2	63.2	1.5	26.4	93.1
07JRM009-007.5A	2.2	4.0	13.8	6.5	20.3	0.4	1.8	2.2	65.2	65.2	0.0	23.6	89.9
07JRM009-015.7A	1.9	2.3	13.2	4.3	17.4	0.0	0.4	0.4	75.2	75.2	2.7	14.0	93.4
07JRM009-016.5A	2.7	4.6	12.7	7.3	20.1	0.0	0.0	0.0	67.6	67.6	1.9	16.6	88.0
07JRM010-003.6A	1.7	1.7	15.5	3.3	18.8	0.0	1.3	1.3	61.9	61.9	1.3	26.4	90.4
07JRM010-005.9A	12.7	5.4	6.6	18.1	24.7	0.6	8.4	9.0	39.8	39.8	7.2	17.5	65.1
07JRM010-024.3A	2.7	2.7	12.1	5.4	17.5	0.0	1.2	1.2	61.1	61.1	1.9	28.0	91.8
07JRM010-033.0A	3.9	5.1	14.2	9.1	23.2	0.0	2.4	2.4	61.4	61.4	1.2	17.7	85.4
07JRM008-005.2A	1.6	2.3	22.7	3.9	26.6	0.0	0.8	0.8	70.7	70.7	3.1	15.2	91.0
07JRM008-022.9A	1.4	1.8	28.0	3.2	31.2	0.7	0.4	1.1	79.4	79.4	2.1	11.7	94.0
07JRM008-027.2A	1.1	1.1	12.1	2.2	14.3	0.4	1.1	1.5	60.7	60.7	1.5	31.3	94.9
07JRM006-001.7A	9.8	6.8	7.7	16.6	24.3	0.9	6.8	7.7	37.9	37.9	2.6	28.1	71.5
07JRM006-005.0A	6.3	6.3	25.4	12.5	37.9	0.0	7.5	7.5	62.9	62.9	2.1	7.1	75.4
07JRM006-006.3A	3.8	3.1	10.0	6.9	16.9	0.0	1.9	1.9	65.4	65.4	0.0	21.9	88.1
07JRM006-007.6A	2.3	6.8	16.5	9.0	25.6	0.0	1.1	1.1	65.0	65.0	0.8	18.4	86.5
07JRM006-009.5A	4.4	4.4	14.0	9.2	23.2	0.4	4.8	5.2	60.8	60.8	2.0	13.6	80.4
07JRM006-014.6A	10.6	6.0	8.5	16.6	25.1	0.4	5.1	5.5	40.4	40.4	5.1	18.7	68.9
07JRM005-002.0A	0.4	3.8	18.3	4.2	22.5	0.0	1.5	1.5	72.5	72.5	2.3	16.0	91.6
07JRM005-008.4A	12.2	6.1	10.9	18.3	29.1	0.0	3.5	3.5	43.0	43.0	4.8	18.3	70.4
07JRM005-011.4A	2.7	5.3	14.1	8.4	22.5	0.4	2.7	3.1	63.4	63.4	3.1	17.6	84.7
07JRM005-014.2A	20.3	10.9	15.9	31.2	47.1	0.7	2.9	3.6	39.1	39.1	2.2	11.6	58.0
07JRM005-020.0A	4.1	6.3	13.8	11.2	24.9	0.7	1.5	2.2	55.0	55.0	3.0	20.1	80.7
07JRM003-001.2A	0.5	3.4	20.8	3.9	24.6	0.0	0.0	0.0	61.8	61.8	1.4	27.5	91.8
07JRM003-001.6A	6.1	1.9	14.4	8.0	22.4	0.4	3.0	3.4	56.7	56.7	1.9	22.4	83.7
07JRM002-004.2A	10.3	9.9	9.9	20.2	30.0	0.9	4.5	5.4	43.5	43.5	0.9	20.2	69.5
07JRM002-007.0A	1.5	5.6	15.0	7.1	22.1	0.0	1.1	1.1	58.1	58.1	1.9	28.8	90.3
07DL002-023.2A	9.7	5.2	8.2	15.0	23.2	2.6	7.9	10.5	47.6	47.6	12.4	5.2	71.2
07DL002-028.6A	10.4	4.7	9.0	15.1	24.1	3.3	17.0	20.3	19.3	19.3	15.1	15.1	58.5
07JRM001-001.0A	4.4	5.2	10.0	9.6	19.7	0.4	1.6	2.0	57.4	57.4	2.8	19.7	81.9
07JRM001-009.1A	8.2	13.7	17.6	22.0	39.6	0.0	4.9	4.9	44.0	44.0	2.2	20.9	68.7
07JRM001-015.5A	2.6	3.8	19.2	6.8	26.1	0.0	1.3	1.3	60.3	60.3	0.9	23.5	85.9
07DL085-081.0M	7.1	11.1	29.2	23.0	52.2	4.4	5.8	10.2	36.3	36.3	6.2	11.1	66.4
09JRM100-17	9.6	4.8	19.1	14.3	33.4	1.7	3.8	5.5	62.1	62.1	0.0	11.9	76.8
09JRM100-49.75	13.5	5.7	19.9	19.3	39.2	2.4	4.1	6.4	64.5	64.5	0.3	7.1	73.0

Table 4.4: Ternary diagram data

Sterling Fm.	Q+	Q+:F:L-	F	Q+:F:L-	L-	Q+:F:L-	Q	Q:F:L	F	Q:F:L	L	Q:F:L	Qm	Qm:F:Lt	F	Qm:F:Lt	Lt	Qm:F:Lt	Q+	Q+:P:K	P	Q+:P:K	K	Q+:P:K
09JRM003-0	37.9		11.2		50.9		27.4		11.2		61.4		22.2		11.2		66.6		77.1		17.6		5.3	
09JRM003-1	28.1		15.7		56.2		17.7		15.7		66.6		12.6		15.7		71.6		64.1		28.2		7.7	
09JRM003-2	34.0		11.1		54.9		21.4		11.1		67.4		15.7		11.1		73.1		75.3		15.2		9.5	
09JRM003-3	44.3		18.7		37.0		29.3		18.7		52.0		19.7		19.7		61.7		70.4		20.1		9.5	
09JRM003-4	35.7		10.0		54.3		29.6		19.0		60.5		22.8		19.0		67.2		78.2		16.2		5.6	
09JRM003-5	34.5		12.8		52.7		22.9		12.8		64.3		17.0		12.8		70.2		73.0		23.3		3.8	
09JRM003-6	30.9		15.2		53.9		26.1		15.2		58.7		17.7		15.2		67.1		67.1		21.3		11.6	
09JRM003-7	33.8		12.1		54.1		26.8		12.1		61.1		19.2		12.1		68.7		73.6		18.4		8.0	
09JRM003-8	30.6		12.8		56.5		25.4		12.8		61.7		19.8		12.8		67.4		70.5		23.9		5.7	
09JRM003-9	31.2		19.2		49.5		22.2		19.2		58.6		15.9		19.2		64.9		61.9		27.4		15.7	
11JRM000-20	47.4		19.7		32.9		35.5		19.7		44.8		25.5		19.7		54.8		70.7		19.7		9.6	
08DL008-001.0A	26.4		17.9		55.7		18.4		17.9		65.7		11.4		17.9		70.6		59.6		37.1		3.4	
08DL008-003.0A	14.9		15.3		69.8		9.9		15.3		74.8		4.5		15.3		80.2		49.2		44.3		6.6	
08DL008-007.0A	11.8		12.8		75.4		6.6		12.8		80.6		4.3		12.9		82.9		48.1		46.2		5.8	
08DL008-008.6A	15.8		14.1		70.1		9.8		14.1		76.1		4.3		14.1		81.5		52.7		41.8		5.5	
08DL008-011.3A	17.2		17.2		65.6		10.9		17.2		71.9		7.4		17.4		75.3		50.0		47.0		3.0	
08DL008-015.8A	13.1		16.8		70.2		11.0		16.8		72.3		7.3		19.8		75.9		43.9		50.9		5.3	
08DL008-025.9B	29.8		17.6		52.7		23.4		17.6		59.0		17.3		17.8		64.9		62.9		35.1		2.1	
08DL007-000.8A	16.2		14.8		69.0		10.5		14.8		74.8		6.7		14.8		78.6		52.3		43.1		4.6	
08DL007-001.0A	20.3		17.5		62.2		15.7		17.5		66.8		9.7		17.5		72.8		53.7		42.7		3.7	
08DL007-004.0A	18.2		17.2		64.5		12.3		17.2		70.4		7.4		17.2		75.4		51.4		40.3		8.3	
08DL007-008.5A	18.6		18.6		62.8		10.6		18.6		70.9		7.0		18.6		74.4		50.0		45.9		4.1	

Table 4.4: Cont.

Sterling Fm.	Q+	Q+:F:L-	F	Q+:F:L-	L-	Q+:F:L-	Q	Q:F:L	F	Q:F:L	L	Q:F:L	Qm	Qm:F:Lt	F	Qm:F:Lt	Lt	Qm:F:Lt	Q+	Q+:P:K	P	Q+:P:K	K	Q+:P:K
08DL007-010.5A		15.6		18.3		66.1		11.1		18.3		70.6		6.7		18.3		75.0		45.9		49.2		4.9
08DL007-011.8A		10.6		19.8		69.6		6.8		19.8		73.4		4.8		18.8		75.4		34.9		60.3		4.8
08DL006-000.3A		15.1		22.2		62.7		6.6		22.2		71.2		1.9		22.2		75.9		40.5		50.6		8.9
08DL006-000.4A		18.6		19.1		62.3		10.1		19.1		70.9		5.0		19.1		75.9		49.3		48.0		2.7
08DL006-003.9A		14.3		21.2		64.6		9.0		21.2		69.8		4.2		21.2		74.6		40.3		56.7		3.0
08DL006-006.2A		18.5		17.5		64.0		11.0		17.5		71.5		6.5		17.6		75.9		51.4		41.7		6.9
08DL006-010.8A		13.7		17.9		68.4		8.0		17.9		74.1		5.2		17.9		76.9		43.3		50.7		6.0
08JRM006-0		38.9		33.8		27.3		37.8		33.8		28.4		32.7		33.8		33.5		53.5		33.9		12.5
08JRM006-1		53.3		30.3		16.4		50.1		30.3		19.6		43.2		30.3		26.5		63.8		26.9		9.3
08JRM006-2		36.2		43.0		20.8		34.5		43.0		22.5		29.1		43.0		27.9		45.7		38.8		15.5
08JRM006-3		42.3		33.3		24.4		40.5		33.3		26.2		35.6		33.3		31.0		55.9		30.8		13.2
11JRM001-0		41.0		33.6		25.4		39.2		33.6		27.2		34.4		33.6		32.0		55.0		34.4		10.6
11JRM001-1		42.8		28.1		29.1		41.1		28.1		30.7		34.8		28.1		37.1		60.3		29.3		10.3
11JRM001-2		37.7		32.7		29.7		37.4		32.7		29.9		30.2		32.7		37.2		53.5		38.3		8.2
11JRM001-3		47.6		32.8		19.7		44.4		32.8		22.8		34.2		32.8		33.0		59.2		30.9		9.9
07JRM011-002.4A		24.2		25.8		50.0		14.4		25.8		59.8		10.8		25.8		63.4		48.5		45.4		6.2
07JRM011-007.4A		26.4		16.6		57.0		21.2		16.6		62.2		14.5		16.6		68.9		61.4		34.9		3.6
07JRM011-017.3A		18.4		20.8		60.9		11.6		20.8		67.6		8.7		20.8		70.5		46.9		44.4		8.6
07JRM011-020.7A		25.0		22.3		52.7		21.2		22.3		56.5		15.2		22.3		62.5		52.9		39.1		8.0
07JRM011-026.5		27.4		14.9		57.7		15.4		14.9		69.7		7.0		14.9		78.1		64.7		27.1		8.2
07DL002-003.7A		22.8		18.6		58.6		15.8		18.6		65.6		10.7		18.6		70.7		55.1		36.0		9.0
09JRM101		51.1		15.8		33.1		35.1		15.8		49.1		22.9		15.8		61.3		76.3		14.2		9.5
09JRM102		57.8		13.7		28.4		31.9		13.7		54.3		17.3		13.7		69.0		80.8		17.0		2.2

Table 4.4: Cont.

Sterling Fm.	Q	Q:P:K	P	Q:P:K	K	Q:P:K	Qm	Qm:P:K	P	Qm:P:K	K	Qm:P:K	Ls+	Ls+:Lv:Lm	Lv	Ls+:Lv:Lm	Lm	Ls+:Lv:Lm
09JRM003-0	70.9		22.3		6.8		66.4		25.8		7.8		46.2		38.7		15.1	
09JRM003-1	52.9		37.0		10.1		44.6		43.6		11.9		29.8		50.0		20.2	
09JRM003-2	65.8		21.1		13.2		58.5		25.5		16.0		52.1		32.7		15.2	
09JRM003-3	61.1		26.4		12.5		51.3		33.0		15.7		56.1		41.9		1.9	
09JRM003-4	74.8		18.7		6.5		69.6		22.5		7.8		39.7		36.9		23.5	
09JRM003-5	64.2		30.8		5.0		57.0		37.0		6.0		51.6		36.8		11.6	
09JRM003-6	63.3		23.8		12.9		53.8		29.9		16.2		23.8		49.7		26.4	
09JRM003-7	68.8		21.7		9.4		61.3		27.0		11.7		41.1		40.1		18.8	
09JRM003-8	66.5		27.1		6.5		60.6		31.8		7.6		45.4		35.6		18.0	
09JRM003-9	53.6		33.3		13.0		45.3		39.3		15.4		38.6		42.9		18.5	
11JRM000-20	64.3		24.0		11.7		56.4		29.3		14.3		47.3		39.7		13.0	
08DL008-001.0A	47.8		47.8		4.3		39.0		55.9		5.1		24.8		56.9		18.3	
08DL008-003.0A	39.2		52.9		7.8		22.5		67.5		10.0		19.8		77.7		11.5	
08DL008-007.0A	34.1		58.5		7.3		25.0		66.7		8.3		19.4		70.8		9.7	
08DL008-008.6A	40.9		52.3		6.8		23.5		67.6		8.8		9.5		75.4		15.1	
08DL008-011.3A	38.9		57.4		3.7		29.8		66.0		4.3		19.8		66.4		13.8	
08DL008-015.8A	39.6		54.7		5.7		30.4		63.0		6.5		8.8		77.9		13.3	
08DL008-025.9B	57.1		40.5		2.4		49.3		47.9		2.8		26.5		54.2		19.3	
08DL007-000.8A	41.5		52.8		5.7		31.1		62.2		6.7		19.4		73.4		7.2	
08DL007-001.0A	47.2		48.6		4.2		35.6		59.3		5.1		15.4		78.9		5.7	
08DL007-004.0A	41.7		48.3		10.0		30.0		58.0		12.0		11.7		82.8		5.5	
08DL007-008.5A	36.2		58.6		5.2		27.5		66.7		5.9		15.3		77.4		7.3	

Table 4.4: Cont.

Sterling Fm.	Q	Q:P:K	P	Q:P:K	K	Q:P:K	Qm	Qm:P:K	P	Qm:P:K	K	Qm:P:K	Ls+	Ls+:Lv:Lm	Lv	Ls+:Lv:Lm	Lm	Ls+:Lv:Lm
08DL007-016.5A	37.7		56.6		5.7		26.7		66.7		6.7		10.9		85.1		4.0	
08DL007-011.8A	25.5		69.1		5.5		19.6		74.5		5.9		11.3		82.3		6.5	
08DL006-000.3A	23.0		65.6		11.5		7.8		78.4		13.7		14.9		80.6		4.5	
08DL006-000.4A	34.5		62.1		3.4		20.8		75.0		4.2		18.5		75.6		5.9	
08DL006-003.9A	29.8		66.7		3.5		16.7		79.2		4.2		17.4		73.4		9.2	
08DL006-006.2A	38.6		52.6		8.8		27.1		62.5		10.4		16.1		74.8		10.1	
08DL006-010.8A	30.9		61.8		7.3		22.4		69.4		8.2		13.1		83.2		3.6	
08JRM006-0	52.8		34.5		12.7		49.2		37.1		13.7		43.8		56.3		0.0	
08JRM006-1	62.4		28.0		9.7		58.8		30.6		10.6		53.8		46.2		0.0	
08JRM006-2	44.5		39.7		15.8		40.3		42.7		17.0		58.3		33.3		8.3	
08JRM006-3	54.9		31.6		13.5		51.7		33.8		14.5		31.3		59.4		9.4	
11JRM001-0	53.8		35.3		10.9		50.6		37.7		11.7		51.9		22.2		25.9	
11JRM001-1	59.4		30.0		10.6		55.3		33.1		11.7		46.4		39.3		14.3	
11JRM001-2	53.4		38.4		8.2		48.0		42.9		9.1		10.0		50.0		40.0	
11JRM001-3	57.6		32.1		10.3		51.1		37.0		11.9		60.0		28.0		12.0	
07JRM011-002.4A	35.9		56.4		7.7		29.6		62.0		8.5		34.7		48.4		16.8	
07JRM011-007.4A	56.2		39.7		4.1		46.7		48.3		5.0		24.1		59.8		16.1	
07JRM011-017.3A	35.8		53.7		10.4		29.5		59.0		11.5		10.8		59.5		20.7	
07JRM011-020.7A	48.8		42.5		8.8		40.6		49.3		10.1		24.1		54.0		21.8	
07JRM011-026.5	50.8		37.7		11.5		31.8		52.3		15.9		27.5		39.7		32.8	
07DL002-003.7A	45.9		43.2		10.8		36.5		50.8		12.7		29.1		48.7		22.2	
09JRM101	69.0		18.6		12.4		59.1		24.5		16.4		44.8		47.2		8.0	
09JRM182	69.9		26.6		3.5		55.7		39.2		5.2		70.8		18.3		9.9	

Table 4.4: Cont.

Beluga Fm.	Q+	Q+:F:L-	F	Q+:F:L-	L-	Q+:F:L-	Q	Q:F:L	F	Q:F:L	L	Q:F:L	Qm	Qm:F:Lt	F	Qm:F:Lt	Lt	Qm:F:Lt	Q+	Q+:P:K	P	Q+:P:K	K	Q+:P:K
08DL001-005.5B1		21.7		16.4		61.8		12.6		16.4		71.0		5.4		16.7		77.8		57.0		39.2		3.8
08DL001-008.8A		28.4		23.2		48.3		17.5		23.2		59.2		8.2		23.7		68.1		55.0		36.7		8.3
08DL001-013.0B1		24.2		25.3		50.5		16.7		25.3		58.1		9.1		25.4		65.5		49.0		43.9		7.1
08DL002-002.4A1		21.4		19.1		60.5		15.7		19.1		66.2		10.0		18.2		71.8		54.2		38.6		7.2
08DL002-004.8		28.6		18.7		52.7		18.2		18.7		63.1		11.8		18.7		69.5		60.4		33.3		6.3
08DL002-006.1A		22.5		20.3		57.2		16.2		20.3		63.5		10.9		20.5		68.6		52.6		45.3		2.1
08DL003-001.9A		20.0		13.3		66.7		13.3		13.3		73.3		6.7		13.4		79.9		60.0		33.8		6.2
08DL003-004.0A1		21.5		22.4		56.1		13.7		22.4		63.9		9.4		22.8		67.8		48.9		44.4		6.7
08DL003-016.5		27.9		25.0		47.1		18.6		25.0		56.4		11.0		25.5		63.5		52.8		39.8		7.4
08DL003-020.3A1		33.8		18.7		49.5		20.7		18.7		62.6		13.6		16.7		69.7		67.0		26.8		6.3
08DL003-021.8A		37.4		29.2		33.3		26.9		29.2		43.9		20.6		29.4		50.0		56.1		39.5		4.4
08DL003-026.1A		32.2		9.0		58.8		22.1		9.0		68.8		15.1		9.0		75.9		78.0		19.5		2.4
08DL004-000.6A		32.2		18.3		49.5		22.6		18.3		59.1		18.7		18.4		70.9		63.8		33.3		2.9
08DL004-002.0A		22.2		27.1		50.7		13.3		27.1		59.6		9.4		27.2		63.4		45.0		45.0		10.0
08DL004-003.0A		23.5		28.3		48.1		16.7		28.3		52.9		9.7		28.5		61.8		45.4		43.3		11.3
08DL004-003.1A1		23.0		27.2		49.7		18.3		27.2		54.5		9.6		27.7		62.8		45.8		44.8		9.4
08JRM016-6		28.3		6.1		65.6		25.4		6.1		68.5		0.0		7.9		92.1		82.2		13.1		4.7
08JRM016-16		18.2		5.4		78.4		10.5		5.4		84.1		0.0		5.7		94.3		75.0		17.6		7.4
07JRM009-005.5A		14.5		0.4		85.2		4.7		0.4		94.9		1.6		0.4		98.0		97.4		2.6		0.0
07JRM009-007.5A		20.6		2.2		77.2		6.6		2.2		91.2		2.2		2.2		95.6		90.3		8.1		1.6
07JRM009-015.7A		17.8		0.4		81.8		4.3		0.4		95.3		2.0		0.4		97.6		97.8		2.2		0.0
07JRM009-016.5A		21.1		0.0		78.9		7.7		0.0		92.3		2.8		0.0		97.2		100.0		0.0		0.0
07JRM010-003.6A		19.8		1.3		78.9		3.5		1.3		95.2		1.8		1.3		96.9		93.8		6.3		0.0
07JRM010-005.9A		26.8		9.8		63.4		19.6		9.8		70.6		13.7		9.8		76.5		73.2		25.0		1.8
07JRM010-024.3A		17.8		1.2		81.0		5.5		1.2		93.3		2.8		1.2		96.0		93.8		6.3		0.0
07JRM010-033.0A		24.0		2.4		73.6		9.3		2.4		88.2		4.1		2.4		93.5		90.8		9.2		0.0

Table 4.4: Cont.

Beluga Fm.	Q	Q:P:K	P	Q:P:K	K	Q:P:K	Qm	QmP:K	P	QmP:K	K	QmP:K	Ls+	Ls+:Lv:Lm	Lv	Ls+:Lv:Lm	Lm	Ls+:Lv:Lm
08DL001-005.5B1		43.3		51.7		5.0		24.4		68.9		6.7		34.6		46.9		19.5
08DL001-008.8A		43.0		46.5		10.5		25.8		60.6		13.6		34.5		43.6		21.8
08DL001-013.0B1		39.8		51.8		8.4		26.5		63.2		10.3		24.2		49.5		26.3
08DL002-002.4A1		46.5		45.1		8.5		35.6		54.2		10.2		21.2		38.1		40.7
08DL002-004.8		49.3		42.7		8.0		38.7		51.6		9.7		33.9		28.6		37.5
08DL002-006.1A		44.4		53.1		2.5		34.8		62.3		2.9		24.6		52.5		22.9
08DL003-001.9A		50.0		42.3		7.7		33.3		56.4		10.3		26.3		24.8		48.9
08DL003-004.0A1		37.8		54.1		8.1		29.2		61.5		9.2		34.8		36.6		28.6
08DL003-018.5		42.7		48.3		9.0		30.1		58.9		11.0		32.7		40.8		26.5
08DL003-020.3A1		55.4		36.1		8.4		44.8		44.8		10.4		36.5		39.1		24.3
08DL003-021.8A		47.9		46.9		5.2		41.2		52.9		5.9		41.2		19.1		39.7
08DL003-026.1A		71.0		25.8		3.2		62.5		33.3		4.2		61.8		8.4		29.8
08DL004-000.6A		55.3		41.2		3.5		36.7		58.3		5.0		34.7		43.6		21.8
08DL004-002.0A		32.9		54.9		12.2		25.7		60.8		13.5		26.5		46.1		27.5
08DL004-003.0A		39.8		47.7		12.5		25.4		59.2		15.5		29.6		46.9		23.5
08DL004-003.1A1		40.2		49.4		10.3		25.7		61.4		12.9		38.5		35.9		25.6
08JRM016-6		80.6		14.3		5.1		0.0		73.7		26.3		82.8		0.5		16.7
08JRM016-16		66.0		24.0		10.0		0.0		70.6		29.4		84.9		0.8		14.3
07JRM009-005.5A		92.3		7.7		0.0		80.0		20.0		0.0		69.3		1.7		29.0
07JRM009-007.5A		75.0		20.8		4.2		50.0		41.7		8.3		73.5		0.0		26.5
07JRM009-015.7A		91.7		8.3		0.0		83.3		16.7		0.0		81.9		3.0		15.2
07JRM009-016.5A		100.0		0.0		0.0		100.0		0.0		0.0		78.5		2.2		19.3
07JRM010-003.6A		72.7		27.3		0.0		57.1		42.9		0.0		69.2		1.4		29.4
07JRM010-005.9A		66.7		31.1		2.2		58.3		38.9		2.8		61.7		11.2		27.1
07JRM010-024.3A		82.4		17.6		0.0		70.0		30.0		0.0		67.1		2.1		30.8
07JRM010-033.0A		79.3		20.7		0.0		62.5		37.5		0.0		76.8		1.5		22.1

Table 4.4: Cont.

Beluga Fm.	Q+	Q+:F:L-	F	Q+:F:L-	L-	Q+:F:L-	Q	Q:F:L	F	Q:F:L	L	Q:F:L	Qm	Qm:F:Lt	F	Qm:F:Lt	Lt	Qm:F:Lt	Q+	Q+:P:K	P	Q+:P:K	K	Q+:P:K
07JRM008-005.2A	27.8		0.8		71.4		4.1		0.8		95.1		1.6		0.8		97.6		97.1		2.9		0.0	
07JRM008-022.9A	31.8		1.1		67.1		3.2		1.1		95.7		1.4		1.1		97.5		96.7		1.1		2.2	
07JRM008-027.2A	14.6		1.5		84.0		2.2		1.5		96.3		1.1		1.5		97.4		90.7		7.0		2.3	
07JRM006-001.7A	25.3		8.0		66.7		17.3		8.0		74.7		18.2		8.0		81.8		76.0		21.3		2.7	
07JRM006-005.0A	39.7		7.9		52.4		13.1		7.9		79.0		6.6		7.9		85.6		83.5		15.5		0.0	
07JRM006-006.3A	17.5		2.0		80.6		7.1		2.0		90.9		4.0		2.0		94.0		89.8		10.2		0.0	
07JRM006-007.6A	26.5		1.2		72.4		9.3		1.2		89.5		2.3		1.2		96.5		95.8		4.2		0.0	
07JRM006-009.5A	24.5		5.5		70.0		9.7		5.5		84.8		4.7		5.5		89.8		81.7		16.9		1.4	
07JRM006-014.6A	27.6		6.1		66.4		18.2		6.1		75.7		11.7		6.1		82.2		81.9		16.7		1.4	
07JRM005-002.0A	23.1		1.6		75.3		4.3		1.6		94.1		0.4		1.6		98.0		93.7		6.3		0.0	
07JRM005-008.4A	31.6		3.8		64.6		10.8		3.8		76.4		13.2		3.8		83.0		89.3		10.7		0.0	
07JRM005-011.4A	23.4		3.2		73.4		8.7		3.2		88.1		2.8		3.2		94.0		88.1		10.4		1.5	
07JRM005-014.2A	50.8		3.9		45.3		33.6		3.9		62.5		21.9		3.9		74.2		92.9		5.7		1.4	
07JRM005-020.0A	26.5		2.4		71.1		11.9		2.4		85.8		4.4		2.4		93.2		91.8		5.5		2.7	
07JRM003-001.2A	25.8		0.0		74.2		4.0		0.0		96.0		0.5		0.0		99.5		100.0		0.0		0.0	
07JRM003-001.6A	23.6		3.6		72.8		8.4		3.6		88.0		6.4		3.6		90.0		86.8		11.8		1.5	
07JRM002-004.2A	31.6		5.7		62.7		21.2		5.7		73.1		10.8		5.7		83.5		84.8		12.7		2.5	
07JRM002-007.0A	22.4		1.1		76.4		7.2		1.1		91.6		1.5		1.1		97.3		95.2		4.8		0.0	
07DL002-023.2A	24.0		10.9		65.1		15.5		10.9		73.6		10.1		10.9		79.1		68.9		23.3		7.8	
07DL002-028.6A	25.6		21.6		52.8		16.1		21.6		62.3		11.1		21.6		67.3		54.3		38.3		7.4	
07JRM001-001.0A	21.0		2.1		76.8		10.3		2.1		87.6		4.7		2.1		93.1		90.7		7.4		1.9	
07JRM001-009.1A	41.4		5.2		53.4		23.0		5.2		71.8		8.6		5.2		86.2		88.9		11.1		0.0	
07JRM001-015.5A	27.7		1.4		70.9		7.3		1.4		91.4		2.7		1.4		95.9		95.3		4.7		0.0	
07DL085-081.0M	52.4		10.2		37.3		23.1		10.2		66.7		7.5		10.7		81.8		83.7		9.2		7.1	
09JRM 100-17	34.6		5.7		59.7		14.8		5.7		79.5		9.9		5.7		84.5		86.0		9.6		4.4	
09JRM 100-49.75	39.7		6.5		53.8		10.5		6.5		74.0		13.7		6.5		79.8		85.9		8.9		5.2	

Table 4.4: Cont.

Beluga Fm.	Q	Q:P:K	P	Q:P:K	K	Q:P:K	Qm	Qm:P:K	P	Qm:P:K	K	Qm:P:K	Ls+	Ls+:Lv:Lm	Lv	Ls+:Lv:Lm	Lm	Ls+:Lv:Lm
07JRM008-005.2A	83.3		16.7		0.0		66.7		33.3		0.0		79.4		3.5		17.1	
07JRM008-022.9A	75.0		8.3		16.7		57.1		14.3		28.6		85.2		2.3		12.5	
07JRM008-027.2A	60.0		30.0		10.0		42.9		42.9		14.3		65.0		1.6		33.5	
07JRM006-001.7A	68.4		28.1		3.5		56.1		39.0		4.9		55.3		3.7		41.0	
07JRM006-005.0A	62.5		37.5		0.0		45.5		54.5		0.0		87.3		2.9		9.8	
07JRM006-006.3A	78.3		21.7		0.0		66.7		33.3		0.0		74.9		0.0		25.1	
07JRM006-007.6A	88.9		11.1		0.0		66.7		33.3		0.0		77.2		0.9		21.9	
07JRM006-009.5A	63.9		33.3		2.8		45.8		50.0		4.2		79.6		2.6		17.8	
07JRM006-014.6A	75.0		23.1		1.9		65.8		31.6		2.6		62.9		7.9		29.1	
07JRM005-002.0A	73.3		26.7		0.0		20.0		80.0		0.0		79.8		2.5		17.6	
07JRM005-008.4A	84.0		16.0		0.0		77.8		22.2		0.0		65.1		7.2		27.6	
07JRM005-011.4A	73.3		23.3		3.3		46.7		46.7		6.7		75.5		3.6		20.9	
07JRM005-014.2A	89.6		8.3		2.1		84.8		12.1		3.0		74.0		4.1		21.9	
07JRM005-020.0A	83.3		11.1		5.6		64.7		23.5		11.8		70.5		3.8		25.7	
07JRM003-001.2A	100.0		0.0		0.0		100.0		0.0		0.0		68.1		1.6		30.3	
07JRM003-001.6A	70.0		26.7		3.3		64.0		32.0		4.0		70.0		2.3		27.7	
07JRM002-004.2A	78.9		17.5		3.5		65.7		28.6		5.7		67.4		1.4		31.3	
07JRM002-007.0A	86.4		13.6		0.0		57.1		42.9		0.0		65.4		2.1		32.5	
07DL002-023.2A	58.8		30.9		10.3		48.1		38.9		13.0		73.0		19.0		8.0	
07DL002-028.6A	42.7		48.0		9.3		33.8		55.4		10.8		39.0		30.5		30.5	
07JRM001-001.0A	82.8		13.8		3.4		68.8		25.0		6.3		71.9		3.5		24.6	
07JRM001-009.1A	81.6		18.4		0.0		62.5		37.5		0.0		65.6		3.3		31.1	
07JRM001-015.5A	84.2		15.8		0.0		66.7		33.3		0.0		71.2		1.0		27.3	
07DL085-081.0M	69.3		17.3		13.3		41.0		33.3		25.6		67.8		11.6		20.7	
09JRM 100-17	72.4		19.0		8.6		63.6		25.0		11.4		83.9		0.0		16.1	
09JRM 100-49.75	75.0		15.8		9.2		67.8		20.3		11.9		89.7		0.5		9.9	

4.10 References Cited

ADKISON, W.L., KELLEY, J.S., and NEWMAN, K.R., 1975, Lithology and palynology of the Beluga and Sterling formations exposed near Homer, Kenai Peninsula: U.S. Geological Survey Open-File Report, 75-383: 104 p.

BEIKMAN, H.M., 1980, Geologic map of Alaska: U.S. Geological Survey Professional Paper PP0171, 1 plate, scale 1:250,000.

BENOWITZ, J.A., 2011, The Topographically Asymmetrical Alaska Range: Multiple Tectonic Drivers Through Space And Time: University of Alaska Fairbanks, Fairbanks, 291 p.

BEST, J.L., ASHWORTH, P.J., BRISTOW, C.S., and RODEN, J., 2003, Three-dimensional sedimentary architecture of a large, mid-channel sand braid bar, Jamuna River, Bangladesh: Journal of Sedimentary Research, v. 73, p. 516-530.

BLODGETT, R.H., and STANLEY, K., 1980, Stratification, bedforms, and discharge relations of the Platte braided river system, Nebraska: Journal of Sedimentary Research, v. 50, p. 139.

BRADLEY, D.C., KUSKY, T., HAEUSSLER, P., GOLDFARB, R., MILLER, M., DUMOULIN, J., NELSON, S.W., and KARL, S., 2003, Geologic signature of early Tertiary ridge subduction in Alaska, *in* Sisson, V.B., Roeske, S.M., and Pavlis, T.L., eds., Geology of a transpressional orogen developed during ridge-trench interaction along the north Pacific margin: Boulder, Geological Society of America, p. 19-49.

BRADLEY, D.C., KUSKY, T., HAEUSSLER, P., KARL, S., and DONLEY, D.T., 1999, Geologic map of the Seldovia quadrangle, Alaska: U.S. Geological Survey Open-File Report 99-18, scale 1:250,000.

BRIDGE, J., COLLIER, R., and ALEXANDER, J., 1998, Large scale structure of Calamus River deposits (Nebraska, USA) revealed using ground penetrating radar: Sedimentology, v. 45, p. 977-986.

BRIDGE, J.S., 1993, The interaction between channel geometry, water flow, sediment transport and deposition in braided rivers: Geological Society, London, Special Publications, v. 75, p. 13.

BRIDGE, J.S., and LUNT, I.A., 2006, Depositional models of braided rivers, *in* Sambrook Smith, G.H., Best, J.L., Bristow, C.S., and Petts, G.E., eds., Braided Rivers; Process, Deposits, Ecology and Management,, International Association of Sedimentologists, p. 11-50.

BUSBY, C., SMITH, D., MORRIS, W., and FACKLER-ADAMS, B., 1998, Evolutionary model for convergent margins facing large ocean basins: Mesozoic Baja California, Mexico: Geology, v. 26, p. 227-230.

BUSBY-SPERA, C.J., 1986, Depositional features of rhyolitic and andesitic volcaniclastic rocks of the Mineral King submarine caldera complex, Sierra Nevada, California: Journal of Volcanology and Geothermal Research, v. 27, p. 43-76.

CANT, D., and WALKER, R., 1978, Fluvial processes and facies sequences in the sandy braided South Saskatchewan River, Canada: Sedimentology, v. 25, p. 625-648.

CLIFT, P.D., DEGNAN, P.J., HANNIGAN, R., and BLUSZTAJN, J., 2000, Sedimentary and geochemical evolution of the Dras forearc basin, Indus suture, Ladakh Himalaya, India: Geological Society of America Bulletin, v. 112, p. 450-466.

COLE, R.B., NELSON, S.W., LAYER, P.W., and OSWALD, P.J., 2006, Eocene volcanism above a depleted mantle slab window in southern Alaska: Geological Society of America Bulletin, v. 118, p. 140-158.

CROWLEY, K., 1983, Large-scale bed configurations (macroforms), Platte River Basin, Colorado and Nebraska: primary structures and formative processes: Bulletin of the Geological Society of America, v. 94, p. 117.

DALLEGGE, T., and LAYER, P., 2004, Revised chronostratigraphy of the Kenai Group from 40Ar/39Ar dating of low-potassium bearing minerals, Cook Inlet Basin, Alaska: Canadian Journal of Earth Science, v. 41, p. 1159-1179.

DEGRAAFF-SURPLESS, K., GRAHAM, S.A., WOODEN, J.L., and MCWILLIAMS, M.O., 2002, Detrital zircon provenance analysis of the Great Valley Group, California: Evolution of an arc-forearc system: Geological Society of America Bulletin, v. 114, p. 1564-1580.

DETTERMAN, R.L., and HARTSOCK, J.K., 1966, Geology of the Iniskin-Tuxedni region: Alaska: U.S. Geolological Survey Professional Paper 512, p. 78.

DETTERMAN, R.L., and REED, B.L., 1980, Stratigraphy, structure, and economic geology of the Iliamna quadrangle, Alaska: U.S. Geological Survey Bulletin, v. 1368-B, p. 86.

DICKIN, A.P., 2005, Radiogenic Isotope Geology: Cambridge, Cambridge University Press.

DICKINSON, W.R., 1985, Interpreting Provenance Relations from Detrital Modes of Sandstones, *in* Zuffa, G.G., ed., Provenance of Arenites: Dordrecht, Deidel Publishing, p. 333-361.

DICKINSON, W.R., 1995, Forearc Basins, *in* Busby, C., and Ingersoll, R.V., eds., Tectonics of sedimentary basins: Cambridge, Blackwell Science, p. 221-261.

DICKINSON, W.R., and SEELY, D.R., 1979, Structure and stratigraphy of forearc regions: AAPG Bulletin, v. 63, p. 2-31.

EBERHART-PHILLIPS, D., CHRISTENSEN, D.H., BROCHER, T.M., HANSEN, R., RUPPERT, N.A., HAEUSSLER, P.J., and ABERS, G.A., 2006, Imaging the transition from Aleutian subduction to Yakutat collision in central Alaska, with local earthquakes and active source data: Journal of Geophysical Research, v. 111.

FERRIS, A., ABERS, G.A., CHRISTENSEN, D.H., and VEENSTRA, E., 2003, High resolution image of the subducted Pacific Plate beneath central Alaska, 50-150 km depth: Earth and Planetary Science Letters, v. 214, p. 575-588.

FIELDING, C.R., 1987, Coal deposition models for deltaic and alluvial plain sequences: Geology, v. 15, p. 661-664.

FILDANI, A., HESSLER, A.M., and GRAHAM, S.A., 2008, Trench-forearc interactions reflected in the sedimentary fill of Talara basin, northwest Peru: Basin Research, v. 20, p. 305-331.

FINZEL, E.S., 2010, Geodynamics of Flat-Slab Subduction, Sedimentary Basin Development, and Hydrocarbon Systems along the Southern Alaska Convergent Plate Margin: University of Purdue, West Lafayette, 401 p.

FISHER, M.A., and MAGOON, L.B., 1978, Geologic framework of Lower Cook Inlet, Alaska: AAPG Bulletin, v. 62, p. 373-402.

FITZGERALD, P.G., SORKHABI, R.B., REDFIELD, T.F., and STUMP, E., 1995, Uplift and denudation of the central Alaska Range; a case study in the use of apatite fission track thermochronology to determine absolute uplift parameters: Journal of Geophysical Research, v. 100, p. 20,175-20,191.

FLORES, R.M., and STRICKER, G.D., 1992, Some facies aspects of the upper part of the Kenai Group, southern Kenai Peninsula, Alaska, *in* Bradley, D.C., and Dusel-Bacon, C., eds., Geologic studies in Alaska by the U.S. Geological Survey, 1991: Reston, VA, U. S. Geological Survey, p. 160-170.

FLORES, R.M., and STRICKER, G.D., 1993, Reservoir framework architecture in the Clamgulchian type section (Pliocene) of the Sterling Formation, Kenai Peninsula, Alaska, *in* Dusel-Bacon, C., and Till, A.B., eds., Geologic Studies in Alaska by the U.S. Geological Survey, 1992: U.S. Geological Survey Bulletin 2068: Reston, p. 118-129.

FLORES, R.M., STRICKER, G.D., and KINNEY, S.A., 2004, Alaska Coal Geology, Resources, and Coalbed Methane potential: U.S. Geological Survey DDS-77.

FOLK, R.L., 1980, Petrology of Sedimentary Rocks: Austin, Hemphill Publishing Co., 182 p.

FUCHS, W.A., 1980, Tertiary tectonic history of the Castle Mountain-Caribou fault system in the Talkeetna Mountains, Alaska: University of Utah, Salt Lake City, 152 p.

GAZZI, P., 1966, Le arenarie del flysch sopracretaceo dell'Appennino modense; correlaziani con il fysch di Monghidoro: Mineralogica e Petrografica Acta, v. 12, p. 69-97.

GRENINGER, M.L., KLEMPERER, S.L., and NOKLEBERG, W.J., 1999, Geographic Information Systems (GIS) compilation of geophysical, geologic, and tectonic data for the Circum-North Pacific: U.S. Geological survey Open File Report 99-422, p. 1.

HAEUSSLER, P., BRUHN, R., and PRATT, T., 2000, Potential seismic hazards and tectonics of the upper Cook Inlet basin, Alaska, based on analysis of Pliocene and younger deformation: Geological Society of America Bulletin, v. 112, p. 1414.

HAEUSSLER, P., O'SULLIVAN, P., BERGER, A.L., and SPOTILA, J.A., 2008, Synchronous exhumation of the Tordrillo Mountains and Denali (Mt. McKinley), Alaska, around 6 Ma, *in* Freymueller, J.T., Haeussler, P.J., Wesson, R.L., and Ekstrom, G., eds., Active Tectonics and Seismic Potential of Alaska: Washington, D.C., American Geophysical Union, p. 269-286

HAEUSSLER, P.J., 2008, An overview of the neotectonics of interior Alaska; far-field deformation from the Yakutat Microplate collision: Geophysical Monograph, v. 179, p. 83-108.

HAEUSSLER, P.J., BRADLEY, D.C., WELLS, R.E., and MILLER, M.L., 2003, Life and death of the Resurrection plate: Evidence for its existence and subduction in the northeastern Pacific in Paleocene–Eocene time: Geological Society of America Bulletin, v. 115, p. 867-880.

HAEUSSLER, P.J., and SALTUS, R.W., 2004, 26 km of offset on the Lake Clark fault since Late Eocene time: U.S. Geological Survey Professional Paper 512, v. 1709-A, p. 4.

HAEUSSLER, P.J., SCHWARTZ, D.P., DAWSON, T.E., STENNER, H.D., LIENKAEMPER, J.J., CINTI, F., MONTONE, P., SHERROD, B., and CRAW, P., 2004, Surface Rupture of the 2002 Denali Fault, Alaska, Earthquake and Comparison with Other Strike-Slip Ruptures: Earthquake Spectra, v. 20, p. 565-578.

HAUG, G.H., MASLIN, M.A., SARNTHEIN, M., STAX, R., and TIEDEMANN, R., 1995, Evolution of northwest Pacific sedimentation patterns since 6 Ma (Site 882), Proc. Ocean Drill.: Program Science Results, v. 145, p. 293-315.

HELMOLD, K.P., LEPAIN, D.L., WILSON, M.D., and PETERSON, S.C., 2012, Petrology and reservoir potential of Tertiary and Mesozoic sandstones, Cook Inlet, Alaska: A preliminary analysis of outcrop samples collected during 2007-2010 field seasons: Division of Geological & Geophysical Surveys Preliminary Interpretive Report.

INGERSOLL, R.V., 1978a, Petrofacies and petrologic evolution of the Late Cretaceous fore-arc basin, northern and central California: Journal of Geology, v. 86, p. 335-352.

INGERSOLL, R.V., 1978b, Submarine fan facies of the Upper Cretaceous Great Valley Sequence, northern and central California: Sedimentary Geology, v. 21, p. 205-230.

INGERSOLL, R.V., 1979, Evolution of the Late Cretaceous forearc basin, northern and central California: Geological Society of America Bulletin, v. 90, p. 813-826.

INGERSOLL, R.V., 1983, Petrofacies and provenance of late Mesozoic forearc basin, Northern and Central California: AAPG Bulletin, v. 67, p. 1125-1142.

INGERSOLL, R.V., FULLARD, T.F., FORD, R.L., GRIMM, J.P., PICKLE, J.D., and SARES, S.W., 1984, The effect of grain size on detrital modes; a test of the Gazzi-Dickinson point-counting method: Journal of Sedimentary Research, v. 54, p. 103-116.

KALBAS, J.L., RIDGWAY, K.D., and GEHRELS, G.E., 2007, Stratigraphy, depositional systems, and provenance of the Lower Cretaceous Kahiltna assemblage, western Alaska Range: Basin development in response to oblique collision: Geological Society of America Special Papers, v. 431, p. 307-343.

KIMBROUGH, D.L., SMITH, D.P., MAHONEY, J.B., MOORE, T.E., GROVE, M., GASTIL, R.G., ORTEGA-RIVERA, A., and FANNING, C.M., 2001, Forearc-basin sedimentary response to rapid Late Cretaceous batholith emplacement in the Peninsular Ranges of southern and Baja California: Geology, v. 29, p. 491-494.

KIRSCHNER, C., and LYON, C., 1973, Stratigraphic and tectonic development of Cook Inlet petroleum province: Arctic geology: American Association of Petroleum Geologists Memoir, v. 19, p. 396-407.

LEPAIN, D.L., WARTES, M.A., MCCARTHY, P.J., STANLEY, R., SILLIPHANT, L.J., PETERSON, S., SHELLENBAUM, D.P., HELMOLD, K.P., DECKER, P.L., MONGRAIN, J.R., and GILLIS, R.J., 2009, Facies Associations, Sand Body Geometry, and Depositional Systems in Late Oligocene–Pliocene Strata, Southern Kenai Peninsula, Cook Inlet, Alaska: Report on Progress During the 2006–07 Field Seasons, *in* LePain, D.L., ed., Preliminary Results of Recent Geologic Investigations in the Homer-Kachemak Bay Area, Cook Inlet Basin: Progress During the 2006-2007 Field Season: Fairbanks, DGGS, p. 1-32.

LINN, A.M., DEPAOLO, D.J., and INGERSOLL, R.V., 1991, Nd-Sr isotopic provenance analysis of Upper Cretaceous Great Valley fore-arc sandstones: Geology, v. 19, p. 803-806.

LINN, A.M., DEPAOLO, D.J., and INGERSOLL, R.V., 1992, Nd-Sr isotopic, geochemical, and petrographic stratigraphy and paleotectonic analysis: Mesozoic Great Valley forearc sedimentary rocks of California: Geological Society of America Bulletin, v. 104, p. 1264-1279.

LITTLE, T.A., and NAESER, C.W., 1989, Tertiary tectonics of the Border Ranges fault system, Chugach Mountains, Alaska; deformation and uplift in a forearc setting: Journal of Geophysical Research, v. 94, p. 4333-4359.

MAGOON, L.B., ADKINSON, W.L., and EGBERT, R.M., 1976, Map showing geology, wildcat wells, Tertiary plant fossil localities, K-Ar age dates, and petroleum operations, Cook Inlet area, Alaska: U.S. Geological Survey Miscellaneous Investigations Series Map I-1019, scale 1:250 000.

MAGOON, L.B., and EGBERT, R.M., 1986, Framework geology and sandstone composition, *in* Magoon, L.B., ed., Geologic studies of the lower Cook Inlet COST No. 1 well, Alaska outer continental shelf: Reston, VA, U. S. Geological Survey, p. 65-90.

MCDOUGALL, I., and HARRISON, T.M., 2000, Geochronology and Thermochronology by the 40Ar/39Ar Method: Journal of Petrology: Oxford, Oxford University Press, 269 p.

MCNEILL, L.C., GOLDFINGER, C., KULM, L.D., and YEATS, R.S., 2000, Tectonics of the Neogene Cascadia forearc basin: Investigations of a deformed late Miocene unconformity: Geological Society of America Bulletin, v. 112, p. 1209-1224.

MIALL, A.D., 1988, Reservoir heterogeneities in fluvial sandstones: lessons from outcrop studies: AAPG Bulletin, v. 72, p. 682-697.

MIALL, A.D., 1994, Reconstructing fluvial macroform architecture from two-dimensional outcrops; examples from the Castlegate Sandstone, Book Cliffs, Utah: Journal of Sedimentary Research, v. 64, p. 146.

MIALL, A.D., and JONES, B.G., 2003, Fluvial architecture of the Hawkesbury Sandstone (Triassic), near Sydney, Australia: Journal of Sedimentary Research, v. 73, p. 531.

MOLL-STALCUP, E.J., 1994, Latest Cretaceous and Cenozoic magmatism in mainland Alaska, *in* Plafker, G., and Berg, H.C., eds., The Geology of Alaska: Boulder, Geological Society of America, p. 589-619.

MORRIS, W.R., and BUSBY-SPERA, C.J., 1988, Sedimentologic evolution of a submarine canyon in a forearc basin, Upper Cretaceous Rosario Formation, San Carlos, Mexico: AAPG Bulletin, v. 72, p. 717-737.

MOXON, I.W., and GRAHAM, S.A., 1987, History and controls of subsidence in the Late Cretaceous-Tertiary Great Valley forearc basin, California: Geology, v. 15, p. 626-629.

NOKLEBERG, W.J., PLAFKER, G., and WILSON, F.H., 1994, Geology of south-central Alaska, *in* Plafker, G., and Berg, H.C., eds., The Geology of Alaska: Boulder, CO, Geological Society of America, p. 311-366.

PAVLIS, T.L., and ROESKE, S.M., 2007, The Border Ranges Fault System, southern Alaska, *in* Ridgway, K.D., Trop, J.M., Glen, J.M.G., and O'Neill, J.M., eds., Tectonic growth of a collisional margin: crustal evolution of southern Alaska: Boulder, Geologic Society of America Special Paper, p. 95-128.

PLAFKER, G., and BERG, H.C., 1994, Overview of the geology and tectonic evolution of Alaska, *in* Plafker, G., and Berg, H.C., eds., The Geology of Alaska: Boulder, Geological Society of America, p. 989-1021.

PLAFKER, G., MOORE, J.C., and WINKLER, G.R., 1994, Geology of the southern Alaska margin, *in* Plafker, G., and Berg, H.C., eds., The Geology of Alaska: Boulder, CO, Geological Society of America, p. 311-366.

PLAFKER, G., NOKLEBERG, W., and LULL, J., 1989, Bedrock geology and tectonic evolution of the Wrangellia, Peninsular, and Chugach terranes along the Trans-Alaska Crustal Transect in the

Chugach Mountains and southern Copper River Basin, Alaska: Journal of Geophysical Research, v. 94, p. 4255-4295.

RAWLINSON, S.E., 1984, Environments of deposition, paleocurrents, and provenance of Tertiary deposits along Kachemak Bay, Kenai Peninsula, Alaska: Sedimentary Geology, v. 38, p. 421-442.

REED, B.L., and LANPHERE, M.A., 1973, Alaska-Aleutian Range Batholith: Geochronology, Chemistry, and Relation to Circum-Pacific Plutonism: Geological Society of America Bulletin, v. 84, p. 2583-2610.

REININK-SMITH, L.M., 1995, Tephra Layers as Correlation Tools of Neogene Coal-bearing Strata from the Kenai Lowland, Alaska: Geological Society of America Bulletin, v. 107, p. 340-353.

REININK-SMITH, L.M., 2010, Variations in alder pollen pore numbers--a possible new correlation tool for the Neogene Kenai lowland, Alaska: Palynology, v. 34, p. 180-194.

REININK-SMITH, L.M., and LEOPOLD, E.B., 2005, Warm Climate in the Late Miocene of the South Coast of Alaska and the Occurrence of Podocarpaceae Pollen: Palynology, v. 29, p. 205-262.

RICHTER, D.H., SMITH, J.G., LANPHERE, M.A., DALRYMPLE, G.B., REED, B.L., and SHEW, N., 1990, Age and progression of volcanism, Wrangell Volcanic Field, Alaska: Bulletin of Volcanology, v. 53, p. 29-44.

RIDGWAY, K.D., TROP, J.M., and FINZEL, E.S., 2011, Modification of continental forearc basins by flat-slab subduction processes: A case study from southern Alaska, *in* Busby, C., and Pérez, A.A., eds., Tectonics of Sedimentary Basins: Recent Advances: Hoboken, Wiley, p. 664.

SAMBROOK SMITH, G., ASHWORTH, P.J., BEST, J.L., WOODWARD, J., and SIMPSON, C.J., 2006, The sedimentology and alluvial architecture of the sandy braided South Saskatchewan River, Canada: Sedimentology, v. 53, p. 413-434.

SAMBROOK SMITH, G., GREGORY, H., ASHWORTH, P., BEST, J., WOODWARD, J., and SIMPSON, C., 2005, The morphology and facies of sandy braided rivers: some considerations of scale invariance.

SCHOLLE, P.A., 1979, A Color Illustrated Guide to Constituents, Textures, Cements, and Porosities of Sandstones and Associated Rocks: Memoir: Tulsa, American Association of Petroleum Geologists, 201 p.

SKELLY, R.L., BRISTOW, C.S., and ETHRIDGE, F.G., 2003, Architecture of channel-belt deposits in an aggrading shallow sandbed braided river: the lower Niobrara River, northeast Nebraska: Sedimentary Geology, v. 158, p. 249-270.

SMITH, N.D., CROSS, T.A., DUFFICY, J.P., and CLOUGH, S.R., 1989, Anatomy of an avulsion: Sedimentology, v. 36, p. 1-23.

SMITH, N.D., and PEREZ-ARLUCEA, M., 1994, Fine-grained splay deposition in the avulsion belt of the Lower Saskachewan River, Canada: Journal of Sedimentary Research, v. 64, p. 159-168.

STOCK, J., and MOLNAR, P., 1988, Uncertainties and implications of the Late Cretaceous and Tertiary position of North America relative to the Farallon, Kula, and Pacific Plates: Tectonics, v. 7, p. 1339-1384.

SURPLESS, K.D., GRAHAM, S.A., COVAULT, J.A., and WOODEN, J.L., 2006, Does the Great Valley Group contain Jurassic strata? Reevaluation of the age and early evolution of a classic forearc basin: Geology, v. 34, p. 21-24.

SWENSON, R., 2001, Introduction to Tertiary tectonics and sedimentation in the Cook Inlet basin: Miscellaneous Publication - Division of Geological and Geophysical Surveys, p. 10-19.

SWENSON, R., 2002, Introduction to Tertiary tectonics and sedimentation in the Cook Inlet basin, *in* Dallegge, T., ed., Geology and Hydrocarbon Systems of the Cook Inlet Basin, Alaska: American Association of Petroleum Geologists Pacific Section/Society of Petroleum Engineers Pacific Regional Conference, May 23-24, 2002, Anchorage, Alaska, p. 11-20.

TRIPLEHORN, D.M., TURNER, D.L., and NAESER, C.W., 1977, K-Ar and Fission-track Dating of Ash Partings in Coal Beds from the Kenai Peninsula, Alaska: A Revised Age for the Homerian Stage-Clamgulchian Stage Boundary: Geological Society of America Bulletin, v. 88, p. 1156-1160.

TROP, J.M., 2008, Latest Cretaceous forearc basin development along an accretionary convergent margin: South-central Alaska: Geological Society of America Bulletin, v. 120, p. 207-224.

TROP, J.M., and RIDGEWAY, K.D., 2007, Mesozoic and Cenozoic tectonic growth of southern Alaska: A sedimentary basin perspective, *in* Ridgway, K.D., Trop, J.M., Glen, J.M.G., and O'Neill, J.M., eds., Tectonic Growth of a Collisional Continental Margin: Crustal Evolution of Southern Alaska: Boulder, Geological Society of America, p. 55-94.

TROP, J.M., and RIDGWAY, K.D., 2000, Sedimentology, stratigraphy, and tectonic importance of the Paleocene–Eocene Arkose Ridge Formation, Cook Inlet-Matanuska Valley forearc basin, Alaska, *in* Pinney, D.S., and Davis, P.K., eds., Short notes on Alaskan Geology: Fairbanks, Division of Geological and Geophysical Surveys Professional Report, p. 129-144.

TROP, J.M., RIDGWAY, K.D., and SPELL, T.L., 2003, Sedimentary record of transpressional tectonics and ridge subduction in the Tertiary Matanuska Valley-Talkeetna Mountains forearc basin, Southern Alaska: Special Paper - Geological Society of America, v. 371, p. 89-118.

TURNER, D.L., TRIPLEHORN, D.M., NAESER, C.W., and WOLFE, J.A., 1980, Radiometric Dating of Ash Partings in Alaskan Coal Beds and Upper Tertiary Paleobotanical Stages: Geology, v. 8, p. 92-96.

WILSON, F.H., DOVER, J.H., BRADLEY, D.C., WEBER, F.R., BUNDTZEN, T.K., and HAEUSSLER, P.J., 1998, Geologic map of central (interior) Alaska: U.S. Geological Survey Open-File Report 98-133-A, 63 p.

WILSON, F.H., HULTS, C.P., SCHMOLL, H.R., HAEUSSLER, P.J., SCHMIDT, J.M., YEHLE, L.A., and LABAY, K.A., 2009, Preliminary geologic map of the Cook Inlet Region, Alaska: Including parts of the Talkeetna, Talkeetna Mountains, Tyonek, Anchorage, Lake Clark, Kenai, Seward, Iliamna, Seldovia, Mount Katmai, and Afognak: 1:250,000 scale quadrangles. Reston, Va.: U.S. Dept. of the Interior, U.S. Geological Survey.

WOLFE, J.A., HOPKINS, D.M., and LEOPOLD, E.B., 1966, Tertiary Stratigraphy and Paleobotany of the Cook Inlet Region, Alaska: Geological Survey Professional Paper, v. 398-A: Washington D.C., U.S. Government Printing Office, 37 p.

ZACHOS, J., PAGANI, M., SLOAN, L., THOMAS, E., and BILLUPS, K., 2001, Trends, Rhythms, and Aberrations in Global Climate 65 Ma to Present: Science, v. 292, p. 686-693, doi: 10.1126/science.1059412.

Chapter 5

Conclusions

5.1 introduction

Our understanding of forearc basins comes primarily from studies of protracted intervals of subduction between normal oceanic crust and continental crust. Typical forearc basin sediment sources the accretionary prism and the magmatic arc. The Miocene to Pliocene terrestrial Beluga and Sterling formations record deposition in Cook Inlet during flat-slab subduction of the Yakutat microplate. These formations crop out at the basin margins with sufficient detail to inform our understanding of forearc basin development during second order subduction events. I document a change in depositional style between these formations and investigated climate and provenance to understand basin evolution.

5.2 Discussion

5.2.1 Depositional Style

The Beluga Fm., exposed along the western and eastern margins of Cook Inlet, was deposited by humid-organic anabranching/single thread fluvial systems. On the east side of the basin, flow is west- directed and on the west side of the basin flow is likely east- directed. Using depositional style, sediment geometry, and geomorphological regional curves from similar climatic and depositional settings in modern rivers, the analog that best fits this formation is the Cumberland Marshes region of the Saskatchewan River.

The Sterling Fm., exposed along the western and eastern margins of Cook Inlet, was deposited by sandy braided fluvial systems. Paleocurrent data from the eastern margin of the basin indicate southward-directed flow. Depositional style, sediment geometry, and geomorphological regional

curves from similar depositional settings in modern rivers gives a range of modern analogs. Sterling Fm. fluvial systems were larger than the modern Platte River but smaller than the modern Brahmaputra River.

5.2.2 Paleoclimate

Palynological analyses of overbank facies indicate vegetation dominated by shrubs (predominately *Alnus*) and herbaceous plants with relatively sparse trees. Carbon stable isotopic analysis of leftover pollen concentrates allowed calculation of mean annual precipitation (MAP). The average MAP was 970 mm a^{-1} with modest variability. The highest variability occurs ~8 Ma with values as high as 3600 mm a^{-1}.

At ~8 Ma, temperatures of the Alaska Gyre in the northern Pacific Ocean, which was about 5°C warmer than today, began to decrease (Romine, 1985). The timing of this decrease in SST correlates with increased variability in the terrestrial precipitation record and may be the cause of this variability. Globally, a reorganization and decline in the throughput of the global water cycle occurred at this time. Monsoon initiation, monsoon intensification, greater seasonality of precipitation, and aridification are attributed to the reorganization in the global water cycle (Lyle et al., 2008). This study documents the northern high latitude precipitation record and provides further evidence for global reorganization of the water cycle.

5.2.3 Provenance

Sandstones of the Beluga Fm. are dominantly litharenites composed of lithic fragments sourced from the accretionary prism on the eastern side of the basin. The western side of the basin is less well constrained but was likely sourced from the Kahiltna Assemblage. The composition of lithic fragments becomes more volcanic in younger strata, indicating an increasingly significant sediment contribution from the volcanic arc.

Sandstones of the Sterling Fm. are dominantly litharenites composed predominantly of lithic fragments from the volcanic arc but with a non-volcanic contribution from the Alaska Range to the north. The Sterling Fm. is similar to the Beluga Fm. in that younger samples contain a greater proportion of volcanic fragments.

The gradual shift from sedimentary lithic fragments to volcanic lithic fragments is interpreted to be a shift from dominantly accretionary prism to dominantly volcanic arc sources. The youngest Sterling Fm. samples are predominantly composed of volcanic fragments, suggesting provenance almost entirely from the volcanic arc.

5.2.4 Basin Reconstruction

Integrating the depositional systems and provenance with available chronostratigraphic control allows for reconstruction of forearc basin evolution. Prior to ~11 Ma humid/organoclastic-style anabranching/single thread channels of the Beluga Fm. received sediment from the accretionary prism on the eastern side of the basin. The western side of the basin is less well-constrained but likely involved eastward- flowing anabranching/single channel streams sourced primarily from the Kahiltna Assemblage. Between ~11 and ~ 8 Ma depositional systems and provenance were changing from Beluga-style deposition to southward-flowing sandy braided fluvial systems of the Sterling Fm. Sterling Fm. fluvial systems were sourced from the volcanic arc. After ~8 Ma the Cook Inlet forearc basin is dominated by sandy braided fluvial systems and by ~6 Ma it is sourced almost entirely from the magmatic arc.

Understanding changes in fluvial style is complicated and necessitates understanding the influence of base level, climate, and tectonics. Of these, base level is not well constrained in Southern Alaska during this time. However, changes due to base-level change propagate towards the hinterland. Fluvial style and provenance changes in Cook Inlet appear to have occurred near the hinterland and propagated downstream. The paleoclimate reconstruction indicates a modest decline in temperature and variations in precipitation. The timing of

precipitation variation postdates changes in fluvial style, making climate an unlikely contributor to the changes in fluvial style. Orogen-scale changes in the western Alaska Range driven by Yakutat microplate subduction is the most likely cause for increased sediment supply that resulted in the change in fluvial style.

Recently, the sediment flux steering concept (Connell et al., 2012a, b) has been introduced to aid in understanding fluvial systems at the basin scale. The sediment flux steering concept postulates that the location and width of the axial and transverse systems in a basin are strongly controlled by relative sediment fluxes ('flux steering') and less influenced by the location of the subsidence maximum and subsidence rate (Connell et al., 2012a, b). Sediment flux in Cook Inlet was highest in fluvial systems draining the basin margins during deposition of the Beluga Fm. sediments. During deposition of the Sterling Fm. sediment flux was highest in the axial fluvial systems derived from the volcanic arc and western Alaska Range. A previously unrecognized exhumation event in the western Alaska Range, starting ~11 Ma, best explains the changes in provenance and depositional systems in the Beluga and Sterling formations.

5.3 References

CONNELL, S.D., WONSUCK, K., PAOLA, C., and SMITH, G.A., 2012, Fluvial Morphology and Sediment-Flux Steering of Axial Transverse Boundaries in an Experimental Basin: Journal of Sedimentary Research, v. 82.

CONNELL, S.D., WONSUCK, K., SMITH, G.A., and PAOLA, C., 2012, Stratigraphic Architecture of an Experimental Basin with Interacting Drainages: Journal of Sedimentary Research, v. 82.

LYLE, M., BARRON, J., BRALOWER, T., HUBER, M., OLIVAREZ LYLE, A., RAVELO, A., REA, D., and WILSON, P., 2008, Pacific Ocean and Cenozoic evolution of climate: Reviews of Geophysics, v. 46.

ROMINE, K., 1985, Radiolarian biogeography and paleoceanography of the North Pacific at 8 Ma, *in* Kennett, J., ed., The Miocene Ocean: Paleoceanography and Biogeography: Boulder, Geological Society of America, p. 237-273.